



HAL
open science

Synthesis of (cyclo)maltooligosaccharide-based glycosaminoglycan mimetics and their interaction with heparin binding growth factors

Rubal Ravinder

► **To cite this version:**

Rubal Ravinder. Synthesis of (cyclo)maltooligosaccharide-based glycosaminoglycan mimetics and their interaction with heparin binding growth factors. Organic chemistry. Université Grenoble Alpes [2020-..], 2020. English. NNT : 2020GRALV034 . tel-03192820

HAL Id: tel-03192820

<https://theses.hal.science/tel-03192820v1>

Submitted on 8 Apr 2021

HAL is a multi-disciplinary open access archive for the deposit and dissemination of scientific research documents, whether they are published or not. The documents may come from teaching and research institutions in France or abroad, or from public or private research centers.

L'archive ouverte pluridisciplinaire **HAL**, est destinée au dépôt et à la diffusion de documents scientifiques de niveau recherche, publiés ou non, émanant des établissements d'enseignement et de recherche français ou étrangers, des laboratoires publics ou privés.

THÈSE

Pour obtenir le grade de

DOCTEUR DE L'UNIVERSITE GRENOBLE ALPES

Spécialité : **Chimie organique**

Arrêté ministériel : 25 mai 2016

Présentée par

Rubal RAVINDER

Thèse dirigée par **Sami HALILA**, Chargé de Recherche, CNRS,
et codirigée par **Romain VIVÈS**, Directeur de Recherche, CNRS

préparée au sein du **Centre de Recherche sur les
Macromolécules Végétales (CERMAV)** et de l'**Institut de
Biologie Structurale (IBS)**
dans l'**École Doctorale Chimie et Sciences du Vivant**

**Synthèse de mimes de
glycosaminoglycanes sulfatés à base de
(cyclo)maltooligosaccharides et leur
interaction avec des facteurs de croissance
liant l'héparine**

**Synthesis of (cyclo)maltooligosaccharide-
based sulfated glycosaminoglycan
mimetics and their interaction with
heparin binding growth factors**

Thèse soutenue publiquement le **7 décembre 2020**
devant le jury composé de :

Madame Angela RUSSELL

Professeure, St John's College, University of Oxford, Rapportrice

Monsieur José KOVENSKY

Professeur des Universités, Université de Picardie, Rapporteur

Madame Chrystel LOPIN-BON

Professeure des Universités, Université d'Orléans, Examinatrice

Madame Sandrine PY

Directrice de Recherche, CNRS, Examinatrice, Présidente du jury

Monsieur Romain VIVÈS

Directeur de Recherche, CNRS, Co-directeur de thèse

Monsieur Sami HALILA

Chargé de Recherche, CNRS, Directeur de thèse



Remerciements

Ce manuscrit est l'aboutissement de trois années de recherche, en qualité de doctorante principalement au sein du Centre de Recherche sur les Macromolécules Végétales (équipe Auto-assemblage de Glycopolymères, Grenoble) mais aussi au sein de l'Institut de Biologie Structurale (groupe Structure et Activité des GlycosAminoGlycanes, Grenoble).

Je tiens tout d'abord à remercier mon directeur de thèse Monsieur Sami HALILA pour m'avoir accueilli au sein du CERMAV. Je le remercie pour son accompagnement, ses idées judicieuses, sa disponibilité et son soutien au cours de ces trois années malgré toutes les difficultés que j'ai pu rencontrer durant ce projet ambitieux et pluridisciplinaire. J'ai énormément appris en glycochimie, et ma passion pour ce domaine n'en a été que renforcée. Sa bonne humeur et son « humour » m'ont aidé à avancer autant sur le plan personnel que professionnel.

Je tiens également à remercier mon co-directeur de thèse Monsieur Romain VIVÈS pour m'avoir accueilli au sein de son équipe à l'IBS. Je le remercie pour sa disponibilité, sa bonne humeur et son accompagnement, et j'espère avoir l'opportunité de faire quelques essais à l'IBS pour renforcer mes compétences. Je le remercie d'avoir pris du temps pour m'expliquer la complexité des glycosaminoglycanes tout au long du projet, mais aussi de m'avoir aidé à comprendre et interpréter les résultats en biologie lors de la rédaction.

J'aimerais ensuite remercier Madame Angela RUSSELL et Monsieur José KOVENSKY, rapporteurs de mon jury, pour avoir accepté de juger ce travail avec bienveillance et pour la discussion qui a suivie la soutenance. Je remercie également Madame Chrystel LOPIN-BON pour avoir examiné ce travail et Madame Sandrine PY, pour avoir en plus présider le jury et pour l'aide pour les réactions d'hydrogénolyse effectuées au sein du laboratoire DCM (Grenoble).

Je souhaite remercier Mesdames Patricia ALBANESE et Carine-Manuela BORGES au laboratoire Gly-CRRET, Croissance, Réparation et Régénération Tissulaires, pour avoir effectué les tests biologiques, pour nos discussions enrichissantes et pour le précieux temps qu'elles m'ont accordé pour m'expliquer les tests et les résultats obtenus.

Mes remerciements s'adressent également à tous les permanents du laboratoire, qui ont créé une atmosphère de travail agréable. J'ai passé de très agréables moments, leurs conseils et leur bienveillance m'ont énormément aidé.

Un très grand merci à tous les non-permanents (anciens et nouveaux) de l'équipe et plus particulièrement à Marie CARRIERE, Charlène EFFLIGENIR, Sophie RENAUD, Justine SOLIER, Cornélia LUNTADILA (les PCG gurlz !), mais aussi à Robin BRAHMI, Shun YAO, Hong LI, Ahlem MNASRI et Julie PERRIN pour cette aventure et ces moments riches en émotions ! Vous avez énormément contribué à l'ambiance de l'équipe, vous m'avez beaucoup aidé, et fait apprécier mon séjour à Grenoble.

Merci également à tous les non-permanents que j'ai rencontré au laboratoire (et je m'excuse d'avance pour ceux que j'ai pu oublier) : Dania, Claire, Simon, Raphael, Vanina, Marie-Carole, Paul C., Fabien, Maeva, Rafael, Robin, Pierre, Antoine, Paul R., Axel, Laurent, Emeline, Céline, Julien, etc. J'ai adoré discuter avec vous tous, votre gentillesse m'émue et j'espère qu'on aura l'occasion de fêter mon diplôme tous ensemble !

Je souhaite exprimer mes profonds remerciements à tous mes amis (dont Emilie, Sylvie, Pauline, Samuel, Merrick et Ghada). Votre présence me fait oublier mes soucis et m'aide à avancer dans ma vie.

Je remercie ma famille, et plus particulièrement mon petit frère, Ravneet, le soleil de ma vie. Ils m'ont appris à toujours me battre, et c'est grâce à eux que j'ai entrepris cette thèse. Aussi un grand merci à la famille de mon conjoint pour m'avoir si chaleureusement accueilli et supporté. Vous êtes des personnes en or.

Enfin, je voudrais remercier mon conjoint, Olivier : merci d'exister.

Résumé en français

Chapitre 1 : Contexte

L'arthrose est une maladie commune affectant les articulations de l'organisme. Dans un organisme sain, l'articulation se compose de deux extrémités d'os protégées par du tissu cartilagineux. Celui-ci est principalement formé d'une matrice extra-cellulaire riche en fibre de collagène, en protéoglycanes (PGs) et en glycosaminoglycanes (GAGs). Un seul type de cellule est présent dans ce tissu avasculaire, les chondrocytes, en charge de la production et la dégradation des composés matriciels et donc de l'intégrité du tissu. C'est lorsque l'équilibre établi par les chondrocytes est rompu que l'arthrose a lieu avec pour principal effet la dégradation du tissu cartilagineux et notamment des protéoglycanes et glycosaminoglycanes.

Lors de stades avancés, la dégradation du cartilage outrepassa la production d'éléments matriciels. Les chondrocytes produisent alors des composés matriciels structurellement altérés incapables de posséder des fonctions physiologiques ce qui contribue à l'inflammation du tissu et à des douleurs au niveau des articulations.

L'arthrose est actuellement la maladie rhumatismale la plus commune dans le monde et est reconnue comme un fardeau pour la santé publique mondiale. Le nombre de patients atteint d'arthrose augmente tous les jours dû au vieillissement de la population et à l'augmentation de la prévalence de l'obésité. Malheureusement, seuls des traitements symptomatiques sont prescrits aux patients car aucun traitement curatif n'a été mis au point à ce jour.

Les thérapies actuelles en développement se basent sur l'ingénierie tissulaire avec la mise en place de réseaux de protéoglycanes et glycosaminoglycanes artificiels ou mimés dans lesquelles des cellules souches mésenchymateuses seraient introduites afin qu'elles puissent se différencier en chondrocytes produisant des éléments matriciels « sains » dans un environnement non-inflammatoire. Cette stratégie a donc été explorée dans le cadre de notre projet.

Les GAGs sont de longues chaînes linéaires de polysaccharides naturels composées de la répétition d'un motif disaccharidique où chaque monosaccharide de la chaîne peut être acétylé, épimérisé ou sulfaté à différentes positions du sucre. La nature du disaccharide, le type de modification ainsi que la position des groupements sulfates sur chaque monomère de sucre sont la source de l'extrême diversité structurale des glycosaminoglycanes. Ces biomolécules hautement chargées négativement sont ubiquitaires dans l'organisme et possèdent une multitude de fonctions structurales et fonctionnelles telles que la croissance, la différenciation et la signalisation cellulaire ou encore la régulation de la bioactivité d'une multitude de protéines dont les facteurs de croissance.

Les GAGs sont communément retrouvés attachés à un corps protéique formant ainsi des PGs. Cette structure leur confère de la multivalence, propriété indispensable pour exercer leurs activités. Le rôle des PGs dans l'organisme est principalement lié aux chaînes de GAGs qu'ils portent.

De par leur implication dans une large gamme de processus physio- et patho-logiques, les GAGs et les PGs sont connus pour être de bonnes cibles thérapeutiques et ont d'ailleurs été étudiés dans le cadre de la croissance des cellules de différents tissus dits « souples ». Cependant, leur obtention difficile est un facteur limitant leur utilisation à des fins thérapeutiques. D'une part, leur extraction à partir de tissus animaliers présente des risques de contamination (par des pathogènes par exemple). De plus, la production de PGs et GAGs variant fortement en fonction du temps et du tissu, aucun lot ne peut être biologiquement identique. D'autre part, leur extrême hétérogénéité structurale rend leur synthèse chimique laborieuse et complexe et mène à la fabrication d'une seule chaîne définie tandis qu'aucune chaîne de GAG naturel ne présente exactement le même motif dans l'organisme.

Pour pallier à ce problème, les scientifiques misent depuis quelques années sur la préparation de mimes de PGs et de GAGs, appelés glycomimétiques. Ces derniers, plus faciles à obtenir en larges quantités, permettent de comprendre le rôle et d'établir des relations structure-activité des biomolécules naturelles afin de pouvoir les utiliser *in fine* comme thérapies. Différents paramètres entrent en jeu dans la préparation de glycomimétiques : le type de squelette de la chaîne (polysaccharides naturels, glycopolymères ou composés non-sucrés synthétiques), la taille de la chaîne, son degré de sulfatation ainsi que sa conformation.

Dans notre projet, nous nous sommes focalisés sur la modification de (cyclo)maltooligosaccharides, en particulier le malto-heptaose, -hexaose et la β -cyclodextrine, ayant des longueurs de chaînes et des conformations tridimensionnelles définies. Ces composés ont déjà fait leur preuve en tant que mimes biologiques de GAGs. Le projet s'articule autour de cinq tâches qui seront développées dans chaque chapitre :

- La sulfatation aléatoire des maltooligosaccharides linéaires et cycliques (libres, fonctionnalisés et greffés) afin de mimer des GAGs et l'évaluation de leur activité biologique ;
- La préparation de maltooligosaccharides cycliques régiosélectivement sulfatés et l'évaluation de leur activité biologique ;
- La fonctionnalisation de l'extrémité réductrice des maltooligosaccharides linéaires par une fonction thiol ou amine en vue de leur couplage sur un polymère ou une biotine ;
- Le greffage des chaînes linéaires fonctionnalisées à une biotine (pour des tests biologiques) ou à un polymère pour créer un mime de PGs.

Chapitre 2 : Obtention de glycomimétiques aléatoirement sulfatés à partir de (cyclo)maltooligosaccharides

Dans ce chapitre, nous nous sommes focalisés sur le maltoheptaose, maltohexaose et la β -cyclodextrine naturels non-modifiés. Ces composés ont été sulfatés aléatoirement à différents degrés (faible, moyen et fort) par variation de la stœchiométrie de l'agent sulfatant, le sulfure de trioxyde. Après caractérisation, ils ont été analysés biologiquement afin de tester l'effet de la longueur de chaîne (malto-hexaose VS heptaose) ainsi que de sa conformation tridimensionnelle (maltoheptaose linéaire VS β -cyclodextrine cyclique) sur l'interaction avec des facteurs de croissance liant l'héparine et leur potentialisation.

Les conditions de sulfatation et notamment leur purification ont d'abord été optimisées avec le maltoheptaose. Un mode-opératoire simple a été adopté pour le traitement des mélanges réactionnels à l'issue de la réaction : une simple neutralisation suivie d'une purification par GPC a permis d'obtenir des produits quasi-purs. Ce protocole a pu également être appliqué pour la β -cyclodextrine. Cependant, ayant des quantités très faibles de maltohexaose (composé coûteux), leur sulfatation n'a pu être effectuée qu'une seule fois avant optimisation.

La caractérisation des (cyclo)maltooligosaccharides sulfatés a été réalisée par quatre méthodes développées ci-après.

La spectroscopie par résonance magnétique nucléaire en proton a permis d'avoir une idée globale du degré de sulfatation au vu de son allure générale. Plus un composé est sulfaté, plus le spectre « shifté » vers les champs faibles, et plus le pic attribué aux protons anomériques est visible comme un multiplet. Nous n'avons malheureusement pas pu attester de la présence de composés anhydros par analyse complémentaire HMBC.

L'analyse SEC-MALS permet d'extraire un bon nombre d'information quant à la composition des mélanges sulfatés. Tout d'abord, l'allure des pics correspondant aux temps de rétention des composés dans le système de chromatographie d'exclusion stérique permet d'avoir une idée de l'homogénéité globale du mélange. Par exemple, les pics gaussiens observés pour la majorité de nos mélanges ont témoigné de leur homogénéité. Ensuite, nous avons observé que les temps de rétention diminuaient avec le degré de sulfatation. Ainsi, les composés hautement sulfatés étaient plus vite élués que ceux moins sulfatés (ce qui concorde avec la taille moyenne des composés). De plus, la SEC-MALS permet d'extraire des informations telles que la masse moléculaire moyenne en poids M_w , la masse moléculaire moyenne en nombre M_n , et l'indice de polydispersité PDI de chaque mélange sulfaté. Globalement, et en accord avec la théorie, ces trois paramètres tendaient à augmenter avec le degré de sulfatation.

L'analyse élémentaire nous a permis de calculer le degré de sulfatation moyen par unité des mélanges sulfatés grâce aux pourcentages en carbone et en soufre. Ce degré augmentait entre les composés faiblement sulfatés et ceux fortement. De plus, les quantités d'azote dans la majorité des échantillons

ont témoigné de la présence de traces d'ammonium carbonate, solvant utilisé lors de la purification des mélanges par GPC.

Enfin, l'analyse infrarouge (FT-IR) nous a permis d'avoir une idée des fonctions chimiques présentes de façon qualitative. Ainsi, nous avons pu confirmer la diminution d'hydroxyles et de l'augmentation de groupements sulfates, le tout sans hydrolyse.

Après leur sulfatation et leur caractérisation, les (cyclo)maltooligosaccharides ont été soumis à des tests biologiques de deux types : le test ELISA qui permet d'évaluer la capacité de compétition entre nos composés et l'héparine pour l'interaction avec des facteurs de croissance liant l'héparine, et le test mitogénique sur cellules BAF32 ou HUVEC qui permet de tester la capacité de nos composés à se comporter comme des glycomimétiques de GAGs en induisant la prolifération cellulaire.

Ainsi, les dérivés modérément et hautement sulfatés des (cyclo)maltooligosaccharides ont semblé avoir de meilleures affinités et ont induit des réponses cellulaires plus intenses que ceux légèrement sulfatés. La taille minimale requise pour l'interaction avec les facteurs de croissance testés a été évaluée à sept unités de sucre en comparant les effets des maltoheptaose et maltohexaose sulfatés mais reste à être confirmée. L'interaction et la potentialisation semblaient varier selon la conformation linéaire ou cyclique des oligosaccharides.

Chapitre 3 : Obtention de glycomimétiques régiosélectivement sulfatés à partir de cyclomaltooligosaccharides

Après avoir découvert que les β -cyclodextrines pouvaient exercer des rôles comparables aux GAGs (voir chapitre 2), nous nous sommes penchés sur l'effet de la position des groupements sulfates sur l'activité biologique de ces composés cycliques. Pour ce faire, la chimie sélective des β -cyclodextrines a été exploitée. Elle se base sur la symétrie de type C_n et la différence de réactivité entre les hydroxyles OH-6, les secondaires OH-2 et OH-3 de ces molécules cycliques. Ainsi, les hydroxyles primaires OH-6 sont les plus réactifs et accessibles, les OH-2 sont les plus acides et les OH-3 sont les moins accessibles et réactifs. Grâce à ces différences, il est possible de sélectivement fonctionnaliser les OH-6 ou bien les OH-2, et de réaliser *via* l'utilisation de groupements protecteurs orthogonaux des *per*-modifications à chacune des positions. Dans ce cadre, de nombreux exemples de fonctionnalisations sélectives ainsi que de stratégie de synthèse ont été développés principalement pour des applications en électrophorèse capillaire.

Nous nous sommes inspirés de quelques-uns d'entre eux pour préparer six composés régiosélectivement sulfatés : les 2S-, 3S-, 6S-, 2,3S-, 2,6S-, et 3,6S- β -cyclodextrines.

Le point de départ de toutes les synthèses a été le même : la préparation de la β -cyclodextrine 6-*O*-*tert*-butyldimethylsilylée. Par la suite, la 6S- β -cyclodextrine a pu être obtenue en cinq étapes. La 2,3S- β -cyclodextrine a nécessité sept étapes, et les positions OH-2 et OH-3 n'ont pas pu être entièrement

sulfatées, probablement dû à la proximité de ces hydroxyles et à l'encombrement stérique des groupements sulfates. De son côté, la 2,6S- β -cyclodextrine n'a pas pu être terminée à temps dû à l'échec d'une étape de désilylation. La 2S- β -cyclodextrine a pu être synthétisée en sept étapes, et la 3,6S- β -cyclodextrine en cinq. Malheureusement, aucune stratégie de synthèse n'a fonctionné pour la 3S- β -cyclodextrine, qui n'a donc pas pu être préparée.

Après caractérisation, les différentes β -cyclodextrines sulfatées ont été soumises à des tests biologiques afin d'évaluer le possible effet de la position des sulfates sur leur activité biologique. Leur habilité à être des compétiteurs avec l'héparine a été évaluée avec FGF-2 et VEGF. Selon le facteur de croissance testé, différents ordres de grandeur des IC50 a été obtenu, et les composés semblaient interagir différemment selon leur motif de sulfatation.

Chapitre 4 : Modification de l'extrémité réductrice de maltooligosaccharides

Afin d'obtenir des mimes de protéoglycanes, il a été envisagé de greffer plusieurs chaînes linéaires de maltooligosaccharides (étant de potentiels mimes de GAGs) sur un polymère bactérien portant soit des fonctions alcènes soit des fonctions acides carboxyliques pendantes. Pour effectuer ce couplage, les chaînes ont été soit thiol- soit amine-fonctionnalisées pour un futur couplage thiol-ène ou amide respectivement.

L'extrémité réductrice étant porteuse d'une fonction aldéhyde, c'est celle qui peut être modifiée chimio-sélectivement par rapport aux autres hydroxyles. Afin d'avoir des adduits fonctionnalisés en un nombre d'étapes limitées, la fonctionnalisation directe sur sucre non-protégé a été choisie. Plus précisément, l'extrémité réductrice des maltooligosaccharides a été modifiée par introduction d'un linker bis-fonctionnalisé (comportent une amine et un(e) thiol/amine).

La piste du couplage thiol-ène a d'abord été investie par la production de maltooligosaccharides thiol-fonctionnalisés puisque le polymère bactérien porte des fonctions alcènes potentiellement modifiables par un couplage thiol-ène. Trois stratégies ont été développées.

La première stratégie s'est basée sur l'utilisation de la cystamine (diamine aliphatique contenant un pont disulfure) et son espèce réduite, la cysteamine. Ce chemin synthétique avait précédemment été développé au sein de l'équipe. Dans un premier temps, l'introduction de la cysteamine, portant un thiol non-protégé, à l'extrémité réductrice a été tentée sur le maltose sans succès. Avec le maltoheptaose, un mélange de trois produits a été obtenu dont deux espèces où le thiol s'est oxydé. A partir de ces observations, les groupements thiols ont dû être introduits sous forme protégée à cause la réactivité des thiols sous forme libre, qui tendent à s'oxyder sous forme de dimères disulfures. La fonction thiol a donc été protégée sous forme de pont disulfure. Un échange thiol-disulfure a été envisagé pour la cysteamine à l'aide du disulfure de pyridyl, composé aromatique et donc UV-actif. Ceci aurait permis un meilleur suivi et une identification rapide des produits thiol-fonctionnalisés. Cependant, cette stratégie s'est

révélée inefficace. Le greffage de la cystamine sur les maltooligosaccharides a ensuite été tenté *via* une amination réductrice ou par amination de Kochetkov. Une nouvelle fois, aucune de ces deux méthodes n'a pu être efficace sur le maltose. D'autres stratégies développées en parallèle de la cystamine/cysteamine (HTL) semblaient par ailleurs mieux fonctionner.

La deuxième stratégie consistait en l'utilisation de l'homocysteine thiolactone (HTL) qui est donc une thiolactone (thiol protégé) portant une amine primaire. L'HTL a dans un premier temps été greffée par amination réductrice au maltoheptaose et au maltose sur de petites quantités. Nous nous sommes ensuite exposés à des difficultés de montée en échelle pour la fonctionnalisation du maltose (destiné à être utilisé pour l'optimisation des conditions de couplage thiol-ène). Sur grosses quantités, un sous-produit contenant un thiol protégé et un thiol libre (correspondant à l'autocondensation de l'HTL à l'extrémité réductrice des chaînes) a été observé à hauteur de 30-50% (calculé à partir du spectre de masse des mélanges obtenu), avec le risque que les thiols libres soient la source de réactions indésirables. Etant donné que les deux produits ne pouvaient que difficilement être séparés en raison de leur similarité structurale, nous avons tenté d'adoucir les conditions de l'amination réductrice en modulant la stœchiométrie des réactifs, les temps de réaction, les solvants, la température et les méthodes de purification. Le pourcentage de sous-produit a pu être diminué à 7% sur une échelle de 4 grammes.

La condensation de Knoevenagel et la fabrication de dérivés d'acide barbiturique est une thématique développée depuis quelques années au sein de l'équipe. Elle a permis de former toute sorte de dérivés (symétriques et asymétriques, portant des fonctions hydrophobes/hydrophiles/« clickables ») pouvant avoir des nombreuses applications. Cette méthodologie a été utilisée pour l'introduction d'une ou deux molécules d'HTL à l'extrémité réductrice des sucres. Nous avons d'abord tenté de synthétiser un dérivé barbiturique symétrique portant deux HTL, sans succès. Par la suite, nous nous sommes penchés sur la préparation d'un dérivé asymétrique portant un éthyle d'une part et un HTL d'autre part. Le composé a enfin été couplé au maltoheptaose et au maltose par condensation de Knoevenagel (dans des conditions légèrement modifiées).

Lors de stades avancés de la thèse et après avoir tenté les couplages thiol-ène avec les composés issus de la stratégie HTL, une troisième et dernière stratégie basée sur les dérivés anthraniliques a rapidement été développée. Ces composés étant UV-actifs et fluorescents, ils permettent un bon suivi des dérivés fonctionnalisés pour les chimistes et les biologistes. Dans un premier temps, nous avons tenté de synthétiser un composé ayant un thiol non-protégé afin d'effectuer des tests de la réaction thiol-ène sans étape préliminaire de déprotection du thiol. Le maltoheptaose a ainsi été couplé à un dérivé anthranilique portant une cysteamine et a été obtenu sous forme de mélange (formation de ponts disulfures) qui a ensuite été réduit par ajout de tributylphosphine et conservé dans des conditions inertes. Dans un deuxième temps, l'anhydride isotoïque a été utilisé en combinaison avec la cystamine pour synthétiser

deux dérivés anthraniliques : un symétrique et un asymétrique. Le dérivé symétrique a ensuite été couplé au maltoheptaose et au maltose par amination réductrice.

Deux des dérivés maltoheptaose thiol-fonctionnalisés (par HTL) ont été soumis à la sulfatation aléatoire pour former, après couplage thiol-ène, un mime de PG. En raison de la faible stabilité de l'HTL en conditions acides et basiques, le protocole de sulfatation développé dans le chapitre 2 a été revu : un piègeur d'acide a été introduit et un seul solvant, le DMF, a été utilisé pour la réaction. Des degrés de sulfatation globalement plus faibles ont été obtenus, probablement en raison du mélange hétérogène entre le piègeur d'acide, le solvant et l'agent sulfatant.

Après plusieurs essais de thiol-ène sur du maltose thiol-modifié non-sulfaté, il s'est avéré que le couplage n'était que peu efficace. Très tardivement dans la thèse, la stratégie a donc été changée pour un couplage amide avec un polymère portant des acides carboxyliques. Ainsi, le maltoheptaose a été fonctionnalisé par une fonction amine.

La préparation d'un linker bis-fonctionnalisé a d'abord été envisagée en faisant réagir l'anhydride isatoïque avec de l'éthylène diamine. La réaction a conduit à une panoplie de produits très similaires s'expliquant par la présence de deux carbonyles électrophiles dans l'anhydride isatoïque et de deux amines dans l'éthylène diamine. Pour pallier à ce problème, le para-nitrophenyl anthranilate, réactif commercial, a plutôt été directement introduit sur le maltoheptaose par amination réductrice, et son ester activé possédant un groupement partant (nitrophénol) a été déplacé à l'aide de l'éthylène diamine. Aucun sous-produit n'a été observé.

Chapitre 5 : Couplage des maltooligosaccharides fonctionnalisés

Le chapitre 5 traite des réactions de couplage thiol-ène et amide entre le sucre et soit la biotine, soit le polymère PHOU. La biotine a ici été utilisée pour deux raisons : une fois transformée en biotine-allyle, elle constitue un composé modèle du polymère PHOU permettant d'optimiser les conditions de la réaction de couplage pour limiter le gaspillage de PHOU ; de plus les adduits maltoheptaose-biotine, une fois sulfatés, peuvent permettre d'effectuer des analyses d'interaction par SPR en tant que mimes potentiels de GAGs (collaborateurs IBS, Grenoble). De son côté, le PHOU est un polyester bactérien biodégradable hydrophobe et possédant des chaînes pendantes d'alcènes terminaux. Ces fonctions peuvent par ailleurs être transformées en acide carboxylique par couplage thiol-ène (collaborateurs ICMPE, Thiais). Le couplage des chaînes de sucre au polymère permettrait d'obtenir des mimes potentiels de PG qui seraient biologiquement évalués.

Afin de mettre en œuvre un couplage thiol-ène radicalaire et photoinitié, la biotine-allyle a été synthétisée en deux étapes en one-pot via l'intermédiaire biotine-NHS. Ensuite, la biotine-allyle et le maltose thiol-fonctionnalisé avec du HTL (préparé au chapitre 4) ont été mis à réagir ensemble dans une réaction en deux étapes (et one-pot) : une première étape consiste à ouvrir la thiolactone par aminolyse

pour libérer la fonction thiol et une seconde étape de réaction du thiol avec la fonction alcène de la biotine. Malgré de nombreuses tentatives en faisant varier des paramètres tels que l'ajout séquentiel des réactifs, les temps de réaction, les conditions inertes, le photoinitiateur ou encore la présence d'agent réducteur, le produit n'a pas pu être isolé. Nous n'avons observé que des mélanges réactionnels incluant une majorité de produit aminolysé et son dimère soufré, ou bien encore un sous-produit qui n'a pas pu être identifié (sur la base du spectre de masse). Les réactifs ont alors été confiés à nos partenaires (ICMPE, Thiais) ayant une expertise en chimie thiol-ène. Ces derniers n'ayant pas non plus réussi la thiol-ène en « one pot – two steps », ils se sont d'abord chargés de l'aminolyse du produit à l'aide de la *n*-butylamine, puis ont ensuite procédé à la thiol-ène à proprement parlé. Ils n'ont malheureusement pu isoler aucun produit à l'issue de leurs essais.

Le couplage thiol-ène a également été tenté sur le polymère PHOU toujours en utilisant le maltose HTL-fonctionnalisé. De même, aucun produit n'a pu être isolé en one pot. D'autres problèmes sont survenus lorsque le couplage a été effectué avec le produit aminolysé isolé précédemment : le PHOU étant hydrophobe et le sucre hydrophile, il a été difficile de trouver un système de solvant permettant de solubiliser les deux. Des sortes de gel impossibles à caractériser ont été formés à l'issue des réactions. La thiol-ène dans le DMSO n'a pu être envisagée qu'avec un dérivé du PHOU, le PHOU-sulfonate (ces fonctions étant censées augmenter la solubilité du polymère dans le DMSO). Seul un petit pourcentage de sucre a pu être greffé au polymère d'après la RMN ¹H. Des essais avec d'autres réactifs tels que la glucosamine et la *N*-acétyl-HTL n'ont pas non plus abouti. La différence de solubilité, l'utilisation d'un thiol protégé, ou encore le système alcène utilisé pourraient expliquer ces échecs.

Le couplage thiol-ène a donc été mis de côté pour se focaliser sur le couplage amide. Les maltooligosaccharides ont préalablement été fonctionnalisés par une amine (chapitre 4). D'abord le maltoheptaose amine-fonctionnalisé a été mis en réaction avec de la biotine-NHS pour former très facilement et rapidement des adduits maltoheptaose-biotine, qui ont été sulfatés à deux degrés de sulfatation (moyen et haut) pour leur future évaluation biologique (tests SPR à l'IBS, Grenoble). Ensuite, les fonctions alcènes du PHOU natif furent entièrement remplacées par des fonctions acides carboxyliques et le PHOU-carboxylate ainsi formé a pu réagir avec le maltoheptaose aminé pour un couplage amide en présence de l'agent de couplage HBTU. Malheureusement, l'adduit maltoheptaose-PHOU n'a pas pu être sulfaté aléatoirement par manque de quantités et de temps.

Conclusions et perspectives

Nous avons dans un premier temps accompli la sulfatation aléatoire des (cyclo)maltooligosaccharides. Après caractérisation, les dérivés sulfatés ont été soumis à des tests biologiques, qui sont encore en cours. Globalement, les dérivés moyennement et hautement sulfatés ont semblé avoir une meilleure affinité pour les facteurs de croissance testés et ont induit des réponses biologiques plus intenses. La

taille minimale de chaîne requise pour l'interaction semblait être de six unités de sucre et la conformation semblait jouer un rôle sur les propriétés biologiques des composés.

La chimie sélective sur les β -cyclodextrines a permis de synthétiser des composés régiosélectivement sulfatés qui sont actuellement en cours d'essais biologiques. Il serait intéressant par la suite d'ouvrir les β -cyclodextrines sulfatées par acétylolyse afin d'obtenir des dérivés maltoheptaose sélectivement sulfatés qui pourraient être comparés à ceux sulfatés aléatoirement.

Dans le but de préparer des mimes de protéoglycanes, les chaînes de maltooligosaccharides ont été thiol- ou amine-fonctionnalisées par différentes méthodes. Les essais thiol-ène de ces chaînes avec le PHOU ou la biotine n'ont pas abouti, alors un couplage amide a été adopté. Les chaînes couplées à la biotine ont été sulfatées à différents degrés pour être soumises à des analyses SPR (collaboration IBS, Grenoble) tandis que les chaînes couplées au polymère PHOU sont actuellement en cours de sulfatation pour être *in fine* évaluées biologiquement en tant que mimes de protéoglycanes.

Abstract

Osteoarthritis (OA) is the most common joint disease, characterized by gradual loss of articular cartilage due to abnormal extracellular matrix (ECM) and changes in chondrocyte morphology and metabolism, associated to sub-endochondral bone remodeling and local synovitis. The burden of this disease has been gradually gaining importance in the last few decades with the aging of the population and the obesity epidemic. Beyond the huge healthcare costs for treatment of OA affecting 70 million individuals in Europe, there is no treatment that can repair the cartilage and stop the progress of OA. Existing therapies, based on hyaluronic acid and chondroitin sulfate injections, are symptomatic and pursue only pain alleviation with no effect on slowing disease progression and on restoring cartilage and chondrocytes functions. In parallel, new therapeutic strategies are currently based on stem cells, but these fragile cells are injected in an inflammatory microenvironment detrimental to their survival and clinical efficacy. Therefore, a more suitable middle is highly mandatory. Our project is born from the observation that OA is closely related to a loss of proteoglycans (PGs), one of the largest components of the ECM. These PGs are not only structural components, but regulators of cell functions also since they interact with growth factors, cytokines, proteinases, adhesion receptors and extracellular matrix components through their sulfated glycosaminoglycan (GAGs) chains. As a consequence, these polysaccharides are new important classes of molecular targets in the fields of biochemistry, pathology and pharmacology. However, due to the natural extractive source of PGs and GAGs and their inherent complexity in terms of relative molecular mass, charge density, sulfation patterns, the relationship with functions are difficult to elucidate and their therapeutic and commercial use is complicated according to their poorly defined structures. Use of well-defined biomimetic structures are therefore the valuable alternatives for therapeutic strategies. Attempts have relied on the idea that a limited number of anionic groups (e.g., sulfate, carboxylate, phosphate) on a smaller oligosaccharide scaffold may overcome the difficulties of working with GAGs or PGs. Examples of these include GAG related polysaccharides of non-mammal origin that have shown to stimulate healing of tissues with similar or higher efficiency than natural GAGs or PGs. And, very recently, glycopolymers based on oligosaccharide repeating units constituting GAG structures have been reported and revealed fascinating ability to recapitulate biological features of natural PGs. Even if only GAGs oligomers (di- up to penta-saccharides) were targeted, their syntheses still pose significant challenges. These shortcomings can be remedied by designing readily accessible GAG oligosaccharide mimetics in order to tune their 3-D structure and to fit the biological binding sites. Additionally, as for natural PGs, multi-presentation of GAG mimetics is an essential task to evaluate the significance of this parameter. Up to date, these approaches have never been investigated, especially in order to promote the articular cartilage homeostasis. Our project aims to develop PG-like biopolymers made of architecturally defined grafted polyesters having simplified sulfated GAG mimetics. These glycomimetics will be assessed for their abilities to interact with growth factors binding to natural GAGs by stimulating cell growth. Forces aligned within this consortium

combined crucial expertise in chemical modification of oligosaccharides (CERMAV, Grenoble), in the preparation of functional polyesters (ICMPE, Paris Est), and in the study of GAGs on the mesenchymal stem cells properties (Gly-CRRET, Paris Est & IBS-Grenoble).

List of figures

FIGURE 1. SCHEMATIC REPRESENTATION OF ARTICULAR CARTILAGE DEPICTING THE CHONDROCYTE SURROUNDED BY COLLAGEN, PROTEOGLYCANS AND ASSOCIATED MATRIX COMPONENTS. REPRODUCED FROM CHEN ET AL. ³	28
FIGURE 2. COMPARISON BETWEEN A HEALTHY KNEE JOINT (A) AND ONE SUFFERING FROM OSTEOARTHRITIS (B). REPRODUCED FROM ⁸	29
FIGURE 3. SCHEMATIC REPRESENTATION OF A PROTEOGLYCAN	31
FIGURE 4. STRUCTURE OF GAG-MIMICKING POLYMER BASED ON CHITOSAN. REPRODUCED FROM LIU ET AL. ⁹⁸	36
FIGURE 5. STRUCTURE OF GAG-MIMICKING POLYMER BY GLY-CRRET GROUP (CRÉTEIL, FRANCE). REPRODUCED FROM IKEDA ET AL. ¹⁰⁹	37
FIGURE 6. STRUCTURE OF GLYCOMIMETIC POLYMER BY MIURA GROUP. REPRODUCED FROM MIURA ET AL. ¹²⁷	39
FIGURE 7. STRUCTURE OF GLYCOMIMETIC POLYMER BY HSIEH-WILSON GROUP. REPRODUCED FROM LIU ET AL. ⁹⁸	40
FIGURE 8. STRUCTURE OF GLYCOMIMETIC POLYMER BY CHAIKOF GROUP. REPRODUCED FROM SUN ET AL. ¹³⁷	41
FIGURE 9. STRUCTURE OF GAG-MIMICKING POLYMER BY MAYNARD GROUP. REPRODUCED FROM MIURA ET AL. ¹²⁷	41
FIGURE 10. STRUCTURE OF GAG-MIMICKING POLYMER BY ZHAO GROUP. REPRODUCED FROM LIU ET AL. ⁹⁸	42
FIGURE 11. SIMPLIFIED STRATEGY OF THE PROJECT WITH THE DIFFERENT TASKS	44
FIGURE 12. ¹ H NMR SPECTRA SUPERPOSITION OF M ₇ AND ITS RANDOMLY SULFATED DERIVATIVES IN D ₂ O AT 298K.....	48
FIGURE 13. (A) SUPERPOSITION OF SULFATED M ₇ SEC-MALS RETENTION TIMES ; (B) SUPERPOSITION OF SULFATED ⁸ CD SEC-MALS RETENTION TIMES	49
FIGURE 14. GRAPH OF MW, PDI VALUES EXTRACTED FROM SEC-MALS ANALYSIS AND DS VALUES FROM ELEMENTAL ANALYSIS OF SULFATED (CYCLO)MALTOOLIGOSACCHARIDES	50
FIGURE 15. FT-IT SPECTRA SUPERPOSITION OF M ₇ AND ITS SULFATED DERIVATIVES	52
FIGURE 16. PRINCIPLE OF COMPETITIVE ELISA TEST	53
FIGURE 17. PRINCIPLE OF MITOGENIC ASSAY ON BAF32 OR HUVEC CELLS.....	54
FIGURE 18. GRAPHIC PRESENTING THE RELATIVE AFFINITY OF SULFATED (CYCLO)MALTOOLIGOSACCHARIDES FOR FGF-2. THE IC ₅₀ VALUE OF HEPARIN MIMETIC WAS USED AS REFERENCE OF 100% OF BINDING AFFINITY, TO CALCULATE THE % OF BINDING AFFINITY OF ALL OTHER TESTED MOLECULES FOR FGF-2.	55
FIGURE 19. PROLIFERATION TESTS OF SULFATED (CYCLO)MALTOOLIGOSACCHARIDES ON BAF32 CELLS IN SYNERGY WITH FGF-2. EFFECT OF INCREASING DOSES (FROM 10 ⁻² TO 10 ² µG/ML) OF (CYCLO)MALTOOLIGOSACCHARIDES WITH FGF-2 WERE TESTED AND COMPARED AS FOLD CHANGE OF PROLIFERATION RATE OF THE CELLS ALONE. INDEPENDENT EXPERIMENTS WERE PERFORMED WITH AT LEAST DUPLICATE WELLS PER CONDITION, AND GRAPHS REPRESENT THE VALUES OBTAINED BY CONDITIONS, MEANS AND STANDARD DEVIATIONS. P VALUES WERE CALCULATED USING AN ORDINARY KRUSKAL WALLIS TEST FOLLOWED BY PAIRWISE COMPARISONS USING THE DUNNETT TEST COMPARED TO CT CONDITIONS WITH FGF-2 ALONE (NS NO SIGNIFICANCE; * <0.05; ** <0.01; *** <0.001; **** <0.0001).	56
FIGURE 20. GRAPHIC PRESENTING THE RELATIVE AFFINITY OF SULFATED (CYCLO)MALTOOLIGOSACCHARIDES FOR VEGF. THE IC ₅₀ VALUE OF HEPARIN MIMETIC WAS USED AS REFERENCE OF 100% OF BINDING AFFINITY, TO CALCULATE THE % OF BINDING AFFINITY OF ALL OTHER TESTED MOLECULES FOR VEGF.	57
FIGURE 21. PROLIFERATION TESTS OF SULFATED (CYCLO)MALTOOLIGOSACCHARIDES ON HUVEC CELLS IN SYNERGY WITH VEGF. EFFECT OF INCREASING DOSES (FROM 10 ⁻² TO 10 ² µG/ML) OF (CYCLO)MALTOOLIGOSACCHARIDES WITH VEGF WERE TESTED AND COMPARED AS FOLD CHANGE OF PROLIFERATION RATE OF THE CELLS ALONE. INDEPENDENT EXPERIMENTS WERE PERFORMED WITH AT LEAST DUPLICATE WELLS PER CONDITION, AND GRAPHS REPRESENT THE VALUES OBTAINED BY CONDITIONS, MEANS AND STANDARD DEVIATIONS. P VALUES WERE CALCULATED USING AN ORDINARY KRUSKAL WALLIS TEST FOLLOWED BY PAIRWISE COMPARISONS USING THE DUNNETT TEST COMPARED TO CT CONDITIONS WITH VEGF ALONE (NS NO SIGNIFICANCE; * <0.05; ** <0.01; *** <0.001; **** <0.0001).	58
FIGURE 22. STRUCTURES OF SULFATED (CYCLO)MALTOOLIGOSACCHARIDES	61
FIGURE 23. STRUCTURE OF B-CYCLODEXTRIN (CYCLOMALTOHEPTAOSE).....	63
FIGURE 24. SCOPE OF REGIOSELECTIVELY MODIFIED B-CYCLODEXTRIN SULFATES BY BAUMANN & RYS ¹⁹⁷	68
FIGURE 25. ¹ H NMR SPECTRUM OF COMPOUND 7 IN CDCl ₃ WITH ITS PEAK INTEGRATION AND ATTRIBUTION	71
FIGURE 26. ¹ H NMR OF COMPOUND 13 IN D ₂ O WITH ITS PEAK INTEGRATION AND ATTRIBUTION	74

FIGURE 27. SEC-MALS RETENTION TIME OF <i>PER-2,3S</i> -B-CYCLODEXTRIN 17	76
FIGURE 28. ¹ H NMR OF COMPOUND 29 IN D ₂ O WITH ITS PEAK INTEGRATION AND ATTRIBUTION	79
FIGURE 29. ¹ H NMR OF COMPOUND 31 IN D ₂ O WITH ITS PEAK INTEGRATION AND ATTRIBUTION	80
FIGURE 30. STRUCTURE AND NAME OF REGIOSELECTIVELY SULFATED B-CYCLODEXTRINS PREPARED	81
FIGURE 31. RELATIVE AFFINITY OF SELECTIVELY SULFATED B-CYCLODEXTRINS WITH FGF-2 (A) AND VEGF (B).....	82
FIGURE 32. STRUCTURE OF PREPARED (<i>TOP</i>) AND UNACHIEVED (<i>BOTTOM</i>) REGIOSELECTIVELY SULFATED B-CYCLODEXTRINS	83
FIGURE 33. END-FUNCTIONALIZATION OF GLYCANS BY TWO METHODS	85
FIGURE 34. STRUCTURES OF CYSTAMINE 34 AND CYSTEAMINE 35	97
FIGURE 35. STRUCTURE OF MONO-, DI-, OR TRI-FUNCTIONALIZED STRUCTURES PREPARED BY REDUCTIVE AMINATION BY VLIST ET AL.	97
FIGURE 36. (A) PRODUCTS OBTAINED FROM THE REDUCTIVE AMINATION OF MALTOHEPTAOSE WITH CYSTEAMINE ; (B) MASS SPECTRUM FROM REDUCTIVE AMINATION OF MALTOHEPTAOSE WITH CYSTEAMINE	99
FIGURE 37. STRUCTURE OF HOMOCYSTEINE THIOLACTONE HYDROCHLORIDE (HTL)	102
FIGURE 38. (A) ¹ H NMR SPECTRA SUPERPOSITION OF COMPOUND 47 WITH NATIVE MALTOHEPTAOSE AND HTL IN D ₂ O ; (B) MASS SPECTRUM OF COMPOUND 47	105
FIGURE 39. MASS SPECTRUM OF THE MIXTURE OBTAINED AFTER REDUCTIVE AMINATION OF MALTOSE WITH HTL ON A 1-GRAM SCALE USING 10 EQUIVALENTS OF HTL AND 30 EQUIVALENTS OF NABH ₃ CN.....	106
FIGURE 40. STRUCTURES OF THE SIDE PRODUCTS FORMED DURING REDUCTIVE AMINATION OF MALTOSE WITH HOMOCYSTEINE THIOLACTONE HYDROCHLORIDE	107
FIGURE 41. MASS SPECTRUM OF THE PRODUCT OBTAINED AFTER REDUCTIVE AMINATION OF MALTOSE WITH HTL ON A 4-GRAM SCALE WITH 2 EQUIVALENTS OF HTL AND 8 EQUIVALENTS OF NABH ₃ CN	108
FIGURE 42. STRUCTURE OF BARBITURIC ACID AND ITS POSSIBLE DERIVATIVES	108
FIGURE 43. EXAMPLES OF C-GLYCOSYLBARBITURATES PREPARED BY KNOEVENAGEL CONDENSATION	109
FIGURE 44. RETROSYNTHESIS OF SYMMETRICAL BARBITURIC ACID BEARING TWO HTL MOIETIES	110
FIGURE 45. ¹ H NMR SPECTRUM OF UNSYMMETRICAL BARBITURIC DERIVATIVE 53 IN CDCl ₃ WITH ITS PEAK INTEGRATION AND ATTRIBUTION (AT 318 K)	111
FIGURE 46. ¹ H NMR SPECTRA SUPERPOSITION OF COMPOUND 54 (BLACK, IN D ₂ O) WITH NATIVE MALTOHEPTAOSE (BLUE, IN D ₂ O) AND COMPOUND 53 (GREEN, IN CDCl ₃).....	113
FIGURE 47. STRUCTURE OF ANTHRANILIC ACID, METHYL ANTHRANILATE AND ISATOIC ANHYDRIDE (<i>FROM THE LEFT TO THE RIGHT</i>) .	114
FIGURE 48. ¹ H NMR SPECTRA SUPERPOSITION OF COMPOUND 58 BEFORE (BLUE) AND AFTER (GREEN) COLUMN PURIFICATION IN DMSO-D ₆ AND ITS PEAK ATTRIBUTION	117
FIGURE 49. PRODUCT OBTAINED AFTER REDUCTIVE AMINATION OF MALTOHEPTAOSE WITH CYSTAMINE-BEARING ANTHRANILIC DERIVATIVE 58	118
FIGURE 50. STRUCTURE OF TWO THIOL-END-FUNCTIONALIZED MALTOHEPTAOSE 47 AND 54 , CHOSEN TO BE RANDOMLY SULFATED	119
FIGURE 51. ¹ H NMR SPECTRA SUPERPOSITION OF AN ATTEMPT OF LIGHTLY SULFATED M ₇ -BHTL IN CONDITIONS PREVIOUSLY DESCRIBED (BLACK) WITH A SUCCESSFULLY PREPARED LIGHTLY SULFATED M ₇ -BHTL (BLUE) AND LIGHTLY SULFATED MALTOHEPTAOSE (GREEN) IN D ₂ O	120
FIGURE 52. ¹ H NMR SPECTRA SUPERPOSITION OF LIGHTLY (BLACK), MODERATELY (BLUE) AND HIGHLY (GREEN) SULFATED M ₇ -BHTL IN D ₂ O	122
FIGURE 53. ¹ H NMR SPECTRA SUPERPOSITION OF LIGHTLY (BLACK), MODERATELY (BLUE) AND HIGHLY (GREEN) SULFATED M ₇ -RHTL IN D ₂ O	123
FIGURE 54. PRODUCTS OBTAINED FROM THE ANTHRANOYLATION OF ISATOIC ANHYDRIDE WITH ETHYLENEDIAMINE.....	126
FIGURE 55. ¹ H NMR SPECTRA SUPERPOSITION OF COMPOUND 74 (BLACK, IN D ₂ O) WITH NATIVE MALTOHEPTAOSE (BLUE, IN D ₂ O) AND PNPA (GREEN, IN CDCl ₃).....	128
FIGURE 56. ¹ H NMR SPECTRA SUPERPOSITION OF COMPOUND 75 WITH ITS PRECURSOR COMPOUND 74 (BLUE) IN D ₂ O	129
FIGURE 57. SCOPE OF THIOLATED AND AMINATED MALTOOLIGOSACCHARIDES THAT WERE SUCCESSFULLY SYNTHESIZED	130
FIGURE 58. THIOL-ENE COUPLING OF THIOL-FUNCTIONALIZED CELLULOSE NANOFIBERS WITH THE POLYMER POLY(VBC-R-VBDMH-R-AMA).....	137
FIGURE 59. STRUCTURE AND NAME OF THIOL-FUNCTIONALIZED MALTOOLIGOSACCHARIDES USED AS MODEL COMPOUNDS FOR THIOL-ENE COUPLING TRIALS.....	138
FIGURE 60. ¹ H NMR SPECTRUM WITH OF COMPOUND 79 ITS PEAK ATTRIBUTION IN DMSO-D ₆	139

FIGURE 61. MASS SPECTRUM OF A THIOL-ENE REACTION TRIAL BETWEEN M ₂ -RHTL 48 AND BIOTIN-ALLYL 79	141
FIGURE 62. MASS SPECTRUM OF THE THIOL-ENE CRUDE AFTER REACTION BETWEEN M ₂ -RHTL 48 AND BIOTIN-ALLYL 79 IN THE PRESENCE OF DMPA PHOTOINITIATOR	142
FIGURE 63. ¹ H NMR SPECTRA SUPERPOSITION OF COMPOUND 83 (AFTER AMINOLYSIS, BLACK) AND 48 (BEFORE AMINOLYSIS, BLUE) IN D ₂ O	143
FIGURE 64. STRUCTURE OF THE VARIANTS OF SUGAR AND N-ACETYL HTL TESTED FOR THIOL-ENE COUPLING BY ICMPE COLLABORATORS	146
FIGURE 65. IMMOBILIZATION OF AMINE-TERMINATED GLYCANS ON NHS-COATED GLASS SLIDES	150
FIGURE 66. STRUCTURE OF M ₇ -RANH ₂ (75).....	150
FIGURE 67. ¹ H NMR SPECTRA SUPERPOSITION OF COMPOUND 90 (BLACK, IN D ₂ O) WITH THE STARTING COMPOUNDS 75 (BLUE, IN D ₂ O) AND 78 (GREEN, IN DMSO-D ₆)	151
FIGURE 68. ¹ H NMR SPECTRA SUPERPOSITION OF PRODUCT 91 (BLACK) AND PHOU-CARBOXYLATE 89 (BLUE)	153
FIGURE 69. SCOPE OF SUCCESSFULLY GRAFTED MALTOOLIGOSACCHARIDES BY AMIDE COUPLING.....	154

List of tables

TABLE 1. CHEMICAL STRUCTURE AND REPRESENTATION BY SNFG (SYMBOL NOMENCLATURE FOR GLYCANS) SYMBOLS ⁴⁷ OF THE DISACCHARIDE BUILDING BLOCK OF FIVE FAMILIES OF GLYCOSAMINOGLYCANS	32
TABLE 2. POTENTIAL ADVANTAGES AND DRAWBACKS OF OLIGOSACCHARIDES.....	37
TABLE 3. MW, MN AND PDI OF SULFATED M ₇ AND ^B CD DERIVATIVES. *COMMERCIALY AVAILABLE	50
TABLE 4. DEGREE OF SULFATION PER SACCHARIDIC UNIT OF THE SULFATED (CYCLO)MALTOOLIGOSACCHARIDES (CALCULATED BY ELEMENTAL ANALYSIS).	51
TABLE 5. MEAN IC ₅₀ VALUES WITH STANDARD DEVIATION FOR SULFATED (CYCLO)MALTOOLIGOSACCHARIDES WITH FGF-2.....	55
TABLE 6. MEAN IC ₅₀ VALUES OF SULFATED (CYCLO)MALTOOLIGOSACCHARIDES AND THEIR STANDARD DEVIATIONS WITH VEGF. MEASURES WERE CONDUCTED IN TRIPPLICATES (N=3) FOR COMPOUNDS EXCEPT FOR M ₇ M, M ₇ H & ^B CDM WHERE N=6.....	57
TABLE 7. SELECTIVE FUNCTIONALIZATION OF PRIMARY HYDROXYLS OF CYCLODEXTRINS	64
TABLE 8. SELECTIVE <i>PER-6-O-TERT</i> -BUTYLDIMETHYLSILYLATION OF NATIVE B-CYCLODEXTRIN	70
TABLE 9. DEGREE OF SULFATION PER SACCHARIDIC UNIT OF <i>PER-2,3S</i> -B-CYCLODEXTRIN 17 (CALCULATED BY ELEMENTAL ANALYSIS). 76	76
TABLE 10. IC ₅₀ VALUES OF RANDOMLY AND SELECTIVELY SULFATED B-CYCLODEXTRINS WITH FGF-2 AND VEGF	81
TABLE 13. SYNTHESIS OF GLYCOSYL THIOLS FROM UNPROTECTED MONOSACCHARIDES WITH LAWESSON REAGENT	87
TABLE 14. SYNTHESIS OF ARYL 1-THIOGLYCOSIDES FROM UNPROTECTED MONOSACCHARIDES WITH DMC REAGENT	88
TABLE 15. PREPARATION OF AMINE-TERMINATED RHAMNOSE BY MECHANOSYNTHESIS	94
TABLE 16. DEGREE OF SULFATION PER SACCHARIDIC UNIT OF THE SULFATED M ₇ -BHTL DERIVATIVES (CALCULATED BY ELEMENTAL ANALYSIS).	122
TABLE 17. DEGREE OF SULFATION PER SACCHARIDIC UNIT OF THE SULFATED M ₇ -RHTL DERIVATIVES (CALCULATED BY ELEMENTAL ANALYSIS).	124
TABLE 22. SCOPE OF GLYCOPEPTIDES PREPARED BY ZHENG ET AL. BY REDUCTIVE GLYCOSYLATION OF NATIVE CARBOYDRATES WITH AZIDES. ^A B:A RATIO >15:1	148
TABLE 23. SEC-MALS ANALYSIS OF SULFATED M ₇	161
TABLE 24. ELEMENTAL ANALYSIS OF SULFATED M ₇	161
TABLE 25. ELEMENTAL ANALYSIS OF SULFATED M ₆	162
TABLE 26. SEC-MALS OF SULFATED ^B CD. *COMMERCIALY AVAILABLE.....	163
TABLE 27. ELEMENTAL ANALYSIS OF SULFATED ^B CD. *COMMERCIALY AVAILABLE	163
TABLE 11. ELEMENTAL ANALYSIS OF <i>PER-2,3S</i> -B-CYCLODEXTRIN 17'	171
TABLE 12. SEC-MALS OF <i>PER-2,3S</i> -B-CYCLODEXTRIN 17'	171
TABLE 18. SEC-MALS OF SULFATED M ₇ -BHTL. (MW, MN AND IP MEASURED ON TRIPPLICATES, HERE THE MEAN VALUE MOY IS GIVEN. STANDARD DEVIATION “±” CALCULATED WITH THE TRIPPLICATE MEASURED VALUES)	183
TABLE 19. ELEMENTAL ANALYSIS OF SULFATED M ₇ -BHTL.....	183

TABLE 20. SEC-MALS OF SULFATED M ₇ -RHTL. (MW, MN AND IP MEASURED ON TRIPPLICATES, HERE THE MEAN VALUE MOY IS GIVEN. STANDARD DEVIATION “±” CALCULATED WITH THE TRIPPLICATE MEASURED VALUES)	184
TABLE 21. ELEMENTAL ANALYSIS OF SULFATED M ₇ -RHTL	184

List of schemes

SCHEME 1. SYNTHESIS OF RANDOMLY SULFATED (CYCLO)MALTOOLIGOSACCHARIDES	47
SCHEME 2. SELECTIVE FUNCTIONALIZATION OF SECONDARY HYDROXYLS OH-2 OF B-CYCLODEXTRIN	65
SCHEME 3. SELECTIVE METHYLATION OF SECONDARY HYDROXYLS OH-2 OF SILYLATED B-CYCLODEXTRIN	65
SCHEME 4. PREPARATION OF <i>PER-6-O</i> -SULFO B-CYCLODEXTRIN BY VINCENT ET AL. ¹⁸⁸	66
SCHEME 5. PREPARATION OF <i>PER-6-O</i> -SULFO-2,3- <i>O</i> -ACYL B-CYCLODEXTRIN BY PARROT-LOPEZ AND COL. ¹⁹²	67
SCHEME 6. PREPARATION OF <i>PER-2-O</i> -SULFO B-CYCLODEXTRIN BY VIGH GROUP ¹⁹³	67
SCHEME 7. PREPARATION OF <i>PER-3,6-O</i> -SULFO-3- <i>O</i> -METHYL B-CYCLODEXTRIN BY VIGH GROUP ¹⁹⁴	68
SCHEME 8. <i>PER</i> -BENZYLATION OF B-CYCLODEXTRIN AND SUBSEQUENT <i>PER-6-O</i> -ACETYLATION	69
SCHEME 9. SELECTIVE <i>PER-6-O</i> -ACETYLATION OF NATIVE B-CYCLODEXTRIN	69
SCHEME 10. SYNTHESIS STRATEGY EMPLOYED FOR SELECTIVELY SULFATED DERIVATIVES (6S; 2S; 2,3S; 2,6S; 3,6S) STARTING FROM B-CYCLODEXTRIN (ALSO SEE APPENDIX)	71
SCHEME 11. PREPARATION OF <i>PER-6S</i> -B-CYCLODEXTRIN STARTING FROM B-CYCLODEXTRIN VIA ACETATE PROTECTION	72
SCHEME 12. PREPARATION OF <i>PER-6S</i> -B-CYCLODEXTRIN STARTING FROM B-CYCLODEXTRIN	72
SCHEME 13. PREPARATION OF <i>PER-2,3S</i> -B-CYCLODEXTRIN 17 VIA SILYLATION OF 7	74
SCHEME 14. PREPARATION OF <i>PER-2,3S</i> -B-CYCLODEXTRIN 17 VIA BENZYLATION OF 9	75
SCHEME 15. PREPARATION OF <i>PER-2,3S</i> -B-CYCLODEXTRIN VIA ACETYLATION OF 12	75
SCHEME 16. PREPARATION OF <i>PER-2,6S</i> -B-CYCLODEXTRIN 24 VIA SILYLATION OF 7 OR NATIVE B-CYCLODEXTRIN	77
SCHEME 17. SYNTHESIS STRATEGY FOR THE PREPARATION OF <i>PER-2,6S</i> -B-CYCLODEXTRIN 24	77
SCHEME 19. SYNTHESIS STRATEGY FOR THE PREPARATION OF <i>PER-2S</i> -B-CYCLODEXTRIN 29	78
SCHEME 20. SYNTHESIS STRATEGY FOR THE PREPARATION OF <i>PER-3,6S</i> -B-CYCLODEXTRIN 31	79
SCHEME 21. SYNTHESIS STRATEGY FOR THE SYNTHESIS OF <i>PER-3S</i> -B-CYCLODEXTRIN 33	81
SCHEME 22. PREPARATION OF TWO NEOGLYCOCONJUGATES STARTING FROM LACTO- <i>N</i> -TETRAOSE BY TWO MEANS: OPEN-RING METHOD (TOP) AND CLOSED-RING METHOD (BOTTOM)	89
SCHEME 23. PREPARATION OF THIOL-END FUNCTIONALIZED DEXTRAN AND ITS MODIFICATION FOR FURTHER SELF-ASSEMBLY INTO GLYCONANOPARTICLES	90
SCHEME 24. OBTENTION OF THIOL-END-FUNCTIONALIZED OLIGOSACCHARIDES BY KOCHETKOV AMINATION WITH CYSTAMINE	90
SCHEME 25. THIOL-FUNCTIONALIZATION OF GLYCAN VIA HYDRAZIDE LINKER BY ZHI ET AL.	91
SCHEME 26. GENERAL METHOD FOR THE COUPLING OF TYPE (A) AND TYPE (B) OXYAMINE LINKERS ON CARBOHYDRATES	91
SCHEME 27. COUPLING OF PIA OLIGOSACCHARIDE WITH <i>N</i> -ALKYLOXYAMINE BEARING A FREE THIOL	92
SCHEME 28. PREPARATION OF MALTOHEPTAOSE GLYCOSYLAMINE BY MICROWAVE-ASSISTED KOCHETKOV AMINATION	93
SCHEME 29. ONE-STEP PREPARATION OF GLYCOSYLHYDRAZIDES STARTING FROM MONO-, DI- AND TETRA-SACCHARIDES	95
SCHEME 30. PREPARATION OF GLYCOSYLAMINE BY REDUCTION OF AZIDE-END FUNCTIONALIZED GLUCOSE	95
SCHEME 31. PREPARATION OF NEOMYCIN B RELATED AMINOGLYCOSIDE BY USING AZIDO-PROTECTING GROUP	96
SCHEME 32. REDUCTIVE AMINATION OF MALTOSE WITH CYSTEAMINE	98
SCHEME 33. REDUCTIVE AMINATION OF MALTOHEPTAOSE WITH CYSTEAMINE	98
SCHEME 34. THIOL-DISULFIDE EXCHANGE OF CYSTEAMINE WITH 2,2'-DIPYRIDYLDISULFIDE	100
SCHEME 35. KOCHETKOV AMINATION OF MALTOSE WITH CYSTAMINE	101
SCHEME 36. STRUCTURES OF THE TWO PRODUCTS POSSIBLE AFTER REDUCTIVE AMINATION OF MALTOSE WITH CYSTEAMINE	101
SCHEME 37. OBTENTION OF A SYMMETRICAL PRODUCT BY REDUCTIVE AMINATION OF MALTOSE WITH CYSTAMINE	102
SCHEME 38. OBTENTION OF AN UNSYMMETRICAL PRODUCT BY REDUCTIVE AMINATION OF MALTOSE WITH CYSTAMINE	102
SCHEME 39. PREPARATION OF A POLYMER BEARING PENDANT HOMOCYSTEINE THIOACTONE MOIETIES, THAT UNDERGOES AMINOLYSIS FOR FURTHER THIOL-X COUPLING	103
SCHEME 40. REDUCTIVE AMINATION OF MALTOHEPTAOSE WITH HOMOCYSTEINE THIOACTONE HYDROCHLORIDE	104

SCHEME 41. REDUCTIVE AMINATION OF MALTOSE WITH HOMOCYSTEINE THIOACTONE HYDROCHLORIDE	106
SCHEME 42. OBTENTION OF SYMMETRICAL AND UNSYMMETRICAL BARBITURIC ACID DERIVATIVES STARTING FROM <i>S,S</i> -DIMETHYL CARBONODITHIOATE OR AN ISOCYANATE	109
SCHEME 43. SYNTHESIS OF A SYMMETRICAL UREA BEARING TWO HTL MOIETIES VIA AN ISOCYANATE	110
SCHEME 44. SYNTHESIS OF AN UNSYMMETRICAL UREA 52 BEARING ONE HTL MOIETY VIA AN ISOCYANATE.....	111
SCHEME 45. KNOEVENAGEL CONDENSATION OF THE HTL-BEARING BARBITURIC ACID WITH MALTOHEPTAOSE	112
SCHEME 46. ANTHRANOYLATION OF ISATOIC ANHYDRIDE WITH AMMONIUM HYDROXIDE.....	114
SCHEME 47. SIDE-PRODUCT FORMATION DURING ANTHRANOYLATION OF ISATOIC ANHYDRIDE WITH AMMONIUM HYDROXIDE	114
SCHEME 48. SYNTHESIS AND GRAFTING OF ANTHRANILIC DERIVATIVE ON THE REDUCING END OF CARBOHYDRATES.....	115
SCHEME 49. PREPARATION OF THIOL-FUNCTIONALIZED MALTOHEPTAOSE 57 BY REDUCTIVE AMINATION WITH CYSTEAMINE-BEARING ANTHRANILIC DERIVATIVE 56	116
SCHEME 50. OBTENTION OF THIOL-FUNCTIONALIZED MALTOHEPTAOSE WITH CYSTAMINE-BEARING ANTHRANILIC DERIVATIVE.....	116
SCHEME 51. REDUCTIVE AMINATION OF MALTOHEPTAOSE WITH SYMMETRICAL CYSTAMINE-BEARING ANTHRANILIC INTERMEDIATE 58	118
SCHEME 52. REDUCTIVE AMINATION OF MALTOSE WITH SYMMETRICAL CYSTAMINE-BEARING ANTHRANILIC INTERMEDIATE 58	118
SCHEME 53. GENERAL SCHEME OF THE RANDOM SULFATION PERFORMED ON M ₇ -BHTL (54)	119
SCHEME 54. RANDOM SULFATION OF M ₇ -RHTL (47)	123
SCHEME 55. PREPARATION OF AMINE-END FUNCTIONALIZED CARBOHYDRATES VIA THE SYNTHESIS OF AN ANTHRANILAMIDE BY CUMMING AND COL	125
SCHEME 56. PREPARATION OF AMINE-END FUNCTIONALIZED CARBOHYDRATES VIA THE SYNTHESIS OF A GLYCOL-CONJUGATE	125
SCHEME 57. PREPARATION OF AN ETHYLENEDIAMINE-BEARING ANTHRANILAMIDE STARTING FROM ISATOIC ANHYDRIDE	126
SCHEME 58. REDUCTIVE AMINATION OF MALTOSE WITH <i>PARA</i> -NITROPHENYL ANTHRANILATE	127
SCHEME 59. REDUCTIVE AMINATION OF MALTOHEPTAOSE WITH <i>PARA</i> -NITROPHENYL ANTHRANILATE.....	128
SCHEME 60. PREPARATION OF AMINE-END FUNCTIONALIZED MALTOHEPTAOSE WITH ETHYLENEDIAMINE	129
SCHEME 61. GENERAL STRATEGIES FOR PREPARING GLYCAN-AGLYCON CONJUGATES	134
SCHEME 62. GLYCOCONJUGATION OF VIRUS-LIKE QB-HAG16 WITH B-1-THIOGLUCOSYL BY RADICAL THIOL-ENE COUPLING	136
SCHEME 63. SYNTHESIS OF BIOTIN-ALLYL 79 VIA BIOTIN-NHS 78	138
SCHEME 64. SYNTHESIS OF BIOTIN-MALEIMIDE 80 VIA BIOTIN-NHS 78	139
SCHEME 65. RADICAL AMINE-THIOL-ENE REACTION OF M ₂ -RHTL 48 AND BIOTIN-ALLYL 79	140
SCHEME 66. AMINOLYSIS OF MALTOSE-RHTL (48) WITH <i>N</i> -BUTYLAMINE	142
SCHEME 67. RADICAL AMINE-THIOL-ENE REACTION OF M ₂ -RHTL-SH 83 AND BIOTIN-ALLYL 79	143
SCHEME 68. RADICAL THIOL-ENE REACTION OF M ₇ -RASH 57 AND BIOTIN-ALLYL 79	144
SCHEME 69. "ONE-POT" PHOTO-INITIATED THIOL-ENE COUPLING OF MALTOSE-RHTL (48) WITH PHOU (76).....	144
SCHEME 70. PHOTO-INITIATED THIOL-ENE COUPLING OF MALTOSE-RHTL-SH (83) WITH PHOU (76).....	145
SCHEME 71. PHOTO-INITIATED THIOL-ENE COUPLING OF MALTOSE-RHTL-SH (83) WITH PHOU-SULFONATE (87)	146
SCHEME 72. PROPOSED MECHANISM FOR THE RITTER REACTION OF UNPROTECTED CARBOHYDRATE WITH A NITRILE	147
SCHEME 73. PREPARATION OF AMIDE-LINKED GLYCOCONJUGATE BY THIOACID-AZIDE LIGATION.....	148
SCHEME 74. SYNTHESIS OF <i>N</i> -GLYCOSYL AMINO ACIDS BY TRACELESS STAUDINGER LIGATION WITH FLUORINATED PHOSPHANES	149
SCHEME 75. PREPARATION OF GLYCOCONJUGATE ADDUCTS BY α -KETOACID/HYDROXYLAMINE LIGATION WITH KDO ANTIGEN POLYSACCHARIDE WITH POLYSTYRENE BEADS.....	149
SCHEME 76. AMIDE COUPLING OF M ₇ -RANH ₂ 75 WITH BIOTIN-NHS 78	150
SCHEME 77. RANDOM SULFATION OF M ₇ -RANH-CO-BIOTIN 90	151
SCHEME 78. AMIDE COUPLING OF M ₇ -RANH ₂ 43 WITH PHOU-CARBOXYLATE 56	152
SCHEME 79. RANDOM SULFATION OF M ₇ -RANH-CO-BIOTIN 91	154

Abbreviations

2M2B	2-methyl-2-butene
ACN	Acetonitrile
AcOH	Acetic acid
AT III	Anti-Thrombin III
^B CD	β-cyclodextrin
Boc	<i>tert</i> -butyloxycarbonyl
BSA	Bovine Serum Albumin
CAN	Ceric ammonium nitrate
Cat.	Catalytic
Cbz	carboxybenzyl
CERMAV	CEntre de Recherches sur les MAcromolécules Végétales
cHexane	Cyclohexane
COSY	COrrrelation SpectroscopY
CuAAC	copper-catalyzed azide-alkyne cycloaddition
DBU	1,8-DiazaBicyclo[5.4.0]Undéc-7-ène
DCC	<i>N,N'</i> -dicyclohexylcarbodiimide
DCM	Dichloromethane
DIPEA	<i>N,N</i> -Diisopropylethylamine
DMAc	Dimethylacetamide
DMAP	4-dimethylaminopyridine
DMC	2-chloro-dimethylimidazolium
DMF	<i>N,N'</i> -dimethylformamide
DMPA	2,2-Dimethoxy-2-phenylacetophenone
DMPU	<i>N,N'</i> -Dimethylpropyleneurea
DMSO	Dimethyl sulfoxide
DP	Degree of polymerization
DS	Degree of sulfation
DTT	dithiothréitol
ECM	Extra-cellular matrix
ELISA	Enzyme Linked ImmunoSorbent Assay
EP	Petroleum ether
Eq.	Equivalent
ESI	Electrospray Ionization
FGF	Fibroblast Growth Factor
FGF-R	Fibroblast Growth Factor Receptor
FT-IR	Fourier Transform – Infrared
GAG	Glycosaminoglycan
Gly-CRRET	Croissance cellulaire, Réparation, et Régénération Tissulaire
GPC	Gel Permeation Chromatography
HBP	Heparin Binding Protein
HBTU	<i>O</i> -(Benzotriazol-1-yl)- <i>N,N,N',N'</i> -tetramethyluronium hexafluorophosphate
Hex	Hexane
HMBC	Heteronuclear Multiple Bond Correlation
HRMS	High Resolution Mass Spectrometry
HS	Heparan Sulfate
HSPG	Heparan Sulfate proteoglycan
HSQC	Heteronuclear Single Quantum Coherence

HTL	Homocysteine ThioLactone
IBS	Institut de Biologie Structurale
ICMPE	Institut de Chimie et des Matériaux Paris Est
KDO	2-Keto-3-Deoxyoctonate
L-Hag	L-homoallylglycine
M ₆	Maltohexaose
M ₇	Maltoheptaose
MALDI	Matrix Assisted Laser Desorption Ionisation
M _n	Molecular mass in number
MUSH	4-methyl-7-sulfanylumbelliferone
M _w	Molecular mass in weight
MW	Microwave
NC	No Competition
NHS	<i>N</i> -hydroxysuccinimide
NMR	Nuclear Magnetic Resonance
OA	Osteoarthritis
PB	Phosphate Buffer
Pd/C	Palladium on Carbon
PDI	Polydispersity Index
PG	Proteoglycan
PHOU	Poly(3-hydroxyoctanoate-co-3-hydroxyundecenoate)
PIA	polysaccharide intercellular adhesin
PNPA	<i>para</i> -nitrophenyl anthranilate
Ppm	Parts per million
Pyr	Pyridine
Quant.	Quantitative yield
RANTES	Regulated upon Activation, Normal T cell Expressed and Secreted
RI	Refractive Index
SEC	Size exclusion chromatography
SEC-MALS	combination of Size Exclusion Chromatography with Multi-Angle Light Scattering
TBAF	Tetrabutylammonium fluoride
TBAI	Tetrabutylammonium iodide
TBDMS	<i>Tert</i> -butyldimethylsilyl
TBTU	<i>O</i> -(Benzotriazol-1-yl)- <i>N,N,N',N'</i> -tetramethyluronium tetrafluoroborate
TCEP	tris(2-carboxyethyl)phosphine
TFA	Trifluoroacetic acid
TGF	Transforming Growth Factor
THF	Tetrahydrofuran
TLC	Thin Layer Chromatography
TMS	trimethylsilyl
TMSOTf	Trimethylsilyl trifluoromethanesulfonate
Tol	Toluene
Tr	Trityl
Ts	Tosyl
UV	UltraViolet
VEGF	Vascular Endothelial Growth Factor
Wt	Weight

CONTENT

REMERCIEMENTS	4
RESUME EN FRANÇAIS.....	6
ABSTRACT	15
LIST OF FIGURES.....	17
LIST OF TABLES	19
LIST OF SCHEMES	20
ABBREVIATIONS.....	22
CHAPTER 1 GENERAL INTRODUCTION	27
1.1 OSTEOARTHRITIS	28
1.2 GLYCOSAMINOGLYCANS AND PROTEOGLYCANS	30
1.2.1 <i>Proteoglycans</i>	30
1.2.2 <i>Structure of glycosaminoglycans</i>	31
1.2.3 <i>Glycosaminoglycans and proteoglycans activities</i>	33
1.2.4 <i>Use of glycosaminoglycans and proteoglycans for therapeutic purposes</i>	34
1.3 GLYCOSAMINOGLYCAN- AND PROTEOGLYCAN-RELATED GLYCOMIMETICS	35
1.3.1 <i>Based on polysaccharides and oligosaccharides</i>	35
1.3.2 <i>Based on glycopolymers</i>	39
1.3.3 <i>Based on non-carbohydrate synthetic polymers</i>	41
1.4 OVERVIEW OF THE PROJECT	43
CHAPTER 2 OBTENTION OF RANDOMLY SULFATED GLYCOMIMETICS STARTING FROM (CYCLO)MALTOOLIGOSACCHARIDES	45
2.1 INTRODUCTION	46
2.2 RESULTS AND DISCUSSION	46
2.2.1 <i>Synthesis and characterization of randomly sulfated (cyclo)maltooligosaccharides</i>	46
2.2.2 <i>Biological assays on randomly sulfated maltooligosaccharides</i>	52
2.2.2.1 Principle of biological assays	52
2.2.2.1.1 Competitive ELISA test.....	52
2.2.2.1.2 Mitogenic assay on BAF32 or HUVEC cells.....	53
2.2.2.2 Biological assays with FGF-2	54
2.2.2.3 Biological assays with VEGF	57
2.2.2.4 Interpretation of the results obtained with FGF-2 and VEGF	59
2.3 CONCLUSION	61
CHAPTER 3 OBTENTION OF REGIOSELECTIVELY SULFATED GLYCOMIMETICS STARTING FROM B- CYCLODEXTRIN 62	
3.1 INTRODUCTION	63
3.1.1 <i>General</i>	63
3.1.2 <i>Per-modification on primary hydroxyls (OH-6)</i>	64
3.1.3 <i>Per-modification on secondary hydroxyls (OH-2)</i>	65
3.1.4 <i>Some examples of regioselectively sulfated β-cyclodextrins preparation</i>	66
3.2 RESULTS AND DISCUSSION	69
3.2.1 <i>Preparation of regioselectively sulfated β-cyclodextrins</i>	69
3.2.1.1 Synthesis of per-6S- β -cyclodextrin 13	72
3.2.1.2 Synthesis of per-2,3S- β -cyclodextrin 17	74
3.2.1.3 Synthesis of per-2,6S- β -cyclodextrin 24	76

3.2.1.4	Synthesis of per-2S- β -cyclodextrin 29	78
3.2.1.5	Synthesis of per-3,6S- β -cyclodextrin 31	79
3.2.1.6	Synthesis of per-3S- β -cyclodextrin 33	80
3.2.2	<i>Biological assays of regioselectively sulfated β-cyclodextrins</i>	81
3.3	CONCLUSION	82
CHAPTER 4	REDUCING-END MODIFICATION OF MALTOOLIGOSACCHARIDES	84
4.1	INTRODUCTION	85
4.1.1	<i>Thiol end-modification of unprotected carbohydrates</i>	86
4.1.2	<i>Amine end-modification of unprotected carbohydrates</i>	92
4.2	RESULTS AND DISCUSSIONS.....	97
4.2.1	<i>Thiol end-functionalization</i>	97
4.2.1.1	Thiol end-functionalization by using cystamine derivatives	97
4.2.1.1.1	Introduction	97
4.2.1.1.2	Grafting of cysteamine onto maltooligosaccharides through reductive amination	98
4.2.1.1.3	Grafting of cystamine onto maltooligosaccharides through reductive and Kochetkov amination ..	100
4.2.1.2	Thiol end-functionalization by using homocysteine thiolactone derivatives	102
4.2.1.2.1	Introduction	102
4.2.1.2.2	Grafting of HTL onto maltooligosaccharides though reductive amination	104
4.2.1.2.3	Grafting of HTL onto maltooligosaccharides through Knoevenagel condensation	108
4.2.1.3	Thiol end-functionalization by using anthranilic derivatives	113
4.2.1.3.1	Introduction	113
4.2.1.3.2	Grafting of cysteamine onto maltooligosaccharides through reductive amination	115
4.2.1.3.3	Grafting of cystamine onto maltooligosaccharides through reductive amination	116
4.2.2	<i>Random sulfation of thiol-end-functionalized maltoheptaose derivatives</i>	119
4.2.2.1	Optimization of sulfation conditions and synthesis of randomly sulfated M ₇ -bHTL	119
4.2.2.2	Synthesis of randomly sulfated M ₇ -rHTL	123
4.2.3	<i>Amine end-functionalization</i>	124
4.2.3.1	Introduction.....	124
4.2.3.2	Amine end-functionalization starting from isatoic anhydride	126
4.2.3.3	Amine end-functionalization starting from para-nitrophenyl anthranilate.....	127
4.3	CONCLUSION	130
CHAPTER 5	COUPLING OF FUNCTIONALIZED MALTOOLIGOSACCHARIDES	132
5.1	INTRODUCTION	133
5.2	RESULTS AND DISCUSSION	135
5.2.1	<i>Thiol-ene coupling</i>	135
5.2.1.1	Introduction.....	135
5.2.1.2	Synthesis of an alkene-bearing biotin.....	138
5.2.1.3	Preliminary tests of the thiol-ene coupling	139
5.2.1.3.1	Thiol-ene reaction of end-functionalized maltose with biotin-allyl.....	139
5.2.1.3.2	Thiol-ene reaction of end-functionalized maltose with PHOU	144
5.2.2	<i>Amide coupling</i>	147
5.2.2.1	Introduction.....	147
5.2.2.2	Amide coupling of amine-modified maltooligosaccharides with biotin-NHS	150
5.2.2.3	Random sulfation of biotin-maltoheptaose conjugates	151
5.2.2.4	Amide coupling of amine-modified maltooligosaccharides with PHOU-carboxylate	152
5.2.2.5	Random sulfation of PHOU-maltoheptaose conjugate	153
5.3	CONCLUSION	154
CHAPTER 6	CONCLUSIONS AND PERSPECTIVES.....	155
6.1	CONCLUSIONS.....	156
6.2	PERSPECTIVES	158

EXPERIMENTAL SECTION	159
MATERIALS AND METHODS	159
SYNTHESIS	160
REFERENCES	190
APPENDIX.....	217

CHAPTER 1

General introduction

1.1 Osteoarthritis

Osteoarthritis is a common disease occurring on body's joints. A joint is a structure where two bones are adjoining (Figure 2). The end of these bones is covered with a protective tissue called cartilage. Articular cartilage is an avascular connective tissue whose functional properties of mechanical support and joint lubrication depend on its extracellular matrix (ECM). ECM is rich in fibrillar collagens, proteoglycans (PGs) and glycosaminoglycans (GAGs).¹ Only one cell-type exists in cartilage, chondrocytes, that are responsible of the synthesis and degradation of ECM components, thereby modulating the structural and functional integrity of the tissue.^{1,2} A schematic illustration of all cartilage components is presented on the Figure 1 below.

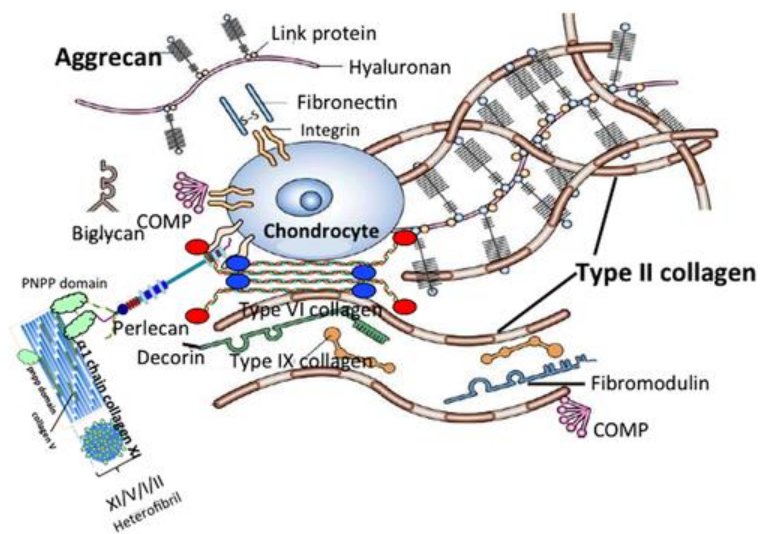


Figure 1. Schematic representation of articular cartilage depicting the chondrocyte surrounded by collagen, proteoglycans and associated matrix components. Reproduced from Chen et al.³

When the delicate balance maintained by chondrocytes in the cartilage is disrupted, the cartilage starts to break down: this degenerative joint disease is called osteoarthritis (OA). OA is characterized by the gradual loss of articular cartilage, chondrocytes death (by apoptosis and autophagy)^{4,5} and synovial inflammation. This causes swelling, pain, joint stiffness and loss of mobility.⁵ In early stages, the cartilage degeneration is offset by the local production of ECM components while in later stages, cartilage destruction considerably exceeds its repair.⁶ In response to the increased destruction of cartilage, chondrocytes produce more ECM components such as proteoglycans, but these latter are structurally altered and may be unable to form healthy ECM.⁷ The Figure 2⁸ presents the comparison between two knees, one healthy (*a*) and one suffering from osteoarthritis (*b*). In the unhealthy one, the exposure of rough bone is due to cartilage destruction, which may no longer protect it. The resulting direct bone-on-bone contact induces the erosion of meniscus as well as the development of osteophytes (or bone spurs). All these deteriorations cause pain and inflammation in the joint region.

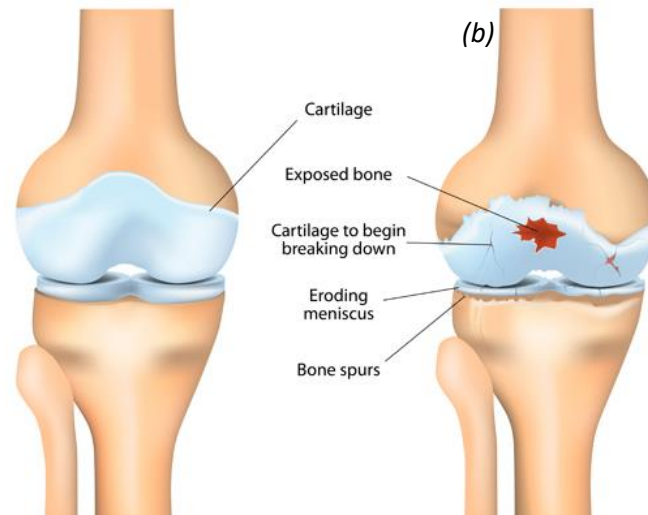


Figure 2. Comparison between a healthy knee joint (a) and one suffering from osteoarthritis (b).
Reproduced from ⁸

Two causes of osteoarthritis may be distinguished : primary osteoarthritis ^{9,10} resulting from gene predisposition and secondary osteoarthritis that frequently occurs after an injury.⁵ The resulting pathology is nevertheless the same : a degenerative process.

Besides affecting physical health, osteoarthritis may impact people’s mental health with symptoms of depression, as demonstrated by a study of Osteoarthritis Initiative.^{11,12}

Osteoarthritis is currently by far the most common rheumatic disorder ¹³ and is recognized as a global public health burden ¹⁴. It is considered as a leading cause of chronic pain ¹⁵ and one of the most significant causes of physical disability in the world.⁵ The number of patients suffering from this disease is growing day by day due to the increasing prevalence of obesity ¹⁶ and the aging of the population ¹⁷. OA currently affects at least 40 million people in Europe and accounts for more than a third of chronic moderate to severe pain. It is strongly age-related, prompting further concerns as population projections suggest that by 2025 there will be over 210 million people in Europe. The National Health Interview Survey estimated that 14 million people in the United States of America were affected by symptomatic knee osteoarthritis in 2018, which represents 4% of the American population. Other studies measured the prevalence of this disease in different joints and different communities around the world.¹⁸⁻²³

The large number of people suffering from osteoarthritis leads to healthcare costs that is currently estimated in Europe at 0.5% of gross national product, reflecting the direct and indirect costs. In a 2003 French macroeconomic study, which involved an estimated 3–4.6 million people with osteoarthritis, the direct costs surpassed €1.6 billion.²⁴ Compared with a similar study led 10 years earlier, the population of patients with osteoarthritis in France increased by 54%.

Current symptomatic therapies rely on the use of anti-inflammatory drugs to relieve patient’s pain.²⁵ Cartilage being avascular, alymphatic and constituted by only one cell-type, the most innovative

approaches to cure osteoarthritis focus on tissue engineering strategies, where a combination of cells, materials and engineering associated with biochemical and physiochemical factors would be used in the aim of improving or replace biological functions. Chondrocytes and mesenchymal stem cells could be applied in a tissue modeling healthy cartilage, leading to cell differentiation into chondrocytes and production of “healthy” ECM components that would result in the repair of cartilaginous tissue.²⁶ This strategy is ultimately in our project perspectives with the creation of a micro-environment of GAG and PG mimetics that would act as a scaffold for mesenchymal stem cells to differentiate into chondrocytes and produce normal GAGs and PGs in injured cartilage.

1.2 Glycosaminoglycans and proteoglycans

1.2.1 Proteoglycans

Proteoglycans (PGs) are large biomolecules found ubiquitously in the organism mainly attached to the cell surface or in the ECM.²⁷ The protein core usually determines the tissue localization of the PG and may in some cases take part in recognition processes.^{28,29} Depending on their localization, multiple classes of PGs may be distinguished. For example, serglycin is found intracellularly while syndecan and glypican are cell-surface PGs interacting with different extracellular proteins for recognition processes. Extracellular matrix PGs include decorin, perlecan and aggrecan. Decorin belongs to the family of small leucine-rich PGs that have ordering functions in tissues (regular structure of cornea for example). Perlecan, located at the basement membrane and in pericellular space, may act as an extracellular storage for growth factors such as FGF and interacts with VEGF in angiogenesis processes.³⁰ Finally, aggrecan is the most abundant PG in ECM-rich tissues such as cartilage where it forms large aggregates with hyaluronan (a non-sulfated GAG).

PGs may also be classified according to their GAG chain contents where those containing heparan sulfate chains, HSPG (heparan sulfate proteoglycan), are the most important and studied class of compounds.

Structurally, PGs are composed of a core protein linked with a number of GAG chains varying from one (e.g. decorin) to more than a hundred (e.g. aggrecan)³¹, that may not be of the same type neither bearing the same sulfation pattern between them (see Figure 3). For example, glypicans contain only one chain type (heparan sulfate) whereas syndecan-1, a family of mammalian syndecan, features two GAG chain types : heparan sulfate and chondroitin sulfate.³² GAG chains' length varies from 20 to 60 kDa in proteoglycans which represents around 40-120 disaccharidic units.³³ They are covalently linked to serine residues of the protein core through their reducing end *via* a motif composed of four monosaccharides : xylose, galactose, galactose and glucuronic acid.³⁴ The presence of a local high concentration of GAG chains allows to create a multivalent (or cluster) effect³⁵⁻³⁷ in recognition processes.

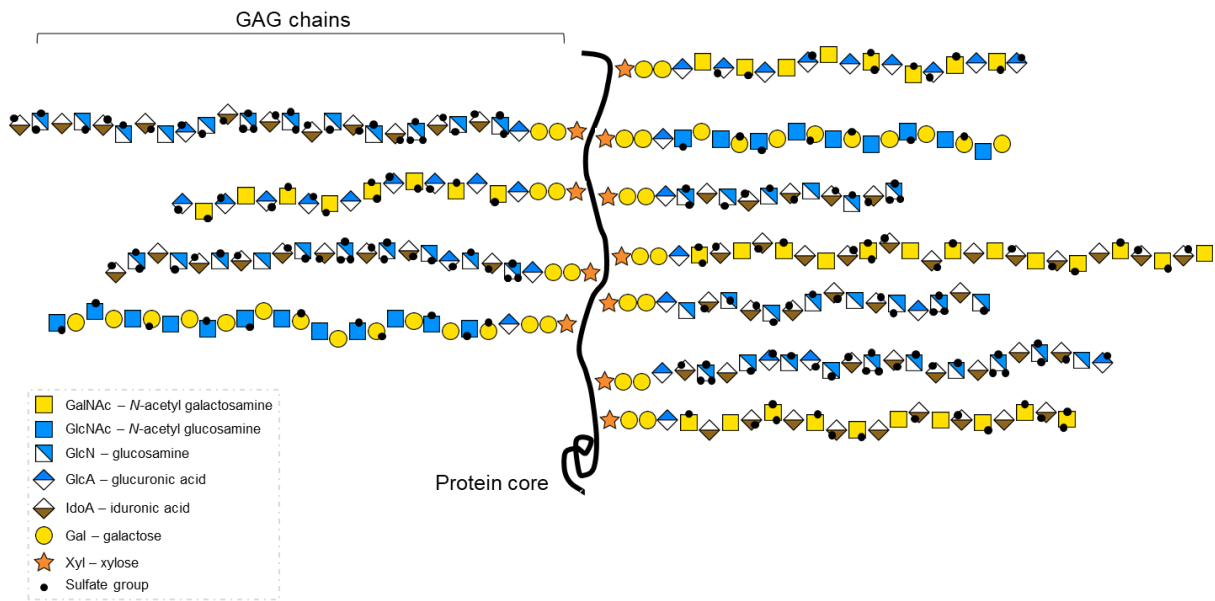


Figure 3. Schematic representation of a proteoglycan

1.2.2 Structure of glycosaminoglycans

GAGs are unbranched polysaccharides with molecular masses ranging from few kDa to over a hundred kDa.²⁷ Each chain consists of a repeating disaccharide unit composed of a hexosamine and a hexose/hexuronic acid and each monosaccharide may be modified heterogeneously : hexosamines may be acetylated, hexuronic acids epimerized and both of them may be sulfated on different positions. The nature, the extent and the position of sulfate groups among the chain are the source of GAGs extensive structural diversity. They are commonly found in the form of proteoglycans (except for hyaluronan).

GAGs may be considered as semi-rigid polymers adopting a helical conformation.^{38,39} These heterogeneous negatively charged polysaccharides may be categorized into five big families according to their saccharide composition and sulfation pattern³⁴, heparin/heparan sulfate, chondroitin sulfate, dermatan sulfate, keratan sulfate & hyaluronan, illustrated in the Table 1.

Heparin and heparan sulfate are both composed of a glucosamine monosaccharide but are different by their iduronic and glucuronic acid contents : heparin is mainly composed of iduronic acid while heparan sulfate comprises both glucuronic and iduronic acids. The glucosamine may be *N*-acetylated or *N*-sulfated, and sulfated on OH-3 and -6 positions. The iduronic (and more rarely glucuronic) acid may be sulfated on their OH-2 position. The distinction between heparin and heparan sulfate is not only based on their carbohydrate structure but also on their PG type and distribution. While HSPG may be covering virtually all cells, heparin proteoglycans (serglycin) are found intracellularly in mast cells.⁴⁰ Heparan sulfate and heparin are the most structurally and functionally diversified GAGs. In addition to the molecular diversity discussed above, they are composed of variable domains⁴¹⁻⁴⁴ : S-domains, which consist of 5-10 highly sulfated disaccharides that are very variable and are, with their high and local degree of sulfation, the usual binding sites of proteins. They are interspaced with A-domains being

poorly sulfated regions. This structural configuration is well observed of heparan sulfate while heparin is more homogeneously highly sulfated among the chain.⁴⁵ Having on average 2.7 sulfate groups per disaccharide units, heparin possesses the highest negative charge density known in Nature.⁴⁶

Chondroitin sulfate repeating unit is composed of *N*-acetyl galactosamine that may bear two sulfate moieties on OH-4 and -6, and of a glucuronic-acid that can be sulfated on OH-2 position. The only difference between chondroitin sulfate and dermatan sulfate is the epimerization at C5 of glucuronic acid into an iduronic acid. A galactose and a *N*-acetyl glucosamine, both possibly sulfated on OH-6, constitute keratan sulfate's disaccharide repeating unit. Finally, hyaluronan is composed of *N*-acetyl glucosamine and a glucuronic acid. It is the only non-sulfated GAG and the only one to be found under free form, i.e., not associated to a PG protein core.

Family of GAG	Chemical structure	Symbol Nomenclature for Glycans (without sulfation pattern)
Heparin & Heparan sulfate		
Chondroitin sulfate		
Dermatan sulfate		
Keratan sulfate		
Hyaluronan		

$R^1 = \text{H or } \text{SO}_3^-; R^2 = \text{Ac or } \text{SO}_3^-$

- GalNAc – *N*-acetyl galactosamine
- GlcNAc – *N*-acetyl glucosamine
- GlcN – glucosamine
- GlcA – glucuronic acid
- IdoA – iduronic acid
- Gal – galactose

Table 1. Chemical structure and representation by SNFG (Symbol Nomenclature for Glycans) symbols⁴⁷ of the disaccharide building block of five families of glycosaminoglycans

GAGs are secreted by the organism, and the molecular structures of GAGs in different cells or even in the same cells at different growth stages is highly variable.⁴⁸ Thus, during aging or in case of pathology, the composition of heparan sulfate for example can vary with important consequences on its protein binding properties.⁴⁹

1.2.3 Glycosaminoglycans and proteoglycans activities

The activity of PGs mainly depends upon their GAG chains⁵⁰ by playing the role of co-receptor for an optimal orientation of signaling proteins towards their receptor, or binding to biomolecules.⁵¹⁻⁵³

Each tissue produces specific structures of GAGs that have different properties. GAGs have numerous roles including cell proliferation and differentiation, cell signalling^{54,55}, regulating the bioactivity of growth factors and mitogenic factors^{56,57}, or inflammation^{31,53}.

The binding activity of GAGs is determined by its type, degree of sulfation, position of sulfation, local concentration⁵⁸ as well as the domain organization cited above^{44,59,60}. For example, heparan sulfate is able to bind to more than a thousand of heparin binding proteins (HBPs) *via* specifically sulfated domains. The binding usually involves electrostatic interactions^{29,61-64} although hydrogen bonding and van der Waals interactions exist with non-charged amino-acids of proteins^{64,29}. Among proteins that interact with GAGs figure chemokines, cytokines, growth factors, morphogens, enzymes, extracellular matrix or adhesion molecules.⁴⁵

The two most studied examples of proteins interactions with specific domains of GAGs are the formation of heparin/antithrombin III (AT III) & HSPG/FGF-R/FGF-2 complexes.

AT III plays a central role in blood coagulation for its ability to inhibit coagulant factors. Its activity depends upon its binding to a specific sequence of heparin or heparan sulfate: a pentasaccharide motif where the glucosamine on the center is 3-*O*-sulfated, which is crucial for the binding and leads to the activation of the protein through conformational changes which allows binding and inhibition of coagulation factors X.⁶⁵⁻⁶⁷ This motif and in particular this 3-*O*-sulfate group are very rare and specific patterns that may only be found in particular domains of heparan sulfate and heparin, indicating the essential role of GAGs in coagulation processes.

The second example deals with FGF-2 and its cell-surface receptor. Heparan sulfate chains (of HSPG) facilitate and stabilize the binding of FGF-2 to its membrane receptor FGF-R by forming a ternary complex.⁶⁸ The minimal motif required for binding to FGF-2 is a hexamer bearing *N*- and 2-*O*-sulfated units. However, promotion of the growth factor activity through the formation of functional FGF-2/FGFR/HS ternary complex is only mediated by longer HS fragments (decamer) composed of *N*-, 2-*O*- and limited 6-*O*-sulfated units (1 or 2).⁶⁹⁻⁷¹ These longer HS fragments may bind both the growth factor and its cell surface receptor, resulting in a stabilized ternary complex able to elicit cell

proliferation. The positioning of sulfate groups may therefore be critical for inducing a specific biological response (here, FGF-2 mediated cell proliferation) indicating that both chain length and sulfation pattern are essential parameters for efficient GAG-protein interactions. It is noteworthy to mention that this structural motif is only applicable to FGF-2 and one specific receptor isoform. For other FGFs and other isoforms receptor, different minimal chain length and sulfation pattern may be needed.

These two examples illustrate the complexity of GAGs interactions with biomolecules, that often require specific sequences with well-defined sulfation patterns. GAGs may bind to proteins to activate their signaling pathway or may simply form complexes to protect them from proteolytic degradation for example.^{72,36}

1.2.4 Use of glycosaminoglycans and proteoglycans for therapeutic purposes

GAGs and PGs are involved in many physiological processes thanks to their biological, mechanical and chemical properties, and are therefore known to have a great therapeutic potential, in tissue engineering for example.⁷³ Many examples of GAG-containing matrices have shown the possibility of growing skin, heart valve, cartilage, vascular grafts and other soft tissues.⁷⁴ Among them, heparin has been the most exploited for clinic applications, yet the only source of heparin are animal tissues⁴⁶ which may expose to contamination risks (pathogens for example) and thus adverse effects. Sulfated GAGs are usually extracted from porcine or bovine trachea, shark cartilage⁷⁵ and rooster combs⁷⁶. Their composition being time- and site-specific (sulfation degree and pattern in constant change), no extracted sample may be biologically identical (batch to batch variability).

Another method to obtain sulfated GAGs and PGs include the preparation of recombinant PGs through genetic engineering.²⁹ Although they constitute a promising alternative for tissue engineering purposes⁷⁷⁻⁷⁹ in the goal of forming matrices for cell growth and differentiation in cartilage for example, their cost, scalability and control of GAG structure limits their use.

Chemical synthesis of GAGs with defined sulfation pattern was also considered. However, due to their structural complexity (molecular mass, degree and position of sulfation, disaccharide composition) GAG synthesis is time-consuming, laborious, very complex and may lead to the preparation of only one specific chain.⁸⁰⁻⁸² On the other side, enzymatic or chemical depolymerization of GAGs provides limited quantities of heterogeneous mixtures.⁸³

The extreme structural diversity of GAGs and PGs therefore limits their therapeutic applications.⁸⁴ To address this issue, scientists investigated the preparation of GAG and PG mimetics, so-called glycomimetics.

1.3 Glycosaminoglycan- and proteoglycan-related glycomimetics

As previously mentioned (see 1.2.4), GAGs and PGs are biomolecules of interest for therapeutic issues as they are involved in many physiological and pathological processes. Understanding their structure-activity relationships is therefore critical. However, their structural diversity hampers their extraction from animal resources and their (bio)synthesis. To address these limitations, scientists started to develop the preparation of synthetic glycomimetics of GAGs and PGs, so-called neo-glycoconjugates. These mimetics are reported to be more stable than natural GAGs and PGs because they resist to glycanase activity.^{85,86} Here, we focused on the chemical approaches of their synthesis. It is noteworthy to mention that PGs being composed of a protein core on which GAG chains are attached, PG mimetics may be considered as the assembly of a polymeric scaffold on which saccharide chains (from mono- to poly-) are attached. Therefore, glycopolymers may be considered as PG mimetics.

Some parameters seem to be important for the preparation of relevant glycomimetics such as the type of GAG chain used, its length and its degree of sulfation. A few examples of each parameter are developed in the following.

1.3.1 Based on polysaccharides and oligosaccharides

In the aim of preparing glycomimetics with readily accessible structures, the modification of natural polysaccharides such as dextran, alginate, cellulose and chitosan was explored⁸⁷⁻⁹⁴ mostly for mimicking heparin. The interest of such approach is that structural nature of polysaccharides is necessarily similar to GAGs. Moreover, most of these natural polysaccharides include bioactivity, biocompatibility, biodegradability, anti-bacterial activity, non-antigenicity, non-immunogenicity as well as non-cytotoxicity. Of course, functional groups incorporation has to be done, and especially, sulfation to closely mimic GAGs. Additionally, polysaccharides are readily available from various resources, abundant and renewable.

Among them, chitin is one of the most abundant polysaccharides on Earth. Chitin is usually extracted from cuticles of various crustaceans (shrimps, crabs) and is composed of linear *N*-acetylated glucosamine. Its variation, chitosan, is partially *N*-deacetylated and provides the possibility of selective sulfation.⁹⁴ Selectively sulfated chitosans were therefore prepared as shown on the Figure 4. Basic conditions allow selective *N*-sulfation of chitosans while acidic ones may allow selective 6-*O*-sulfation. and their anticoagulant activities were assessed. While *N*-sulfated chitosan had no significant anticoagulant activity, 3,6-*O*-disulfated chitosan was highly active in accordance with previous publications.⁹⁵⁻⁹⁷ In addition, it was observed that the bioactivity of sulfated chitosan was dependent on the degree of sulfation and molecular weight of the polysaccharide.

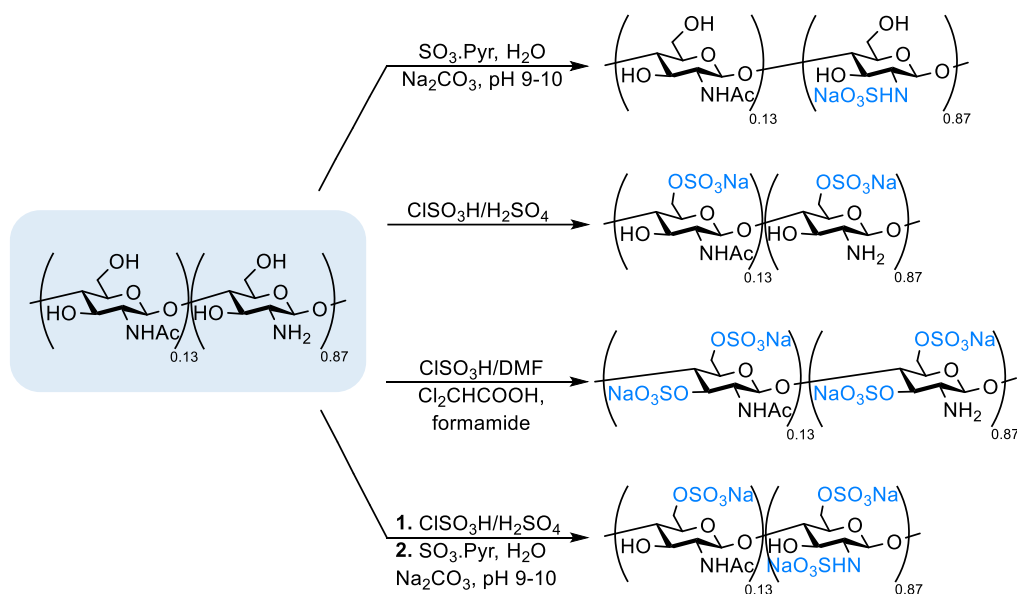


Figure 4. Structure of GAG-mimicking polymer based on chitosan. Reproduced from Liu et al.⁹⁸

Besides their anticoagulant properties, sulfated chitosans exhibited high affinities for specific growth factors.^{99–103} However, structural heterogeneity is observed on natural polysaccharides (chain length for example), and their chemical modification on specific positions of each monomer might not be possible.

Other polysaccharides of non-animal origin were used for tissue engineering purposes as they were reported to be more efficient to stimulate healing of tissues than natural GAGs, including fucoidan^{104,105}, or sulfated dextran^{82,106–108}.

Dextran was widely used as polymeric scaffold to create GAG mimetics partly thanks to its approved use in clinics as plasma volume expander and its ease of modification. The most well-known class of semi-synthetic heparin mimetic reported is carboxymethyl benzylamide sulfonate dextrans. These polymers were extensively developed by the Gly-CRRET group (Créteil, France).^{82,109–112} They bear benzylsulfonate and carboxymethyl groups along the linear chain whose respective ratios allow their anticoagulant/antithrombotic activities.⁸² Moreover, they are suggested to replace GAGs and PGs in injured tissues by forming a scaffold supporting the activity of HBPs.^{110,112–116} Their efficiency is well recognized as they are currently used for the treatment of skin and eye ulcer.¹¹⁷

Albanese et al.¹¹⁰ reported the comparison between two different dextran-based GAG mimetics (structure on Figure 5) that had the same molecular weight and the same degree of substitution of carboxymethyl and sulfate groups.¹¹¹ They differed only by the presence or absence of acetyl groups.

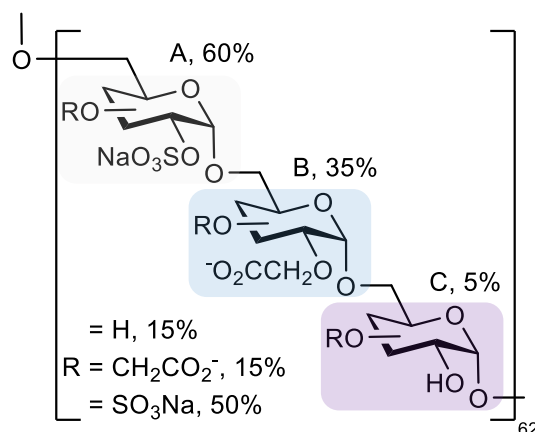


Figure 5. Structure of GAG-mimicking polymer by Gly-CRRET group (Créteil, France). Reproduced from Ikeda et al.¹⁰⁹

They compared their ability to induce mobilization of hematopoietic stem and progenitor cells in mice as GAG mimetics with fucoidan (naturally sulfated polysaccharide known to induce it).^{118,119} The group found out that the mimetics, that had a superior sulfate content than Fucoidan, were less efficient for mobilization, suggesting that an optimal but not maximal degree of sulfation is required for biological activity. In addition, they reported a better affinity of the acetylated GAG mimetic compared to the unacetylated one, suggesting that acetylation of GAGs might be important for interaction with proteins.

On the other side, the extraction of a marine branched exopolysaccharide by Jouault et al.¹²⁰ that was later modified by depolymerization and sulfation presented some structure similarities with heparin (presence of oversulfated domains and of uronic acid). Oversulfated fractions were found to possess a lower anticoagulant activity than heparin, but they could induce angiogenesis and cell proliferation by interacting with FGF-2 and VEGF.¹²¹ They later demonstrated that the mimetic could also interact with TGF- β 1, which is known for its positive effects on driving the chondrogenic differentiation of mesenchymal stem cells in cartilage.¹

Polysaccharides are polydisperse high molecular weight bio-sourced materials which make the perfect control and reproducibility of their modification difficult. Low molecular weight polysaccharides, so-called oligosaccharides, as GAG mimetics may be more advantageous because of structurally defined molecules with reduced side-effects. The potential advantages and drawbacks of such compounds are summarized in the Table 2.

Advantages	Drawbacks
Better pharmacokinetics	Potential toxicity
Better bioavailability	High cost
Synthetic or semi-synthetic source	Weaker avidities for GAG-binding proteins
Better dose control monitoring	Binding selectivity issues

Table 2. Potential advantages and drawbacks of oligosaccharides

Driven by the success story of GlaxoSmithKline in 2001, that registered fondaparinux as a new antithrombin drug called Arixtra®¹²², a glycomimetic which was designed using the natural pentasaccharide sequence responsible for the activity of heparin as template, many researchers looked for various sulfated oligosaccharides as GAG-mimetics.

Maltooligosaccharides were investigated as GAG mimetics because of well-defined structures. Wall et al. prepared 17 sulfated oligosaccharides and assessed their anticoagulant activities as heparin mimetics.¹²³ They found out that the influence of chain length was particularly evident with the maltooligosaccharide series. While sulfated di-, tri-, and tetra-saccharides displayed almost no anticoagulant activity, malto-pentaose, -hexaose and -heptaose were much more effective. From maltotetraose to maltopentaose, a 19-fold increase of anticoagulant activity was observed. The group pointed out the interesting features of maltooligosaccharides as heparin mimetics even though their activities were about two times lower to low molecular weight heparin.

More recently, Köhling et al.⁶³ prepared a library of defined oligohyaluronan in order to elucidate the effect of chain length, sulfation pattern and anomeric substitution effects on GAG recognition by regulatory proteins (cytokines, growth factors etc.). They found out that the oligosaccharides' length had a strong impact on binding affinities. Elongation of chains (from tetra- to hexa-saccharides) resulted in a general increase in binding affinities. They suggested, in accordance with Hsieh-Wilson group¹²⁴, that tetramers represented the minimum length required for GAG-protein interaction. Additionally, the absence of negatively charged groups on GAG mimetics showed no binding with regulatory proteins while an increase of sulfation degree was in favor of binding. Electrostatic interactions were essential to promote GAG binding with biomolecules.

Foxall et al.¹²⁵ prepared randomly sulfated maltooligosaccharides with chain lengths varying from one to seven units that were almost completely sulfated. For maltoheptaose, five derivatives containing increasing number of sulfates were prepared. The compounds were tested for their ability to block the interaction between FGF-2 and biotinylated heparan sulfate. They found out that maltohexaose was the minimum size required for significant activity. Whether the reducing end of maltooligosaccharides was left unchanged or was reduced, similar activities were observed. Maltoheptaose was the most potent, even more than heparin itself. The more maltoheptaose was sulfated, the more FGF-2 – heparan sulfate interaction was inhibited. Highly sulfated maltoheptaose was found to also inhibit endothelial cell growth. This inhibition was dependent on the sulfation level. Maltoheptaose with intermediate sulfation degrees stimulated cell growth but this latter decreased with higher sulfation degrees. However, sulfated maltoheptaose was not cytotoxic as its presence in a medium of endothelial cells did not induce cell deaths.

Later, Parish et al.¹²⁶ investigated sulfated oligosaccharides including maltooligosaccharides as heparan sulfate mimetics to inhibit angiogenesis and heparanase activity (anticancer applications). They found

that maltohexaose was the most potent inhibitor of *in vitro* human angiogenesis. More than four saccharide units in length were important for antiangiogenic activity. In addition, increasing chain length of maltooligosaccharides (until seven units) resulted in the increase of FGF – membrane heparan sulfate interaction inhibition which was in accordance with previous studies.¹²⁵ Saccharides from five to seven units were comparable heparanase inhibitors. Moreover, maltohexaose exhibited increased inhibition of heparanase activity with the degree of sulfation until a plateau, while antiangiogenic activity was observed on highly sulfated derivatives.

To summarize, maltooligosaccharides with a minimum size of tetrasaccharide and moderate sulfation degree were able to induce biological activity.

1.3.2 Based on glycopolymers

The preparation of polymers bearing glycans (glycopolymers) as side-chains was extensively developed in the aim of preparing glycomimetics with more controlled structures, especially sulfation patterns.

Linear polymers bearing pendant *N*-acetyl glucosamine end-functionalized with phenyl acrylamide and selectively sulfated on different hydroxyls were prepared by Miura group as shown on the Figure 6.¹²⁷ To do that, they selectively sulfated the monosaccharide on OH-6, -4, -3, or -3,4,6 positions prior to the copolymerization step with acrylamide. Polymers with different molecular weights sugar contents were obtained (from 10 to 100%). Later, they focused on the polymer bearing 6-sulfo *N*-acetyl glucosamine for biological tests.^{128,129} The addition of sulfated glycopolymers inhibited the aggregation of amyloid β peptides, which is detrimental in the case of Alzheimer amyloidosis. This inhibition depended on the percentage of sugar content in the polymer and low molecular weight glycopolymers exhibited stronger inhibition because of their greater mobility.

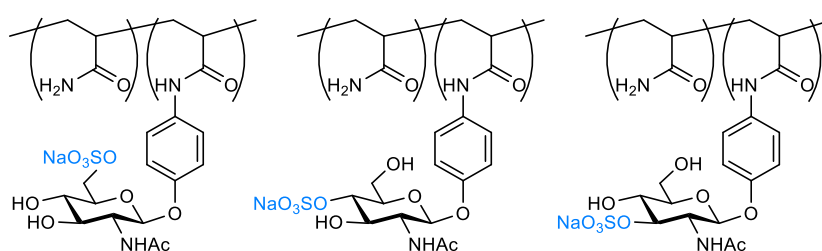


Figure 6. Structure of glycomimetic polymer by Miura group. Reproduced from Miura et al.¹²⁷

Still aiming to decipher the role of the multivalent architecture found in GAG or PG structures, Hsieh-Wilson et al. proposed to investigate ring-opening metathesis polymerization of protected sulfated di- or tetra-saccharides monomers, representative of repetitive building blocks of native GAGs (like chondroitin sulfate, heparin and heparan sulfate) that were next fully deprotected^{130–133} (Figure 7).

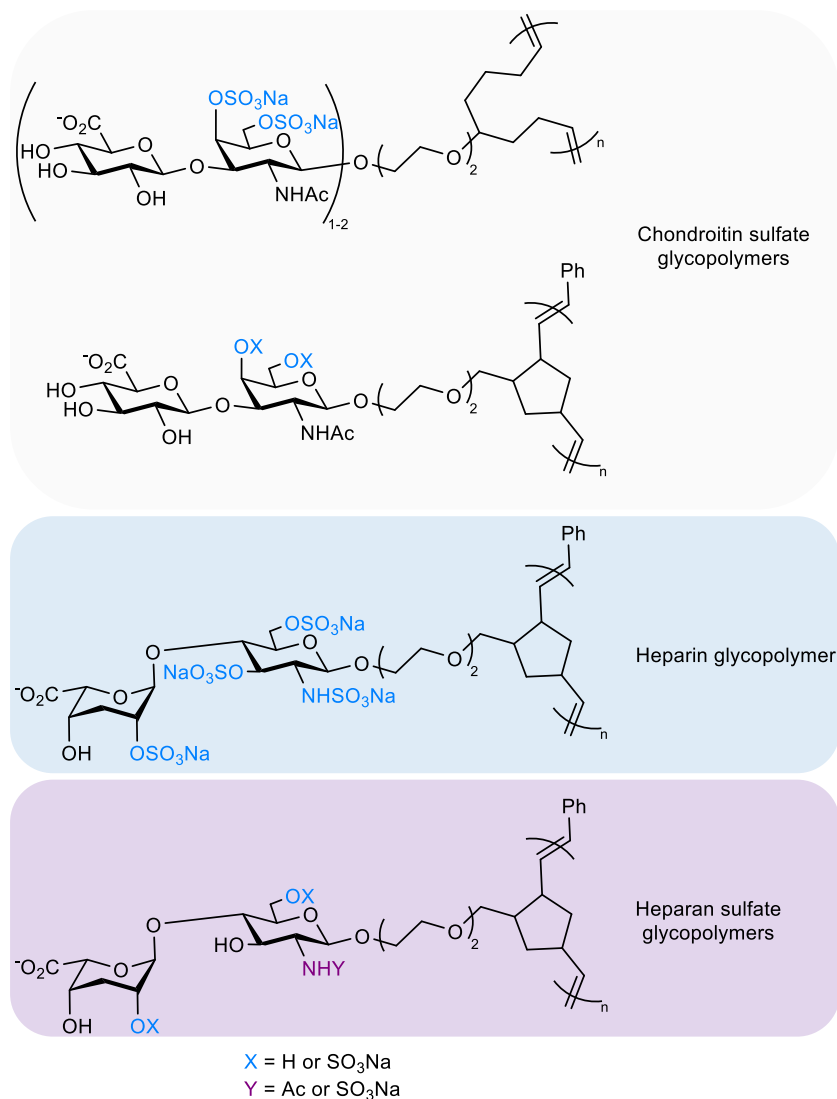


Figure 7. Structure of glycomimetic polymer by Hsieh-Wilson group. Reproduced from Liu et al.⁹⁸

These kind of GAG glycomimetic polymers showed biological activities similar to natural GAG polysaccharides. Chondroitin sulfate mimicking polymer displayed both neurite outgrowth and growth cone collapse assays, heparin mimetic exhibited potent antifactor Xa and antithrombin activity and heparan sulfate mimicking glycopolymers showed strong avidities to the proinflammatory chemokines RANTES. These bioinspired glycopolymers recapitulating the biological activities of GAGs are very encouraging and promising even if the main drawback of this strategy relies on the synthesis of complex oligosaccharide building blocks.

A simpler strategy was reported by Chaikof group on the preparation of glycopolymers bearing *per*-sulfated *N*-acetyl glucosamine or lactose.^{134–137} The structure of the glycomimetic with lactose is displayed on the Figure 8. They found out that the glycopolymers could interact with FGF-2 and exhibit anti-coagulant activity as a function of molecular weight of the polymers, sugar ratios and sulfation degree. They later demonstrated that the glycopolymer with a controlled molecular weight of 9.3 kDa

and a lactose content of 57% could protect FGF-2 from proteolysis, acid- and heat-induced degradation.¹³⁸

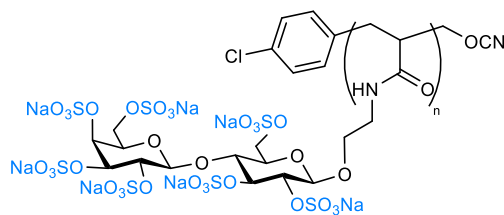


Figure 8. Structure of glycomimetic polymer by Chaikof group. Reproduced from Sun et al.¹³⁷

Glycopolymers are certainly the most readily accessible glycomimetics. Their synthesis can be achieved by multiple polymerization techniques and their molecular weight may be more or less controlled. Pendant saccharides can be modified with sulfate groups either before or after polymerization. However, in spite of breakthrough advances in polymer science, the precise control of the composition, molecular weight and chain sequence of GAG mimicking polymers is still difficult. In addition, they may be desulfated under acidic conditions, and the preparation of glycomonomers may still be challenging.⁴⁶

1.3.3 Based on non-carbohydrate synthetic polymers

In view of the difficulty to properly design carbohydrate leads that generally require multistep routes, non-carbohydrate glycomimetics are an appealing alternative. Non-carbohydrate GAG-related mimetics are usually anionic polymers recapitulating the negative charge displayed along the sulfated GAG polysaccharide backbone.

Maynard group¹³⁹ investigated the preparation of heparin-mimicking neo-GAG based on poly(styrene sulfonic acid-*co*-(poly(ethylene glycol) methacrylate) polymer. They found out that this polymer was able to bind to fragments of FGF and VEGF thanks to the acidity generated by sulfonic acid-bearing polymer. Then, they conjugated the polymer to FGF-2 through disulfide bond¹⁴⁰ as shown in the Figure 9 to see whether the polymer could act as a GAG by stabilizing FGF-2, which is positively charged. The group found out that the growth factor had indeed a higher stability under high and low temperature, acidic conditions and in the presence of a protease. The co-polymer also enhanced cell growth.

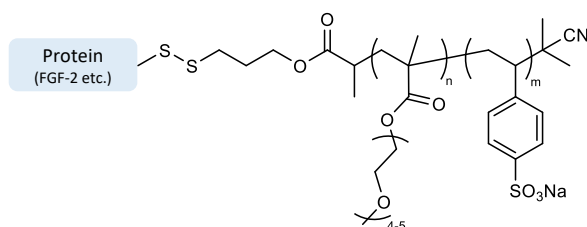


Figure 9. Structure of GAG-mimicking polymer by Maynard group. Reproduced from Miura et al.¹²⁷

Zhao's group proposed the preparation of heparin mimetics with a polymer bearing negative charges coming from sulfonate and carboxylic groups, poly(styrene sodium sulfonate *co*-sodium methacrylate).

The structure, displayed on the Figure 10, demonstrated a decreased protein adsorption and platelet adhesion compared to unmodified surfaces.¹⁴¹

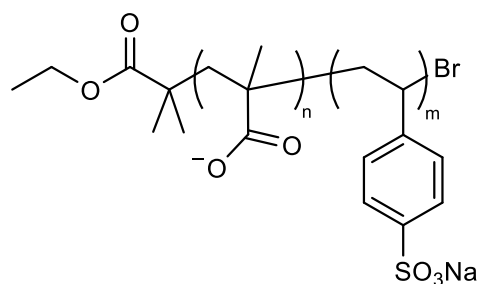


Figure 10. Structure of GAG-mimicking polymer by Zhao group. Reproduced from Liu et al.⁹⁸

In spite of their ease of synthesis, these anionic polymers as non-carbohydrate GAG mimetics are usually polydisperse and not degradable (petro-sourced materials). More importantly, their activities were found to be lower than natural GAGs, natural sulfated polysaccharides or glycopolymers.⁴⁶

Other seminal works have been done based on multi-display of sulfated carbohydrates on nanostructured materials due to their high surface-area-to-volume ratio, which can support high concentrations of bioactive GAG mimetics that can ultimately enhance their activity. There a few exciting examples of GAG mimetic functionalized nanomaterials that will not be developed here.^{142–144}

In conclusion, the monosaccharide composition, the amount and positions of the sulfate groups, the molecular weight and the overall conformation are all recognized to influence the bioactivity of a GAG. While natural polysaccharides seem as promising as glycopolymers, their polydisperse nature and structural complexity might hinder their use for structure-activity relationships. Chain length superior to four units and moderate to high degrees of sulfation were generally found to be important factors for biological activity. Finally, maltooligosaccharides seem to be a good compromise as they are plant-sourced oligosaccharides (no possible contamination compared to animal source) that were found to take part in several biological processes implying GAGs and PGs. Glycomimetic satisfying these criteria were investigated in our project.

1.4 Overview of the project

In the context of osteoarthritis, the strategy of the project is to propose a favorable environment for mesenchymal stem cells to reconstruct the articular matrix by preparing structurally simplified GAG and PG mimetics (see [1.3](#))¹. The aim of the study was to understand the role of chain length, conformation, charge density, sulfate position and multivalency for the interaction of newly synthesized glycomimetics with proteins involved in osteoarthritis. All these parameters could be assessed with one class of molecules : (cyclo)maltoligosaccharides.

(Cyclo)maltooligosaccharides were chosen as promising compounds for many reasons : (i) they are naturally occurring oligosaccharides presenting a defined structure considering chain length and conformation, (ii) they are composed of glucose units, which is among ten of the most abundant monosaccharides found in mammalian tissues (2.5% of total monosaccharides found)^{145,146} so no immune response may be elicited by their use in organism, (iii) they are quite stable in the joints as only one class of enzyme, α -amylases¹⁴⁷, may cleave their glycosidic linkage in the digestive system of living organisms, (iv) their sulfated derivatives present interesting biological properties (see [1.3.1](#)), (v) regioselective modification of cyclomaltooligosaccharides can be performed at different hydroxyl positions for extracting important data on structure/biological interactions relationships.

In practice, our multidisciplinary project was developed between four laboratories : mainly the CERMAV (Grenoble) for their expertise in glycochemistry, Gly-CRRET (Créteil) for biological assays *in vitro* and *ex vivo* skills, ICMPE (Thiais) for their knowledge in polymer chemistry, and a team at IBS (Grenoble) for their competence on GAG structure and activity.

The strategy was based on (cyclo)maltooligosaccharides of defined length, six and seven sugar units, that already proved their biological activities (see [1.3.1](#)). The first part of the project consisted in random sulfation of potential GAG mimetics. Linear malto-hexaose & -heptaose and β -cyclodextrin (the cyclic equivalent of maltoheptaose) were randomly sulfated at different degrees (low, medium, high) and assayed to estimate the degree of sulfation and the importance of structural conformation needed to elicit biological activity as potential monovalent GAG mimetics (performed by our collaborators of Gly-CRRET, Créteil). Then, regioselective sulfation on β -cyclodextrin was achieved by using the chemistry of cyclomaltooligosaccharides, known for their C_n symmetry. Selectively sulfated cyclodextrins were later biologically assayed to understand the role of sulfate position on their biological activity.

In order to get a multivalent structure able to potentially mimic PGs, linear maltooligosaccharides were also end-functionalized for their future coupling performed by ICMPE collaborators with a biodegradable bacterial polyester polymer, PHOU (poly(3-hydroxyoctanoate-co-3-hydroxyundecenoate)).

The project was structured around four main tasks, that will be developed in the following chapters and that are illustrated on the Figure 11 :

- 1) Random sulfation of (cyclo)maltooligosaccharides and their biological evaluation ([chapter 2](#));
- 2) Preparation of potential cyclic GAG mimetics by regioselective sulfation and their biological evaluation ([chapter 3](#));
- 3) Thiol- and amine-end-functionalization of potential linear GAG mimetics, and their random sulfation, for their future grafting by thiol-ene or amide coupling respectively ([chapter 4](#));
- 4) Preparation of potential PG mimetics by grafting of potential linear GAG mimetics on a biodegradable polymer scaffold and their random sulfation ([chapter 5](#)).

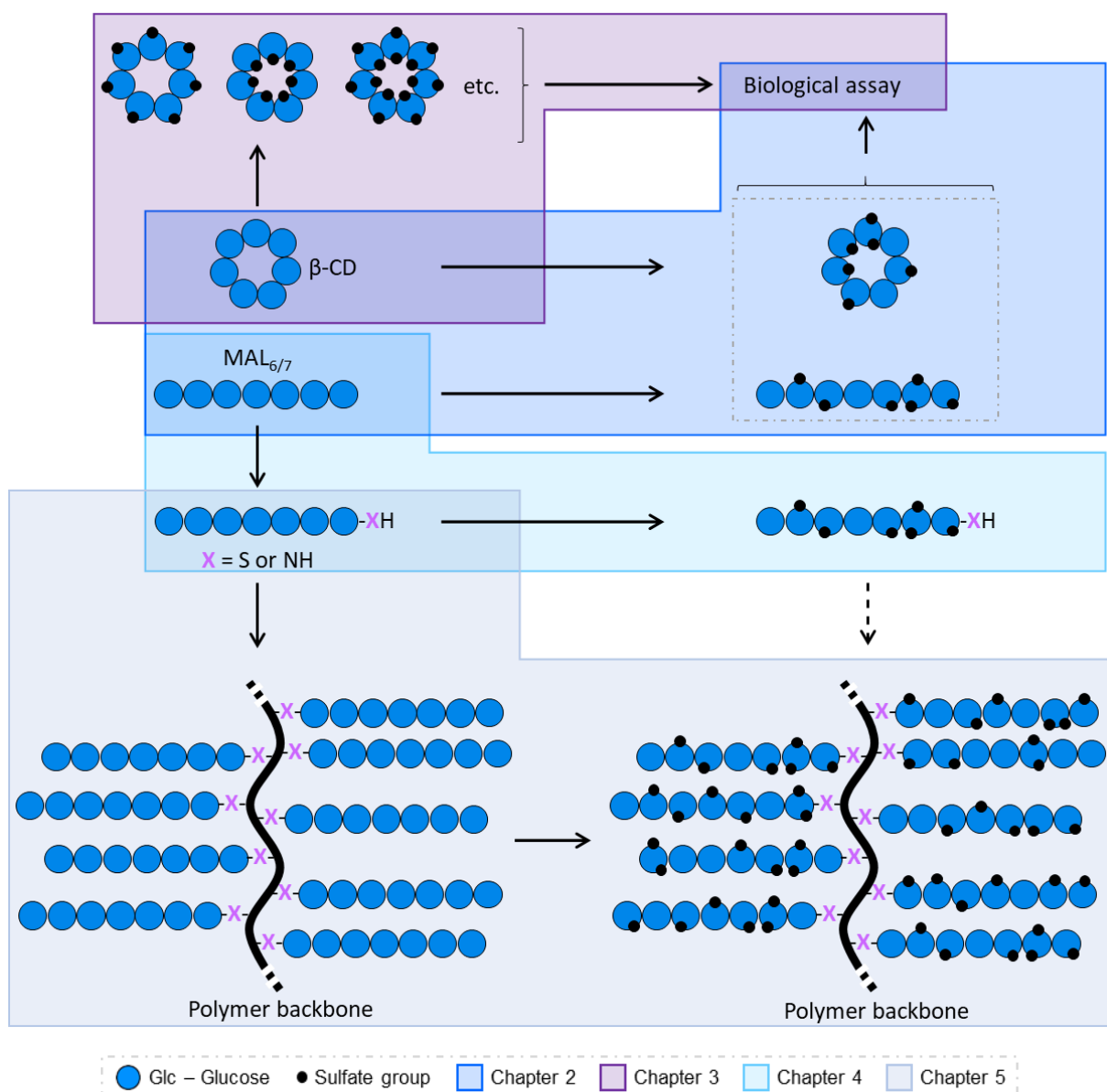


Figure 11. Simplified strategy of the project with the different tasks

CHAPTER 2

Obtention of randomly sulfated glycomimetics starting from (cyclo)maltooligosaccharides

2.1 Introduction

Heparin binding proteins interact with heparin and heparan sulfate chains at cell surface or in the extracellular matrix to mediate physiological activities. Among HBP's figure FGF-2 and VEGF.

FGF-2 (or bFGF for basic fibroblast growth factor) is part of a large family of polypeptide growth factors¹⁴⁸ and VEGF represents a family of glycoproteins involved in vasculogenesis, lymphangiogenesis and angiogenesis¹⁴⁹. Their important feature is their binding to heparin/heparan sulfate.^{150,151,152} These interactions stabilize the growth factors (especially FGF-2) to thermal denaturation and proteolysis¹⁵³ but also regulate their biological activities^{56,154,155}. They also allow (through HSPG or free-form HS/heparin) growth factors to activate their receptors on cells.^{152,156,157}

FGF-2 and VEGF were found to be implicated in osteoarthritis. While FGF-2 has a controversial role by being associated to anabolic and catabolic events¹⁵⁸, VEGF mediates mainly destructive and inflammatory reactions^{159,160}.

Studies suggested that linear sulfated maltooligosaccharides could potentially mimic the role of heparin/heparan sulfate (see [1.3.1](#) & ¹⁶¹). On the other side, sulfated cyclic maltooligosaccharides and more precisely β -cyclodextrins were found to have interesting properties as heparin mimetics, for the binding of FGF-2 or for antiangiogenic activity.^{162–164} They required a minimum of 10 sulfate groups (representing a moderate degree of sulfation) and higher doses than those needed for heparin for binding. β -cyclodextrins could also exert these effects under polymeric forms.^{163,164}

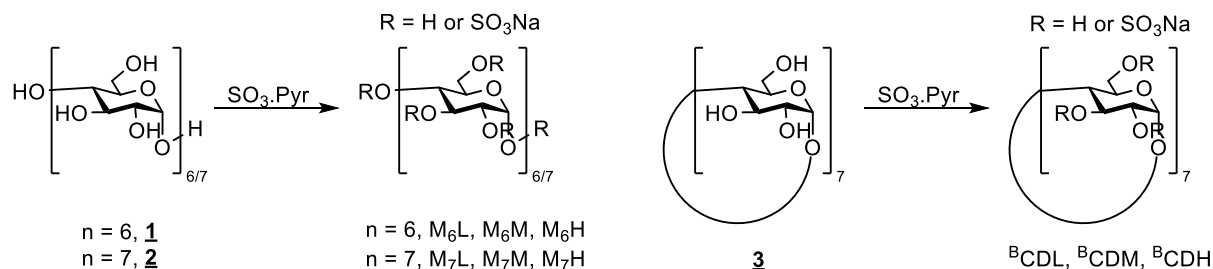
As preliminary studies for evaluating the biological effects of sulfated (cyclo)maltooligosaccharides in the context of osteoarthritis, the binding and activity of such compounds was measured with FGF-2 and VEGF. (Cyclo)maltooligosaccharides were in this chapter randomly sulfated to determine whether an interaction of the prepared glycomimetics with biomolecules could be established or not, and if the sulfation degree had an influence on this interaction. Structural configuration of glycomimetics for their potential biological activity was evaluated by using linear and cyclic sulfated oligosaccharides: maltohexaose/-heptaose vs β -cyclodextrin. Also, the effect of chain length on the interaction was assayed by comparing sulfated maltoheptaose (DP 7) and maltohexaose (DP 6).

2.2 Results and discussion

2.2.1 Synthesis and characterization of randomly sulfated (cyclo)maltooligosaccharides

Natural and unmodified oligosaccharides (M_6 **1**, M_7 **2** and B CD **3**) were sulfated at three degrees of sulfation (DS) by changing the stoichiometry of the sulfation reagent. Typically, three degrees of sulfation per monosaccharide (DS) were targeted by controlling the stoichiometry of sulfur trioxide•pyridine complex per hydroxyl (equiv./OH): 0,5 equivalents of sulfur trioxide pyridine complex per hydroxyl for the lightly sulfated ($M_{6/7}L$, B CDL), 1 eq./OH for the moderately sulfated ($M_{6/7}M$,

^BCDM) and 2 to 5 eq./OH for the highly sulfated one (M_{6/7}H, ^BCDH). Randomly sulfated (cyclo)maltooligosaccharides were obtained as shown on the Scheme 1. The sulfation procedure was optimized with maltoheptaose **2** by varying different reaction parameters (solvent, temperature, reaction time and purification).



Scheme 1. Synthesis of randomly sulfated (cyclo)maltooligosaccharides

First, the oligosaccharides were sulfated according to the procedure described by Parish et al.¹²⁶ in a mixture of solvents (DMF/pyridine 2/3 v/v) for two hours at 80°C. However, the long workup procedure did not allow to afford pure products because of the contamination with pyridinium salts and solvents (observed by ¹H NMR). Sulfated maltohexaose (M₆L, M₆M and M₆H) being prepared only once due to their availability, their sulfation procedure and work-up was carried out in early stages of the project according to this procedure. Another simpler work-up reported by Papy-Garcia et al.¹¹¹ was adopted for maltoheptaose that required, after completion of the reaction, a simple step of pH neutralization followed by dialysis purification affording almost pure products. Pyridinium salts were also observed in some cases. To overcome this problem, a modified procedure of Chaikof and co-workers¹³⁷ was approved for maltoheptaose and cyclodextrin: the reaction was carried out in inert conditions in DMF at a lower temperature of 60°C resulting in more homogeneous mixture of products (see sulfated cyclodextrins). As our products were aimed to be biologically assayed, a purification by gel permeation chromatography (GPC) was opted instead of the dialysis for maltoheptaose and cyclodextrin derivatives, providing very pure products yet containing small traces of ammonium carbonate, that is used in its aqueous solution as the solvent for GPC purification.

After purification, the lyophilized products, obtained as complex mixtures, were characterized by different methods (¹H NMR, SEC-MALS, FT-IR & elemental analysis).

Based on the overall look of the spectra, the nuclear magnetic resonance ¹H allowed to have an idea of the degree of sulfation of the different derivatives along with their purity (contamination with salts or solvents). As an example, a superposition of ¹H NMR spectra of native maltoheptaose (M₇, black) with lightly (M₇L, green), moderately (M₇M, orange) and highly (M₇H, red) sulfated maltoheptaose is presented on the Figure 12.

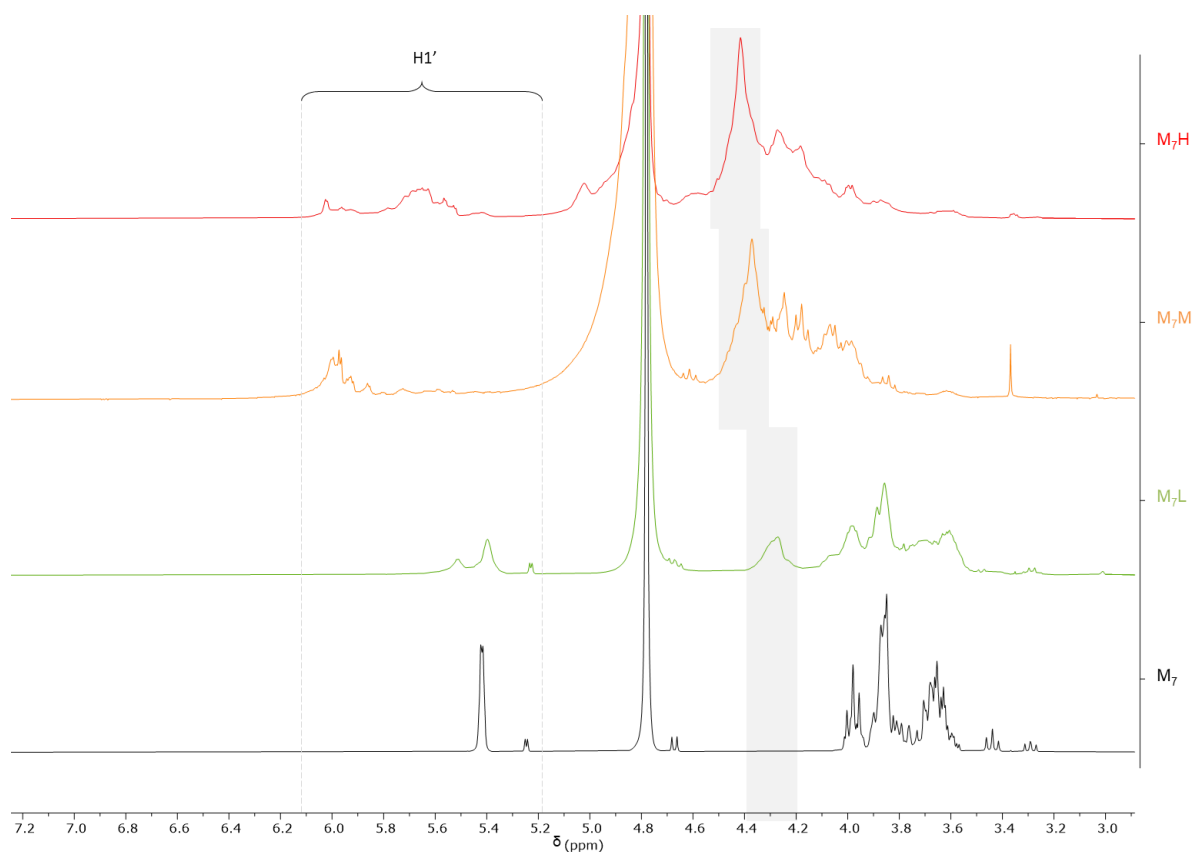


Figure 12. ^1H NMR spectra superposition of M_7 and its randomly sulfated derivatives in D_2O at 298K

The peak attributed to anomeric protons ($\text{H}^{1'}$), that usually appeared as a doublet around 5.40 ppm in native carbohydrates (M_7 spectrum in black), was after sulfation seen as a multiplet in every sample (see green, orange and red spectra), indicating that the chemical environment of each anomeric proton changed depending on the position that was sulfated. The more the polysaccharide was sulfated, the less the original $\text{H}^{1'}$ peak was observed. Furthermore, after sulfation, a big peak appeared around 4.30 ppm corresponding to the methylene of the primary hydroxyl once this position was sulfated (see gray zone on each spectra). As expected, this peak tended to gain in intensity when the degree of sulfation of the oligosaccharides increased. It is well-known that sulfation of hydroxyl group in glycosyl residues causes a significant deshielding of geminal and vicinal proton resonance. A geminal proton is deshielded by about 0.6 ppm, some variations with axial or equatorial orientation being apparent. The effect of sulfate group on a vicinal proton is also dependant on the relative orientations of the two groups the, being the largest when the both groups are equatorial in the pyranoside ring.¹⁶⁵ The formation of 1,6-anhydro bridge motif in reducing monomers of sulfated (cyclo)maltooligosaccharides as suggested by Yeh et al.¹⁶¹ could not be confirmed by HMBC experiment (no spot between $\text{H}^{1'}$ and C6 observed) due to the complex attribution of ^1H NMR spectra obtained.

Another method to have an idea of the degree of sulfation is size exclusion chromatography coupled with a light scattering detector, a refractometer and a UV detector (SEC/MALS). This method allows to calculate the molecular weight of macromolecules based on their refractive index value (RI) that can be

calculated for each molecule for more accurate measurements. Here we used the RI of dextran sulfate ($dn/dc=0.142$) as a reference for our samples, that are complex mixtures of products. Only M_7 and ^BCD derivatives could be analyzed (not enough quantities of sulfated M_6). SEC/MALS measurements were conducted on triplicates and retention times of products are presented in Figure 13.

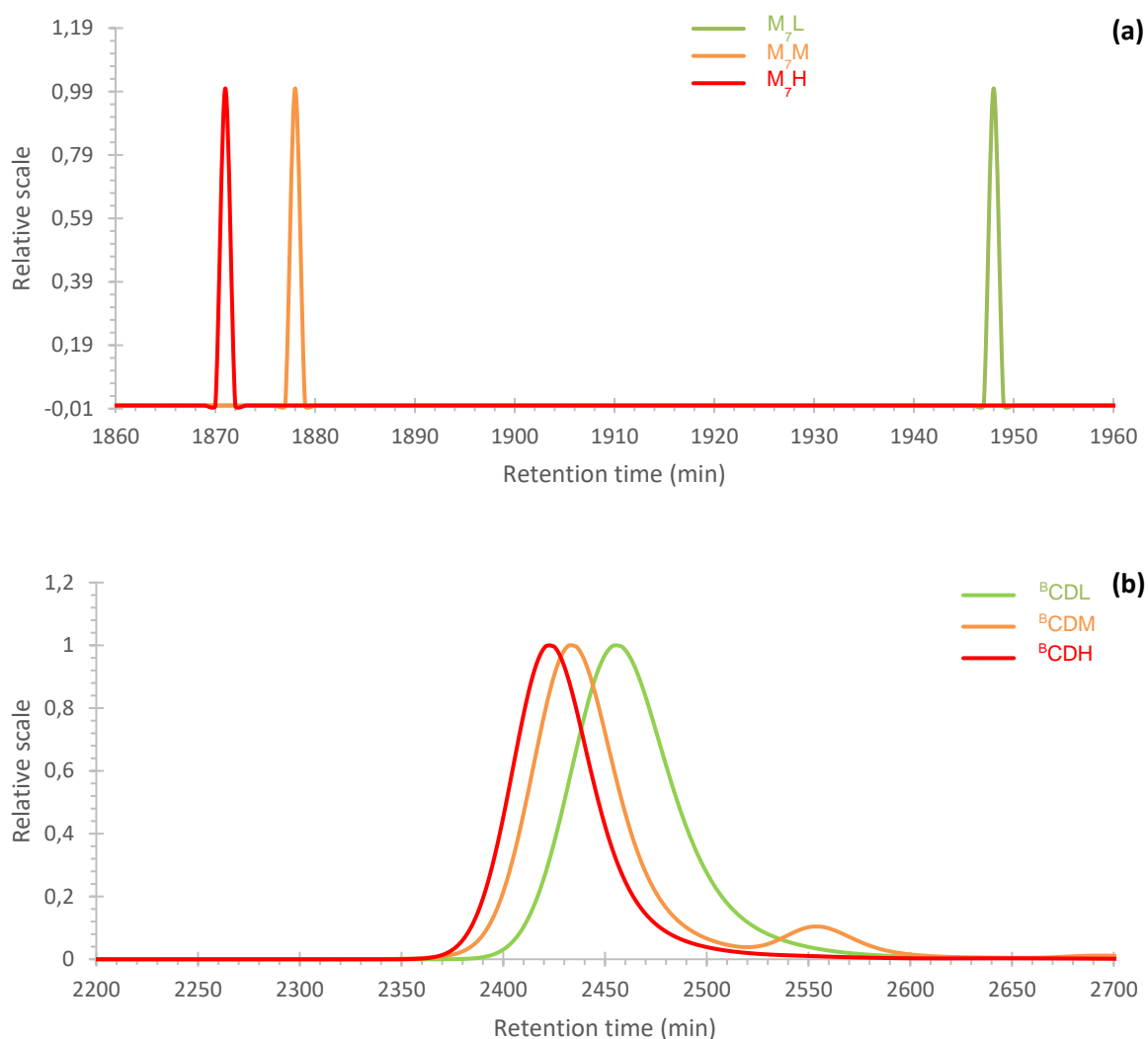


Figure 13. (a) Superposition of sulfated M_7 SEC-MALS retention times ; (b) Superposition of sulfated ^BCD SEC-MALS retention times

M_7 derivatives (Figure 13a) and sulfated ^BCD (Figure 13b) showed clear gaussian curves for retention times suggesting homogeneous mixtures. Sulfation seemed to have effectively occurred as GPC peaks shifted to lower retention times with the increase of molecular weight. It is noteworthy to mention that moderately and highly sulfated derivatives (red and orange, Figure 13) showed more similar retention times compared to lightly sulfated ones. This phenomenon is well-observed on Figure 13a (even though for both graphs, the difference of retention times does not exceed 100 min between highly and lightly sulfated products) and indicates more structural similarity in terms of number of sulfate groups between them.

SEC-MALS data of sulfated derivatives are summarized on the Table 3. The polydispersity indexes PDI observed were greater than 1 for all the sulfated products, confirming that each batch is composed of a plethora of similar products, and this index seemed to globally increase with the degree of sulfation.

Sample		Mw		Mn		PDI (Mw/Mn)	
		Mean	±	Mean	±	Mean	±
M ₇	Low	1722	53	1281	28	1.344	0.012
	Medium	2415	31	1320	15	1.830	0.025
	High	2910	167	1649	57	1.765	0.066
^B CD	Low	1665	3	1241	37	1.342	0.044
	Medium*	2274	19	1477	14	1.540	0.003
	High	2543	39	1559	17	1.632	0.022

Table 3. Mw, Mn and PDI of sulfated M₇ and ^BCD derivatives. *commercially available

The data showed an increase of weight average molecular weight Mw with the degree of sulfation from 1722 to 2910 g.mol⁻¹ for M₇ derivatives and from 1665 to 2543 g.mol⁻¹ for sulfated ^BCD. This confirmed that the number of grafted sulfate moieties increased between lightly and highly sulfated products. The number average molecular weight Mn was in each case lower than Mw, which was typical for polydisperse polymers and evolve in the same manner as Mw and PDI. Figure 14 summarized Mw, PDI and DS values of each sulfated derivatives.

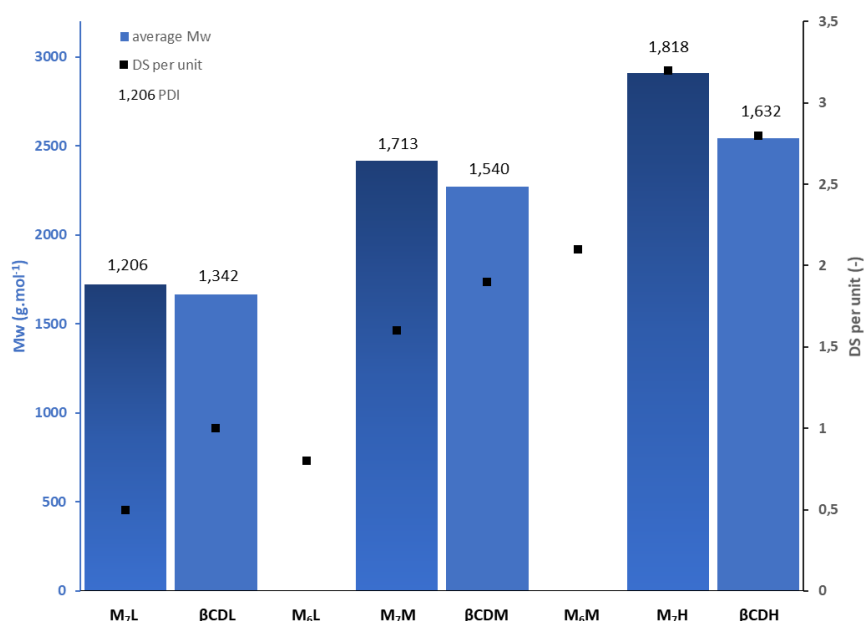


Figure 14. Graph of Mw, PDI values extracted from SEC-MALS analysis and DS values from elemental analysis of sulfated (cyclo)maltooligosaccharides

Mw and PDI values increased accordingly to DS for sulfated M₇ (dark blue) and ^BCD (lighter blue).

Further analysis on sulfated (cyclo)maltooligosaccharides using elemental analysis were carried out. This method allowed for the evaluation the average degree of sulfation per unit (DS) of all sulfated products. The results are presented in Table 4. As expected, the DS increased from 0.5 sulfate moiety

per sugar unit to 3 for sulfated M₇ and from 1 to 2.8 for ^BCD derivatives. Concerning the M₆ batches, the DS increased from 0.8 to 2.1 between the lightly and moderately sulfated derivatives, but the highly sulfated one showed a DS of only 0.6. Due to a lack of starting material, the sulfation reaction experiment could not be reproduced.

Sample		C	H	N	S	DS
		[wt%]	[wt%]	[wt%]	[wt%]	
M ₇	Low	30.844	5.999	3.152	7.003	0.5
	Medium	20.532	5.475	5.826	14.444	1.6
	High	14.832	4.716	8.473	21.009	3.2
M ₆	Low	25.451	4.496	0.016	9.259	0.8
	Medium	17.696	5.466	6.870	16.618	2.1
	High	28.680	5.905	3.034	7.968	0.6
^B CD	Low	25.144	5.754	5.192	11.790	1.0
	Medium*	17.498	3.421	0.000	14.680	1.9
	High	15.441	5.074	7.936	19.007	2.8

Table 4. Degree of sulfation per saccharidic unit of the sulfated (cyclo)maltooligosaccharides (calculated by elemental analysis).

A qualitative analysis of sulfated (cyclo)maltooligosaccharides could be obtained from Fourier-transform infrared spectroscopy (FT-IR). As an example, infrared spectra superposition of M₇ and its lightly, moderately, and highly sulfated derivatives is presented on the Figure 15. The broad hydroxyl stretching vibration band O-H around 3300 cm⁻¹ seemed to decline with the increase of the degree of sulfation. The band at 2900 cm⁻¹, corresponding to carbon-hydrogen stretching, was present before and after sulfation as well as the strong band at 990 cm⁻¹, corresponding to carbon-oxygen stretching and carbon-carbon bending. This may show that no hydrolysis occurred during the reactions. More importantly, a strong band appeared after sulfation : the sulfur-oxygen double-bond stretching band S=O at 1200 cm⁻¹, whose intensity varied as a function of the degree of sulfation, attesting that sulfation did succeed.

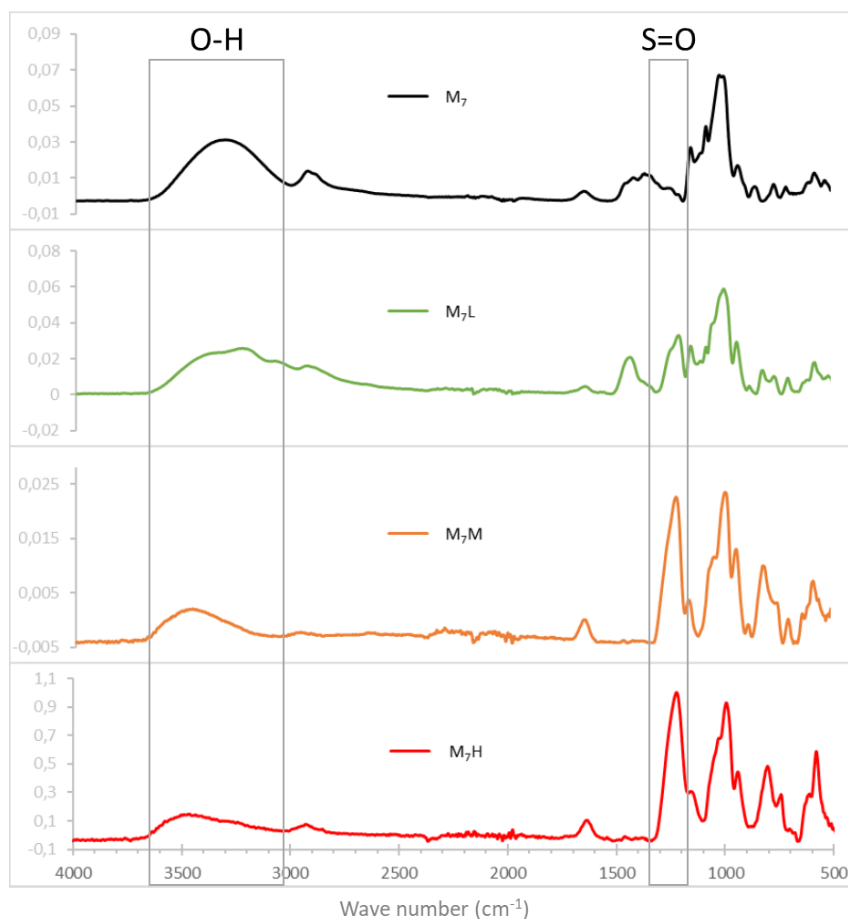


Figure 15. FT-IT spectra superposition of M_7 and its sulfated derivatives

After being characterized, the sulfated (cyclo)maltooligosaccharides were submitted to biological assays performed by our collaborators (Gly-CRRET, Créteil).

2.2.2 Biological assays on randomly sulfated maltooligosaccharides

2.2.2.1 Principle of biological assays

2.2.2.1.1 Competitive ELISA test

Our collaborators first measured the relative affinity of our randomly sulfated (cyclo)maltooligosaccharides being potential GAG mimetics for a given growth factor by competitive ELISA (Enzyme-Linked Immunosorbent Assay) test, which is explained and illustrated on the Figure 16.

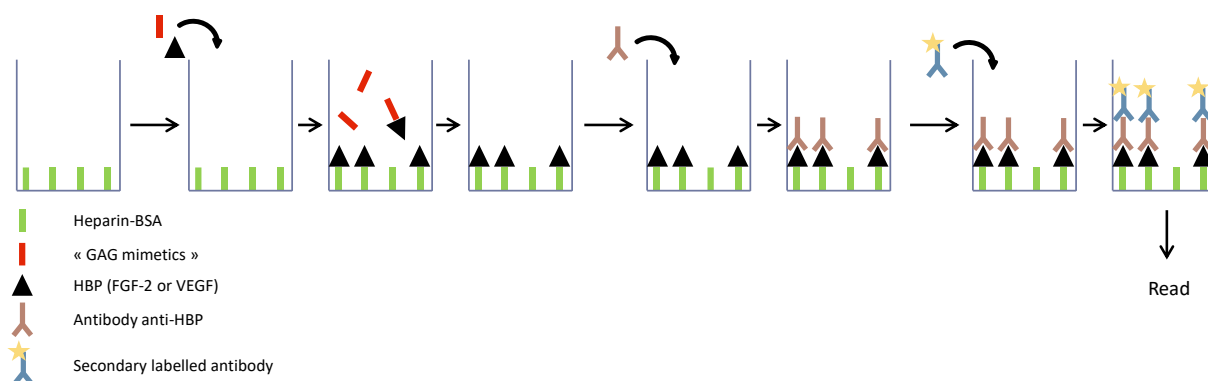


Figure 16. Principle of competitive ELISA test

In this assay, each well of a plate was coated with heparin by using the heparin-BSA complex. The heparin being fixed, a known and constant mass concentration of HBP and a concentration of “GAG mimetics” was added to the well. Our “GAG mimetics” in solution acted as competitors of surface immobilized heparin for binding to the HBP. After incubation, a washing step eliminated all free HBP and “GAG mimetics” bound or not to HBPs. A primary antibody anti-HBP was then added and bound to all the heparin immobilized HBP left in the well. After a washing step to eliminate the excess of unbound antibody, a secondary labelled antibody recognizing specifically the first antibody was added to the well. Finally, after a last washing step to eliminate excess of labelled secondary antibody, the quantity of HBP bound to heparin was measured as a function of the fluorescence intensity of each well. The less the signal, the more HBP were fixed to our “GAG mimetics”, proving a significant interaction between sulfated maltooligosaccharides and these HBPs.

This assay was carried out on a 96-well plate, with different concentrations of “GAG mimetics” in wells where each concentration of “GAG mimetic” was tested at least two times. Two positive controls were used for the experiment : heparin and a heparin mimetic (a randomly sulfated polysaccharide known to efficiently bind both HBPs). The IC₅₀ value of the heparin mimetic was fixed as 100% and the relative affinity of our “GAG mimetics” compounds was compared to this reference.

From the fluorescence measurement of all the wells with different concentrations of “GAG mimetics”, the IC₅₀ values (concentration of “GAG mimetics” for which 50% of HBP remain bound to the immobilized heparin) of our compounds were calculated.

2.2.2.1.2 Mitogenic assay on BAF32 or HUVEC cells

Binding and signalling of the mitogenic growth factor FGF-2 by our sulfated maltooligosaccharides was analyzed using BAF32 cell assay. BAF32 cells are a model system developed to identify heparan sulfate and heparin structures that interact with FGFs and their receptors¹⁶⁶. They consist of transfected lymphocytes that express FGF receptors at their surface but lack cell-surface heparan sulfate chains that stabilize the interaction between FGF-2 and its receptor (see 1.2.3). To proliferate, these cells thus require the presence of FGF-2 as well as addition of exogenous heparin/heparan sulfate in the medium

to form biologically active ternary complexes between cell surface FGF receptors, FGF-2 and heparin/heparan sulfate ¹⁶⁷. In our case, this assay was realized to test if randomly sulfated maltooligosaccharides are efficient promoters of FGF-depending proliferation, and thus mimicking heparin/heparan sulfate.

HUVEC cells present VEGF receptors as well as heparan sulfate on their cell surface. VEGF and its receptor require the presence of cell-surface or free-form heparin/heparan sulfate to induce biological response. However, higher concentrations of heparin/heparan sulfate or their mimetics induce an inhibition of the fixation of VEGF to its cell receptor thus inhibiting cell growth. In this assay, we tested the ability of sulfated (cyclo)maltooligosaccharides to inhibit cell growth by mimicking free-form GAG mimetics.

The principle of the method is explained in the following and illustrated in the Figure 17.

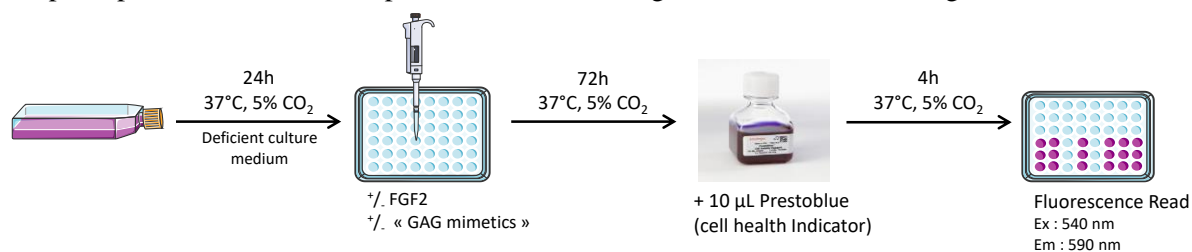


Figure 17. Principle of mitogenic assay on BAF32 or HUVEC cells

BAF32/HUVEC cells were cultured in similar conditions. Here, the cell culture of BAF32 cells is detailed. BAF32 cells were grown for 24 hours at 37°C in a serum-free culture medium with 5% CO₂ (fixed parameter of the incubator allowing cell growth). This serum deficiency is necessary for all cells to reach the quiescent stage. Each well of a 96-well plate was differently filled with a constant concentration of dormant BAF32 cells and FGF-2, and variable concentrations of potential GAG mimetics. The plate was then incubated for 72 hours at 37°C. After that, Prestoblué®, a reagent permitting cell viability quantification by fluorescence ¹⁶⁸, was added to each well and cells were incubated for 4 more hours at 37°C. Finally, the fluorescence was read on the plate, and alive cells in wells were quantified.

On the 96-well plate, positive and negative control tests were also realized to assess the validity of the assay.

2.2.2.2 Biological assays with FGF-2

Our collaborators realised their biological assays with two HBPs. The one presented here is FGF-2. Thanks to their competitive ELISA assays (preliminary results), they calculated the mean IC₅₀ value of sulfated (cyclo)maltooligosaccharides when they were acting as competitors of heparin for binding with FGF-2 (triplicate measurements, n=3, were performed for each compound except for M₇M, M₇H & ^BCDM where n=6). The mean IC₅₀ values are presented with their standard deviation on the Table 5.

Compounds	Heparin	Hep mim	M ₇ L	^B CDL	M ₆ L	M ₇ M	^B CDM	M ₆ M	M ₇ H	^B CDH
Mean IC ₅₀ for FGF-2 (µg/mL)	0.05	0.55	NC	1634	NC	104.4	71.4	NC	8.5	465
	±0	±0.04		±767		±34.6	±11.8		±4.7	±114

Table 5. Mean IC₅₀ values with standard deviation for sulfated (cyclo)maltooligosaccharides with FGF-2.

As can be seen on the table, no competition (NC) was observed for sulfated M₆ and for lightly sulfated M₇. Moreover, the IC₅₀ values were considerably high for β-cyclodextrin lightly and highly derivatives. Moderately sulfated M₇ and ^BCD and highly sulfated M₇ seem to be the most competitive components against heparin.

Using the mean IC₅₀ values presented on Table 5, a graph presenting the relative affinity of different “GAG mimetics” with FGF-2 compared to the value of the heparin mimetic, fixed as the reference, was traced and presented on the Figure 18.

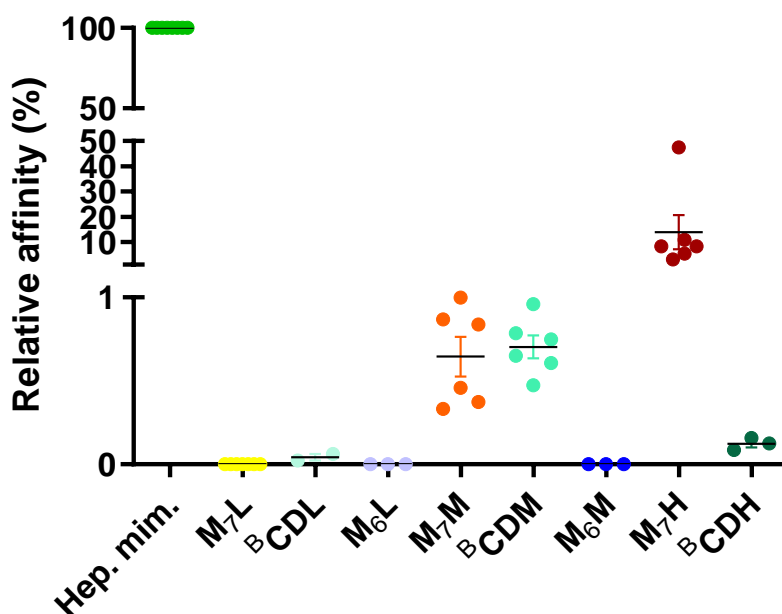


Figure 18. Graphic presenting the relative affinity of sulfated (cyclo)maltooligosaccharides for FGF-2. The IC₅₀ value of Heparin mimetic was used as reference of 100% of binding affinity, to calculate the % of binding affinity of all other tested molecules for FGF-2.

Lightly sulfated (cyclo)maltooligosaccharides seemed to exhibit no inhibition with heparin for FGF-2. We observed an increasing tendency of M₇ derivatives to compete with heparin with the degree of sulfation. Interestingly, highly sulfated M₇ revealed a relative affinity up to 10%, while the one of ^BCDH drastically dropped to 0.2%. However, M₆ derivatives did not seem to interact with FGF-2 no matter their degree of sulfation.

The compounds were then submitted to the mitogenic assay on BAF32 cells. The figure 19 summarizes the effect of sulfated (cyclo)maltooligosaccharides (at different concentrations) on BAF32 cell

proliferation. Positive controls were evaluated with heparin and heparin mimetic and negative controls were performed for all “GAG mimetics” (two first assay of each graph, black and grey).

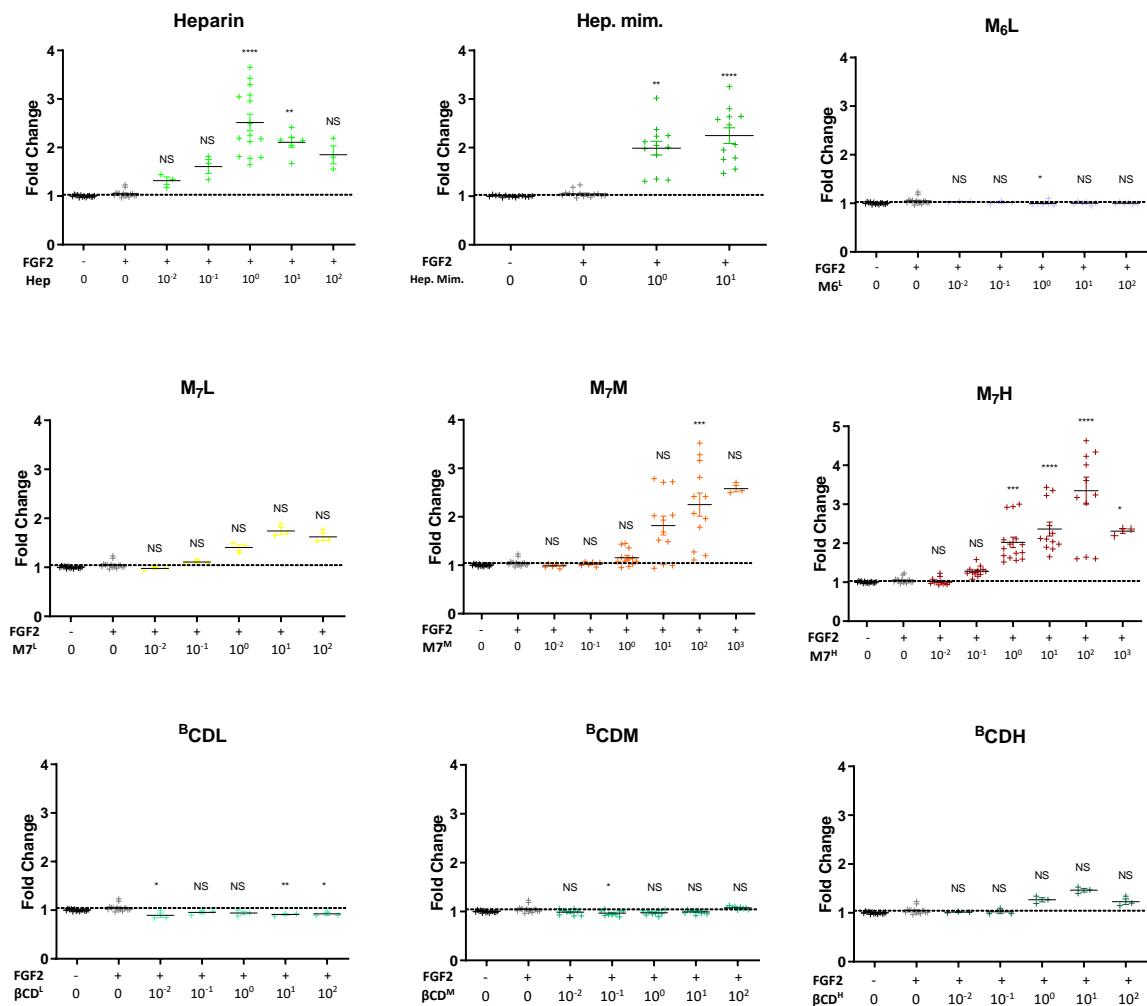


Figure 19. Proliferation tests of sulfated (cyclo)maltooligosaccharides on BAF32 cells in synergy with FGF-2. Effect of increasing doses (from 10^{-2} to 10^2 $\mu\text{g/ml}$) of (cyclo)maltooligosaccharides with FGF-2 were tested and compared as fold change of proliferation rate of the cells alone. Independent experiments were performed with at least duplicate wells per condition, and graphs represent the values obtained by conditions, means and standard deviations. P values were calculated using an ordinary Kruskal Wallis test followed by pairwise comparisons using the Dunnett test compared to CT conditions with FGF-2 alone (NS no significance; * <0.05 ; ** <0.01 ; *** <0.001 ; **** <0.0001).

Cells alone exhibited a fluorescence set at one, the base value of proliferation (without induction or inhibition of cell proliferation). As expected, the absence and the presence of FGF-2 alone did not influence the proliferation rate of cells (negative controls, NS). The concomitant presence of FGF-2 with a natural GAG or a GAG mimetic (heparin and heparin mimetic, positive controls) allowed the significant increase of proliferation by 2-3-fold change for mass concentration around 1-10 $\mu\text{g/mL}$.

No induction of cell growth was noticed for M_6 derivatives with this assay. As observed previously with the ELISA test, no binding seemed to occur with FGF-2 while this step is required for the activation of

a receptor. M₇L did not significantly increase cell proliferation. M₇M and M₇H both allowed BAF32 cell growth at comparable rates of proliferation but at higher concentrations than positive controls (2-4-fold changes). The rate of cell proliferation then decreased when higher concentrations of “GAG mimetics” were added as can be seen with M₇H derivative. ^BCD derivatives globally did not modulate cell proliferation (although ^BCDH seemed to slightly induce cell growth).

2.2.2.3 Biological assays with VEGF

The second HBP tested by our collaborators was VEGF. As for FGF-2, the ELISA tests allowed to calculate the mean IC₅₀ value of sulfated (cyclo)maltooligosaccharides when they were acting as competitors of heparin for VEGF. Their mean IC₅₀ values are presented with their standard deviation on the Table 6.

Compounds	Heparin	Hep mim	M ₇ L	^B CDL	M ₆ L	M ₇ M	^B CDM	M ₆ M	M ₇ H	^B CDH
Mean IC ₅₀ for VEGF (µg/mL)	0.06	0.32	100.5	132	NC	2.9	3	NC	1.6	2
	±0.02	±0.05	±56.3	±25		±1.4	±0		±1.2	±1

Table 6. Mean IC₅₀ values of sulfated (cyclo)maltooligosaccharides and their standard deviations with VEGF. Measures were conducted in triplicates (n=3) for compounds except for M₇M, M₇H & ^BCDM where n=6

As for FGF-2, no competition was observed for sulfated M₆. Compared to the other IC₅₀ values, those of lightly sulfated compounds were the highest. More interesting values were obtained with sulfated M₇ and ^BCD in the order of some µg/mL.

As previously, a graph representing the relative affinity of each “GAG mimetics” with VEGF and with a heparin mimetic as the reference value is presented on the Figure 20 by using the mean IC₅₀ values presented on the Table 6 (preliminary results).

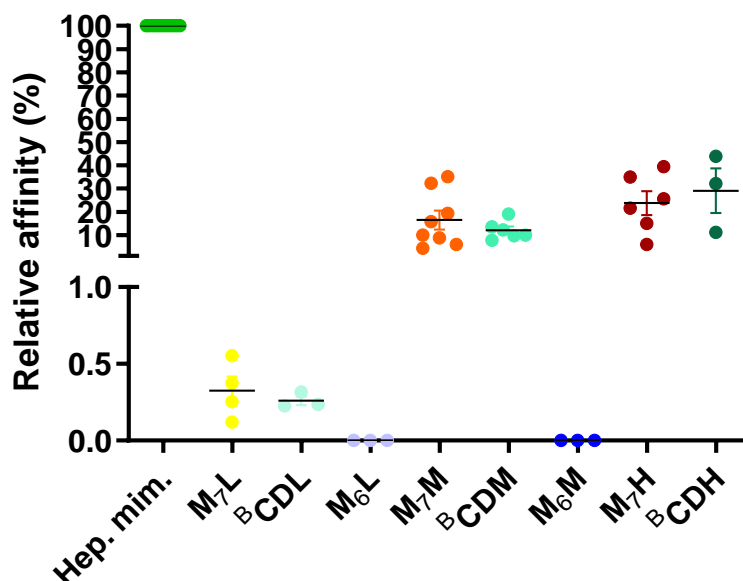


Figure 20. Graphic presenting the relative affinity of sulfated (cyclo)maltooligosaccharides for VEGF. The IC₅₀ value of Heparin mimetic was used as reference of 100% of binding affinity, to calculate the % of binding affinity of all other tested molecules for VEGF.

While M₇L, & ^BCDL seem to have relative affinity values of about 0.3%, no competition with heparin was observed for M₆L and M₆M. As for FGF-2, M₆ derivatives did not seem to interact with VEGF. Moderately sulfated seven-unit compounds (M₇M & ^BCDM) had similar relative affinities of about 10-15%. And highly sulfated M₇ and ^BCD exhibited relative affinities of about 30%. We therefore observed an increasing inhibition tendency for sulfated M₇ and ^BCD with the degree of sulfation.

Sulfated (cyclo)maltooligosaccharides were then submitted to the mitogenic assay on HUVEC cells in synergy with VEGF, as illustrated on the figure 21.

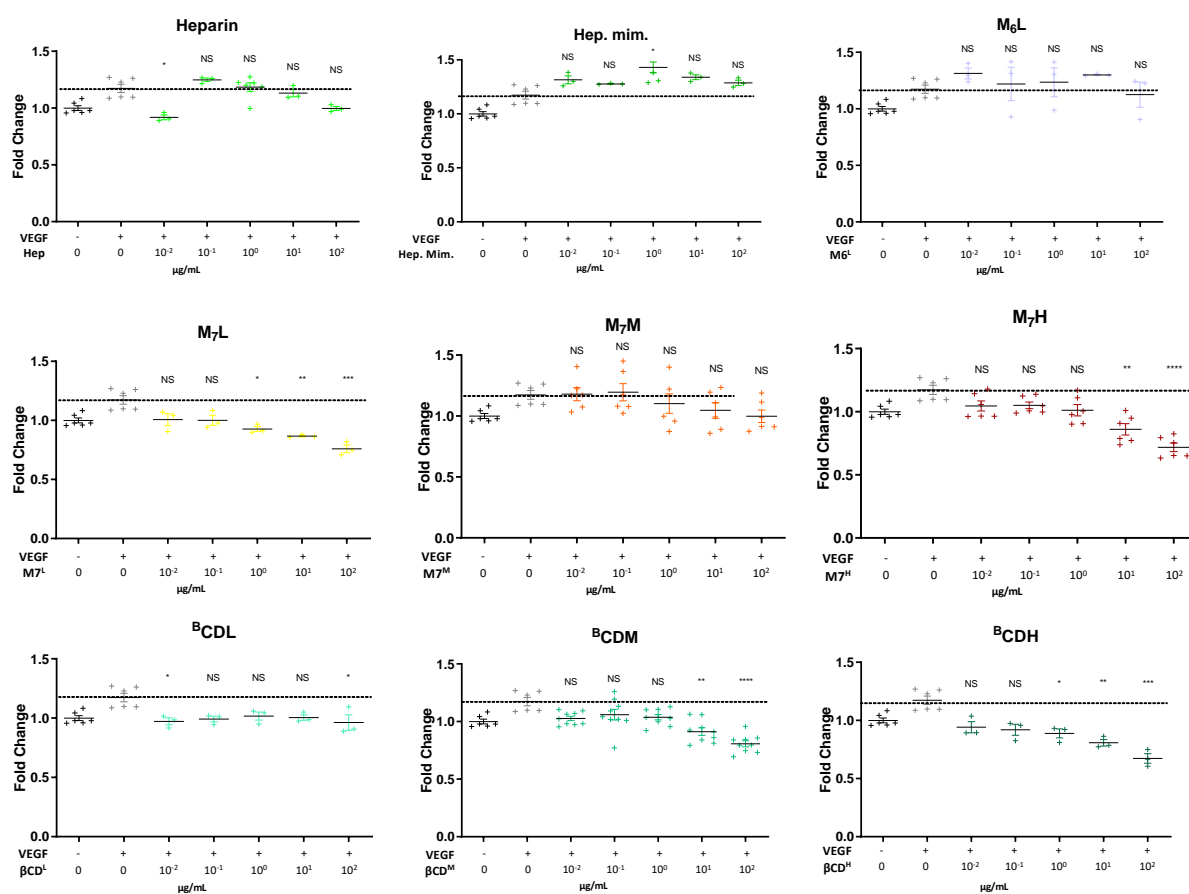


Figure 21. Proliferation tests of sulfated (cyclo)maltooligosaccharides on HUVEC cells in synergy with VEGF. Effect of increasing doses (from 10⁻² to 10² µg/ml) of (cyclo)maltooligosaccharides with VEGF were tested and compared as fold change of proliferation rate of the cells alone. Independent experiments were performed with at least duplicate wells per condition, and graphs represent the values obtained by conditions, means and standard deviations. P values were calculated using an ordinary Kruskal Wallis test followed by pairwise comparisons using the Dunnett test compared to CT conditions with VEGF alone (NS no significance; * <0.05; ** <0.01; *** <0.001; **** <0.0001).

The proliferative rate of cells alone was reported as one, and was slightly increased 1.2 times when VEGF alone was added to the culture media (activation of the receptor by formation of the ternary complex HSPG/VEGF-R/VEGF). The concomitant presence of VEGF with a natural GAG (heparin) at high doses seemed to inhibit cell growth. On the opposite, the heparin mimetic did not seem to have any effect on cell growth.

M₆ did not elicit cell growth inhibition, which may be explained by the absence of binding of M₆ to VEGF (observed with the ELISA assay on VEGF). All M₇ derivatives exhibited cell growth profiles similar to heparin. At low doses, no significant effect was observed but M₇L and M₇H seemed to inhibit significantly cell proliferation by 1/3 at high concentration ($p < 0.001$ for M₇L and $p < 0.0001$ for M₇H at $10^2 \mu\text{g/mL}$). Similar profiles (as for heparin and sulfated M₇) for ^BCD derivatives were observed. It is noteworthy to mention that the inhibition seemed to increase as a function of the sulfation degree of ^BCD derivatives. On the contrary to mitogenic assays on BAF32 for FGF-2, here no effect of the structural conformation was observed : cell proliferation was modulated similarly by seven-unit linear and cyclic compounds.

2.2.2.4 Interpretation of the results obtained with FGF-2 and VEGF

Two growth factors belonging to the family of HBPs, FGF-2 and VEGF, were used to evaluate the potential biological effects of sulfated (cyclo)maltooligosaccharides previously synthesized and characterized (see [2.2.1](#)).

The preliminary ELISA tests allowed to determine the mean IC₅₀ values of each compounds and then to evaluate their relative competition with heparin for each growth factor. For some compounds, only two or three values could be measured, explaining the absence of statistical analysis for these tests. More assays are currently being performed.

The mitogenic assay of BAF32 or HUVEC cells allowed to evaluate the effect of sulfated compounds at various concentrations on the cell proliferation. Preliminary results of the assays may allow to observe interesting features and dress hypotheses with the furnished data.

First, the M₆ series did not seem to compete with heparin for binding of each growth factor (to be confirmed) and did not have any effect on neither on BAF32 and HUVEC cell growth. This demonstrates that these compounds may not be able to efficiently mimic biologically active GAG structures for the tested growth factors. On the contrary, the M₇ series elicited biological properties while only bearing one more glucose unit and having similar sulfation degrees. It may be speculated that if the binding does not depend on the sulfate density present on the compounds, this one-sugar-unit difference between maltohexaose and maltoheptaose derivatives is necessary for the binding for FGF-2 and VEGF, and that the minimal length for recognition and binding to these growth factors is seven units.

Then, the proliferation tests on BAF32 and HUVEC cells allowed to emphasize the importance of the concentration of GAGs and their mimetics to mediate biological processes. For the ones that elicited a response in synergy with FGF-2, BAF32 cell growth increased with the concentration of “GAG mimetics” until a maximum accordingly to heparin and heparin mimetic profiles. Passed this point, the proliferation decreases. This might be due to the excess of “GAG mimetics” in the medium which could limit the FGF-2 recognition by its receptor. Some “GAG mimetics” therefore mediated BAF32 cell

growth in a dose-dependent manner. For the “GAG mimetics” that elicited a response in synergy with VEGF, no significant inhibition was observed at low doses, but a strong inhibition rapidly emerged at higher doses. This effect has previously been documented in literature.^{154,157} Cell growth could therefore be inhibited by some “GAG mimetics” also in a dose-dependent manner. It is noteworthy to mention that an effect of the degree of sulfation (for M₇ and BCD derivatives) on the modulation of cell proliferation was observed. Interestingly, an effect of structural conformation (sulfated M₇ vs ^BCD) was observed for BAF32 mitogenic assay but not in the case of HUVEC cell proliferation.

It is known that BAF32 cell growth can only be enhanced by the presence of free-form heparin/heparan sulfate or their mimetics (as abundant chondroitin sulfate was shown to have no effect on the proliferation of cell deficient in HSPGs)⁶⁰. Some of M₇ derivatives allowing significant cell proliferation, it may be postulated that such compounds act specifically as mimetics of heparin or heparan sulfate type GAGs.

In addition, some compounds such as ^BCDL for VEGF and ^BCDM for FGF-2 seemed to be able to bind to the corresponding growth factors but did not elicit biological response by modulating cell proliferation. This illustrates the fact that the effect of GAG mimetics on both ligands and receptors may depend on two events: the affinity of GAG mimetics for the ligand and/or receptor (binding) and the ability to induce a biological response (activation). In other terms, to be recognized as GAGs for the cell surface receptor, our sulfated compound must bind to it and elicit a response.

Finally, the effect of cyclomaltooligosaccharides was observed to drastically change between FGF-2 and VEGF (no significant effect vs inhibition of cell growth respectively). ^BCD derivatives had almost no binding with FGF-2 and no significant effect on cell proliferation, but strongly interacted with VEGF by inhibiting cell growth as much as sulfated M₇. This may illustrate the difference of binding motif needed for each growth factor.

More generally, highly sulfated maltooligosaccharides exhibited higher binding for HBPs and elicited more intense biological responses (cell proliferation) than lightly sulfated ones. The reason for that is for the moment unclear. It may be thanks to the presence of more sulfate groups on glycans or because for higher sulfation degrees, more sulfating reagent was introduced allowing the sulfation of less accessible positions on sugars that might be important for the binding with these growth factors (difference between sulfation degree and sulfation pattern).

These preliminary hypotheses and tendencies are still to be confirmed by more studies. In particular, our compounds remain to be tested for their synergistic effects with other FGFs members such as FGF-8 and FGF-18 (that contribute to cartilage homeostasis). For example, the role of FGF-8 has been identified as a catabolic mediator in rat and rabbit articular cartilage, but its precise biological impact on human adult articular cartilage remains unknown.¹⁵⁸

2.3 Conclusion

We performed and optimized the protocol for randomly sulfated (cyclo)maltooligosaccharides whose structures are presented on the figure 22 below.

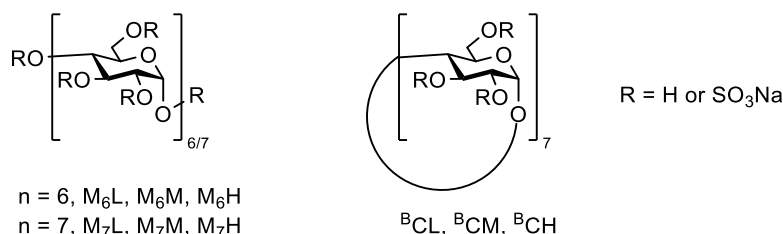


Figure 22. Structures of sulfated (cyclo)maltooligosaccharides

After being characterized by 1H NMR, SEC-MALS, FT-IR and elemental analysis, the compounds were submitted to biological assays. Two tests were carried out to evaluate their ability to mimic natural GAGs by using FGF-2 and VEGF as HPBs. The ELISA tests allowed to measure the relative affinity of sulfated (cyclo)maltooligosaccharides for growth factors, and thereby their binding abilities. The mitogenic assay on BAF32 and HUVEC cells allowed to attest their efficacy by eliciting cell growth. Globally, moderately and highly sulfated exhibited more affinity and elicited more intense responses than lightly sulfated derivatives. The minimal chain length required for biological activity was estimated at seven sugar units. Binding affinities and cell growth were different depending on the linear or cyclic conformation of oligosaccharides. More biological tests still remain to be carried out to confirm these assumptions.

Selective chemistry on β -cyclodextrins may allow us to confirm the role of sulfate groups position and DS with the preparation of selectively sulfated maltooligosaccharides.

CHAPTER 3

Obtention of regioselectively sulfated glycomimetics starting from β -cyclodextrin

3.1 Introduction

3.1.1 General

Cyclodextrins (or cyclomaltooligosaccharides) are a series of non-reducing cyclic oligomers composed of α -1,4-linked D-glucofuranosyl units in 4C_1 conformation, a 'chair' conformation where the superscript number indicates the carbon atom located above the reference plane of the chair and the subscript number the one located below, this plane being made up by C-2, C-3, C-5 and the ring oxygen. Their natural production is realized by enzymatic degradation of starch by cyclodextrin glycosyl transferases.¹⁶⁹

The most common cyclodextrins are formed of six, seven or eight repetitive units (respectively α -, β - and γ -cyclodextrins). Their C_n -symmetry (n being the number of glucose units)¹⁷⁰ allows them to possess two structural rims formed by primary hydroxyls (OH-6) and secondary hydroxyls (OH-2 & -3).

β -cyclodextrins (B CD) are the most commonly employed for chemical modification. Their structure, presented on the figure 23, is particularly rigid because of intramolecular hydrogen bonding between OH-2 and OH-3, explaining their poor solubility in water¹⁷¹.

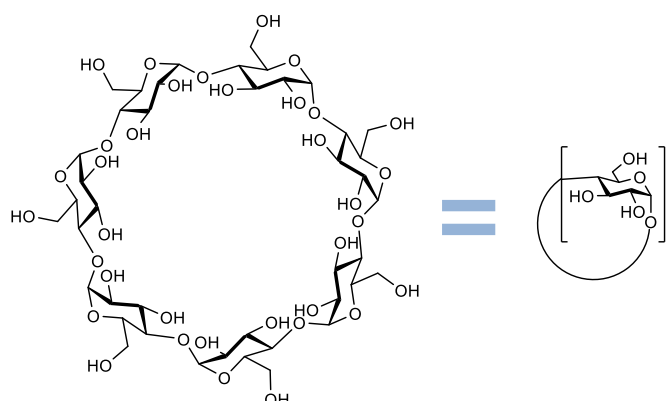


Figure 23. Structure of β -cyclodextrin (cyclomaltoheptaose)

These cyclic macromolecular structures bear abundant hydroxyls (18, 24 or 31 in α -, β - and γ -cyclodextrins respectively), that may nonetheless be categorized. Primary hydroxyls (OH-6) are the most accessible and the most nucleophilic. OH-2 are the most acidic ($pK_a=12.2$)¹⁷² because the hydrogen of the hydroxyl is involved in a hydrogen bonding with the anomeric oxygen, and finally OH-3 are the least reactive. In spite of that, preparation of regioselectively modified cyclodextrin derivatives still needs strategies based on protecting groups. Their modification remains a challenge for organic chemists due to statistical factors imposed by the great number of hydroxyls but was nevertheless reviewed.^{173,174}

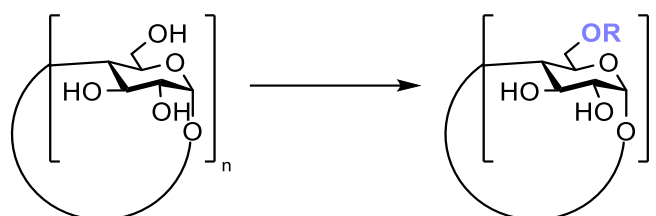
Cyclodextrins being versatile molecules, they find applications in a plethora of fields ranging from drug-delivery systems¹⁷⁵⁻¹⁷⁷ to supramolecular chemistry^{178,179}.

In our project, we were interested in the synthesis of selectively *per*-modified cyclodextrin derivatives in the goal of preparing well-defined and biologically active GAG and PG mimetics. Moreover, structural analysis of such compounds by ^1H & ^{13}C NMR may be easier thanks to their C_n symmetry.

3.1.2 *Per*-modification on primary hydroxyls (OH-6)

Primary hydroxyls (OH-6) may be directly modified selectively in the presence of electrophiles such as alkyl or silyl halides. To do so, the use of a weak base or a basic solvent allows to neutralize the formed acid and to avoid cyclodextrin degradation, which is less stable in acidic conditions.

Thanks to their nucleophilicity, they may be more selectively functionalized than their secondary counterparts. Some examples of modified α - and β - cyclodextrins will be provided in the following, as shown on the Table 7 below.



	OR	Yield for n=6	Yield for n=7
(a)	OTs	12%	/
(b)	Br	93%	80%
	I	/	88%
(c)	OTBDMS	75%	83%
(d)	OTr	62%	55%

Table 7. Selective functionalization of primary hydroxyls of cyclodextrins

Direct *per*-tosylation of primary hydroxyls of α -cyclodextrin in pyridine by Umezawa provided a poor yield of 12% (Table 7a)¹⁸⁰. *Per*-halogenation is also a popular way to modify the primary rim of cyclodextrins. The conversion of native cyclodextrin into its *per*-bromo or -iodo derivative may be carried out in DMF in the presence of triphenylphosphine with bromine or iodine, and affords high yields from 80 to 93% (Table 7b)¹⁸¹. 6-halogenated and -tosylated derivatives are a class of important precursors as they render carbon 6 particularly electrophile.

More commonly employed *per*-silylation is usually employed with the widely used *tert*-butyldimethylsilyl chloride. The reaction leads to high yields of 75% of product for α -cyclodextrin and 83% for β -cyclodextrin (Table 7c)^{182,183}.

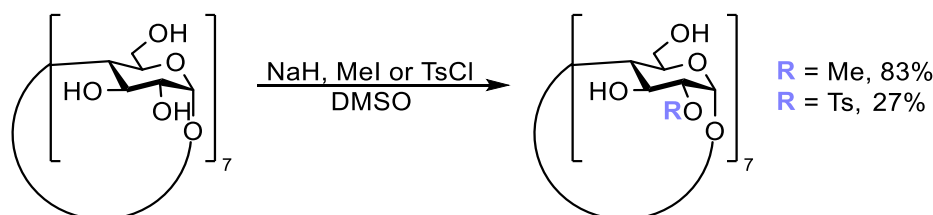
The introduction of trityl group on OH-6 positions was achieved by Zhang et al.¹⁸⁴ under harsh conditions: native cyclodextrins were reacted with trityl chloride at 80°C, and extra portions of reagent were added each day for five days. Moderate yields of compounds were obtained (Table 7d).

Selective per-methylation^{182,183} or *per*-azidation¹⁸⁵ of the primary rim of cyclodextrin could however not be obtained starting from native cyclodextrins.

3.1.3 *Per*-modification on secondary hydroxyls (OH-2)

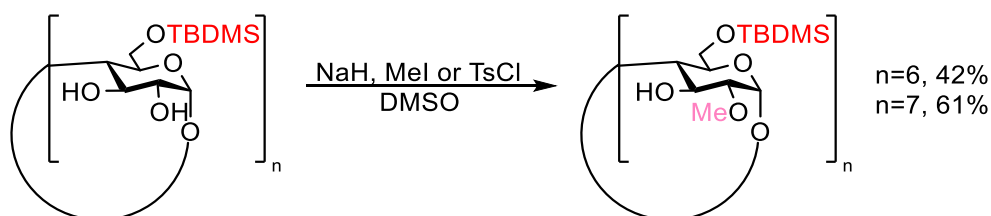
Selective functionalization of secondary hydroxyls of cyclodextrins seems way more challenging than for primary hydroxyls. This is caused by the steric hindrance of this rim (twice more hydroxyls than primary rim) and hydrogen bonding between OH-2 and -3 allowing less flexibility for the structure. The modification of OH-2 relies on their acidic properties.

Per-methylation and -tosylation of OH-2 positions was achieved by reactive native cyclodextrins with sodium hydride and methyl iodide or tosyl chloride¹⁸⁶ providing *per*-2-methylated and *per*-2-tosylated β -cyclodextrin with 83% and 27% respectively, as shown on the Scheme 2.



Scheme 2. Selective functionalization of secondary hydroxyls OH-2 of β -cyclodextrin

However, *per*-2-*O*-modifications are often accompanied by modifications on OH-6 as well. To solve this problem, primary alcohols are masked in advance in most of the synthetic strategies. As an example, the primary rim is often protected by TBDMS groups. Next, OH-2 may be selectively methylated using a strong base. By doing so, Takeo et al. obtained 42% of *per*-6-*O*-tert-butyldimethylsilyl-*per*-2-*O*-methyl α and β cyclodextrins with 42 and 61% respectively^{182,183}, as displayed on the Scheme 3.



Scheme 3. Selective methylation of secondary hydroxyls OH-2 of silylated β -cyclodextrin

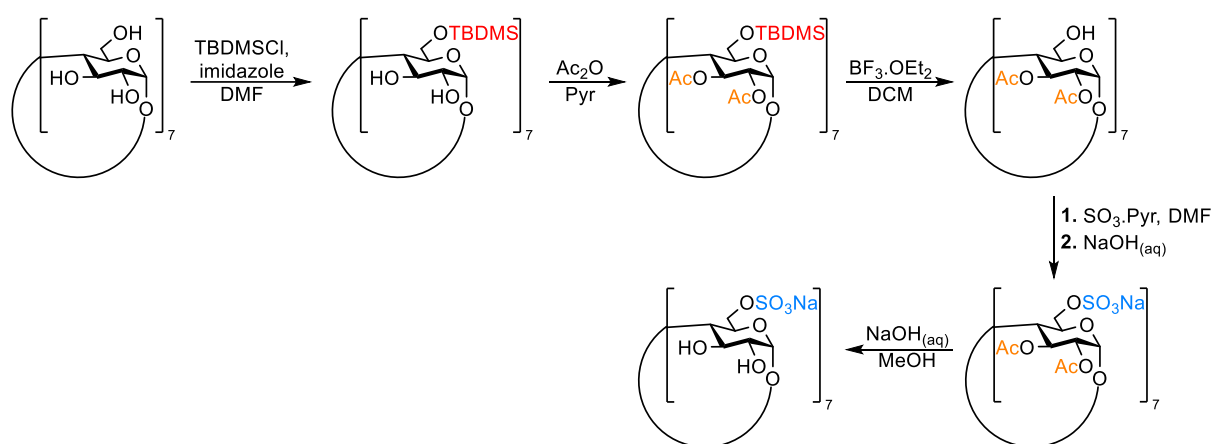
Instead of methylation, Ward et al.¹⁸⁷ realized a selective benzylation, allylation or ethylation of OH-2 positions after TBDMS group protection of primary rim with low to moderate yields (52%, 43% and 30% respectively after column purification).

For our project, we were inspired by many multi-step synthesis strategies described in literature for the preparation of a library of regioselectively sulfated glycomimetics based on (cyclo)maltooligosaccharides.

3.1.4 Some examples of regioselectively sulfated β -cyclodextrins preparation

We were interested in the synthesis of regioselectively sulfated *per*-(2 and/or 3 and/or 6)-*O*-sulfo β -cyclodextrin derivatives. Such compounds were extensively developed by Vigh group for capillary electrophoresis. Some usual synthetic pathways extracted from literature will be showed in the following.

Synthesis of *per*-6-*O*-sulfo β -cyclodextrin was reported as shown on the Scheme 4 by his group.¹⁸⁸ First, they *per*-functionalized OH-6 positions with TBDMS groups thanks to Takeo & co-workers' procedure.¹⁸³ Secondary alcohols were then *per*-acetylated and silyl groups were removed with boron trifluoride diethyl etherate in DCM. Next, primary alcohols were selectively sulfated with sulfur trioxide pyridine complex in DMF and finally, acetate groups were removed. The compound was then used in capillary electrophoresis for separation purposes thanks to its differential complexation properties. Later, the compound was reused as a reference to compare randomly highly sulfated cyclodextrin between them.¹⁸⁹



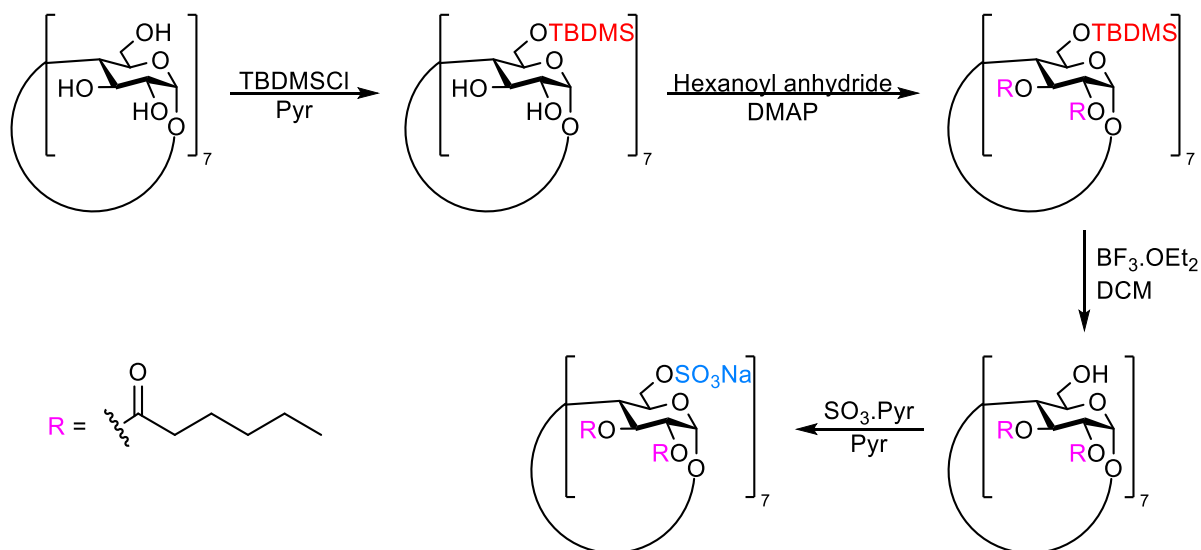
Scheme 4. Preparation of *per*-6-*O*-sulfo β -cyclodextrin by Vincent et al.¹⁸⁸

The group also reported the synthesis, one year later, of *per*-2,3-*O*-dimethyl-6-*O*-sulfo β -cyclodextrin by a similar approach involving protection of secondary hydroxyls by methyl groups instead of acetates for better enantioselectivity.¹⁹⁰

Bols group¹⁹¹ prepared a cyclodextrin-based artificial enzyme by synthesizing mono-, di- and hepta-modified cyclodextrin derivatives. Similarly to the previous strategy developed above (Scheme 4), *per*-2,3-*O*-diacetate β -cyclodextrin was prepared according to Takeo group procedure.¹⁸³ The intermediate was then sulfated with sulfur trioxide pyridine complex in pyridine with 92% yield, and was finally

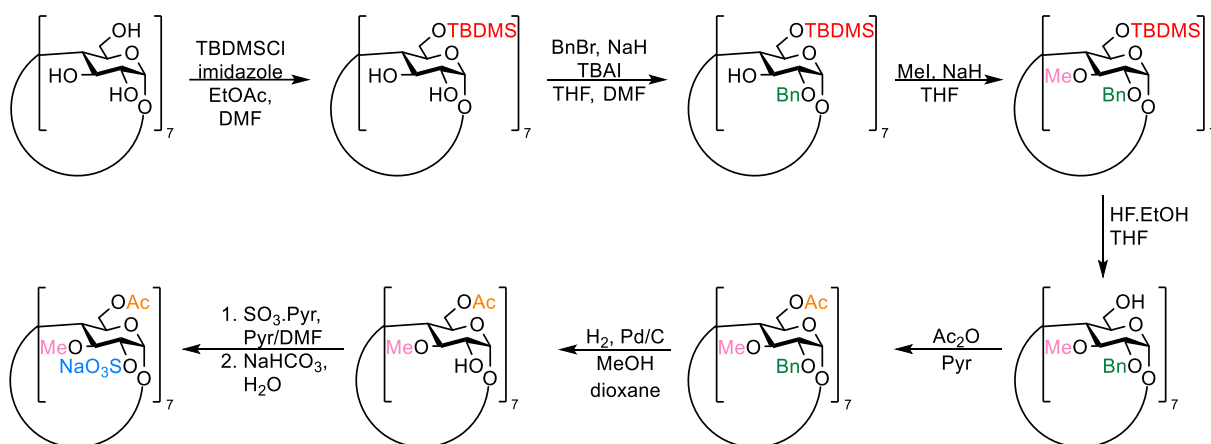
deprotected by using sodium methoxide in methanol to provide the final *per*-6-*O*-sulfo β -cyclodextrin with 88% yield.

Parrot-Lopez group¹⁹² reported the synthesis of less common derivatives with the preparation of amphiphilic acyl-sulfated β -cyclodextrins as shown on the Scheme 5 below. The pathway used for these derivatives was similar to previous reported strategies.



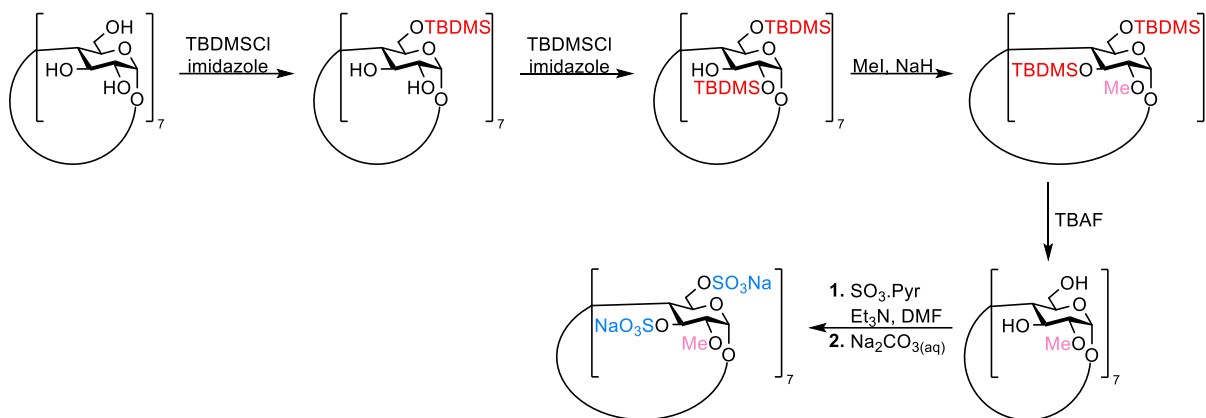
Scheme 5. Preparation of *per*-6-*O*-sulfo-2,3-*O*-acyl β -cyclodextrin by Parrot-Lopez and col.¹⁹²

Other than 6-sulfo β -cyclodextrins, other positions could be sulfated. As an example, Tutu & Vigh¹⁹³ prepared a *per*-2-sulfo β -cyclodextrin derivative as shown on the Scheme 6 below still for capillary electrophoresis. The strategy began by the classic *tert*-butyldimethylsilylation. A selective benzylation on OH-2 and subsequent methylation of OH-3 were carried out. The TBDMS groups were then replaced by acetate groups, being more stable in the acidic conditions used for sulfation that took place right after deprotection of OH-2.



Scheme 6. Preparation of *per*-2-*O*-sulfo β -cyclodextrin by Vigh group¹⁹³

In the continuity of preparing chiral resolving agents, the same group investigated the preparation of *per*-3,6 cyclodextrin sulfates.¹⁹⁴ They explored the *tert*-butyldimethylsilylation of OH-6 and -2 as reported earlier.^{195,196} In methylating conditions, silyl groups of OH-2 migrated on OH-3, allowing OH-2 to be *per*-methylated. Next, desilylation and subsequent sulfation afforded the compound *per*-3,6-*O*-sulfo-3-*O*-methyl β -cyclodextrin as shown on the Scheme 7.



Scheme 7. Preparation of *per*-3,6-*O*-sulfo-3-*O*-methyl β -cyclodextrin by Vigh group¹⁹⁴

To the best of our knowledge, preparation of a library of selectively sulfated β -cyclodextrins was only reported once by Baumann & Rys¹⁹⁷ in the goal of conceiving heparin mimics. In this paper, the authors tested the ability of compounds to bind with cationic dyes. They prepared six regioselectively sulfated derivatives still containing their hydroxyl protecting groups (structures on Figure 24). The synthesis of the orthogonally protected intermediates has not been described and full sulfation could only be achieved for *per*-2-*O*-sulfo and *per*-6-*O*-sulfo cyclodextrins.

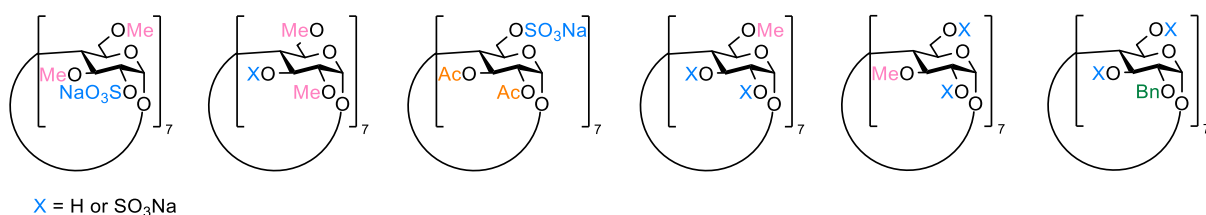


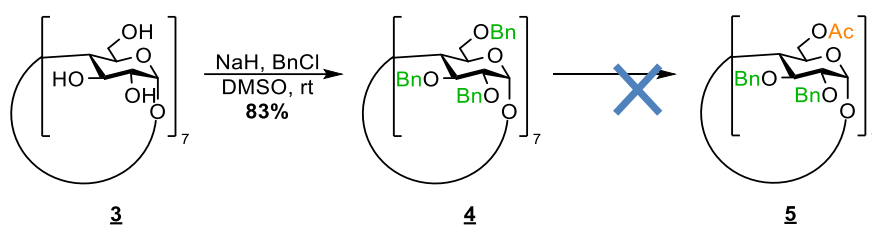
Figure 24. Scope of regioselectively modified β -cyclodextrin sulfates by Baumann & Rys¹⁹⁷

In our project, we also targeted the preparation of six regioselectively sulfated β -cyclodextrin derivatives fully deprotected as glycosaminoglycan mimetics in order to evaluate the influence of the position of sulfation, the charge density and the cyclic conformation of the maltooligosaccharide on its interaction with GAG-binding proteins.

3.2 Results and discussion

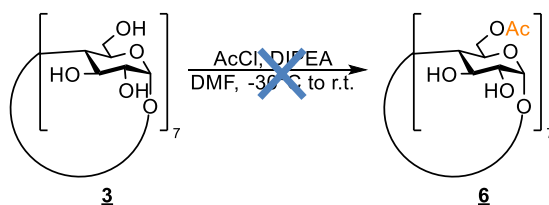
3.2.1 Preparation of regioselectively sulfated β -cyclodextrins

The starting point of the whole synthesis consisted in selectively targeting the primary hydroxyls of β -cyclodextrin. The very first idea was to protect all hydroxyls, and realise a subsequent selective reaction on primary ones as illustrated on the Scheme 8. *Per*-benzylation was carried out according to Lecourt et al. procedure¹⁹⁸ with sodium hydride and benzyl chloride in DMSO. Liquid chromatography on silica gel afforded 83% of pure compound **4** on a 10-gram scale whose ¹H NMR spectrum was in accordance with literature. Next, the goal was to replace benzyl groups on position 6 (OH-6) by acetate groups with TMSOTf in acidic conditions as reported in literature.^{187,199} Despite multiple tries, the reaction afforded a plethora of products impossible to isolate.



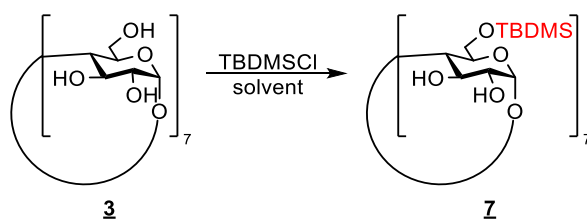
Scheme 8. *Per*-benzylation of β -cyclodextrin and subsequent *per*-6-*O*-acetylation

A direct *per*-acetylation on OH-6²⁰⁰ was later tried with ethyldiisopropylamine and acetyl chloride in DMF as shown on Scheme 9. Almost no conversion was observed by TLC plates after one night.



Scheme 9. Selective *per*-6-*O*-acetylation of native β -cyclodextrin

Finally, the preparation of *per*-6-*O*-*tert*-butyldimethylsilyl β -cyclodextrin **7** was investigated as starting point of all products. This crucial step was achieved by reacting β -cyclodextrin with *tert*-butyldimethylsilyl chloride at room temperature as shown on the Table 8.



Entry	Equiv. TBDMSCl	Base	Solvent	Scale	Result
(a)	8	Pyridine		100 mg	No reaction or mixture
(b)	8	Imidazole	DMF	100 mg	No reaction
(c)	12	Pyridine		100 mg	Mixture
(d)	8.4	Pyridine		100 mg	Mixture
(e)	8.4	Pyridine		1 g	18-34% yield
(f)	8.4	Pyridine		13 g	83% yield

Table 8. Selective *per-6-O-tert*-butyldimethylsilylation of native β -cyclodextrin

The first trial (Table 8a) was carried out accordingly to Fügedi's procedure¹⁹⁶ by dissolving 100 mg of previously lyophilized β -cyclodextrin in dry pyridine and adding the silylating reagent (8 equiv. diluted in pyridine) dropwise to the reaction mixture. No transformation was observed based on TLC plates. Addition of activated molecular sieves 4 Å and of extra portions of TBDMSCl and applying very inert conditions resulted in a mixture of silylated products, including a minority of targeted product **7** and under-silylated derivatives no matter the reaction time (from one night to four days). Conditions reported by Takeo et al.¹⁸² were then tested (Table 8b), still on a 100-milligram scale, by mixing β -cyclodextrin and imidazole in DMF, and adding TBDMSCl dropwise. According to the TLC plate, almost no reaction was observed. The procedure of Ashton²⁰¹ that is very similar to Fügedi's¹⁹⁶ yet requiring 12 equivalents of TBDMSCl was also carried out (Table 8c). A mixture of products was still observed on TLC plates, but the addition of extra portions of silylating reagent did not allow any evolution of the reaction and the targeted compound **7** could not be separated from under-silylated products by liquid chromatography on silica gel. Finally, a last protocol reported by Vogel & Murphy²⁰² was tried. β -cyclodextrin was dissolved in pyridine during half an hour, then TBDMSCl was added in one portion without prior dilution in pyridine at room temperature. The reaction, ineffective on small scale (100 mg, Table 8d), showed three spots on the TLC plate after one night on a 1-gram scale (Table 8e). As suggested by the procedure, one extra portion of TBDMSCl was added in the reaction mixture to convert the more polar spot (minor) into an apolar one for better column separation. Purification by liquid chromatography on silica gel provided 18-34% of pure targeted product **7**. Surprisingly, the same reaction carried out on multi-gram scale (Table 8f) provided 83% of pure product, whose ¹H NMR spectrum in CDCl₃ displayed on the figure 25 was in accordance with literature. The two additional peaks at 1.24 and 3.72 ppm were attributed to residual ethanol (part of the solvent system used for chromatography purification).

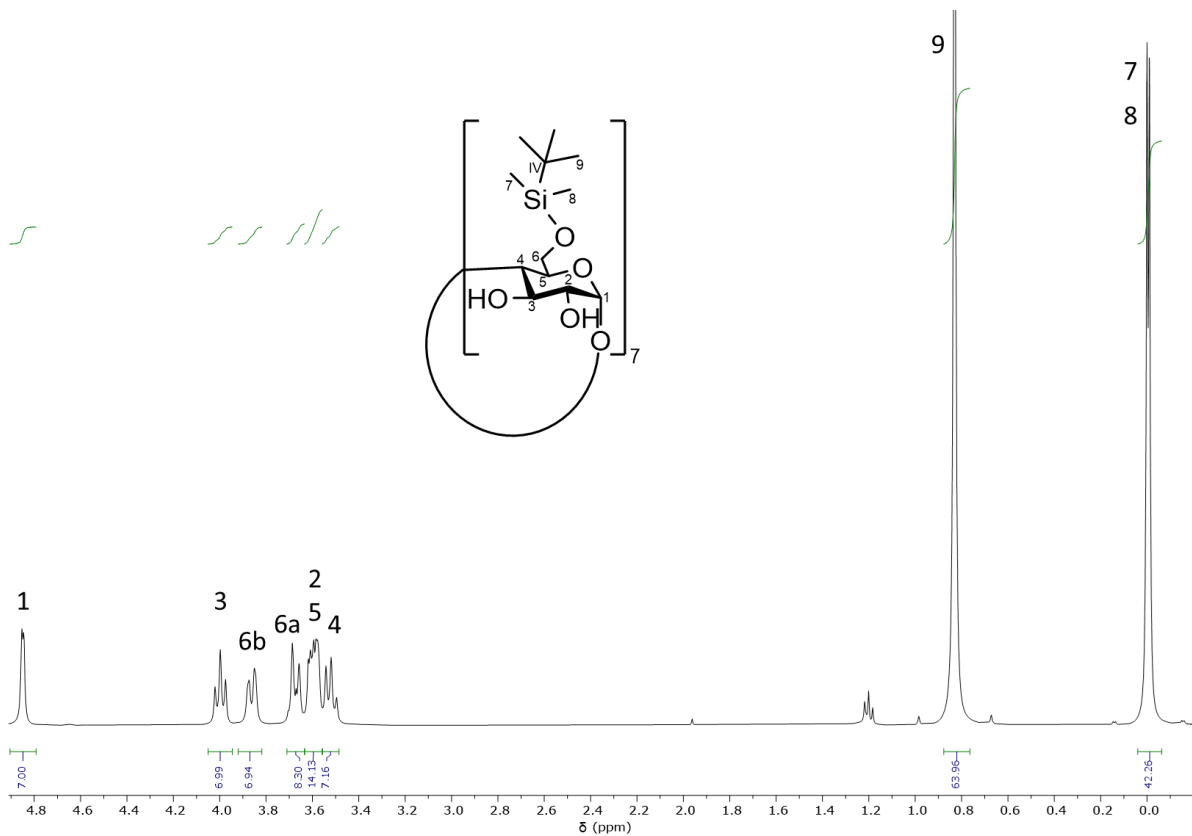
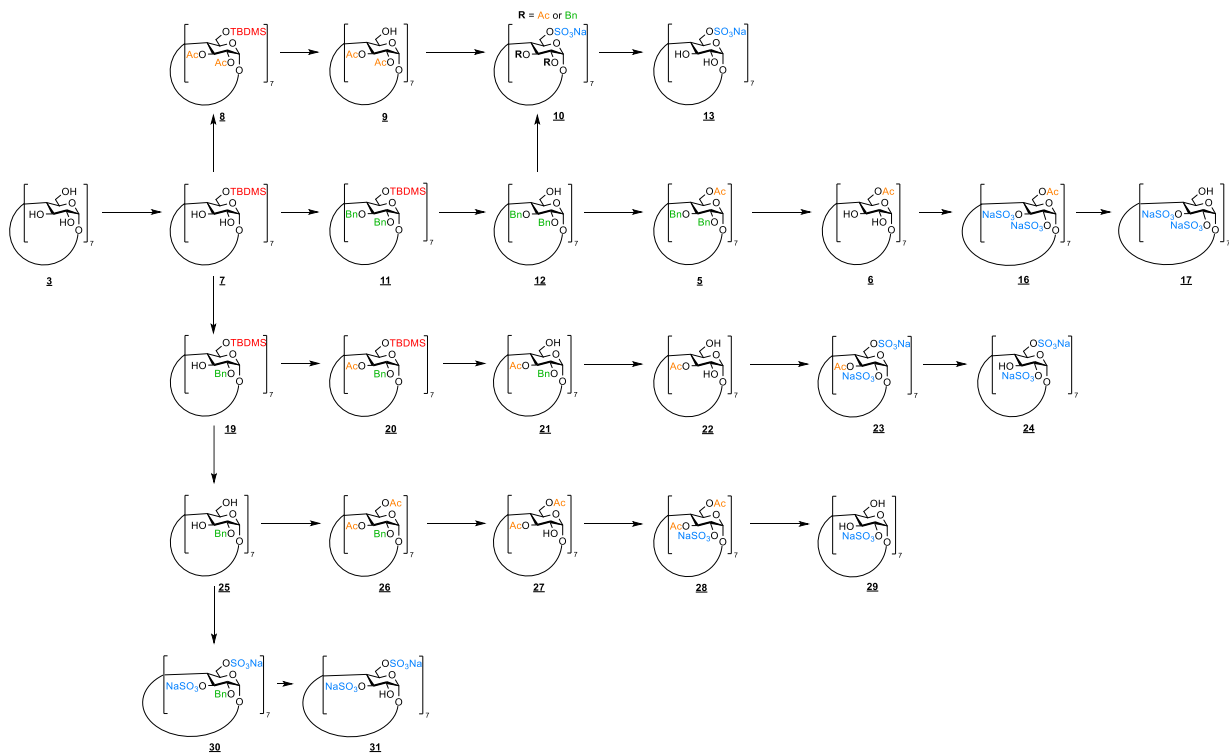


Figure 25. ^1H NMR spectrum of compound **7** in CDCl_3 with its peak integration and attribution

Starting from the key intermediate *per-6-O-tert-butyldimethylsilyl* β -cyclodextrin **7**, the following synthetic routes for obtaining each selectively sulfated derivative were undertaken (Scheme 10).

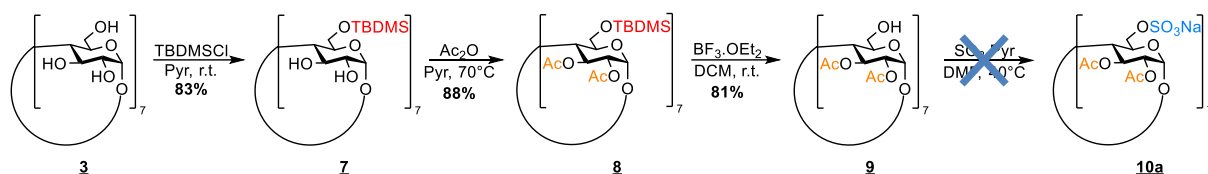


Scheme 10. Synthesis strategy employed for selectively sulfated derivatives (6S; 2S; 2,3S; 2,6S; 3,6S) starting from β -cyclodextrin (also see Appendix)

In the following, the preparation of each sulfated derivative of β -cyclodextrin will be developed.

3.2.1.1 Synthesis of *per*-6S- β -cyclodextrin **13**

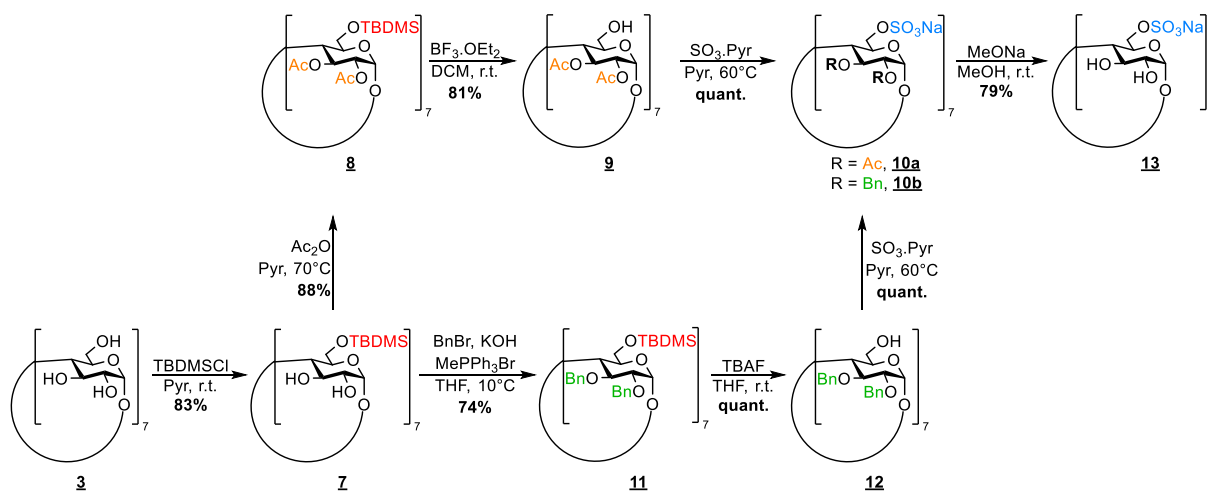
The preparation of *per*-6S- β -cyclodextrin **13**, selectively sulfated on OH-6, was first carried out as illustrated on the Scheme 11.



Scheme 11. Preparation of *per*-6S- β -cyclodextrin starting from β -cyclodextrin *via* acetate protection

Silylated intermediate **7** was *per*-acetylated on OH-2 and -3 by classical conditions, *i.e.* acetic anhydride in pyridine at 70°C²⁰³ providing 88% yield of intermediate **8** after chromatography purification. Next, TBDMS groups were selectively deprotected by using boron trifluoride diethyl etherate in DCM²⁰³ and the intermediate **9** was obtained after chromatography on silica gel with 81% yield. This latter underwent sulfation on OH-6 positions with sulfur trioxide pyridine complex in DMF at 40°C.^{111,191} A column purification followed by ¹H NMR analysis suggested that the product was not fully sulfated, and leaving the reaction longer with or without 2-methyl-2-butene (2M2B), an acid scavenger supposed to capture free protons formed in the medium, led to partial deacetylation according to ¹H NMR analysis. Acidic and non-anhydrous conditions employed for sulfation may have caused hydrolysis of acetate esters.²⁰⁴

In parallel of sulfation trials with acetate groups, another pathway (illustrated on the Scheme 12) was investigated implying the protection of OH-2 and -3 of β -cyclodextrin derivatives by benzyl groups, supposed to be one of the most stable protecting group in acidic and basic conditions, but harder to remove compared to acetyl groups.



Scheme 12. Preparation of *per*-6S- β -cyclodextrin starting from β -cyclodextrin

Intermediate **7** was thereby submitted to *per*-2,3-*O*-benzylation according to the procedure of McKee & Green^{205,206} with sodium hydride, benzyl bromide and tetrabutylammonium iodide as catalyst in THF at reflux. A mixture of products was observed on TLC plate. Other protocols^{198,207} led to similar mixtures. The reactions did not evolve after extra additions of BnBr and NaH as suggested by Bálint et al.²⁰⁸ In their paper, they reported procedures applicable on large scale. Their protocol was then carried out on a 2-gram scale with the use of KOH as base and drying agent and benzyl bromide in THF at 10°C. In this reaction, methyltriphenylphosphonium bromide was also used as phase transfer catalyst²⁰⁹ between the gel formed at 10°C and THF. A mixture of under-benzylated products was also observed on TLC plates (based on the expected retardation factor of the product). However, on the contrary to the previous procedure, extra additions of reagents could make the reaction evolve. Additional portions of KOH and BnBr were therefore added until one main spot on TLC plate was left. The reaction was finally treated after 10 days and 5 additions of reagents. Interestingly, the three very close spots observed in the classic eluent system petroleum ether/ethyl acetate (9/1 v/v) could be efficiently separated in petroleum ether/dichloromethane (5/5 v/v) by liquid chromatography on silica gel. Pure intermediate **11** was afforded with 74% yield. TBDMS groups of this intermediate were then removed with tetrabutylammonium fluoride trihydrate in THF at room temperature over one night.²⁰⁸ A precipitation in water afforded a quantitative yield of intermediate **12**, with no trace of residual TBAF salts based on the ¹H NMR spectrum. *Per*-6-*O*-sulfation of compound **12** was carried out with sulfur trioxide pyridine complex in pyridine at 60°C as reported by Parrot-Lopez & co-workers.¹⁹² After one weekend, the product was purified by chromatography affording compound **10b** with a quantitative yield. Surprisingly, the procedure applied to the acetylated intermediate **9** also provided compound **10a** with a quantitative yield with no removal of acetate groups. Pyridine solvent was found to be a better choice for sulfation. Finally, a deprotection of acetate groups, being more easily removable than benzyl groups, was achieved accordingly to Uccello-Barretta procedure²¹⁰ with freshly prepared sodium methoxide in methanol. The final compound *per*-6-*O*-sulfated **13** was provided pure with 79% yield after GPC purification and was fully characterized (¹H NMR on Figure 26). Final compound *per*-6S-β-cyclodextrin was obtained with an overall yield of 47-48% over 5 steps (depending on the pathway used). It is noteworthy to mention that mass spectrometry of cyclodextrin sulfates was carried out using electrospray ionization although multi-charged compounds were obtained because MALDI ionization caused desulfation of compounds.²¹¹

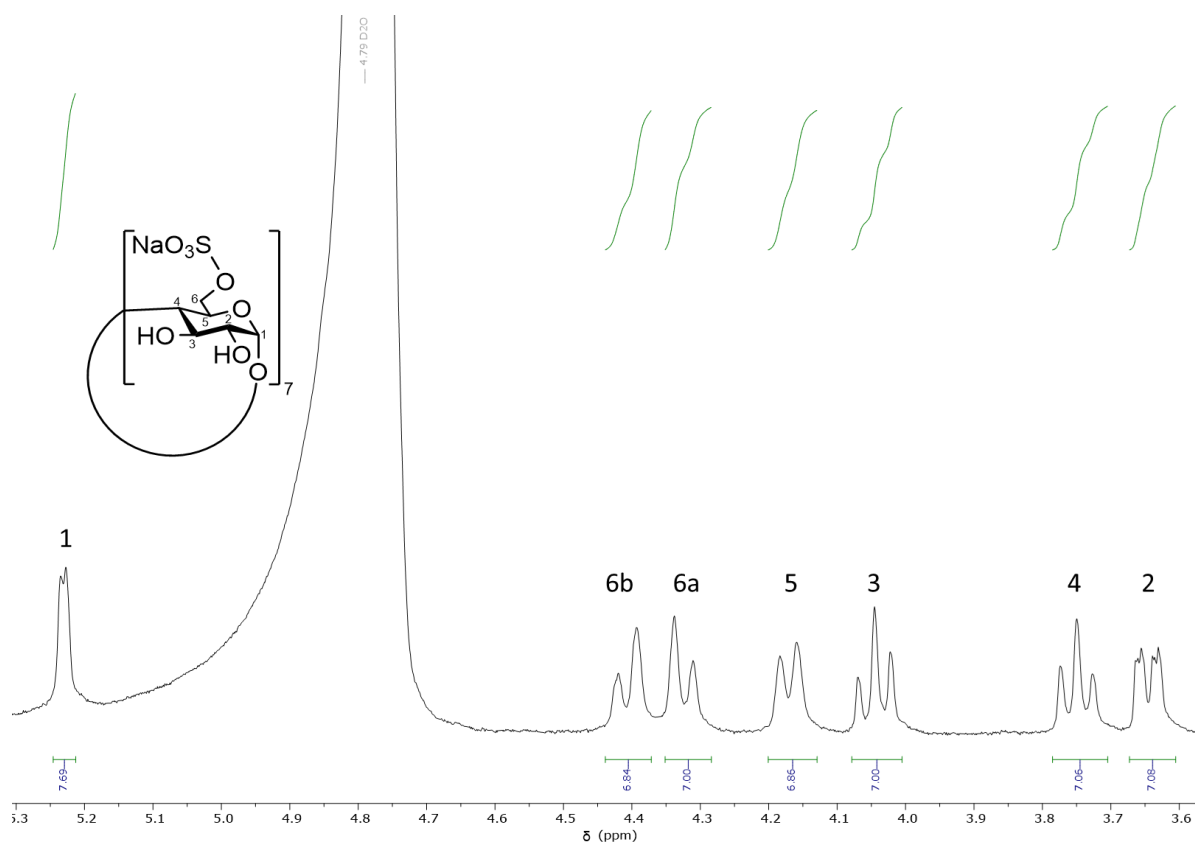
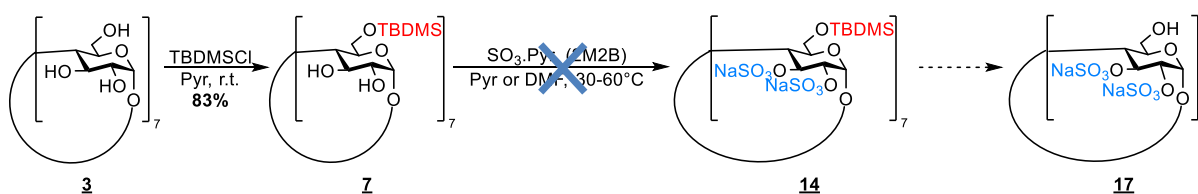


Figure 26. ^1H NMR of compound **13** in D_2O with its peak integration and attribution

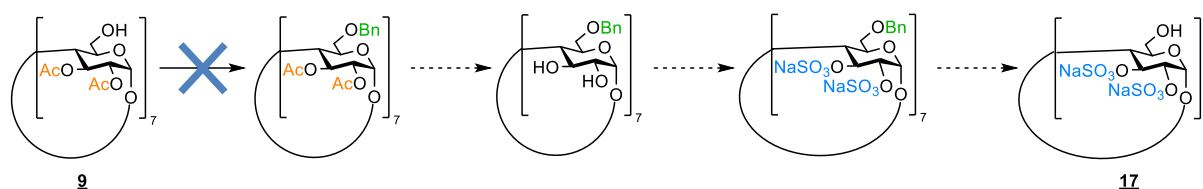
3.2.1.2 Synthesis of *per*-2,3S- β -cyclodextrin **17**

The synthesis strategy of *per*-2,3S- β -cyclodextrin followed is illustrated on the Scheme 13. In the goal of saving synthesis steps, the intermediate *per*-6-*O*-*tert*-butyldimethylsilyl β -cyclodextrin **7** was submitted to sulfation in different conditions previously employed in pyridine or DMF^{111,191,192} with and without acid scavenger 2M2B to afford **14**. Unfortunately, silyl groups were each time partially hydrolyzed due to the acidic medium necessary for sulfation.



Scheme 13. Preparation of *per*-2,3S- β -cyclodextrin **17** via silylation of **7**

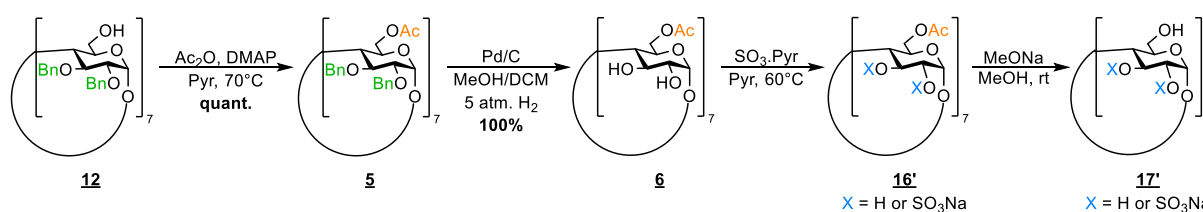
A longer synthesis strategy starting from intermediate **9** previously synthesized (see 3.2.1.1) was investigated where a *per*-6-*O*-benzylation of this intermediate followed by acetate group removal and sulfation of OH-2 and -3, and subsequent benzyl group deprotection would finally provide *per*-2,3S- β -cyclodextrin **17** (Scheme 14).



Scheme 14. Preparation of *per*-2,3S- β -cyclodextrin **17** via benzylation of **9**

The first step consisting in *per*-6-*O*-benzylation of **9** was carried out according to a modified procedure of Meppen et al.²¹². Benzyl chloride, silver oxide (I) and sodium bicarbonate were mixed together with compound **9** and activated molecular sieves 4 Å in anhydrous Tol/DCM (3/1 v/v). A total conversion of starting material into four products was observed on TLC plates, however small quantities were isolated after liquid chromatography on silica gel. Another method based on the *in situ* preparation of benzyl triflate (Oike et al.²¹³) and its subsequent reaction with compound **9** according to a modified procedure of Uemura group¹⁸³ was tested with no conclusive result as well.

As the benzylation reaction seemed to cause problem for β -cyclodextrin derivatives, a similar pathway than above was investigated starting from the intermediate **12**, already benzylated. A *per*-6-*O*-acetylation of this compound, debenylation and subsequent sulfation of OH-2 and -3 and a final deacetylation would afford *per*-2,3S- β -cyclodextrin (Scheme 15).



Scheme 15. Preparation of *per*-2,3S- β -cyclodextrin via acetylation of **12**

Compound **12** was *per*-6-*O*-acetylated in classic conditions with anhydride acetic and DMAP in pyridine at 70°C. MALDI analysis of product **5**, obtained with a quantitative yield, displayed a major peak corresponding to the product $[M+Na]^+$ at $m/z=2713.469$ and a minor peak that would correspond to the product with one missing benzyl group at $m/z=2623.400$. This second and unsymmetrical product not being observed on the 1H NMR spectrum, it was suggested to be formed by mass fragmentation. Next, debenylation of secondary alcohols was carried out by catalytic hydrogenation with palladium on carbon in EtOAc/MeOH (3/5 v/v) in an atmosphere of hydrogen. No conversion was observed based on TLC plates. The reaction was relaunched at 5 atm of H_2 in anhydrous MeOH and a minimum of DCM for one night and afforded the intermediate **6** with a 100% yield after a simple filtration on celite. The sulfation step of this intermediate was conducted in previously described conditions with sulfur trioxide pyridine complex in pyridine at 60°C. After one night, the reaction was treated showing an incomplete sulfation according to the mixture observed on 1H NMR spectrum. The mixture was then resubmitted to sulfation in the same conditions. After two night, no notable change was observed on 1H NMR spectrum.

Less accessible OH-3 positions and steric hindrance of sulfate groups on the secondary rim might explain this incomplete sulfation. Baumann & Rys¹⁹⁷ had also encountered difficulties in preparing some of their *per-3-O*-sulfated derivatives : the mass spectrum (ESI-) indicated the presence of multiple under-sulfated products. The crude **16'** was treated as is, and was deacetylated with sodium methoxide in methanol. Purification by GPC provided compound **17'**, whose average sulfation degree was estimated to be of 1.2, meaning that an average of 1.2 sulfate group are present per unit. According to these results, almost half of the hydroxyls could not be sulfated and the presence of residual ammonium carbonate (GPC eluent) was observed in the lyophilized sample. The results of elemental analysis are presented on the Table 9 below.

Sample	C [wt%]	H [wt%]	N [wt%]	S [wt%]	DS
<i>Per-2,3S</i> - β -cyclodextrin 17	23.975	5.460	5.637	12.912	1.2

Table 9. Degree of sulfation per saccharidic unit of *per-2,3S*- β -cyclodextrin **17** (calculated by elemental analysis).

Although the product was obtained as a mixture, SEC-MALS analysis showed a nice gaussian curve for the retention time of the product (Figure 27), indicating a homogeneous sulfation of the product.

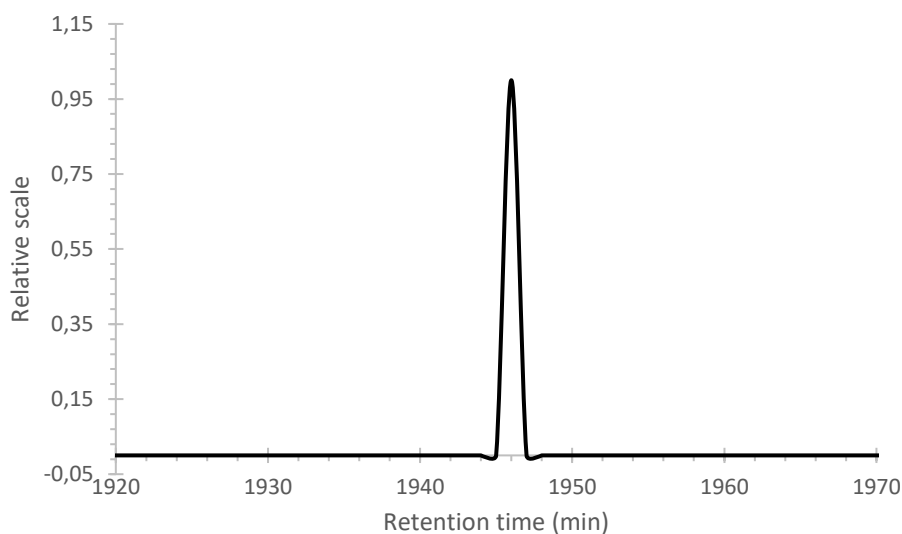
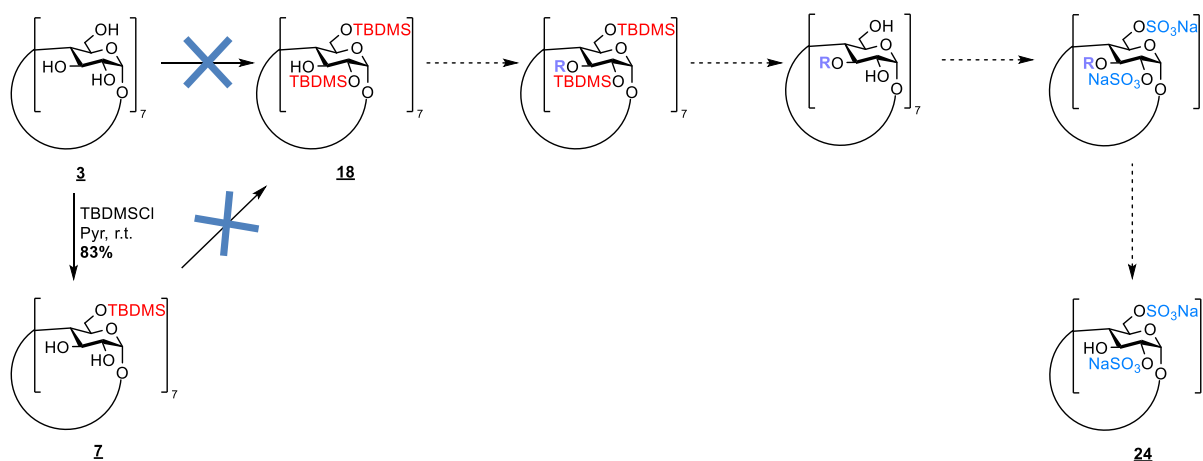


Figure 27. SEC-MALS retention time of *per-2,3S*- β -cyclodextrin **17**

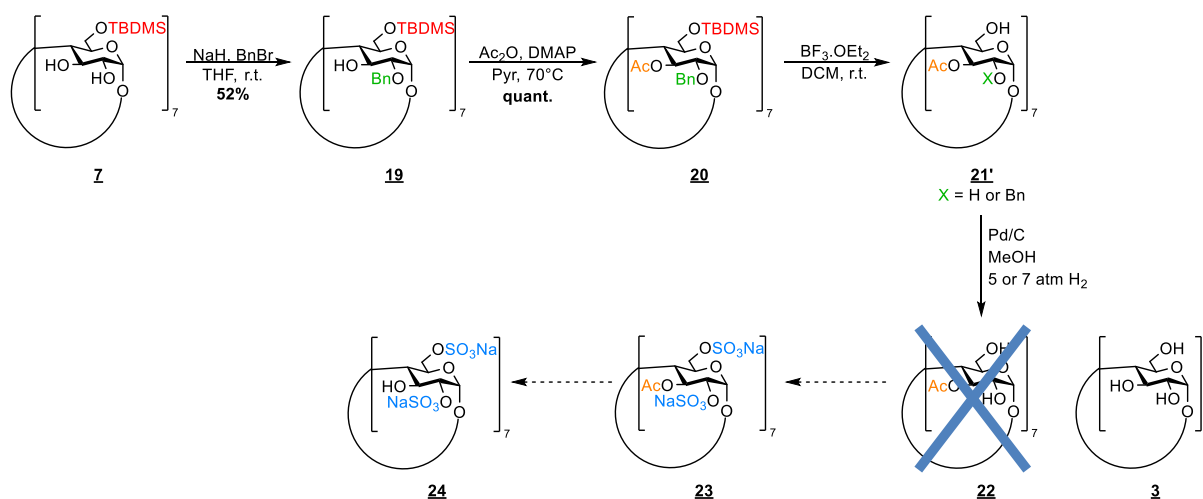
3.2.1.3 Synthesis of *per-2,6S*- β -cyclodextrin **24**

Preparation of *per-2,6S*- β -cyclodextrin **24** was first envisioned by synthesizing *per-2,6-O*-di-*tert*-butyldimethylsilyl β -cyclodextrin **18** (scheme 16). After protection of OH-3 and subsequent removal of TBDMS groups, sulfation and a final deprotection would afford compound **24**.



Scheme 16. Preparation of *per*-2,6S- β -cyclodextrin **24** via silylation of **7** or native β -cyclodextrin

The silylation of OH-6 and -2 was first carried out according to Fügedi procedure.¹⁹⁶ Native β -cyclodextrin was mixed with TBDMSCl and imidazole in DMF at 80°C. After one day, a mixture of products was observed on the TLC plate. Similarly, the protocol described by Ashton²¹⁴ with DMAP in DMF/pyridine at 100°C led to a mixture of under-silylated products. Optimized conditions used for the synthesis of *per*-6-*O*-*tert*-butyldimethylsilyl β -cyclodextrin (see 3.2.1²⁰²) were finally tried, with no success. They were also applied directly on *per*-6-*O*-*tert*-butyldimethylsilyl β -cyclodextrin **7**, but led to the addition of only one more TBDMS group. Faced with the difficulty of obtaining compound **18**, another synthesis strategy was investigated (Scheme 17).



Scheme 17. Synthesis strategy for the preparation of *per*-2,6S- β -cyclodextrin **24**

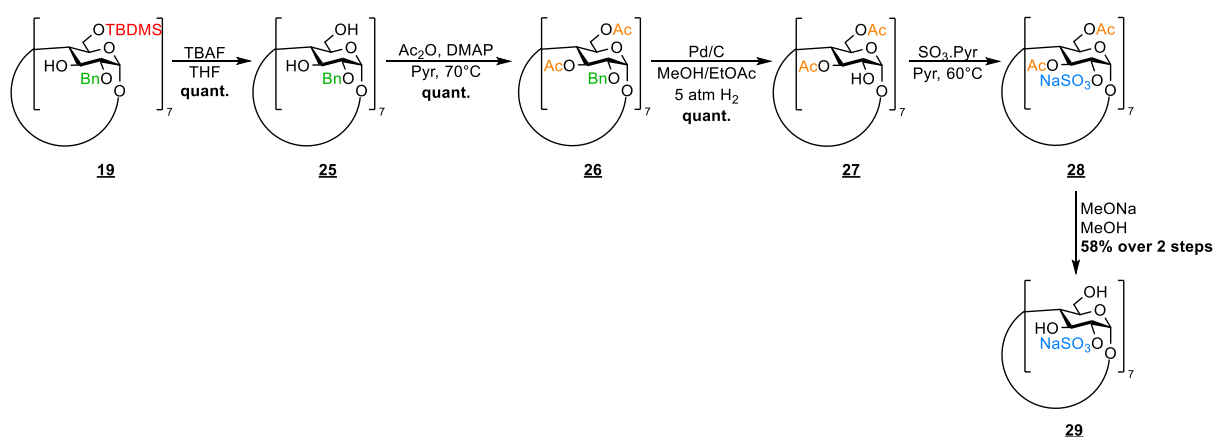
Starting from intermediate **7**, a regioselective benzylation on OH-2 was carried out with barium oxide, barium hydroxide octahydrate and benzyl bromide either in DMF (Takeo et al.¹⁸³) or in H₂O/THF (Hamelin et al.²¹⁵). In both solvent systems, a mixture of products was observed based on TLC plates. More classical conditions reported by Ward et al.¹⁸⁷ using sodium hydride (7.7 equiv.) and benzyl bromide (7 equiv.) in DMF were tried, leading to a mixture of under-benzylated products as well. When

10 equivalents of reagents were mixed in THF with *per-6-O-tert*-butyldimethylsilyl β -cyclodextrin, the targeted product **19** could be isolated from one very similar product (TLC plate) after column purification with 52% yield. Intermediate **19** was then *per-3-O*-acetylated with acetic anhydride, DMAP in pyridine at 70°C with a quantitative yield. Next, a desilylation of compound **20** was carried out with TBAF in THF as reported by Bálint et al.²⁰⁸ According to its mass spectrum, the targeted compound **21** ($m/z=2081.841$) was accompanied by a side-product missing one acetate group ($m/z=2039.842$) likely stemming by the basicity of TBAF. To palliate this problem, boron trifluoride diethyl etherate in DCM²⁰³ was used. Surprisingly, the targeted compound **21** was minor while partially debenzylated derivatives were observed. This mixture of products, named **21'**, submitted to catalytic hydrogenation at 7 atm of H₂ in MeOH with traces of H₂O led to the formation of native β -cyclodextrin **3**. The same result was observed in MeOH with minimum DCM at 5 atm of H₂.

The intermediate **21** (after desilylation) could not be obtained pure and the synthesis could not be finished due to a lack of time.

3.2.1.4 Synthesis of *per-2S*- β -cyclodextrin **29**

Preparation of *per-2S*- β -cyclodextrin **29** was investigated from the intermediate **19** previously synthesized (see 3.2.1.3) as illustrated on the Scheme 19.



Scheme 18. Synthesis strategy for the preparation of *per-2S*- β -cyclodextrin **29**

Compound **19** was desilylated according to Bálint et al. procedure²⁰⁸ with TBAF in THF overnight, affording intermediate **25** with a quantitative yield which was *per*-acetylated on OH-6 and -3 with anhydride acetic and DMAP in pyridine at 70°C. Compound **26** was obtained with a quantitative yield as well and was then debenzylated with palladium on carbon in MeOH with minimum EtOAc under 5 atm of H₂ providing intermediate **27** with a quantitative yield. This latter was then sulfated on OH-2 using sulfur trioxide pyridine complex in pyridine at 60°C and (compound **28**) was subsequently deacetylated with sodium methoxide in MeOH. The crude was then purified by GPC yielding 58% of product **29** over two steps yet slightly accompanied by partially sulfated derivatives (see peaks and

integrations of ^1H spectrum). The symmetry observed of the ^1H NMR spectrum of this final compound **29** displayed on Figure 28 is a proof that the compound was regioselectively sulfated on OH-2 position. The HRMS (ESI-) showed the product at $m/z=422.50959$ corresponding to the $[\text{M}+3\text{H}-7\text{Na}]^+$ form of compound **29**.

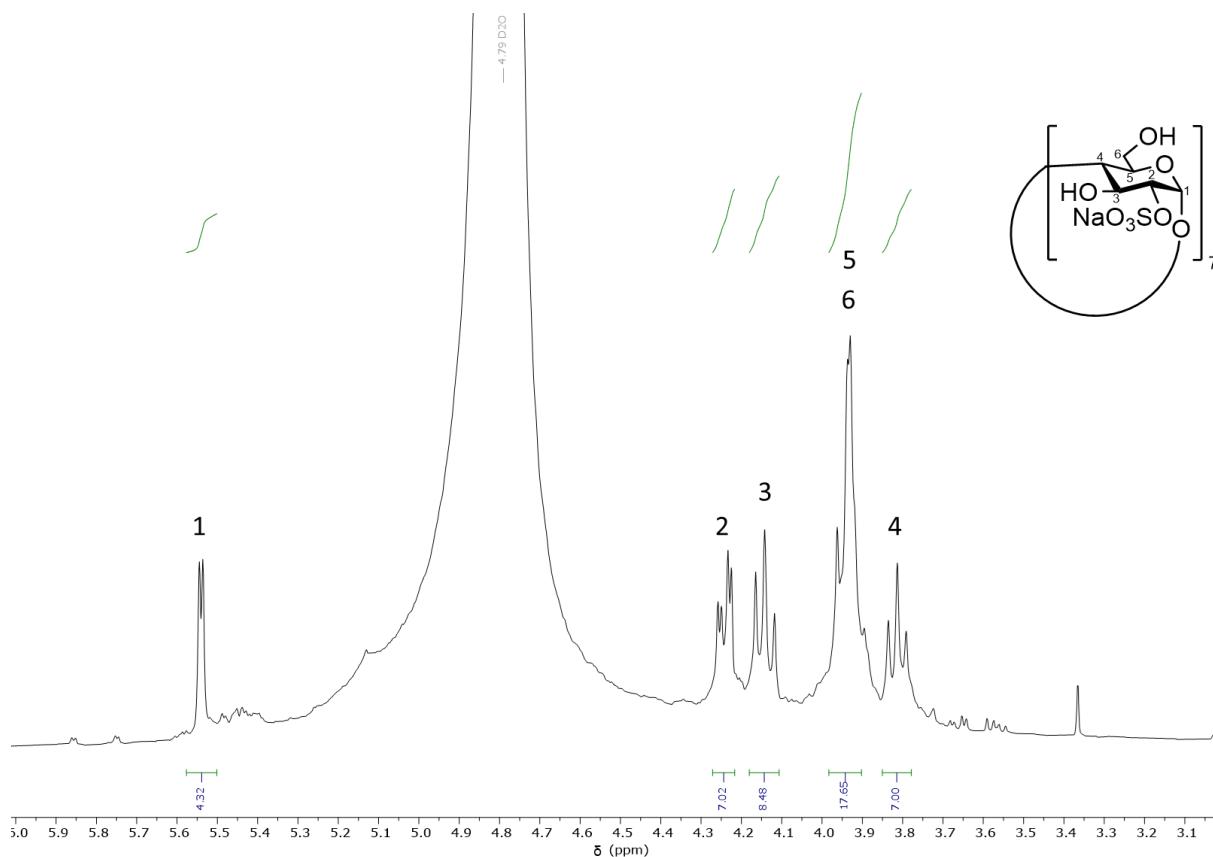
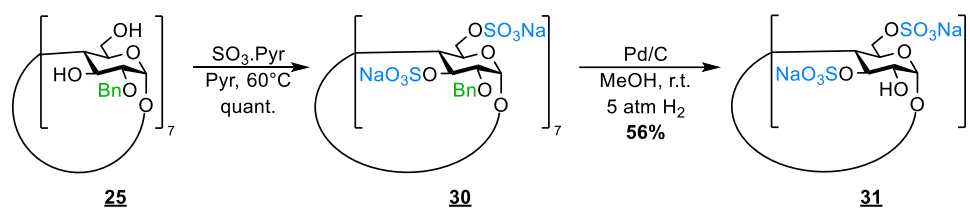


Figure 28. ^1H NMR of compound **29** in D_2O with its peak integration and attribution

3.2.1.5 Synthesis of *per*-3,6S- β -cyclodextrin **31**

Synthesis of *per*-3,6S- β -cyclodextrin **31** could be achieved within two steps starting from intermediate **25** previously synthesized as illustrated by the Scheme 20 below.



Scheme 19. Synthesis strategy for the preparation of *per*-3,6S- β -cyclodextrin **31**

Compound **25**, benzylated on OH-2, was sulfated with sulfur trioxide pyridine complex in pyridine at 60°C , and the product **30**, obtained with a quantitative yield, was debenzylated. The first trials of catalytic hydrogenation were performed in MeOH at atmospheric pressure of H_2 as reported by

Angibeaud & Utile.¹⁹⁹ No conversion was observed on TLC plate. The protocol of Bálint et al.²⁰⁸ using hydrazine carbonate was not effective either: according to TLC plate, slightly more polar and more apolar products were formed during the reaction, suggesting partial debenzylation as well as desulfation. Finally, the procedure requiring palladium on carbon in MeOH under 5 atm of H₂ afforded 56% of compound **31**. The product was purified by HPLC chromatography and sent to biologist collaborators (Gly-CRRET, Créteil). The ¹H NMR spectrum with attribution of this final compound is presented on the Figure 29. Due to the large peak of NMR solvent D₂O, peaks attributed to OH-3 and OH-6b are not clearly visible and all peaks integration are not exact.

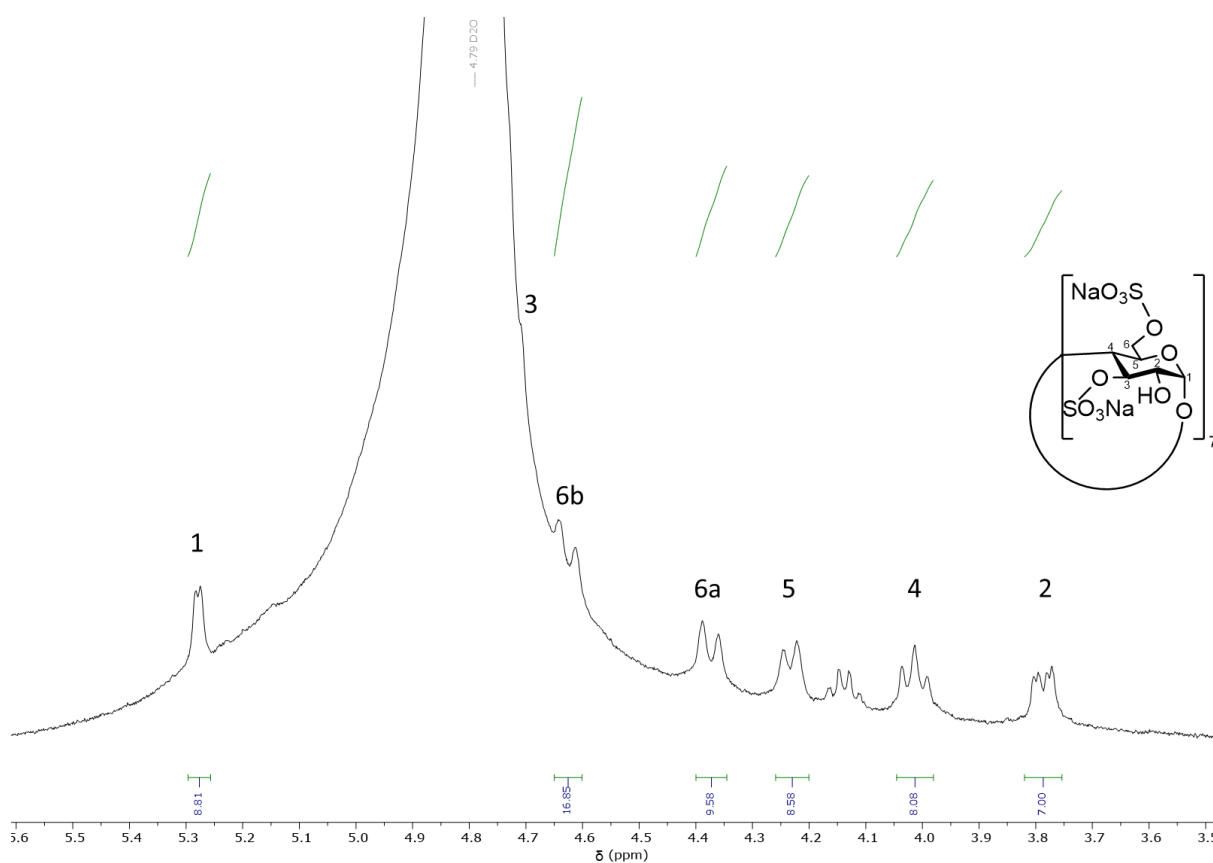
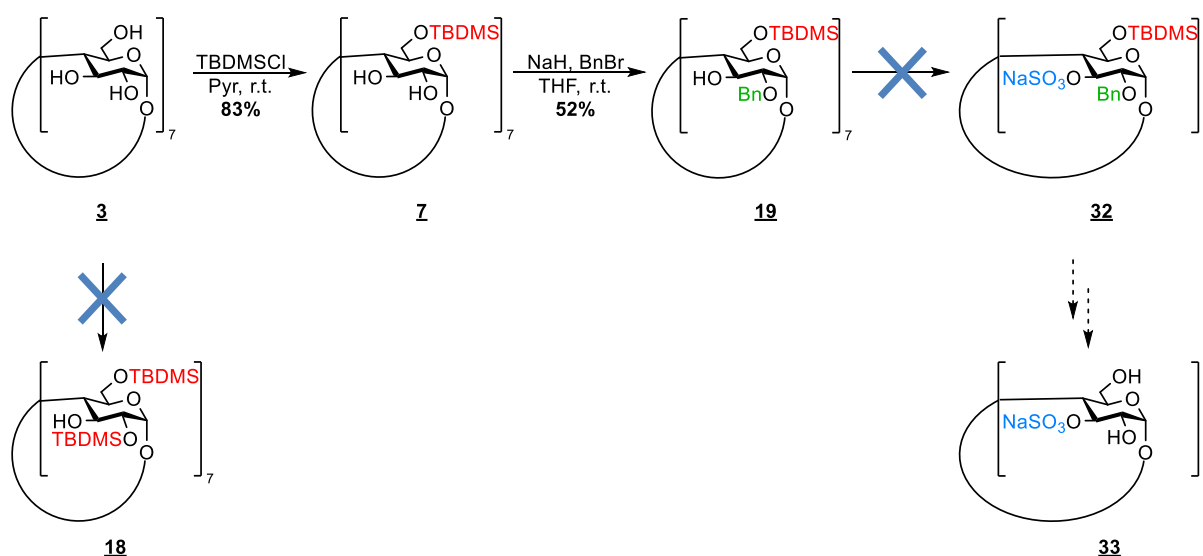


Figure 29. ¹H NMR of compound **31** in D₂O with its peak integration and attribution

3.2.1.6 Synthesis of *per*-3S- β -cyclodextrin **33**

The preparation of *per*-3S- β -cyclodextrin **33** was first investigated with the preparation of *per*-2,6-*O*-*tert*-butyldimethylsilyl β -cyclodextrin **18**. However, as this compound could not be prepared, a longer pathway was then envisioned with the sulfation on OH-3 of the intermediate **19** (Scheme 21). However, as observed in part 3.2.1.2 with the sulfation of intermediate **7**, TBDMSCl groups were found not to be stable enough under the acidic conditions required for sulfation even in pyridine with the addition of acid scavenger. This compound **33** could therefore not be prepared.



Scheme 20. Synthesis strategy for the synthesis of *per*-3S- β -cyclodextrin **33**

3.2.2 Biological assays of regioselectively sulfated β -cyclodextrins

As for randomly sulfated (cyclo)maltooligosaccharides, regioselectively sulfated β -cyclodextrins (structure on figure 30) were submitted to biological assays in order to evaluate the potential effect of the position of sulfation on the biological activity of such compounds.

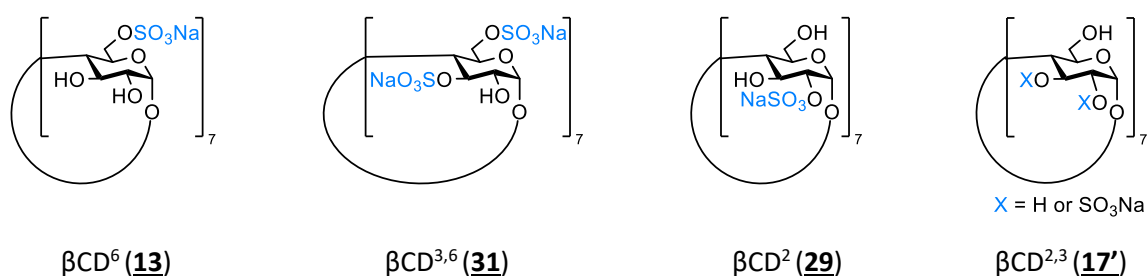


Figure 30. Structure and name of regioselectively sulfated β -cyclodextrins prepared

Preliminary assays were carried out and are presented. Only competitive ELISA tests could be performed (see 2.2.2.1.1 for the principle). The IC₅₀ values of all β -cyclodextrin derivatives were calculated for FGF-2 and VEGF, and are presented on the table 10 below. The values were compared with previously prepared randomly sulfated β -cyclodextrins (see 2.2.1).

($\mu\text{g/mL}$)	^B CDL	^B CDM	^B CDH	βCD^6	$\beta\text{CD}^{3,6}$	βCD^2	$\beta\text{CD}^{2,3}$
IC ₅₀ for FGF-2	1634 ± 767	88 ± 14	465 ± 114	8200 ± 2650	1301 ± 1644	6309 ± 5391	6830 ± 2970
IC ₅₀ for VEGF	132 ± 25	3 ± 0	2 ± 1	198 ± 166	166 ± 154	328 ± 44	7 ± 4

Table 10. IC₅₀ values of randomly and selectively sulfated β -cyclodextrins with FGF-2 and VEGF

The IC₅₀ values for FGF-2 binding were very high and polydisperse regarding to their standard deviation (especially for $\beta\text{CD}^{3,6}$ and βCD^2). For VEGF, IC₅₀s were in the same range order as those of randomly sulfated ones.

The relative affinity of selectively sulfated compounds compared with a heparin mimetic, whose affinity was set as the reference, and randomly sulfated β -cyclodextrin B CDM (used in [CHAPTER 2](#)) are presented on the figure 31 (preliminary results).

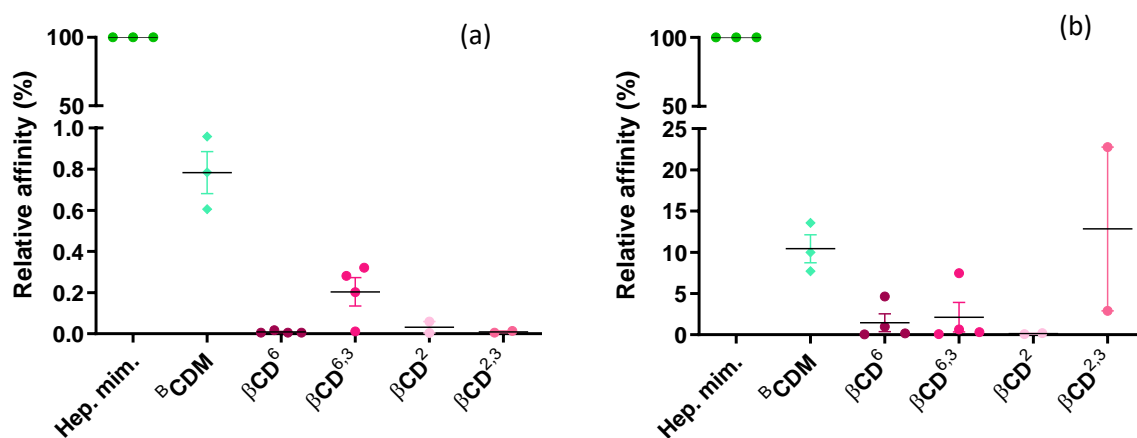


Figure 31. Relative affinity of selectively sulfated β -cyclodextrins with FGF-2 (a) and VEGF (b)

No relative affinity for FGF-2 was greater than 1% for randomly and selectively sulfated β CDs. Concerning VEGF, a negligible relative affinity was observed for β CD⁶ and β CD^{3,6}. Interestingly, partially sulfated compound 2,3S- β -cyclodextrin (β CD^{2,3}) may seem to exhibit a relative competition of about 12%, which is similar to the one of B CDM.

For the moment, no hypotheses neither statistical analysis (enormous error bar & only duplicate measures for some of the compounds) can be made based on these preliminary results. More assays need to be performed to accumulate significant data. In addition, a study of all regioselectively compounds could give a more comprehensive view on the positions interesting for the interaction with FGF-2 and VEGF.

3.3 Conclusion

Six regioselectively sulfated β -cyclodextrin derivatives were targeted in the goal of obtaining cyclic maltooligosaccharides with well-defined sulfation patterns. Starting from a key intermediate, heptakis-(6-*O*-*tert*-butyldimethylsilyl)- β -cyclodextrin **7**, multiple pathways were investigated. To resume, three cyclic derivatives were successfully obtained (6S (**13**), 2S (**29**), and 3,6S (**31**)), one compound could only be partially sulfated (2,3S (**17'**)) and two compounds could not be prepared due to incompatible protecting groups and a lack of time (2,6S (**24**) and 3S (**33**)). The structures of all the products are presented on the Figure 32.

Partially sulfated 2,3S (**17'**), 6S-, 2S- and 3,6S- β -cyclodextrins (**13**, **29** and **31** respectively) were sent to our biologist collaborators (Gly-CRRET, Créteil) for early-stage assays. Depending on the growth factor tested, very different range orders of IC₅₀ were obtained for the compounds. More biological

assays remain to be performed to make assumptions on the role of the position of sulfate groups and the DS.

Regarding the low bindings observed for these cyclic compounds, one of the perspectives would be to open the cyclodextrins by acetolysis to obtain linear maltoheptaoses with well-defined sulfation patterns. These selectively sulfated maltoheptaose may later be compared with the randomly sulfated one to assess the effect of sulfate position on the biological properties of these potential GAG mimetics.

An interesting perspective would be to perform an acetolysis of regioselectively sulfated β -cyclodextrins. By doing so, linear maltoheptaoses with defined sulfation patterns would be obtained, and their biological properties could also be compared to those of randomly sulfated maltoheptaoses.

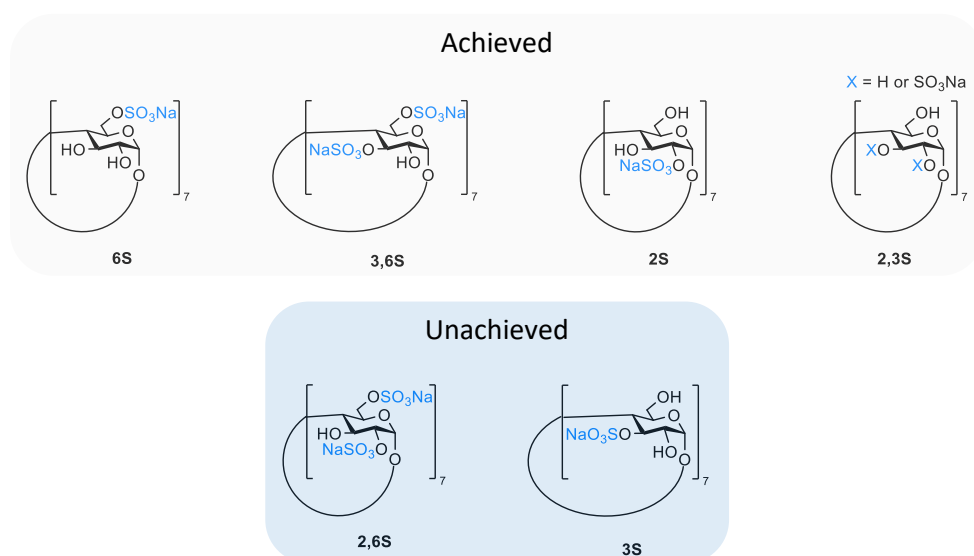


Figure 32. Structure of prepared (*top*) and unachieved (*bottom*) regioselectively sulfated β -cyclodextrins

CHAPTER 4

Reducing-end modification of maltooligosaccharides

4.1 Introduction

All carbohydrates, with few exceptions, possess a reducing end at the extremity of their chains. This reducing end is characterized by the presence a hemiacetal moiety at the anomeric position of the ending closed-form saccharide that is in equilibrium with the opened-ring form generating an aldehyde moiety (“masked” aldehyde). The reducing end anomeric position of each carbohydrate chain is therefore prone to react with nucleophiles, and can be chemoselectively functionalized. It is naturally the target of choice for producing (neo)glycoconjugates. Amine and thiol functions are usually chemically introduced for their ability to react with well-known electrophiles such as activated carboxylic acid, α -halogeno-ketone, activated alkenes and so on. Therefore, glycochemists developed different methods to incorporate an amine or a thiol function at the reducing end of glycans, for which two main pathways can be distinguished, as shown on the figure 33 below.

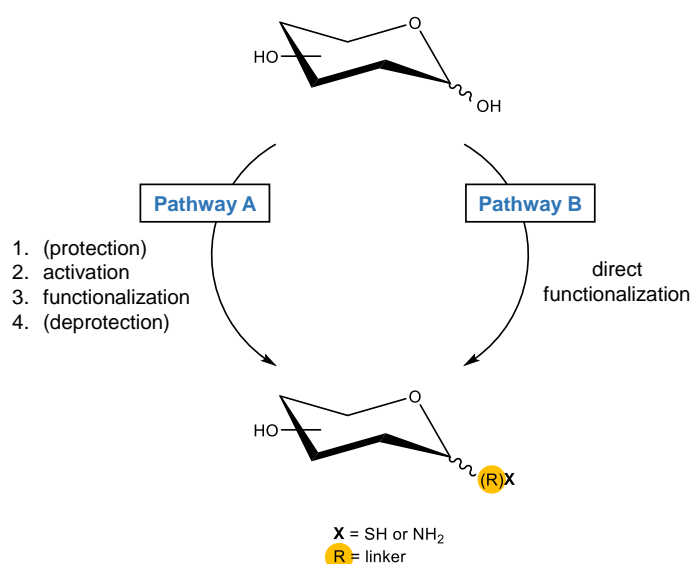


Figure 33. End-functionalization of glycans by two methods

The transformation of the hemiacetal alcohol into an amine or a thiol affording respectively *N*- and *S*-glycosyl derivatives is presented by the **pathway A** (figure 33). This transformation usually passes through a key step of activation of the anomeric position with an activating group. A prior protection of all positions is sometimes performed to activate the anomeric position and protect the other functions. In rare cases, the activation is realized prior to the protection of all other positions. The promoting group is further replaced by the desired function (for all possible methods to form 1-thioglycosides, see review ²¹⁶). This method is well-known for glycosylation reactions of native & non-native glycans. In the cases where no activation is needed, a protection of all other positions is still required.²¹⁷

Besides, the type of glycan end-functionalization might have an effect on the future linkage in the goal of forming (neo)glycoproteins as the proximity between the glycan and the future aglycon seems to be an important point. In Nature, glycans are spaced from protein by the mean of four monosaccharides.

While using the pathway A, no spacing is added during the coupling between the *N*- or *S*-glycosyls and the polymeric structure mimicking a protein core. These disadvantages along with the 2-or-more step procedure to provide these types of compounds limit their use to form complex glycoconjugates.

The **pathway B** (figure 33) consists in the direct attack of a nucleophile onto the anomeric position of unprotected carbohydrate. The nucleophiles commonly used are part of a bis-functionalized linker and are generally introduced at early stages of carbohydrate modification. The introduced linker must thereby be stable enough to withstand the later synthesis steps and its bearing functionality enables the carbohydrate conjugation with a variety of carbohydrates or aglycons. This single-step method does not need any activation and can be performed on unprotected carbohydrates. Along with the conjugation feature, the linker can in some cases provide new functionalities such as UV absorbance, fluorescence or temporary function protection that can easily be removed. Among linker functionalities figure classic functions such as amines, alcohols or activated ester. Other “clickable” groups such as alkene and azide were extensively developed starting from the 90’s due to their biological orthogonality and various applications.²¹⁸

Only direct end-modifications on unprotected carbohydrates were developed in our project, and will be discussed further.

4.1.1 Thiol end-modification of unprotected carbohydrates

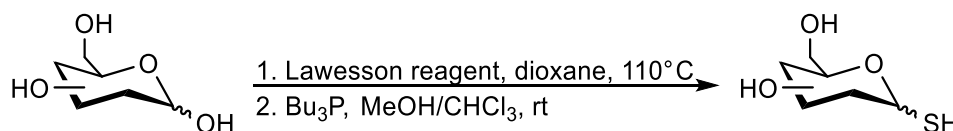
Thiols display a high reactivity toward various substrates as they are more acidic than alcohols, pK_a of 10-11 vs 15-16 for alcohols, and more nucleophilic especially in basic solutions.²¹⁹ They can undergo a wide range of reactions from nucleophilic substitution to radical addition.²²⁰ Regardless of their high reactivity and versatility, thiols suffer from a lack of selectivity when multiple functional groups are present. In addition to their common malodorous and volatile properties, thiol reagents are commercially less available compared to other reagents such as alcohols and amines.^{221,222} More importantly, they are sensitive to oxidation as they can form disulfide bonds.²²² Avoiding side-reactions involving thiol functions including their undesirable sulfation right after their introduction on glycans relies on their protection. But the possibilities for thiol protecting groups are lowered compared to those for alcohols or amines. Some conditions are required for the protecting group to be efficient: (i) it must be easily introduced at the beginning of the synthesis and removed prior to conjugation step, and (ii) it must be tolerant to the other steps.²²³ Various thiol protecting group have been reported especially for solid-phase peptide synthesis, but their introduction or removal needs to be performed in strongly basic, acidic or reductive conditions, which limits their use. Along with the lack of orthogonality, these reactions might be low yielding.

Preparing thiol-glycosides from unprotected carbohydrates have been reported by many groups. In the following, examples from literature to synthesize such challenging compounds were developed.

Yanase & Funabashi²²⁴ developed methods for preparing *tert*-butyl 1-thio- functionalized carbohydrates from unprotected mono- and di-saccharides in trifluoroacetic acid. The thiol-modified products were subsequently per-acetylated. They then evaluated the α : β ratio of each compound by ¹H NMR, affirming a main 1,2-*cis* selectivity. However, no thiol-functionalized carbohydrate was obtained as one anomer (9:1 ratio of 1,2-*cis*:1,2-*trans* in the best case), and the yields were relatively low (34% of one anomer in the best case).

Funabashi et al. also succeeded in preparing diphenyl- and trimethylenethio-dithioacetals of saccharides in trifluoroacetic acid from seven unmodified mono- to tri-saccharides in an effort to provide a generally applicable and versatile approach.²²⁵ The dithio-modified carbohydrates were blocked in their open form configuration, and cleavage of interglycosidic linkages could not be completely avoided. Once again, the products were subsequently per-acetylated after thiol-modified carbohydrate formation.

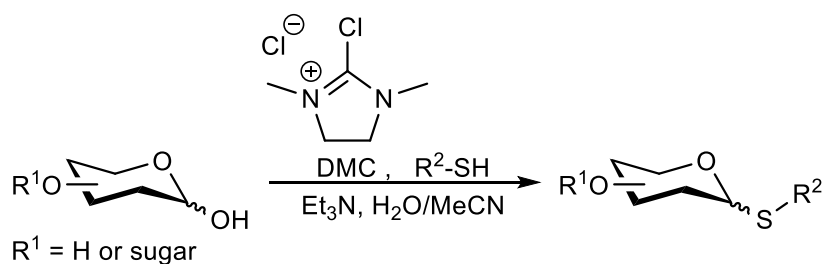
Later, Davis group²¹⁷ reported the use of the Lawesson reagent with monosaccharides such as D-glucose, D-mannose and D-galactose as presented on the Table 13. The reagent was used as an electrophile and source of sulfur allowing the replacement of anomeric alcohol by a thiol function. A subsequent reduction of unwanted disulfide formation was carried out with tributylphosphine yielding 63-71% of pure *S*-glycoside after chromatographic separation. However, this method required extensive heating and long reaction times, and as for previous methods, the final products were obtained as anomeric mixtures. They also needed a careful storage under reductive conditions.



Substrate	Yield	α : β ratio
D-glucose	71%	1:6
D-mannose	63%	α anomer
D-galactose	70%	1:4

Table 11. Synthesis of glycosyl thiols from unprotected monosaccharides with Lawesson reagent

Shoda and co-workers developed the formation of *S*-aryl glycosides from unprotected mono- and di-saccharides by using 2-chloro-dimethylimidazolium (DMC) reagent in basic medium.²²⁶ *S*-aryl glycosides are commonly used as glycosyl donors for glycosylation^{227,228} or as precursors of glycosyl halides or sulfoxides²²⁹⁻²³¹. The aryl 1-thioglycosides were obtained within one hour of reaction with excellent yields (from 90% to quantitative) and main or exclusive β -selectivity (Table 14).



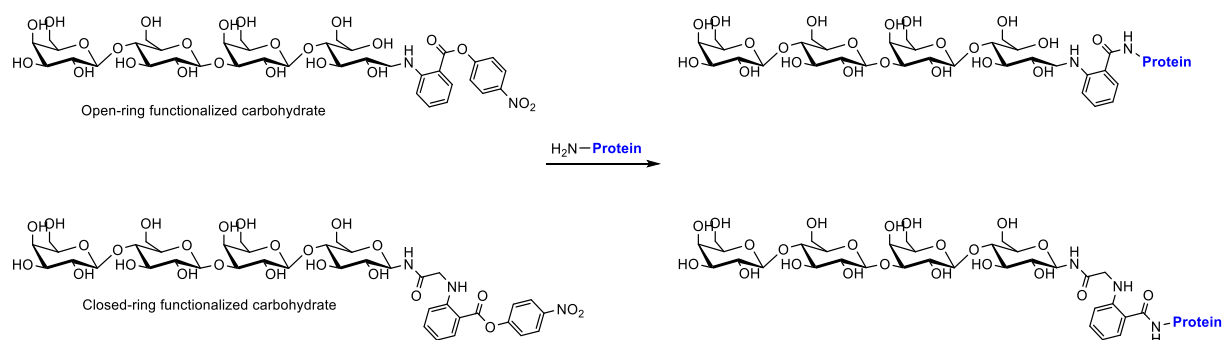
Entry	Substrate	v/v H ₂ O/MeCN, temperature (°C)	R ² -SH (equiv.)	Yield (%), β:α
1	D-glucose	1/1, -15	(5)	Quant., 6.7:1
2	D-glucose	1/1, 0	(7)	93, 4.5:1
3	D-glucose		(3)	90, 10:1
4	D-glucose	1/1, r.t.	(5)	90, β
5	D-glucose	1/1, 0		91, β
6	Cellobiose			
7	Lactose	4/1, 0	(5)	Quant., β
8	Laminaribiose			
9	Melibiose			

Table 12. Synthesis of aryl 1-thioglycosides from unprotected monosaccharides with DMC reagent

They later demonstrated the DMC-mediated synthesis of fluorescently labelled carbohydrates, once again starting from unprotected oligosaccharides in aqueous medium by grafting the 4-methyl-7-sulfanylbulliferone (MUSH) fluorophore²³² (for more information about DMC-assisted formation of *S*-aryl and *S*-alkylglycosides see review³⁷).

Instead of transforming the hemiacetal, another method for the preparation of thiol end-modified carbohydrates consists in the direct introduction of a spacer bearing a thiol function onto unprotected carbohydrates. The thiol is either present from the beginning in a masked state or introduced in the final step of synthesis. In polymer chemistry, efforts have been put to efficiently utilize thiol chemistry without using tedious protection/deprotection strategy. In order to limit purification steps and quicken polymer preparation, byproduct-free processes were developed for macromolecular structure synthesis. Some thiol moieties have been integrated, mostly in cyclic forms to mask the sulfhydryl function, such as cyclic dithiocarbonates, ethylene sulfide, 2-iminothiolane (also known as Traut's reagent) or thiolactones (for more information, see review²³³).

Aside from the classical and widely used glycosylation, which was presented by the pathway **A** (Figure 33), few methods exist to introduce a spacer on the reducing end of unprotected carbohydrate. It was demonstrated that the spacer and the linkage method might have an effect on the biological properties of the neo-glycoconjugate and must be wisely chosen. Prasanphanich et al.²³⁴ studied this effect on a small glycan, lacto-*N*-neotetraose, that was linked by two different methods shown in the scheme 22 : one that leaves the reducing end in its opened form, and the other one that leaves the ring closed. Despite their similarities, the immune response elicited by the two different neoglycoconjugates was divergent, indicating that the reducing end linker and linkage type might be crucial for immune response.

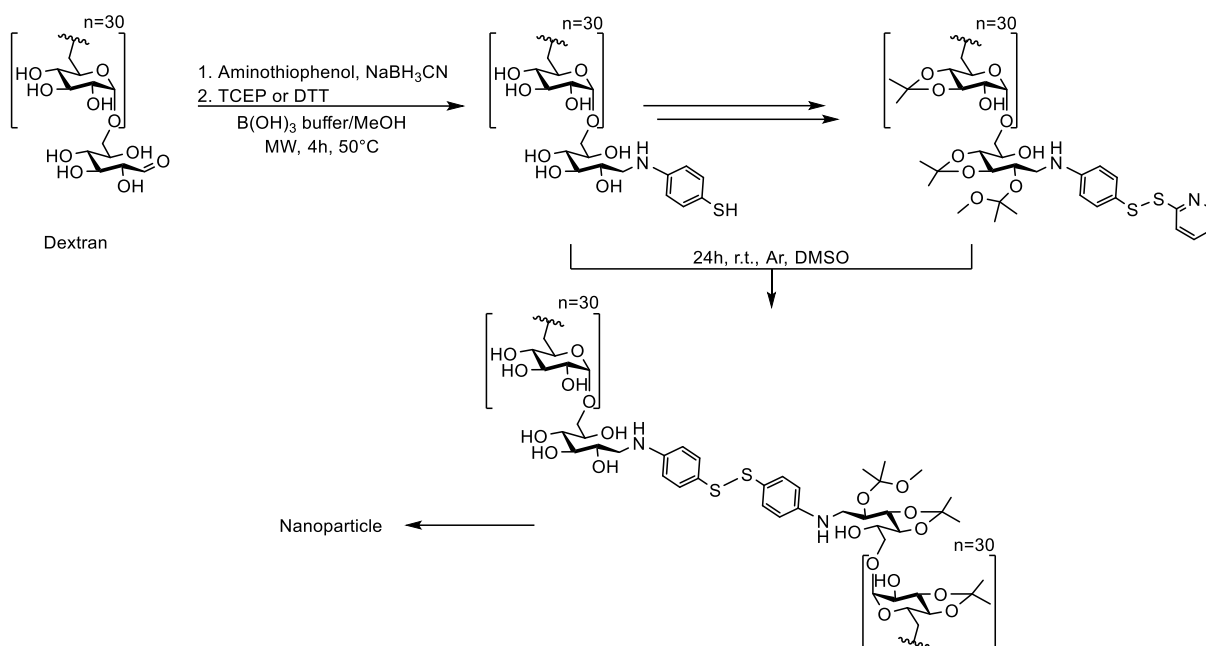


Scheme 21. Preparation of two neoglycoconjugates starting from lacto-*N*-tetraose by two means: open-ring method (top) and closed-ring method (bottom)

The most common reaction to end-functionalize a carbohydrate is reductive amination.²³⁵ The amine-bearing compound reacts with the anomeric latent aldehyde of the glycan in a condensation reaction, providing an imine species that is reduced by a hydride source (usually sodium cyanoborohydride) to yield a 1-amino-1-deoxyglycitol, also named glycamine.²³⁶ This method presents several advantages : one amine-bearing compound is grafted per glycan chain allowing an easy quantification, the grafting is performed on glycans in a single step without prior activation of the anomeric position and the process is usually high-yielding. It however also presents disadvantages: large excess of the amine-bearing compound and of reducing agent are often necessary and the open-ring form of the reducing end might alter protein interaction²³⁶ and glycan antigenicity²³³ although most protein-carbohydrate interactions occur at the non-reducing end.

Reductive amination possesses a wide range of application: it was used to graft fluorescent tags on carbohydrate chains for analysis²³⁸⁻²⁴⁰, but mostly used to attach carbohydrate chains to carbohydrates or proteins/aglycons as illustrated on the following example.

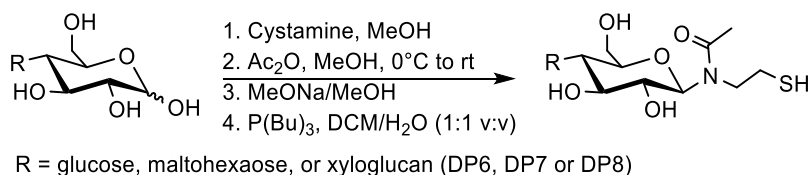
Breitenbach et al.²⁴¹ end-functionalized a dextran polymer with 4-aminothiophenol by reductive amination and ensured that all thiols were free by reducing the potential disulfides formed. They subsequently protected the free thiol with dipyrindyl disulfide in order to realize a further thiol-disulfide exchange forming a block-co-polymer that would later assemble to constitute glyconanoparticles, as shown on the Scheme 23.



Scheme 22. Preparation of thiol-end functionalized dextran and its modification for further self-assembly into glyconanoparticles

The introduction of an arylamine as part of the spacer allows a better detection and analysis of functionalized adducts thanks to the additional UV and fluorescent properties as suggested Guerry et al.²⁴²

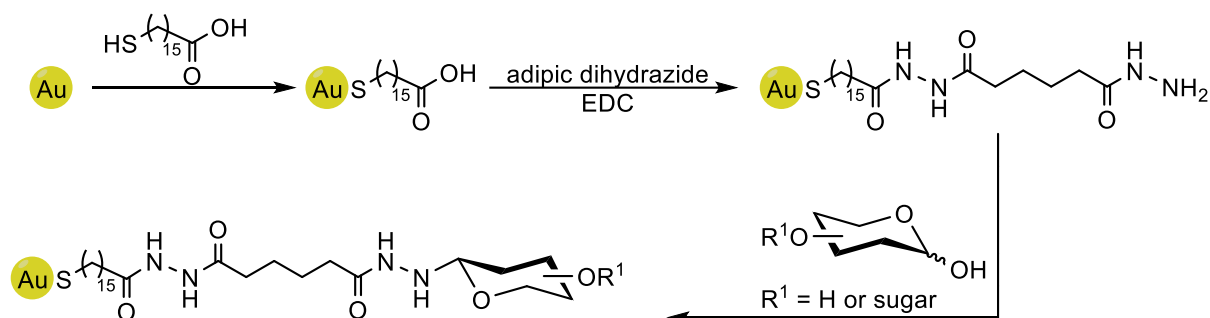
On the contrary to reductive amination, the formation of end-functionamized glycans by Kochetkov amination leaves the reducing end in a close-form ring, and predominantly in a β configuration²⁴³. Usually, the reaction is carried out with ammonium carbonate to synthesize the corresponding glycosylamine. Nevertheless, a modified procedure of this reaction enables the formation of thiolated glycans by using a substituted amine carrying a thiol moiety. Thiol-end functionalization strategy using cystamine is a chemistry that was previously developed and published in the team²⁴⁴. The multi-step functionalization based on amination was performed onto three products: maltose, maltoheptaose and xyloglucan oligosaccharides, as presented in the Scheme 24. Kochetkov amination of the anomeric carbon of the carbohydrate with cystamine was first performed. Without purification, the introduced secondary amine was chemoselectively acetylated in methanol with acetic anhydride for stability reasons. Some *O*-acetylations that might occur were later selectively deprotected with sodium methoxide in methanol. Finally, the disulfide bridge was reduced by using tributylphosphine providing cysteamine-functionalized oligosaccharides.



Scheme 23. Obtention of thiol-end-functionalized oligosaccharides by Kochetkov amination with cystamine

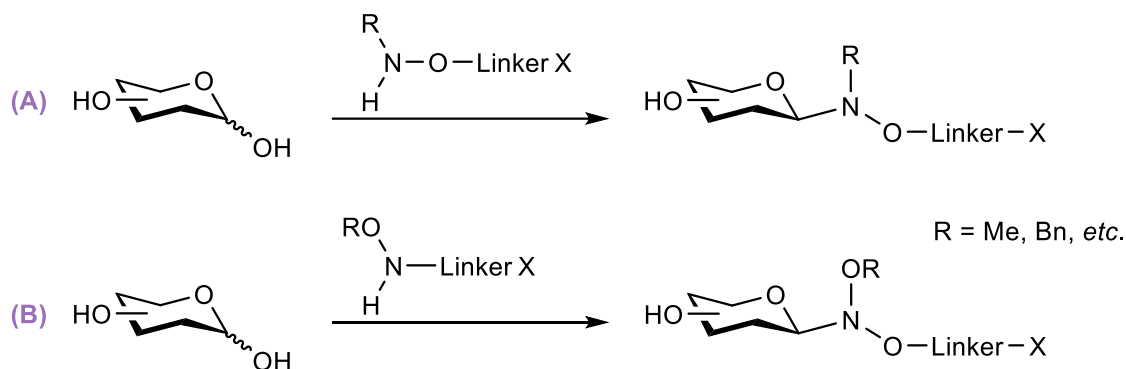
Kochetkov amination however presents some disadvantages such as slow speed of the reaction and the use of large excess of amine derivatives.

To address these problems, oxime and hydrazide-based strategies were developed. It allows the facile introduction of a variety of linkers in aqueous conditions²⁴⁵. Oxime bonds form rapidly and in high yields from the reaction between aldehydes and hydroxylamine derivatives. However, the formed neoglycosides are blocked in their open configuration. On the contrary, end-modification of glycans with hydrazide groups lead predominantly to closed-form configuration. Zhi et al.²⁴⁶ prepared carbohydrate microarrays on gold surface by attaching unprotected glycans on their surface *via* a hydrazide linker, illustrated on the Scheme 25. 16-mercaptohexadecanoic acid was first self-assembled to gold-coated glass slides thanks to its free thiol, the homobifunctional spacer adipic dihydrazide was then attached on the carboxylic acid on one extremity and the second one was grafted on the oligosaccharides. It is noteworthy that hydrazide linker reacted with the open-form glycan providing a hydrazone, which cyclized to predominantly form the corresponding β -pyranose form.²⁴⁷



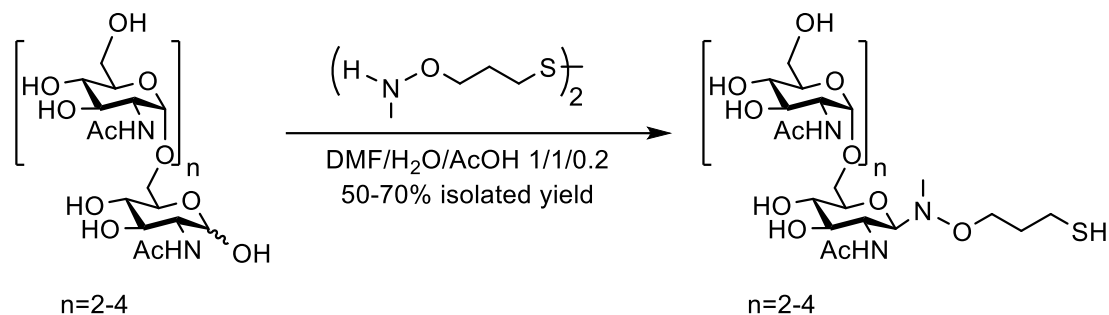
Scheme 24. Thiol-functionalization of glycan *via* hydrazide linker by Zhi et al.

Similarly to hydrazides and oximes, the oxyamine group allows the grafting of a variety of linkers, but may also be cleaved by acidic hydrolysis to provide native carbohydrates. Two general strategies ((A) and (B)) may be used for the preparation and conjugation of oxyamine linkers to carbohydrates, as shown on the Scheme 26 below. But in practice, the majority of glycoconjugates are from type (A) rather than type (B).²⁴⁸



Scheme 25. General method for the coupling of type (A) and type (B) oxyamine linkers on carbohydrates

Such as reductive amination and oxime conjugation, attachment of glycans with oxyamine spacers leads to predominantly open-form carbohydrates^{249,250}. This may be overcome by using *N*-methylated amino-oxy linkers^{251–253} which promotes the formation of exclusively β -linked glycoconjugates. Leung et al.²⁵⁴ described the conjugation between PIA polysaccharide (polysaccharide intercellular adhesin) and a heterobifunctional linker bearing a disulfide, as illustrated on the Scheme 27 below. Prior to the conjugation, the disulfide of *N*-alkyloxyamine was reduced to the free thiol. The conjugation with mild acid catalysis (catalytic amount of acetic acid) provided a β -oriented thiol-functionalized oligosaccharide with 50-70% yield after isolation by size exclusion chromatography.



Scheme 26. Coupling of PIA oligosaccharide with *N*-alkyloxyamine bearing a free thiol

To resume, as documented in the literature and above, many thiol-functionalization methods exist with and without linkers. In addition to the type of linker, the method for its conjugation onto glycans may vary. Amine-functionalization may be more documented as it is a common linkage found in Nature.

4.1.2 Amine end-modification of unprotected carbohydrates

Amines are widely found in Nature in amino acids, plant alkaloids, or glycans. They may undergo different reactions to be introduced on the reducing end of carbohydrates. There are two main drawbacks related to the preparation of glycosylamines: their low stability due to the rapid hydrolysis in neutral or acidic solutions (fast hydrolysis occurs at pH 1.5 to 9^{255–259}) and the formation of *N*-glycosylcarbamate and diglycosylamine as secondary reaction products^{243,256–258,260}. In addition, simple glycosylamine, *N*-alkyl and -aryl glycosides can freely undergo mutarotation similarly to unsubstituted hemiacetal of native carbohydrates, which renders them less stable than *O*-glycosides for example, this latter being blocked in one configuration³⁷.

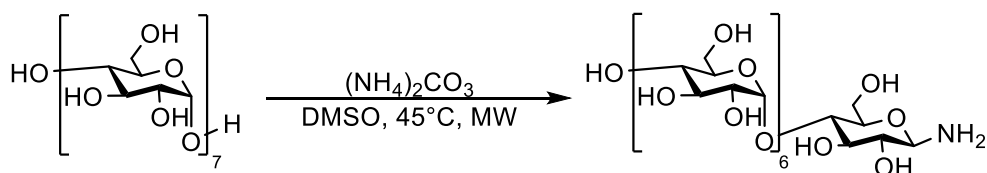
Lobry de Bruyn^{261,262} was the first to prepare aminated derivatives of monosaccharides (glucose, fructose, mannose, sorbose and galactose) by mixing them preferably in methanol with ammonia. He had already discovered the formation of diglycosylamines as side-products for some of the monosaccharides, which was then fully characterized by Isbell group²⁶³.

Later, Mitts and Hixon introduced the condensation reaction between different amines and D-glucose under reflux²⁶⁴. Kochetkov and co-workers later optimized the reaction to form glycosylamines but the slow speed and excess of ammonium hydrogen carbonate rendered the purification laborious. This

reaction, called the Kochetkov amination, has been widely used in the purpose of optimizing it and for efficient glycan derivatization. However, even though *N*-glycosides are generally more stable in the β -anomer configuration, a mixture of anomers is often observed ²⁶⁵.

Some upgrades of the synthesis were provided by Likhoshesterov et al. ²⁵⁵ with the use of mixtures of ammonium carbamate and aqueous ammonia. The procedure tested with a range of mono- and disaccharides including 2-acetamido-2-deoxy-hexoses provided more stable glycosylammonium carbamates that could be converted to corresponding glycosylamine with high yields and globally lowered reaction times.

As an emerging technique, microwave irradiation has been used for the preparation of glycosylamines by Kochetkov amination. Liu et al. ²⁶⁶ described the glycosylamine transformation of maltoheptaose in non-aqueous DMSO to prevent glycosylamine from degradation, as shown on the Scheme 28. The glycosylamine prepared within 30 minutes at 45°C required only 5-fold excess (w/w) of ammonium carbonate over maltoheptaose and was used for further labelling with tris(2,4,6-trimethoxyphenyl)phosphonium acetic acid *N*-hydroxysuccinimide ester (TMPP-Ac-Osu)²⁶⁷⁻²⁶⁹. This conjugation step was performed to introduce a charged group onto maltoheptaose for a simpler MALDI analysis.



Scheme 27. Preparation of maltoheptaose glycosylamine by microwave-assisted Kochetkov amination

With the growing interest for environmentally friendly approaches with green chemistry, solvent-free procedure for glycosylamine preparation was developed by Wadouachi group ²⁷⁰. Their mechanosynthesis using high speed ball milling enabled the preparation of a scope of amine-functionalized carbohydrates *via* linkers. For example, the reaction of L-rhamnose with diamines to obtain monosubstituted saccharide yielded 95-96% of product without waste as one equivalent of each reactant was used, as shown on the Table 15 below. This innovative procedure yet requires specific equipment and a good knowledge of mechanosynthesis.

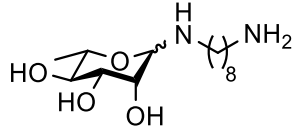
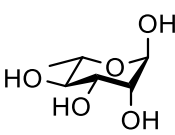
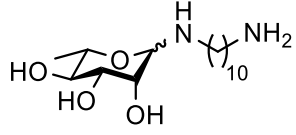
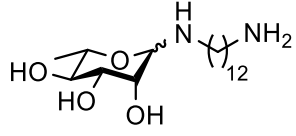
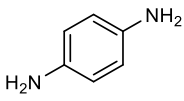
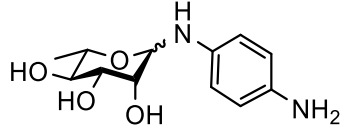
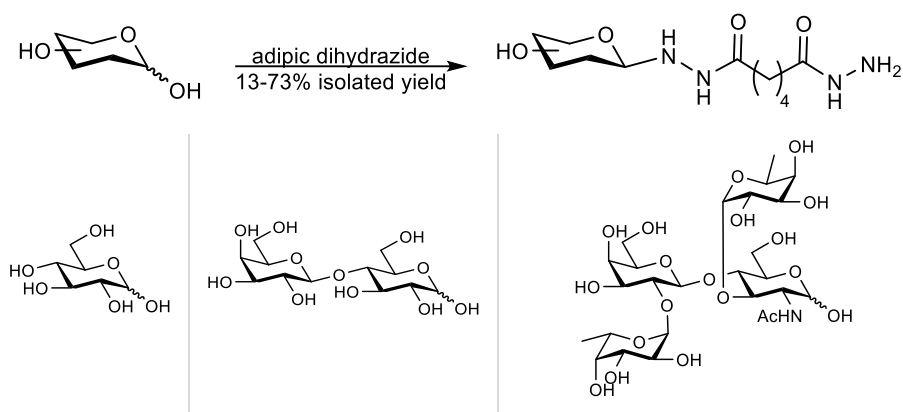
Entry	Sugar	Amine	Time (h)	Product	$\alpha:\beta$ ratio	Yield (%)
1		$\text{H}_2\text{N}(\text{CH}_2)_8\text{NH}_2$			87:13	96
2		$\text{H}_2\text{N}(\text{CH}_2)_{10}\text{NH}_2$	1.5		90:10	95
3	(L-rhamnose)	$\text{H}_2\text{N}(\text{CH}_2)_{12}\text{NH}_2$			96:4	96
4					85:15	95

Table 13. Preparation of amine-terminated rhamnose by mechanosynthesis

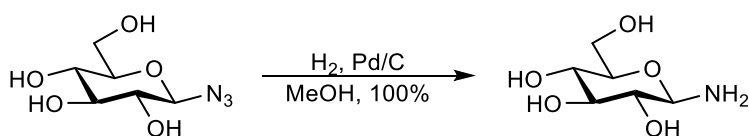
As developed previously (see 4.1.1), a popularly-used method for the end-functionalization of carbohydrates is reductive amination. Using bisfunctionalized linkers enables the preparation of amine-modified glycans that are stable, yet present only in open-ring form. Parekh and co-workers²³⁹ described the preparation of fluorescently and radio-labelled glycans with more than 80% yield by reductive amination with using 2-aminobenzamide. This methodology was also more recently developed by Cummings groups (see 4.2.3).

Hydrazide linkers may be used for the derivatization of unprotected carbohydrates through the formation of hydrazones. The one-step preparation of glycosylhydrazide was reported by Flinn et al.²⁴⁷, leaving the reducing end structure intact. Mono-, di- and tetra-saccharides were reacted with the bifunctional spacer adipic dihydrazide as shown on the Scheme 29 below. Although mild conditions were used with no aggressive activating agent, no general methodology could be applied due to the variation of yields depending on glycan types and length. Moreover, reaction times were found to be longer for tetrasaccharides.



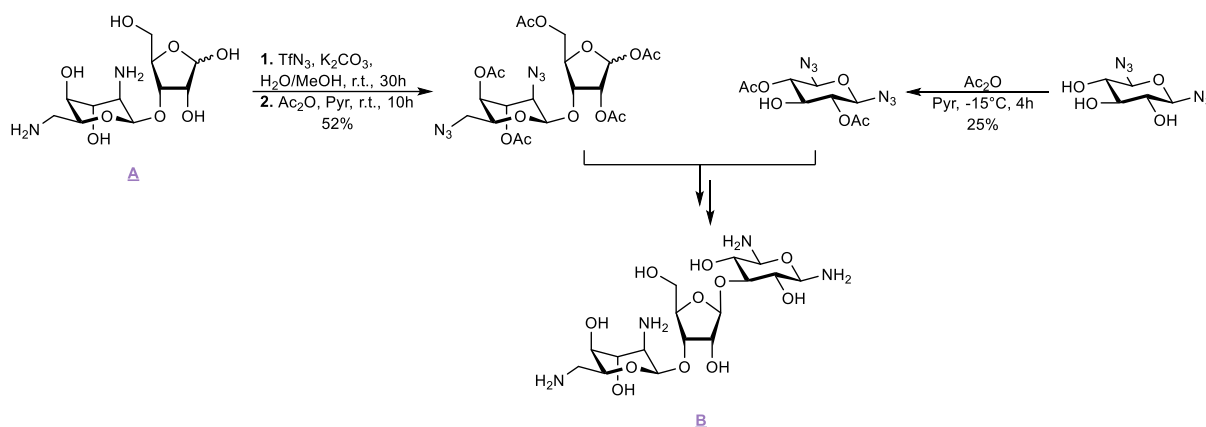
Scheme 28. One-step preparation of glycosylhydrazides starting from mono-, di- and tetra-saccharides

A last commonly used method for the preparation of amine-functionalized carbohydrates in a protected form relies on the azide chemistry. Many protecting groups were described for amine functions, in which the *tert*-butyloxycarbonyl (Boc), acetate (Ac) and carboxybenzyl (Cbz) are the most employed in carbohydrate and peptidic chemistry. Similarly to thiols, a few of them can be introduced and removed very easily. However, azides were found to be convenient amine protecting groups. In addition to their orthogonal applicability in copper-catalyzed azide-alkyne cycloaddition (CuAAC) reactions and their stability, they can be reduced into amines in later stages of carbohydrate modification (for more information about azides, see ²⁷¹). The reduction of unprotected glycosylazide to form the corresponding amine was demonstrated by de Barros et al. ²⁷² Catalytic hydrogenation was performed onto a β -oriented 1-azido-1-deoxy-glucose, which yielded 100% of pure glycosylamine as shown on the Scheme 30 below.



Scheme 29. Preparation of glycosylamine by reduction of azide-end functionalized glucose

As a more complex example, Griffey group ²⁷³ prepared neomycin B related aminoglycosides by using azido-protecting group. As shown on the scheme 31, the amines were converted into azides by diazo transfer on compound **A** and reduced back into amines after glycosylation by Staudinger reduction using phosphine complex in mild conditions to provide compound **B**.



Scheme 30. Preparation of neomycin B related aminoglycoside by using azido-protecting group

Although azides are widespread in carbohydrate chemistry, their use includes two additional steps (protection/deprotection) in the synthesis, for which the yields vary from 60-100%.

The strategy adopted in our project consisted in introducing a linker bearing an activated ester with a leaving group stable enough to endure all steps before its substitution by a free amine. By this means, no protection was needed as the free amine was introduced at the last stage of carbohydrate modification, right before its coupling to the polymer backbone. Carbohydrates were therefore functionalized *via* a linker bearing an amine, 4-nitrophenyl anthranilate, which was grafted by reductive amination similarly to Cumming group strategy (see 4.2.3).

In the goal of obtaining glycosaminoglycan mimetics, linear maltooligosaccharides were reducing end functionalized by a sulfhydryl or an amine moiety. As a reminder, several chains of these monovalent structures were planned to be grafted to a polymeric skeleton in order to obtain proteoglycan mimetics, that have the advantage to be multivalent. The polymeric structure chosen, PHOU, being a biodegradable polyester bearing pendant terminal alkene functions, the grafting was first conceived to be realized by a thiol-ene chemistry. For such ligation, the GAG mimetics have to be thiol-functionalized at their extremity, but under a protected form. Three main strategies were used to end-functionalize maltooligosaccharides with a protected thiol moiety. Since maltoheptaose (from natural source or synthetically obtained from β -cyclodextrin) is an expensive oligosaccharide, maltose (DP2) was used in most cases to fine-tune the experimental conditions, this latter being readily available. After obtention of thiol end-functionalized maltoheptaose, two of them were chosen to be randomly sulfated at different degrees for their future coupling to PHOU polymer in order to obtain PG mimetics.

In a later stage of the project, it was found that the thiol-ene coupling was a real challenge. An amide coupling between carboxylated PHOU and an amine-functionalized maltoheptaose was therefore proposed. Only one strategy was developed, based on the similar thiol-functionalization developed lately.

4.2 Results and discussions

4.2.1 Thiol end-functionalization

4.2.1.1 Thiol end-functionalization by using cystamine derivatives

4.2.1.1.1 Introduction

Cystamine (**34**) is a symmetrical molecule consisting of two primary amines linked by a short alkyl chain and a disulfide bridge. Breaking the disulfide bond releases two cysteamine molecules **35**, the reduced form of cystamine with a free thiol. Their structures are presented below (Figure 34). The aim of this part was to react the amine on the terminal anomeric position of carbohydrates through an amination reaction.

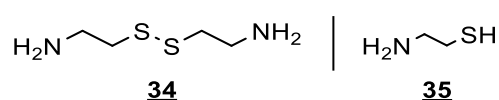


Figure 34. Structures of cystamine **34** and cysteamine **35**

The thiol-end functionalization strategy using cystamine is a chemistry that was developed and published in the team ²⁴⁴. The multi-step functionalization starting from a Kochetkov amination was described above (see 4.1.1).

Reductive amination was also conceived for the introduction of cystamine. In the approach of van der Vlist et al. ²⁷⁴, reductive amination was used to synthesize a variety of mono-, di-, or tri-amine-functionalized products starting from maltoheptaose. The structures are presented in the figure 35. Similarly to Gauche et al. ²⁷⁵ procedure, the reagents were reacted in an incubator at high temperature. However, the reaction times were significantly longer.

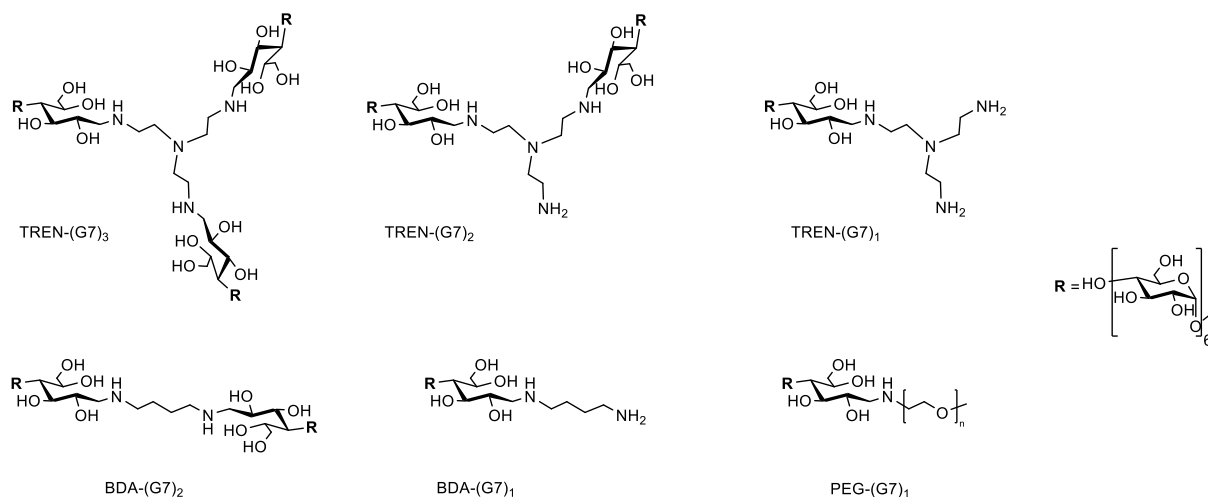
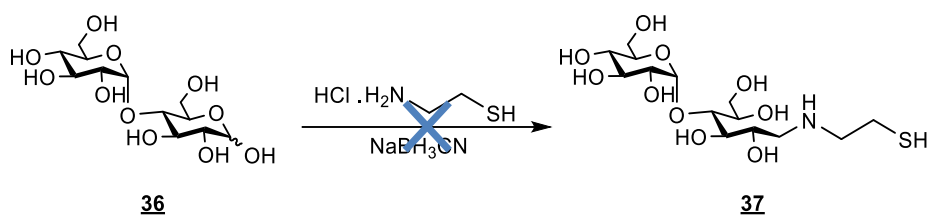


Figure 35. Structure of mono-, di-, or tri-functionalized structures prepared by reductive amination by Vlist et al.

To attach cystamine or its reduced form cysteamine to the anomeric position of saccharides, four ways were investigated.

4.2.1.1.2 Grafting of cysteamine onto maltooligosaccharides through reductive amination

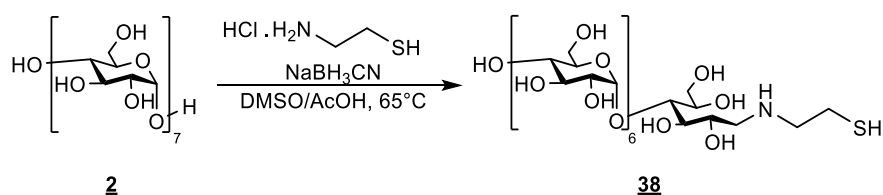
The first way investigated to graft a thiol function onto maltooligosaccharides was done without thiol protection. The goal of this reaction was to evaluate the need of thiol protection. If the product was effectively functionalized with a free thiol, it could be readily accessible for the further thiol-ene coupling. On the contrary, if the product was obtained as a mixture of free thiol and dimerized thiol, protection of this function would be necessary. For this purpose, a reductive amination of maltose **36** was carried out by using cysteamine **35** as shown in the scheme 32.



Scheme 31. Reductive amination of maltose with cysteamine

The reductive amination was conducted with an equimolar ratio of maltose and cysteamine hydrochloride, and eight equivalents of sodium cyanoborohydride reducing agent at 65°C in a mixture of DMSO/AcOH. After twenty-two hours of reaction, the starting material seemed to disappear on TLC plate to give a very polar product. The ¹H NMR analysis of the isolated product showed neither the expected product, neither the starting material, but a mixture of saccharides where the peaks assigned to anomeric protons was seen as a multiplet instead of the initial doublets. It was hypothesized that a mixture of products was present, including one issued from reduction and possibly one from hydrolysis of maltose. The reaction was tried a second time in different conditions described by Gauche et al.²⁷⁵. In this way, one equivalent of maltose was mixed with two equivalents of cysteamine and of sodium cyanoborohydride in a mixture water/methanol acidified with acetic acid at 80°C. The TLC plate showed that no reaction had occurred within three hours. Reductive amination, which is usually a quick reaction, did not work with maltose in two different conditions although all reactants were well-characterized and pure. As maltoheptaose was the definitive carbohydrate to be thiol-functionalized, the reductive amination was later tried on this oligosaccharide.

A trial of reductive amination onto maltoheptaose **2** was carried out, as shown in the scheme 33, but in harsher conditions than previously: one equivalent of sugar, ten equivalents of cysteamine hydrochloride, and thirty equivalents of sodium cyanoborohydride were solubilized in a mixture of DMSO/acetic acid at 65°C.



Scheme 32. Reductive amination of maltoheptaose with cysteamine

Interestingly, the TLC plate showed a total conversion of the starting material into a slightly more polar product and the ^1H NMR analysis indicated that the doublets assigned to reducing end anomeric proton were still present. However, the aspect of the spectrum suggested a mixture of a major and a minor product as well as the presence of salts. The mass spectrometry analysis displayed the presence of three products: the targeted product M₇-cysteamine **38** at $m/z=1214.32$, an oxidized side-product M₇-cystamine **38a** at $m/z=1289.39$ where the free thiol was oxidized into a disulfide bond due to the excess of cysteamine in the medium, and the dimer product M₇-cystamine-M₇ **38b** at $m/z=816.47$ also obtained by oxidative dimerization. The structures of these three products and the mass spectrum of the reaction are presented in the figure 36.

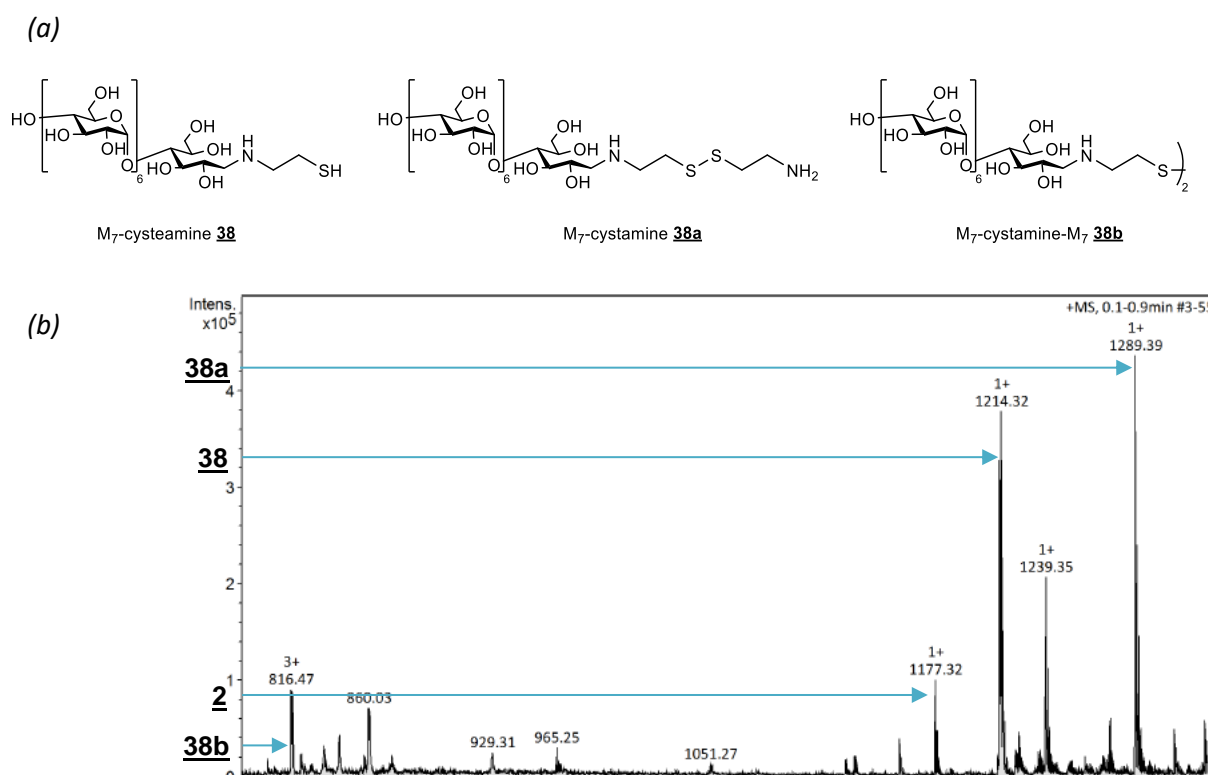
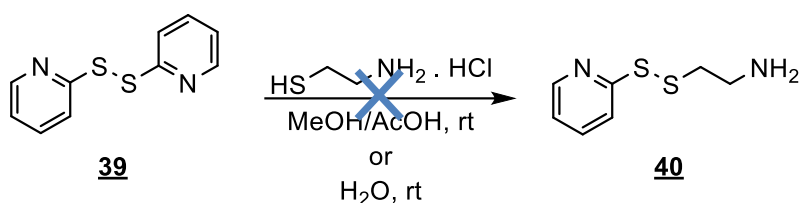


Figure 36. (a) Products obtained from the reductive amination of maltoheptaose with cysteamine ; (b) Mass spectrum from reductive amination of maltoheptaose with cysteamine

This evidenced that our thiolated product suffered from oxidation into disulfide bond. In these conditions, the thiol was not stable enough to be recovered in the form of a single product. The mixture of products was not further purified by breaking this bridge allowing us to reach the pure targeted product for the reason that the product should have been stored and manipulated for further reactions or characterizations very carefully.

This group of reactions proved the necessity to protect the sulfhydryl function in order to obtain well-defined products. The protection was envisioned to be realized in the form of a disulfide bond.

To do so, the free thiol of cysteamine **35** was intended to be protected by a disulfide bond thanks to a thiol-disulfide exchange using pyridyl disulfide **39** to avoid its dimerization, as presented in the Scheme 34. This reagent is commonly used for this type of reaction and has the advantage to provide a UV-active product. Once coupled to the saccharide, it allows the easy identification of the product during further reactions, by TLC for example. In the same way, the removal of this UV-active moiety providing a non-UV-active saccharide with a free thiol can be easily assessed.



Scheme 33. Thiol-disulfide exchange of cysteamine with 2,2'-dipyridyldisulfide

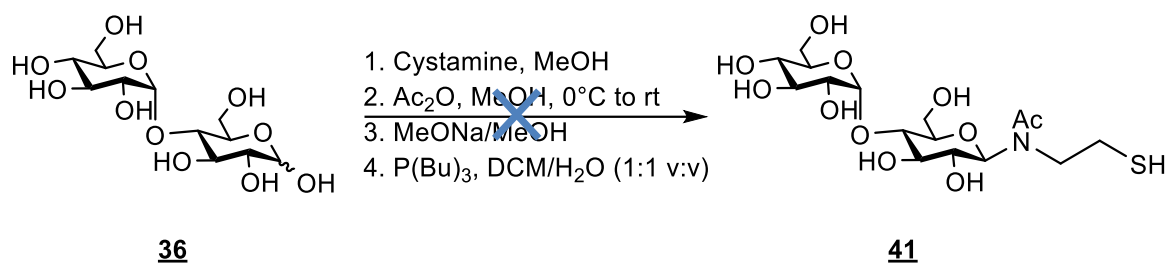
A thiol-disulfide exchange was carried out ²⁷⁶ by mixing 1.2 equivalents of cysteamine hydrochloride with one equivalent of 2,2'-dipyridyldisulfide **39** in aqueous solution, but only led to the breakage of the initial disulfide bond. Different conditions ^{277,278,279} were then tested by reacting one equivalent of cysteamine hydrochloride with two equivalents of 2,2'-dipyridyldisulfide in a mixture of methanol/acetic acid. After one night, cysteamine was no longer visible on TLC plate, but three other spots appeared in addition to the UV-active starting material. The references claimed to obtain the pure product by precipitating the reaction mixture in diethyl ether. However, by doing so, none of the four products were separated.

Considering that no cysteamine-grafted product was obtained, another similar strategy was built up to protect this thiol function as a disulfide bond by using cystamine.

4.2.1.1.3 Grafting of cystamine onto maltooligosaccharides through reductive and Kochetkov amination

To graft a protected thiol on the anomeric position of glycans, two types of amination were developed simultaneously, Kochetkov and reductive amination. In both cases, the grafted products of this reaction were aimed to possess a thiol that would, after disulfide bond breakage of cystamine, be readily accessible for the further thiol-ene coupling.

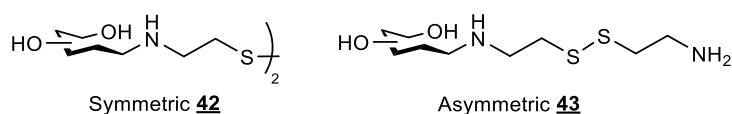
The Kochetkov amination previously published in the team and described above (4.1.1) was tried onto maltose using cystamine dihydrochloride, as presented in the Scheme 35.



Scheme 34. Kochetkov amination of maltose with cystamine

Prior to the reaction, cystamine dihydrochloride was converted into its salt-free form with sodium hydroxide. Then, maltose and cystamine free-base in a 1/10 molar ratio were reacted together in methanol until maltose was fully converted into a very polar product on TLC plate. After a rapid precipitation to remove the excess of cystamine, an acetylation of the secondary amine newly introduced was achieved by reacting the crude with acetic anhydride in methanol. The formed acetic acid was then removed by azeotropic evaporation. The product was taken back in methanol and the eventual hydroxyls that were acetylated during the previous step were selectively removed with sodium methoxide in methanol. The crude product was then neutralized with Amberlite H⁺ form. Finally, the disulfide bond was reduced by using tributylphosphine in a mixture of dichloromethane/water, and the side-products were removed thanks to an extraction. However, this lengthy five-step procedure afforded a very small quantity of a brown residue that did not seem to be the product according to the TLC.

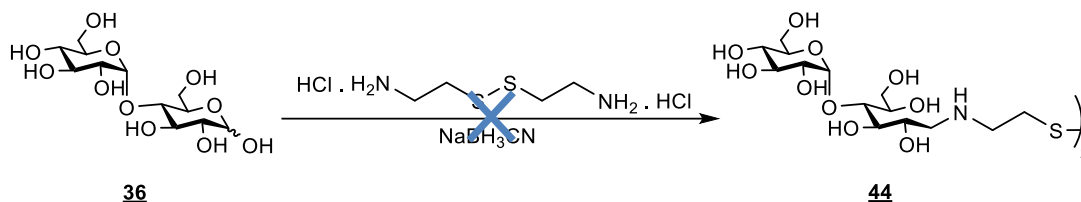
In parallel of Kochetkov amination, cystamine was introduced by reductive amination. Two sets of products could be obtained thanks to the presence of two amines on cystamine, whose structures are presented on the Scheme 36 below: (i) glycan-cystamine-glycan **42**, leading to a symmetrical product that after disulfide bond breakage, would give two identical products, (ii) glycan-cystamine **43**, by using a modified procedure of van der Vlist et al.²⁷⁴.



Scheme 35. Structures of the two products possible after reductive amination of maltose with cystamine

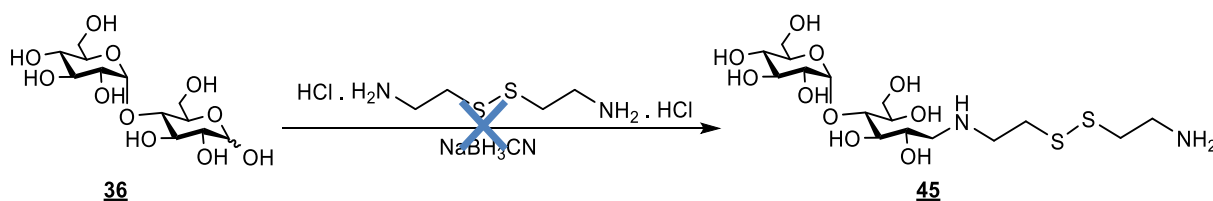
To obtain the symmetrical product **44** (Scheme 37), maltose was mixed with cystamine dihydrochloride in a 2/1 molar ratio and sodium cyanoborohydrate (eight equivalents) in a mixture of DMSO/acetic acid at 65°C. No reaction was observed even after addition of maltose and reducing agent extra portions. It was hypothesized that the reaction would be more efficient if cystamine was salt-freed, as for the reaction presented above. So, a step of converting cystamine dihydrochloride into its salt-free form was added prior to the reaction. By doing so, maltose was converted into a very polar product (according to TLC), similarly to reductive aminations with cystamine. As previously, the ¹H NMR analysis of this product was not conclusive: the peak corresponding to anomeric protons was seen as a multiplet, and

the aspect of the spectrum suggested a mixture of products probably coming from reduction of maltose and hydrolysis. The reaction was also carried out in the conditions described in Gauche et al.²⁷⁵. However, once again, no conversion of maltose was observed based on TLC plate. Despite many tries, the symmetrical product has never been obtained.



Scheme 36. Obtention of a symmetrical product by reductive amination of maltose with cystamine

An attempt to synthesize the unsymmetrical glycan-cystamine **45** product was carried out in the conditions described by Gauche et al.²⁷⁵ (Scheme 38). One equivalent of maltose was mixed with two equivalents of cystamine dihydrochloride and sodium cyanoborohydride in a mixture of water/acetic acid at 80°C. After one night, maltose was fully converted to a very polar product according to TLC plate (no elution), which was assumed to be a failure as the retardation factor of the product was expected to be similar than the one of maltose.



Scheme 37. Obtention of an unsymmetrical product by reductive amination of maltose with cystamine

Unfortunately, none of the symmetrical neither unsymmetrical product could be obtained with the protocols used on maltose. Faced with the difficulty of obtaining the targeted products, efforts were put into grafting a protected thiol function by another strategy that was developed in parallel.

4.2.1.2 Thiol end-functionalization by using homocysteine thiolactone derivatives

4.2.1.2.1 Introduction

Thiolactones are four-, five-, or six-membered cyclic thioesters (respectively β -, γ - and δ -thiolactone). In this family of compounds, γ -thiolactone, and especially homocysteine- γ -thiolactone (HTL, **46**), is predominant for its availability and synthetic applicability. HTL is a small yet very functional molecule, whose structure is presented on the Figure 37.

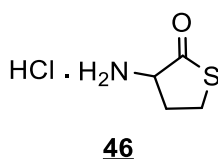
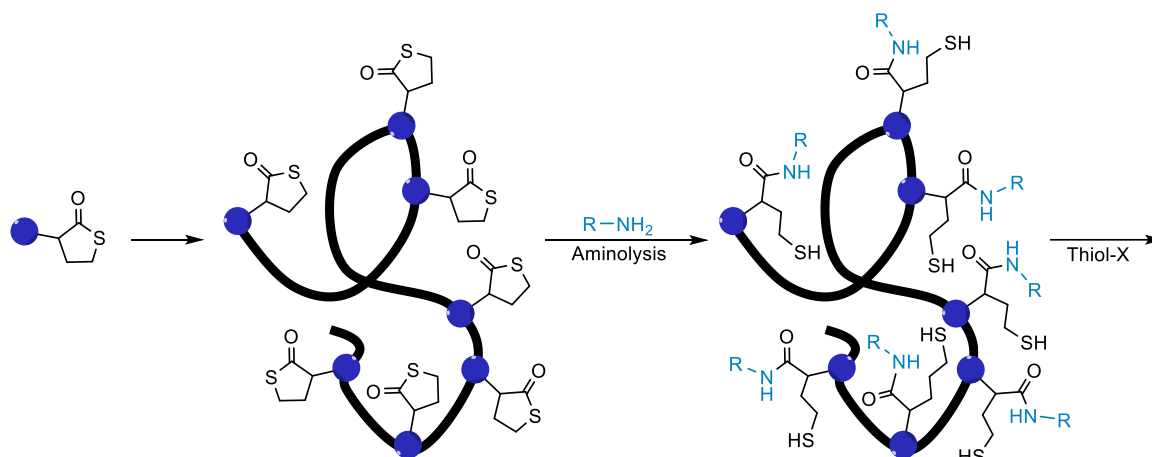


Figure 37. Structure of homocysteine thiolactone hydrochloride (HTL)

The thiolactone chemistry has been extensively developed by Du Prez group who used the reagent and its derivatives in order to create multi-thiol bearing polymers ²⁸⁰. Concerning its properties, HTL is commercially available in its hydrochloride salt form (for amine stability problems) as a bulk chemical. Its amine possesses a particularly low pK_a of 6.67 because of the electron-withdrawing effect of the sulfur atom. Ring opening of thiolactone can be achieved by hydrolysis and alcoholysis in basic medium, or by simple aminolysis. The amine can be transformed into a very reactive isocyanate by phosgene treatment ²⁸¹, which may be hazardous. The main drawback of HTL is its instability because of possible self-condensation due to the presence of a primary amine capable of aminolysis. On the other hand, this small molecule allows double functionalization in addition to its UV activity: a wide variety of amines can be employed to open the ring, and the subsequently released thiol can undergo many reactions such as nucleophilic attack, thiol-ene or disulfide bond formation. In the following example, Du Prez group ^{282,283} prepared polymers bearing HTL moieties along the chain, that are opened by the action of an amine (to note that additional groups can be introduced by the amine, leading to additional properties). Next, the liberated thiol underwent to thiol-X reactions, as displayed on the following Scheme 39.



Scheme 38. Preparation of a polymer bearing pendant homocysteine thiolactone moieties, that undergoes aminolysis for further thiol-X coupling

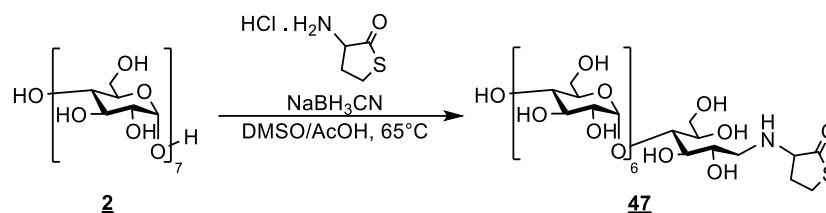
They also studied the effect of the amine used for the aminolysis on the efficiency of ring opening, suggesting that aliphatic amines were the most rapid and efficient.

The primary amine present on α of the carbonyl can undergo different reactions. It can be transformed into an isocyanate for further coupling reactions ^{281,284,285} or be protected by acetylation to take advantage of the thiolactone chemistry ²⁸⁶. This amine can also be subjected to grafting *via* amidation ^{287,288} or amination.

Our approach consisted in coupling HTL to carbohydrates through a chemoselective reaction on the anomeric position according to two routes : reductive amination and Knoevenagel condensation.

4.2.1.2.2 Grafting of HTL onto maltooligosaccharides through reductive amination

Reductive amination was first considered since HTL could be directly introduced at the anomeric position of maltooligosaccharides. As for cysteamine-grafted maltoheptaose (see 4.2.1.1.2), modified conditions of van der Vlist et al.²⁷⁴ protocol were used as shown in the Scheme 40. The reaction of maltoheptaose **2** with ten equivalents of homocysteine thiolactone hydrochloride **46** and thirty equivalents of sodium cyanoborohydride at 65°C was completed within two hours in a mixture of DMSO/acetic acid.



Scheme 39. Reductive amination of maltoheptaose with homocysteine thiolactone hydrochloride

The pure product **47** was obtained after four precipitation-centrifugation cycles in acetonitrile with a quantitative yield. As shown on the Figure 38a, the ^1H NMR spectrum of compound **47** displayed the peaks corresponding to carbohydrate protons between 3.25 and 5.51 ppm, as well as those corresponding to HTL between 2.2 and 4.4 ppm. The superposition of spectra offers a good indication that no starting material was left, and that HTL was successfully grafted onto maltoheptaose. The mass spectrum presented on the figure 38b shows one predominant peak at $m/z=1276.288$ corresponding to the product in the $[\text{M}+\text{Na}]^+$ form. One residual peak of maltoheptaose in the form of $[\text{M}_7+\text{Na}]^+$ also appears, but can be considered as a side-product of mass fragmentation as the TLC plates and ^1H NMR spectrum did not show any signs of residual maltoheptaose.

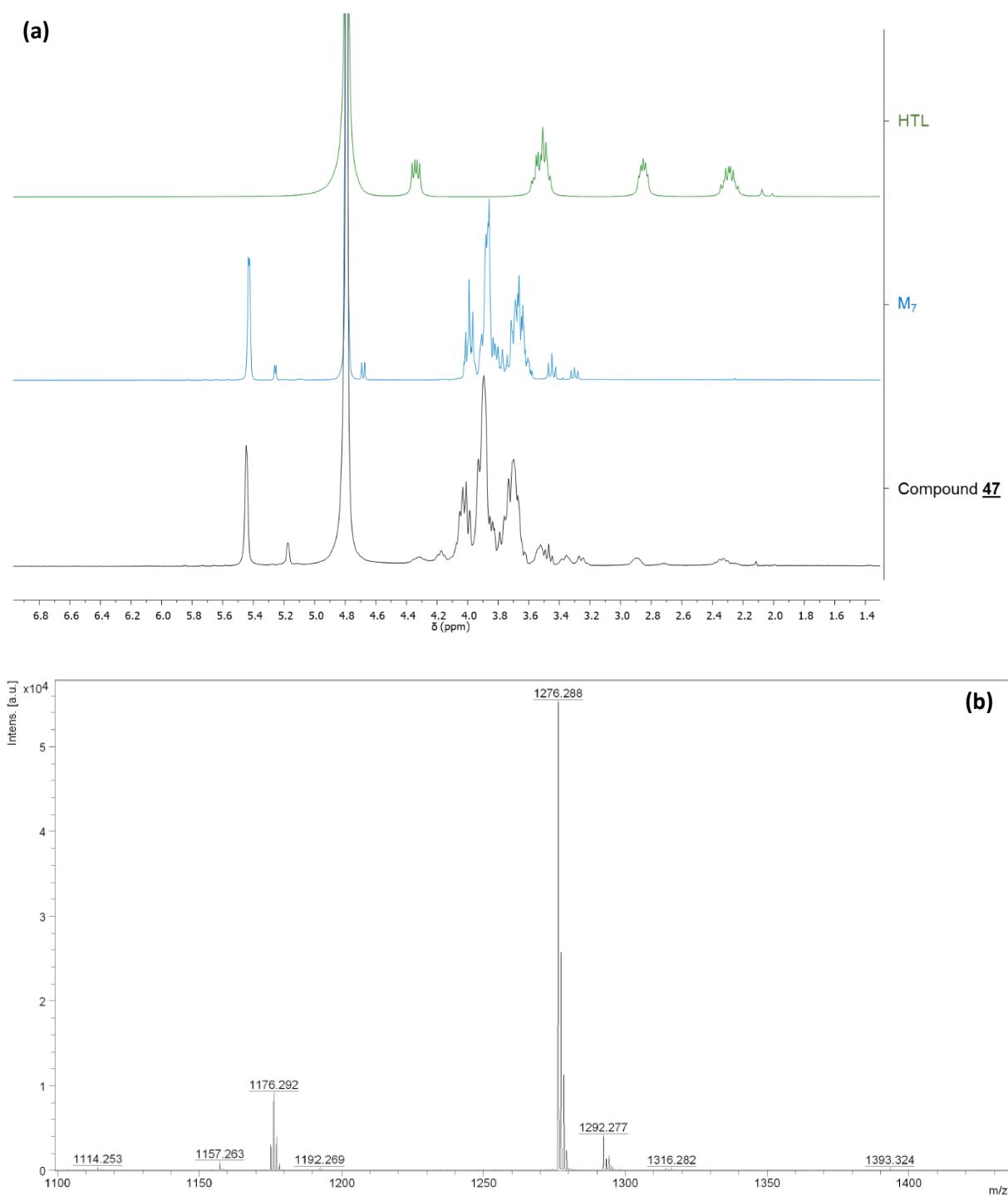
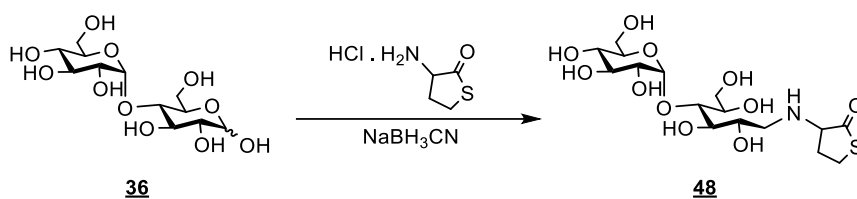


Figure 38. (a) ^1H NMR spectra superposition of compound **47** with native maltoheptaose and HTL in D_2O ; (b) Mass spectrum of compound **47**

To further perform some trials of the thiol-ene coupling and optimize this critical reaction, a smaller and cheaper saccharide, maltose, was selected to be HTL-functionalized. To do so, maltose was submitted to a reductive amination with HTL hydrochloride (Scheme 41) in the same conditions as for maltoheptaose.



Scheme 40. Reductive amination of maltose with homocysteine thiolactone hydrochloride

The reaction on small quantities provided the product **48** with a quantitative yield. However, when changing the scale, although the ^1H NMR spectra were very similar on small and large quantities, the product **48** could not be obtained pure. This was evidenced by the appearance of a peak on mass spectrometry analysis (see Figure 39 below) at $m/z=561.15$, whose intensity varied from 30 to 50% compared to the targeted product ($m/z=444.09$ $[\text{M}+\text{H}]^+$). This new peak corresponded to a side-product where the thiolactone moiety of the newly formed product, maltose-HTL, was opened by the amine of a second HTL molecule (self-condensation, compound **48a**).

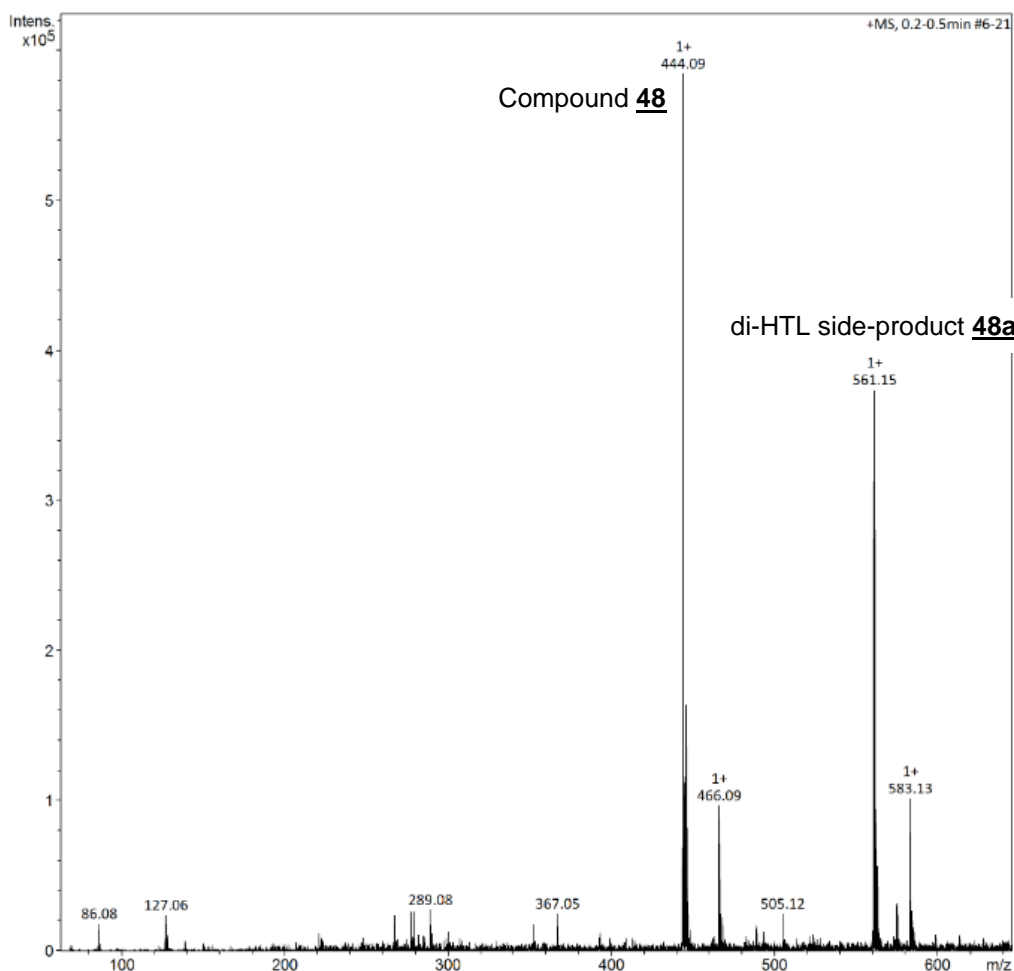


Figure 39. Mass spectrum of the mixture obtained after reductive amination of maltose with HTL on a 1-gram scale using 10 equivalents of HTL and 30 equivalents of NaBH_3CN

The compound named di-HTL side-product **48a**, whose structure is shown on figure 40, was thereby composed of a free thiol and a protected thiol. This side-reaction was considered to be due to the excess

of HTL used for reductive amination. It was estimated that the isolation of compound **48** would be challenging due to the similarity of structures and polarity (no difference of frontal elution on TLC).

To avoid the phenomenon, many conditions as the temperature, the solvents, the equivalents of reagents and the purification methods were changed. First, the number of equivalents of HTL/sodium cyanoborohydride were decreased to 5/15 then to 2.5/8 when performing the reaction on a 1-gram scale: this allowed to decrease the amount of side-product to 20%. When 2/8 molar ratios of HTL/reducing agent were reacted with maltose, this percentage was reduced to 17%. On a small scale, the ratio of 1.5/8 equivalents provided only 9% of side-product, and when equimolar ratios of maltose and HTL were mixed with eight equivalents of reducing agent, no side-product was observed. However, on a 4-gram scale, the purification process became troublesome: the precipitation-centrifugation cycles did not separate salts and solvents from the product, neither did the size exclusion chromatography that followed these cycles. To limit the number of precipitation-centrifugation cycles necessary to eliminate DMSO, another mixture of solvents was tested: water/acetic acid. Equimolar ratios of maltose and HTL were reacted with eight equivalents of reducing agent in this new system of solvent at 65°C. The work-up procedure was lightened and almost no side-product was observed, however a second peak appeared on mass spectrum at $m/z=367.22$: reduced maltose **48b** (figure 40).

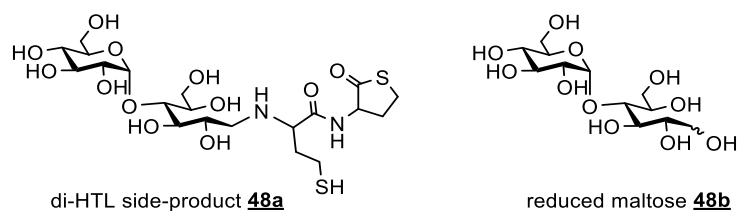


Figure 40. Structures of the side products formed during reductive amination of maltose with homocysteine thiolactone hydrochloride

To avoid this second side-product, the quantity of reducing agent was decreased to four equivalents, but this ended to a uncomplete conversion of maltose. A last solvent system, water/methanol, was tested at a higher temperature of 80°C for a variety of molar ratios of HTL/reducing agent. Also, the pH variation was tested by changing the quantities of acetic acid added. All these conditions led to bigger quantities of side-products (including reduced maltose, di-HTL-maltose, and *N*-acetylated maltose-HTL). Thus, these choices were all set aside. The first conditions using a mixture of DMSO/acetic acid at 65°C were found to be the best on large scale. Reacting one equivalent of maltose and two of HTL with eight equivalents of reducing agent yielded 68% of product **48** including 7% of di-HTL side-product. The mass spectrum is presented on the figure 41.

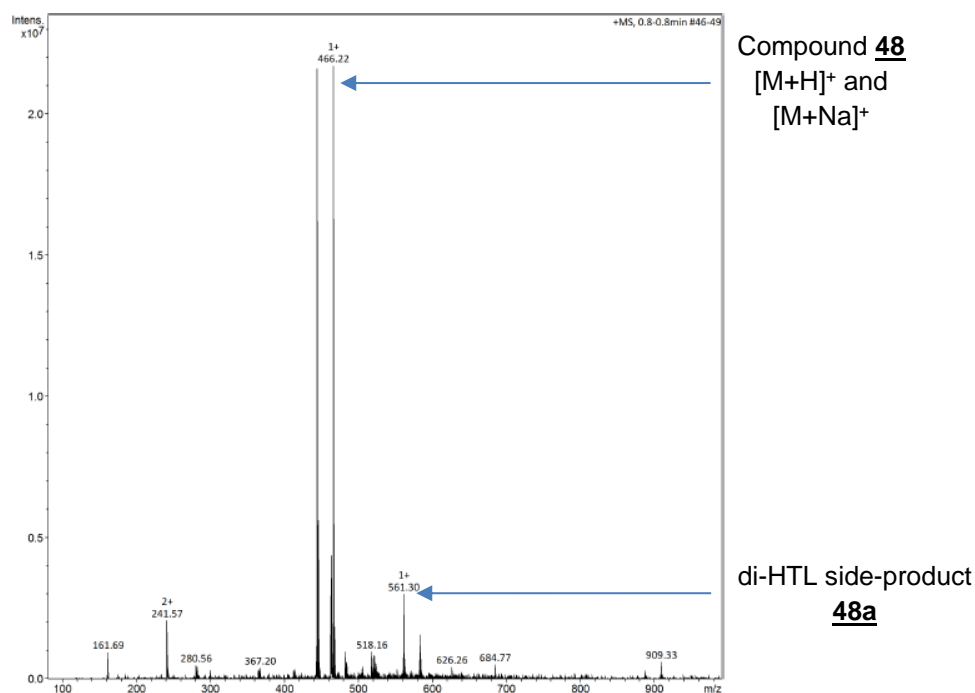
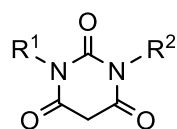


Figure 41. Mass spectrum of the product obtained after reductive amination of maltose with HTL on a 4-gram scale with 2 equivalents of HTL and 8 equivalents of NaBH_3CN

In parallel of the reductive amination, another approach based on the barbituric acid chemistry was conceived in order to incorporate one or two homocysteine thiolactone moieties at the extremity of maltooligosaccharides.

4.2.1.2.3 Grafting of HTL onto maltooligosaccharides through Knoevenagel condensation

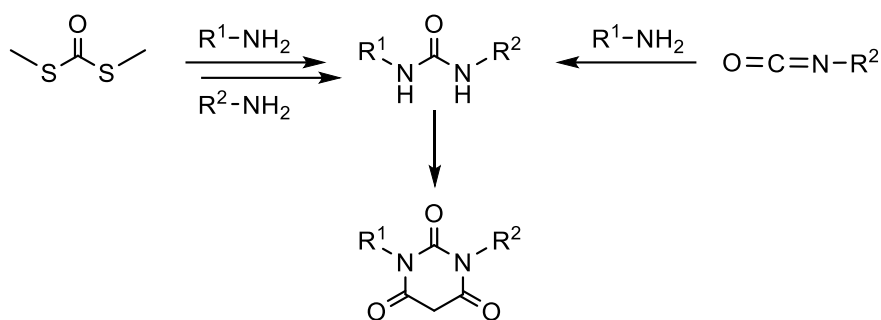
Barbituric acids are symmetrical cyclic compounds possessing two imides, three carbonyl functions and an active methylene. These compounds are very interesting in term of structure as they can be the source of various derivatives, as presented in the figure 42.



$\text{R}^1 = \text{R}^2 = \text{H}$, barbituric acid

Figure 42. Structure of barbituric acid and its possible derivatives

Barbituric acids can be amine-functionalized on their imides with diverse moieties in a symmetrical or unsymmetrical way. Biltz & Wittek²⁸⁹ were among the firsts to explore this chemistry by synthesizing a range of barbituric acid derivatives. More recently, Silverman and col. produced a collection of symmetrical and unsymmetrical barbituric acids either starting from *S,S*-dimethyl carbonodithioate²⁹⁰, either starting from an isocyanate^{291,292} as depicted in the scheme 42 below.



Scheme 41. Obtention of symmetrical and unsymmetrical barbituric acid derivatives starting from *S,S*-dimethyl carbonodithioate or an isocyanate

The active methylene of barbituric acids can be easily deprotonated due to the acidity of the hydrogen (which has a pK_a around 4-5 depending on the barbituric acid derivative). The formed carbanion, stabilized by carbonyl groups, can undergo reactions such as attachment with the anomeric carbon of carbohydrates. This coupling involving the anomeric carbonyl group and a carbanion is called the Knoevenagel condensation. The formation of *C*-glycosides was extensively developed by Galbis Perez and coll.^{293,294} that reported the one-step preparation of *C*-glycosylbarbiturates and *C*-glycosylbarbituric acids with good yields and without any prior protection step. They functionalized a collection of monosaccharides with di-methylbarbiturate (D-glucose, D-galactose, D-mannose, D-xylose, D-ribose, and D-arabinose). Examples of some *C*-glycosylbarbiturate prepared are illustrated in the figure 43 below.

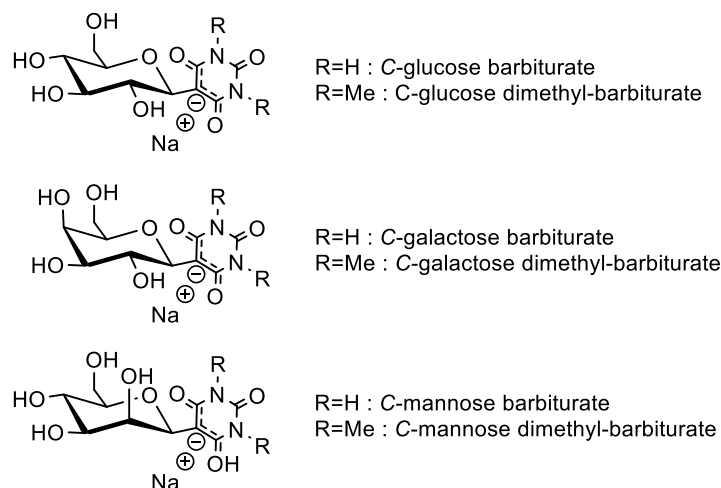


Figure 43. Examples of *C*-glycosylbarbiturates prepared by Knoevenagel condensation

This Knoevenagel coupling was more recently performed by Critchley and Clarkson²⁹⁵ with usual dimethylbarbituric acid on mono- or di-saccharides such as galactose, lactose, cellobiose and maltose. Recently, in our team, Portier et al.²⁹⁶ promoted this chemistry with a set of mono- and disaccharides and of barbituric acid derivatives to create series of interesting “clickable” *C*-glycoconjugates from protecting-group free carbohydrates.

Similarly, the barbituric acid chemistry offers the possibility to graft either one or two HTL moieties onto oligosaccharides' reducing end. Attaching two HTL moieties was envisioned to latter give the opportunity of cross-linking between carbohydrate chains and alkene-bearing polymer during the thiol-ene step.

In this regard, a barbituric acid bearing two HTLs was targeted (compound **50**). The retrosynthesis, described in the figure 44, was inspired from Silverman and coll. ^{291,292}. Starting from HTL hydrochloride **46**, a symmetrical urea (**49**) could be obtained, and this latter could be cyclized using malonyl chloride. After being prepared, the barbituric derivative could be grafted to the anomeric position of saccharides through Knoevenagel condensation.

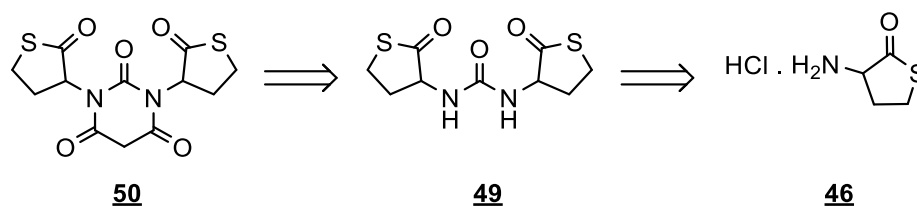
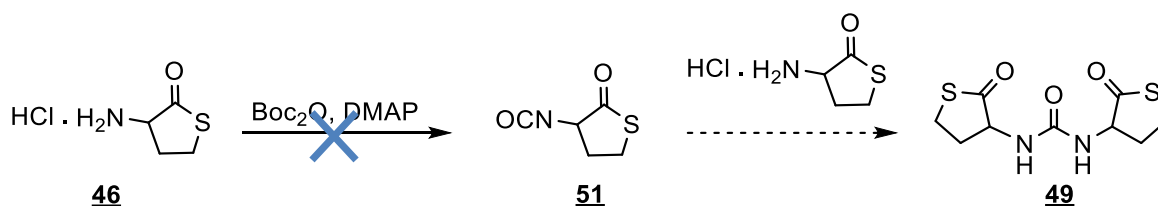


Figure 44. Retrosynthesis of symmetrical barbituric acid bearing two HTL moieties

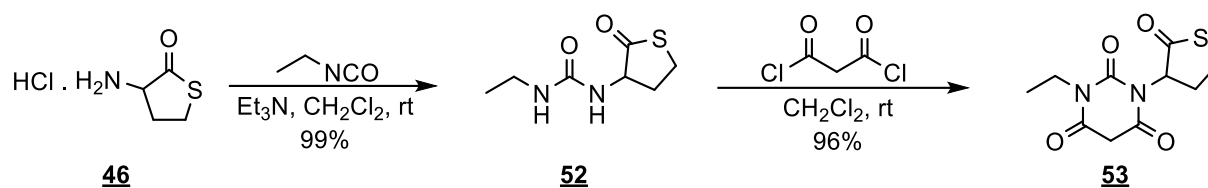
To obtain the symmetrical urea derivative **49**, a first try was carried out by employing carbonyldiimidazole/homocysteine thiolactone hydrochloride in a 1/2 molar ratio in the presence of the base DBU in *tert*-butanol at 40°C ²⁹⁷. The mixture led, after one night, to a mixture of products including the starting material. A second try by changing the base to triethylamine provided a mixture of products. Replacing *tert*-butanol by dry dichloromethane did not improve the reaction regardless of the base employed, neither did the change of temperature (from 40°C to room temperature). The other approach inspired from Silverman et col. ²⁹⁰ was thereby investigated. *S,S'*-dimethyldithiocarbonate and HTL were reacted in a 1/2 molar ratio in water at 60°C. This trial showed a TLC plate where the starting material was converted into a very polar product, that was assumed to come from side-reactions (self-condensation and/or hydrolysis).

Another strategy was to transform the amine of HTL into an isocyanate (compound **51**) as described by Knölker et al. ²⁹⁸, and to latter attach it to an HTL molecule to form the symmetrical urea (**49**). The synthesis strategy is illustrated in the scheme 43. However, the isocyanate could not be obtained. More harsh conditions could be employed to form the isocyanate by the mean of triphosgene ²⁸⁴ but this protocol was considered too hazardous to be tried. The preparation of a symmetrical urea was left out, and efforts were put to synthesize a urea bearing only one HTL moiety.



Scheme 42. Synthesis of a symmetrical urea bearing two HTL moieties *via* an isocyanate

The barbituric derivative **53** bearing one HTL was obtained by two steps illustrated on the Scheme 44. Starting from homocysteine thiolactone hydrochloride **46** and ethyl isocyanate in dry dichloromethane in the presence of triethylamine, the unsymmetrical urea **52** was provided with 99% yield. Next, a cyclisation of the urea with malonyl chloride in dry dichloromethane afforded the pure barbituric derivative **53** with 90% yield²⁹². The procedure could be performed in a one-pot reaction yielding 96% of compound **53** after column purification, whose ¹H NMR spectrum, with some minor ethylacetate contamination, is presented on the figure 45.



Scheme 43. Synthesis of an unsymmetrical urea **52** bearing one HTL moiety *via* an isocyanate

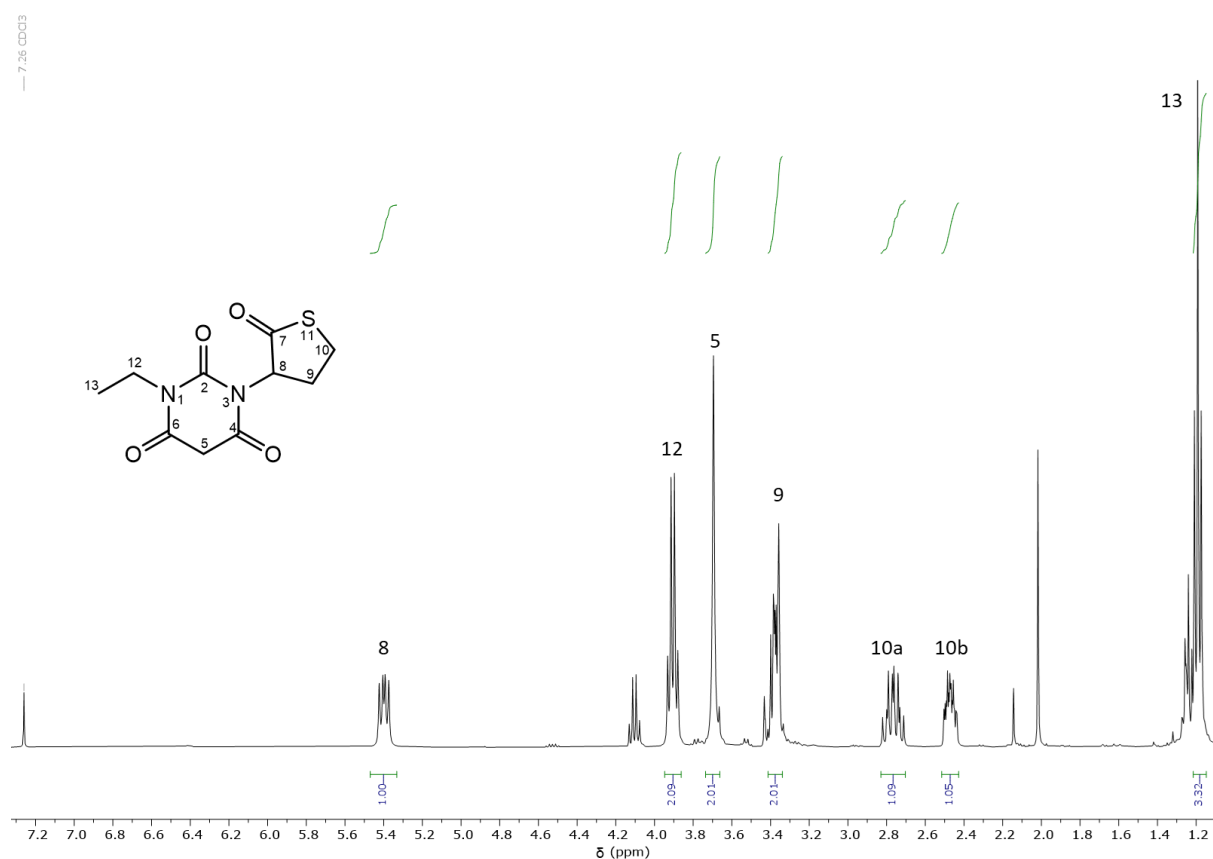
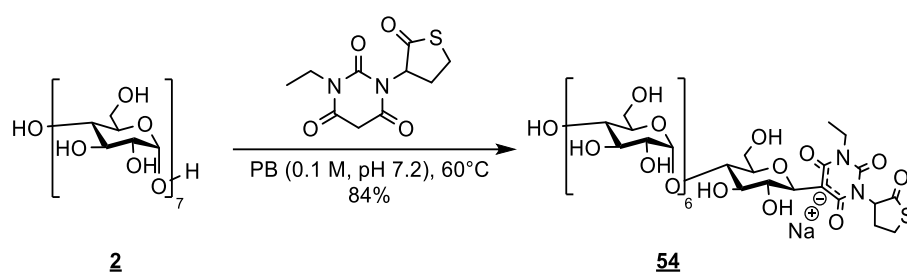


Figure 45. ¹H NMR spectrum of unsymmetrical barbituric derivative **53** in CDCl₃ with its peak integration and attribution (at 318 K)

After that, the Knoevenagel condensation of the unsymmetrical barbituric acid **53** and maltoheptaose **2** was carried out (Scheme 45). In the first experiment, an equimolar ratio of maltoheptaose and the barbituric acid derivative were mixed at 80°C in water in the presence of the weak base sodium bicarbonate (NaHCO₃) to reach pH 7. According to TLC, the conversion was not total, and the product was accompanied by a sugar side-product a bit less polar. The product could not be completely separated

by liquid chromatography on silica gel from this impurity. It was observed by mass spectrometry that maltoheptaose had been hydrolysed into maltohexaose, maltopentaose, etc. Lowering the temperature to 60°C allowed to decrease the quantity of hydrolysed product but did not enable the reaction to be total. To have more control on the pH of the medium, the reaction was then carried out in a phosphate buffer (0,1M; pH=7,2) at 60°C. No hydrolysed product was observed, and the conversion evolved for an almost-total reaction. 77% of pure C-glycosylbarbiturate **54** were obtained after column purification. The reaction was scaled-up to afford 83% of pure product. Temperature and mostly pH were found out to be important for this reaction to avoid hydrolysis of maltooligosaccharides.



Scheme 44. Knoevenagel condensation of the HTL-bearing barbituric acid with maltoheptaose

The ¹H NMR superposed spectra of compound **54** with native maltoheptaose **2** and unsymmetrical barbituric acid **53** is presented on the figure 46. From 3.25 to 5.46 ppm, the intense peaks attributed to maltoheptaose protons seem unchanged and more importantly, the reducing end anomer proton at 4.67 ppm (β-anomer) and 5.25 ppm (α-anomer) disappeared which confirmed the substitution on this position. The coupling constant of the anomeric proton with H-2 indicates that the glycoconjugate **54** is in β-configuration. Peaks from compound **53** are also present although their bad resolution. The superposition of ¹H NMR spectra, the ¹³C NMR and HRMS spectra, indicate that both maltoheptaose and barbituric derivative successfully grafted together.

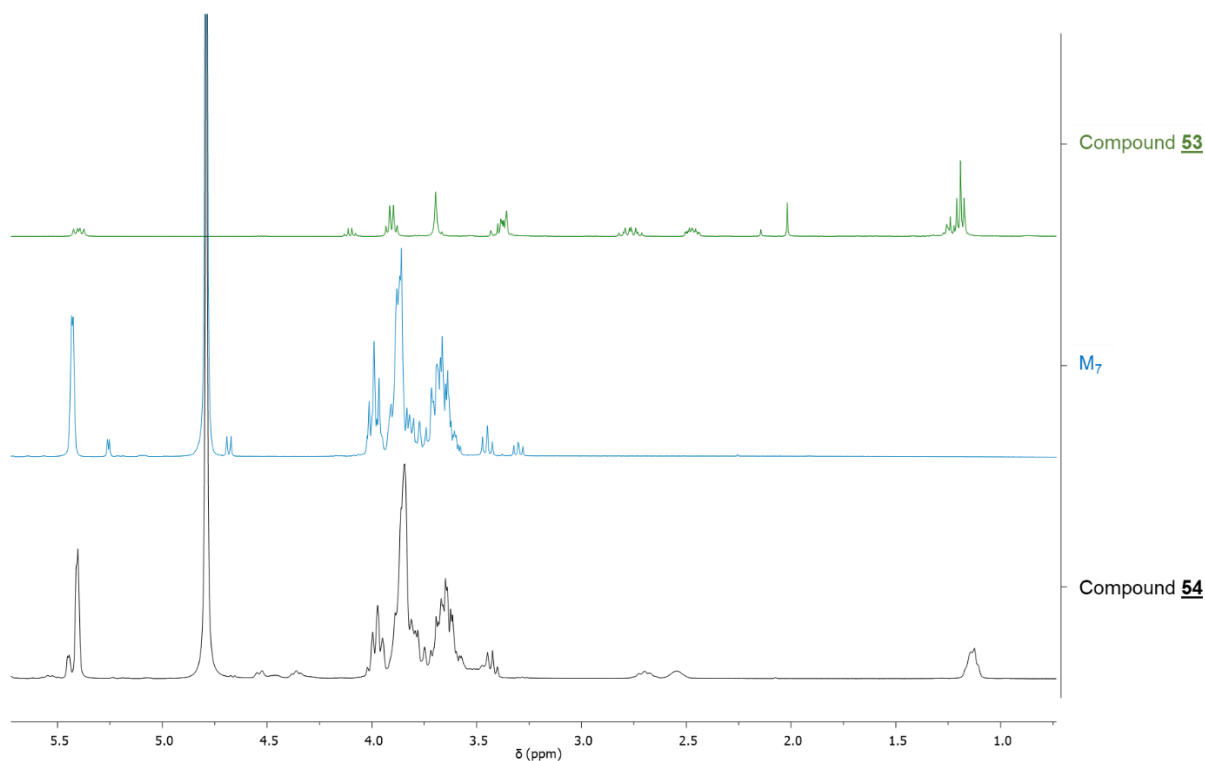


Figure 46. ^1H NMR spectra superposition of compound **54** (black, in D_2O) with native maltoheptaose (blue, in D_2O) and compound **53** (green, in CDCl_3)

The same reaction was carried out on D-glucose and D-maltose in order to perform some sulfation and thiol-ene trials. Yields of 63% and 68% were obtained respectively (compounds **54bis** and **54tris**). However, the small mono- and di-saccharides encountered stability and purification problems.

HTL-functionalized maltoses were submitted to thiol-ene optimization tests while HTL-functionalized maltoheptaoses were randomly sulfated to prepare glycosaminoglycan mimetics. It was shown that HTL was an acid- and base-labile moiety that could hardly withstand sulfation conditions (see 4.2.2). To overcome this problem, another strategy to thiol-end-functionalize maltooligosaccharides was developed lately. This last method allowed to afford UV-active product by discovering the chemistry of anthranilic derivatives.

4.2.1.3 Thiol end-functionalization by using anthranilic derivatives

4.2.1.3.1 Introduction

Anthranilic acid is an aromatic compound bearing a primary amine in *ortho* position of a carboxylic acid. Being able to act as a base or as an acid, this compound is therefore amphoteric. It has many commercial derivatives including methyl anthranilate, that is widely used in perfume industry or as a flavor additive, and isatoic anhydride, a versatile starting material for synthesis²⁹⁹. Their structures are presented on the figure 47 below.

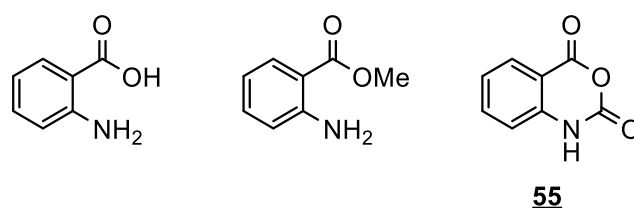
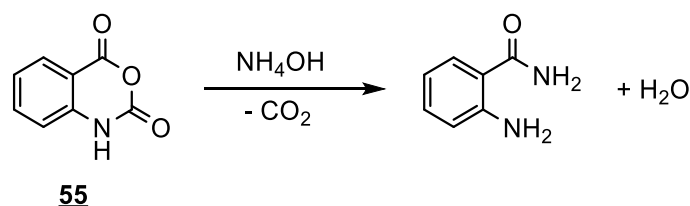


Figure 47. Structure of anthranilic acid, methyl anthranilate and isatoic anhydride (from the left to the right)

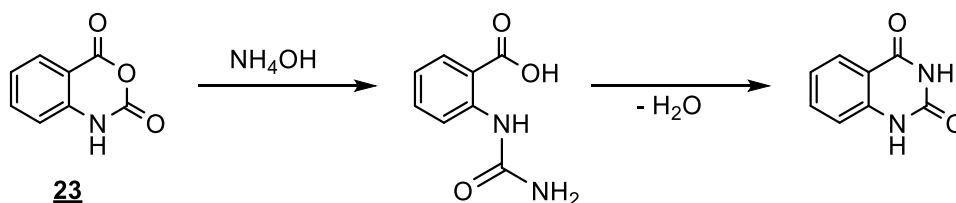
Isatoic anhydride (compound **55**) is the source of a wide range of transformations, leading to a variety of applications from pharmaceuticals to fragrances³⁰⁰. For example, starting from it, five-, six- and seven-membered heterocycles can be prepared (for more information see review³⁰¹).

Among these transformations was developed the benzoxazine dione ring opening by the action of a nucleophile, providing a free amine and subsequent loss of carbon dioxide, also called anthranoylation. This reaction was first performed with ammonium hydroxide by Kolbe³⁰², who discovered by accident the formation of anthranilamide, as illustrated on the scheme 46 below.



Scheme 45. Anthranoylation of isatoic anhydride with ammonium hydroxide

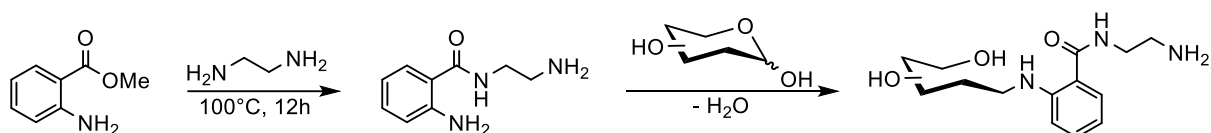
The anthranoylation was performed using different nucleophiles, but the best yields were obtained with amines. However, a second side-product resulting from a different ring cleavage was observed by Sheibley^{303,304} with halogenated isatoic anhydride derivatives. It implied the nucleophilic attack on the carbonyl on α of the amine and subsequent loss of water allowing the ring to recyclize as explained by Staiger & Wagner³⁰⁵ in the Scheme 47. It was found that the second product formation depended on the solvent of the reaction³⁰⁶, the molar ratio of the amine, its concentration but also its bulkiness³⁰⁷.



Scheme 46. Side-product formation during anthranoylation of isatoic anhydride with ammonium hydroxide

The solvent was found to be critical to suppress this side-reaction, and a variety of anthranilamides could be prepared by changing the amine in solvents such as DMF, DMAc or DMSO³⁰⁸. The prepared derivatives were biologically assayed and some of them were found to possess anti-inflammatory or

antitumor activities. The preparation of anthranilamides for biological applications was more recently developed by Cummings et al.²³⁷ in order to graft the synthesized entities on the reducing end of carbohydrates. Anthranilic derivatives have the advantage to provide fluorescent and UV active compounds. These features allow the compounds to be easily identified by chemists, but also by biologists. In one step, they easily prepared a fluorescent anthranilic derivative starting from methyl anthranilate and they grafted it on a pentasaccharide by reductive amination. The employed strategy is illustrated in scheme 48.



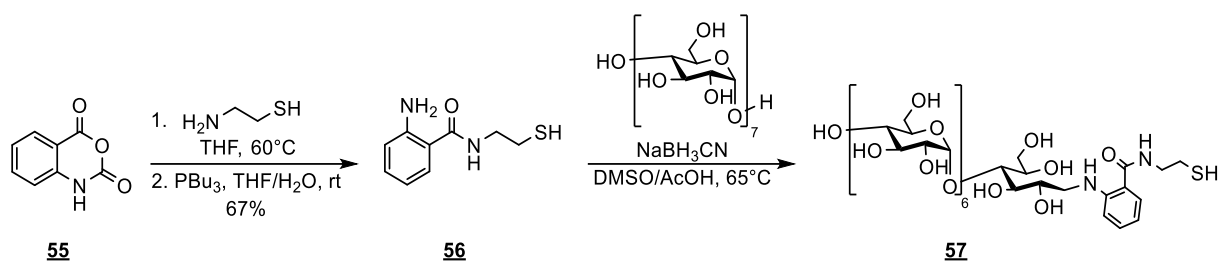
Scheme 47. Synthesis and grafting of anthranilic derivative on the reducing end of carbohydrates

Lately, this grafting was promoted by the synthesis of functionalized maltoheptaose with anthranilic derivatives bearing clickable functions in our team (work not published). Starting from isatoic anhydride, they first prepared functionalized anthranilic derivatives with good yields (more than 80%), and they performed the reductive amination with maltoheptaose with a 100% of yield.

The anthranilic derivative chemistry was carried out in the same conditions as previously. A two-step strategy was conceived to introduce cysteamine or its oxidized form cysteamine on the reducing end of carbohydrates.

4.2.1.3.2 Grafting of cysteamine onto maltooligosaccharides through reductive amination

In order to reproduce the synthesis previously developed in our team, maltoheptaose was planned to be end-functionalized by an anthranilic derivative bearing a cysteamine moiety. This reaction was carried out to obtain a free thiol, readily accessible for thiol-ene coupling. To do so, isatoic anhydride **55** and cysteamine **35** were grafted in tetrahydrofuran at 60°C. The product, obtained in the form of a monomer or a dimer (formation of a disulfide bond), was submitted to reduction by using tributyl phosphine in a mixture of tetrahydrofuran and water according to the procedure of Ayers & Anderson³⁰⁹, and kept without further purification in inert atmosphere in the fridge, affording 67% of product **56**. This reaction crude was then submitted to a reductive amination with maltoheptaose in the same conditions as 4.2.1.1.2, as shown on the Scheme 49. Briefly, the starting material was reacted with ten equivalents of cysteamine-bearing anthranilic derivative **56** and thirty of sodium cyanoborohydride in DMSO/acetic acid at 65°C under inert atmosphere. A hardly characterizable mixture of products including oxidized dimer was obtained according to mass spectrometry. This latter was expected as the work-up of the reaction could not be done in inert conditions.

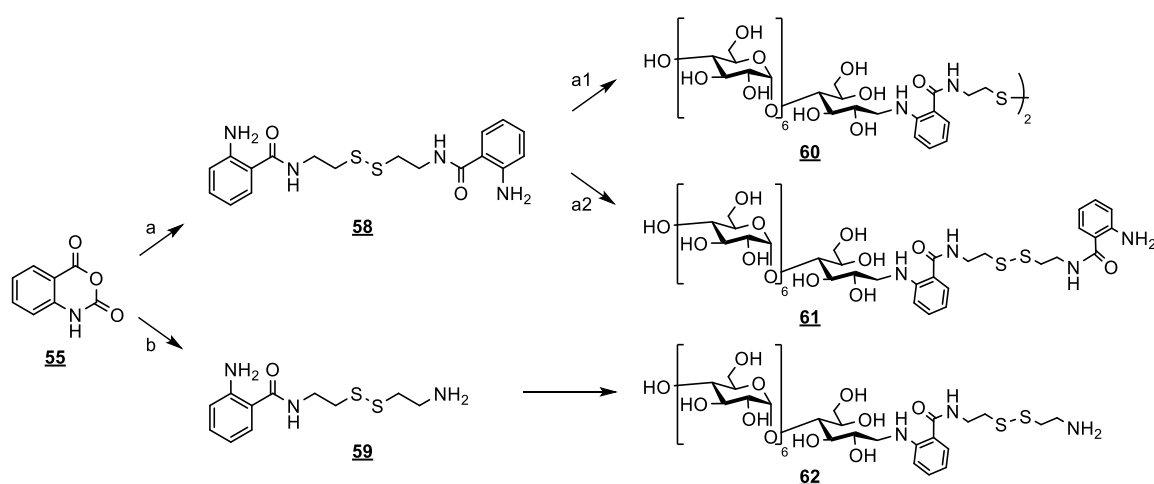


Scheme 48. Preparation of thiol-functionalized maltoheptaose **57** by reductive amination with cystamine-bearing anthranilic derivative **56**

The storage and manipulation of free thiolated product was observed to add steps in the synthesis, leading to low yields and problems of purification. So, this strategy was put aside to concentrate on thiol protection with the use of cystamine with anthranilic derivatives.

4.2.1.3.3 Grafting of cystamine onto maltooligosaccharides through reductive amination

As previously said, cystamine contains two equivalent amines thanks to its symmetry, meaning that either symmetrical or unsymmetrical anthranilic derivatives can be synthesized starting from it, as illustrated on the scheme 50 below.



Scheme 49. Obtention of thiol-functionalized maltoheptaose with cystamine-bearing anthranilic derivative

Starting from isatoic anhydride **55**, a symmetrical anthranilic intermediate **58** could be obtained via the pathway **a**. This entity bearing two equivalent arylamines could undergo reductive amination symmetrically to obtain a dimer (path **a1**, compound **60**) or unsymmetrically (path **a2**, compound **61**), leading in both cases to a thiol protected by a disulfide bond. The other possibility would be to graft only one of cystamine's amines on isatoic anhydride in order to obtain the unsymmetrical anthranilic derivative **59** via the pathway **b**. This latter, reacted with maltoheptaose, would similarly lead to a protected thiol (compound **62**). The first approach (pathway **a**) involving the preparation of a symmetrical anthranilic intermediate was investigated.

Prior to the reaction, cystamine dihydrochloride was freed from its salts with sodium hydroxide. Free-base cystamine was then reacted with isatoic anhydride in a ½ molar ratio in tetrahydrofuran at 60°C. The brown product **58** obtained could either be purified by chromatography to afford 81% of a white pure product, or be used without further purification with a quantitative yield. The ¹H NMR analysis shown on figure 48 did not show any significant difference between the two products (peak at 3.31 ppm corresponding to water traces in DMSO-d₆ & same peak integration (not shown)), and the purification of this intermediate did not affect the effectiveness of further steps.

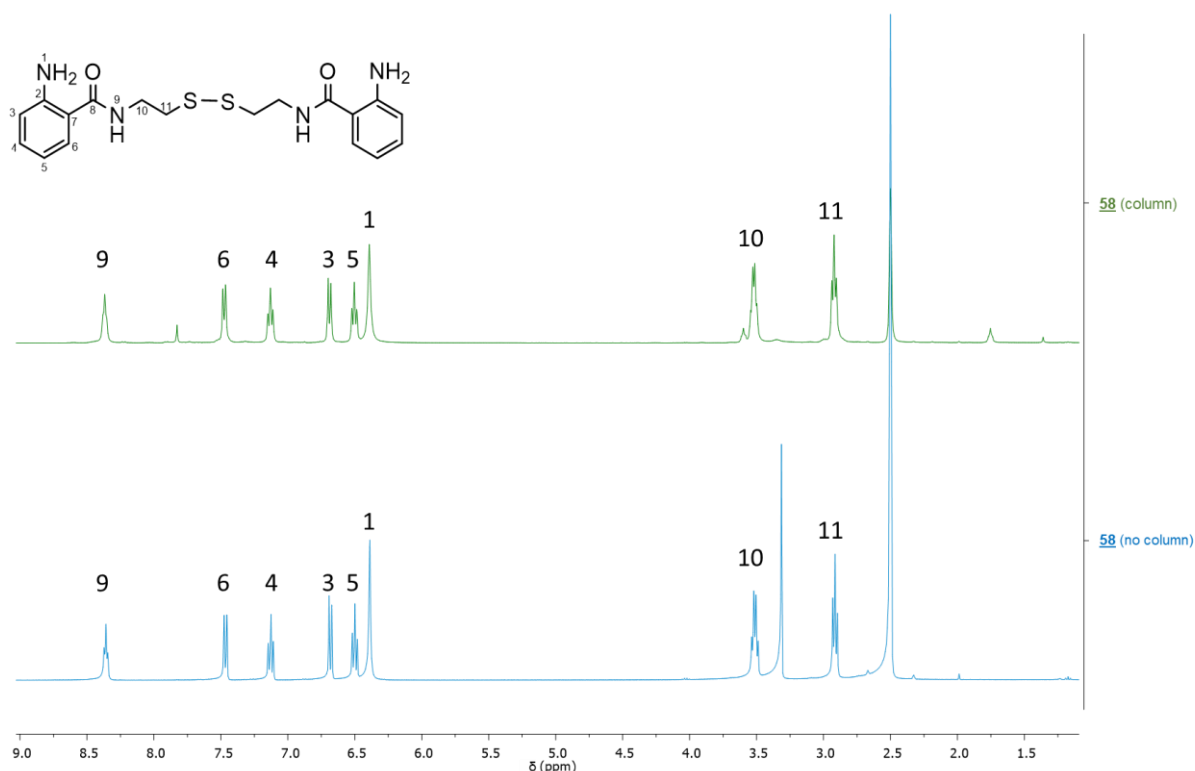


Figure 48. ¹H NMR spectra superposition of compound **58** before (blue) and after (green) column purification in DMSO-d₆ and its peak attribution

The symmetrical anthranilic derivative could be further attached to one or two maltoheptaose moieties as previously mentioned (Scheme 50, pathways **a1** and **a2**).

To obtain the symmetrical thiol-functionalized maltoheptaose (pathway **a1**), reductive amination was first carried out with four equivalents of maltoheptaose, one equivalent of anthranilic derivative **58** and thirty of reducing agent. As a result, a mixture of three unpurifiable products was obtained according to mass spectrum: unreacted and/or reduced maltoheptaose [M₇+Na]⁺ at m/z=1175.372, M₇-A-cysteamine **57** as a sodium salt at m/z=1355.448 where the disulfide bond was broken, and M₇-A-cystamine-A-M₇ **60** at m/z=2686.902 [M+Na]⁺, the targeted product. To get rid of the excess of maltoheptaose, two equivalents instead of four were reacted with the cystamine-bearing anthranilic derivative **58** in the same conditions as above. However, another product was observed in addition to the three previous: M₇-A-cystamine-A **61** at m/z=1549.500 in its sodium salt form, the unsymmetrical thiol-functionalized

maltoheptaose (pathway **a2**). The structures of all products obtained are presented on the figure 49. Faced with the difficulty to obtain the pure product with a good yield, the symmetrical maltoheptaose derivative **60** was shelved while the preparation of the unsymmetrical derivative **61** was carried out.

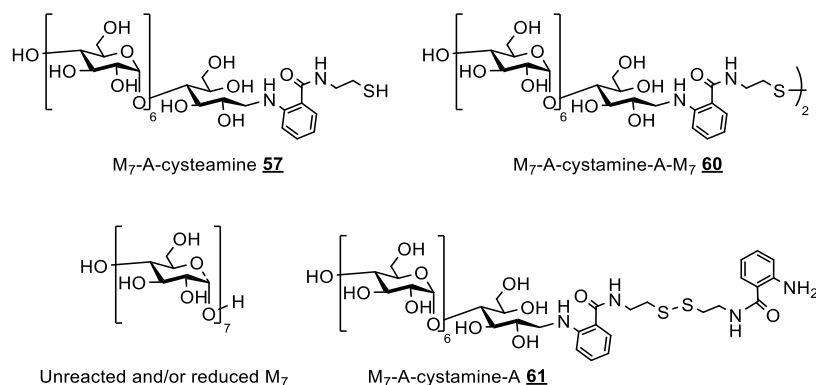
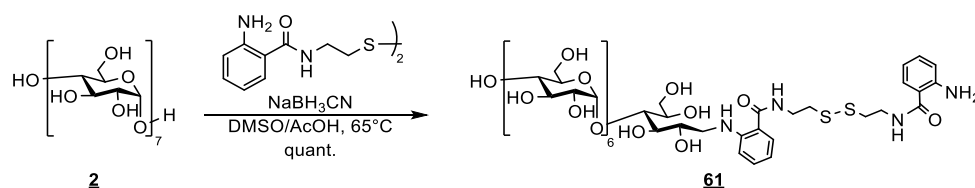


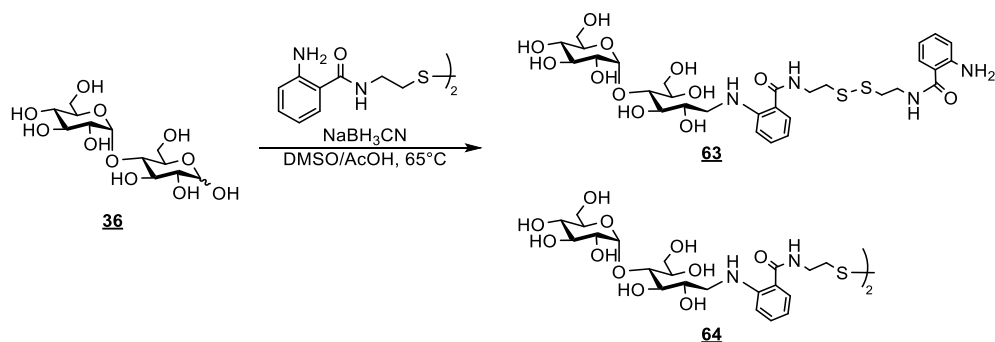
Figure 49. Product obtained after reductive amination of maltoheptaose with cysteamine-bearing anthranilic derivative **58**

To obtain the unsymmetrical thiol-functionalized maltoheptaose (pathway **a2**), previous conditions of reductive amination (see 4.2.1.1.2) were applied as shown on scheme 51. The product was obtained with a quantitative yield.



Scheme 50. Reductive amination of maltoheptaose with symmetrical cysteamine-bearing anthranilic intermediate **58**

The reductive amination of maltoheptaose with the symmetrical anthranilic intermediate seemed to work well on maltoheptaose. As previously, the reaction was tested on maltose in order to optimize the further thiol-ene coupling with this cheaper and more accessible carbohydrate. Same conditions as above were applied on maltose **36**. However, a minority of symmetrical dimer M₂-A-cysteamine-A-M₂ **64** as well as a minority of reduced maltose were observed as side-products (according to ¹H NMR and MS), as illustrated on the Scheme 52.



Scheme 51. Reductive amination of maltose with symmetrical cysteamine-bearing anthranilic intermediate **58**

In the aim of preparing carbohydrate-polymers mimicking natural PGs, some thiol-functionalized maltoheptaose were randomly sulfated for a future coupling with the PHOU polymer provided by our ICMPE collaborators (Thiais).

4.2.2 Random sulfation of thiol-end-functionalized maltoheptaose derivatives

As a reminder, three thiol-end-functionalized maltoheptaose were synthesized. Two of them, that were developed in early stages of the project, were submitted to random sulfation in the goal of preparing sulfated glycopolymers with native PHOU. Structures of these two thiol-terminated maltoheptaose are presented in the Figure 50.

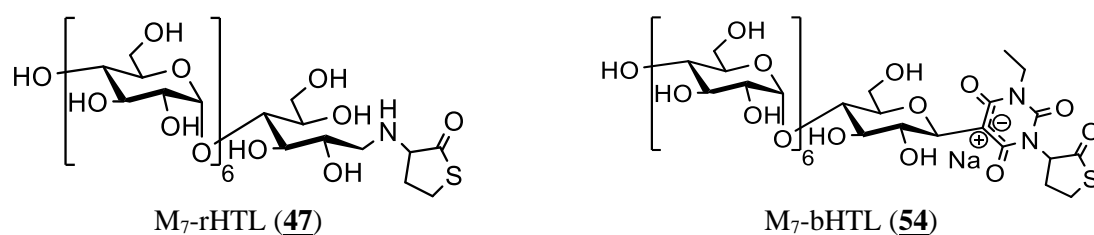
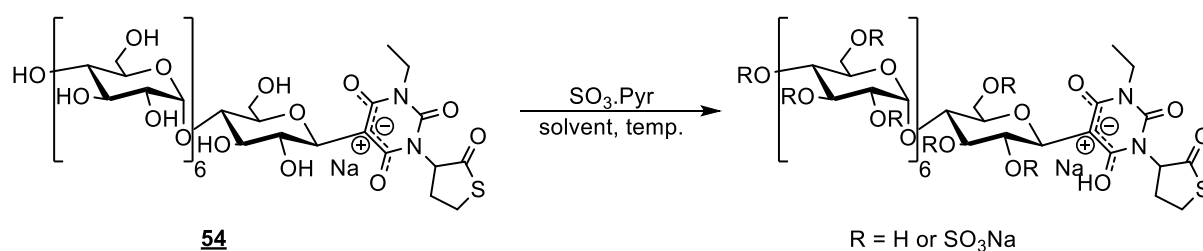


Figure 50. Structure of two thiol-end-functionalized maltoheptaose **47** and **54**, chosen to be randomly sulfated

Both structures were submitted to sulfation at three different degrees (lightly, moderately and highly sulfated) in conditions being beforehand optimized with M₇-bHTL derivatives.

4.2.2.1 Optimization of sulfation conditions and synthesis of randomly sulfated M₇-bHTL

To obtain randomly sulfated end-functionalized maltoheptaose derivatives, many procedures were tried varying solvent, temperature and reactants. Optimizations of the reaction conditions were performed on M₇-bHTL (**54**) as illustrated on the Scheme 53.



Scheme 52. General scheme of the random sulfation performed on M₇-bHTL (**54**)

The procedure previously reported for random sulfation of unmodified M₇ and ^BCD (see [CHAPTER 1](#)) was first tested. Briefly, M₇-bHTL (**54**) and sulfur trioxide pyridine complex (stoichiometry depending on the degree of sulfation targeted) were reacted together in a mixture of DMF/pyridine at 80°C. The ¹H NMR spectrum of obtained mixture (Figure 51) was superposed with the spectrum of a successful attempt (see later, blue) and the one of a sulfated native maltoheptaose, that were all aimed to be lightly sulfated derivatives. The ¹H NMR spectra resulting from such procedure showed almost no peak of

reducing end aglycon, HTL, and the general aspect of the spectrum seemed a bit different from the one of natural maltooligosaccharides (see highlighted zone on figure 51).

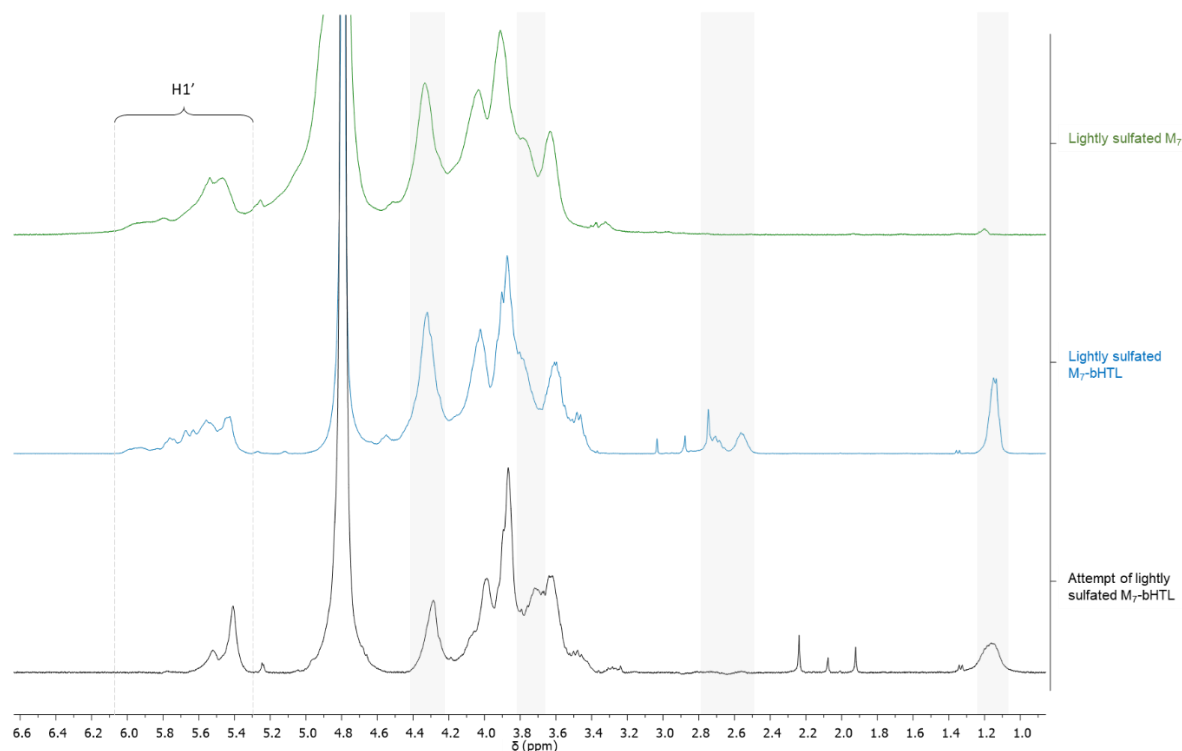


Figure 51. ^1H NMR spectra superposition of an attempt of lightly sulfated M_7 -bHTL in conditions previously described (black) with a successfully prepared lightly sulfated M_7 -bHTL (blue) and lightly sulfated maltoheptaose (green) in D_2O

The product obtained was then analyzed by SEC-MALS to assess the obtention of one homogeneously sulfated mixture of products. However, two or three populations having either very low either high to very high Mw (calculated on the basis of their elution time) that could not be possible in both extreme cases (no sulfation and complete sulfation) were observed. The FI-IR analysis showed almost no peak corresponding to sulfate esters around 1200 cm^{-1} , and the broad hydroxyl vibration peak at 3300 cm^{-1} and carbonyl group of HTL were also almost inexistent. All these data together suggested that the reaction led to undistinguished mixture of product, being partially sulfated with a clear hydrolysis of HTL. Decrease of the reaction temperature to 50°C in DMF/pyridine solvent system did not show any change.

Pyridine alone was tested as solvent for the reaction at 80°C , surprisingly leading to greater mixture of products including not negligible quantities of starting material (assessed by ^1H NMR by superposing spectra of the crude and of M_7 -bHTL (**54**)). This was likely due to the insolubility of product in the solvent resulting in the formation of gummy residues from the beginning of the reaction.

Then, DMF alone was tested as solvent providing similar mixtures of products as DMF/pyridine solvent system at 80°C, but leading very lightly sulfated maltoheptaose derivatives without hydrolysis of HTL for the lowest degrees of sulfation.

To overcome hydrolysis of HTL, 2-methyl-2-butene (2M2B), a volatile acid scavenger reported by Papy Garcia et al.¹¹¹ was added to the reaction mixture in a 8/1 2M2B/SO₃.Pyr ratio, and temperature was decreased to 30°C to avoid its evaporation. In DMF/pyridine (2/3 v/v) solvent, HTL was not hydrolyzed anymore but a mixture of unreacted starting material along with final products was observed. Changing the solvent for DMF alone allowed to obtain lightly and moderately sulfated M₇-bHTL derivatives (Figure 51 below). Methyl protons of the barbiturate at 1.17 ppm and peaks attributed to HTL methylene between 2.40 and 2.80 ppm in addition to the slight shift towards low field confirms the presence of sulfated carbohydrate without HTL hydrolysis.

Concerning the highest degree of sulfation, larger quantities of insoluble 2M2B necessary for the reaction to proceed without hydrolysis induced poorly sulfated products, diminishing the 2M2B/SO₃.Pyr ratio from 8/1 to 2/1 proved to be ineffective. The reaction conditions were no longer optimized although the targeted highly sulfated M₇-bHTL derivative seemed to have a similar degree of sulfation to the lightly one (Figure 52 below). Additional peaks between those attributed to methylene at position 6' after sulfation (big peak around 4.35 ppm) and those attributed to position 2' from 5' (between 3.39-4.10 ppm) were observed. Moreover, peaks between 2.40 and 2.90 ppm attributed to HTL protons were less defined. All these observations indicated possible partial degradation of sample as previously observed without acid scavenger 2M2B. The ¹H NMR spectra superposition of all three sulfated derivatives after dialysis purification is presented on the Figure 52 below.

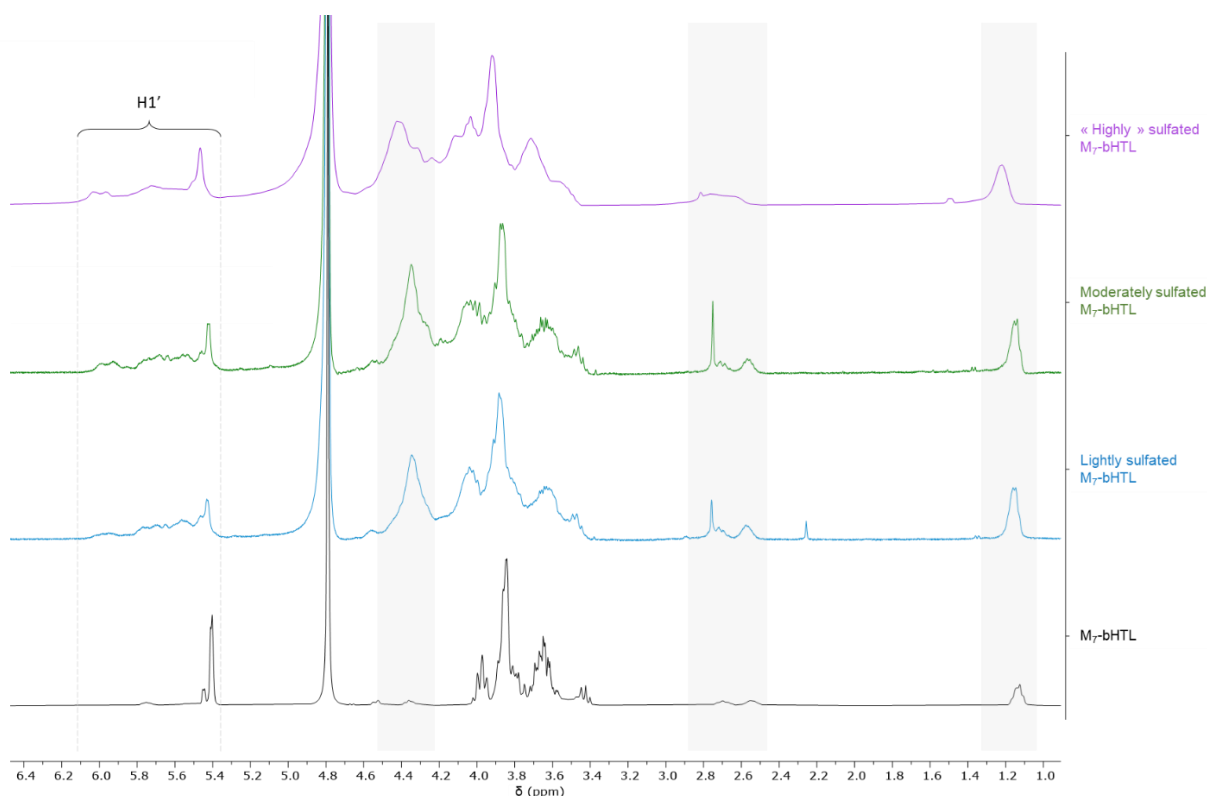


Figure 52. ^1H NMR spectra superposition of lightly (black), moderately (blue) and highly (green) sulfated $\text{M}_7\text{-bHTL}$ in D_2O

As for sulfated (cyclo)maltooligosaccharides, SEC-MALS analysis of three sulfated derivatives was carried out. Lightly sulfated $\text{M}_7\text{-bHTL}$ was characterized by a M_w of $2233 \text{ g}\cdot\text{mol}^{-1}$, the moderately by a M_w of $2560 \text{ g}\cdot\text{mol}^{-1}$. As expected with ^1H NMR, many populations including the targeted one were observed for highly sulfated $\text{M}_7\text{-bHTL}$ with M_w varying from 1746 to $1844 \text{ g}\cdot\text{mol}^{-1}$.

For a precise determination of the average degree of sulfation, elemental analysis was performed (Table 16). Lightly and moderately sulfated maltoheptaose derivatives presented a degree of sulfation of 0.8 and 1.4 respectively, in accordance with previous data. The mixture composing “highly sulfated” $\text{M}_7\text{-bHTL}$ exhibited a degree of sulfation of 1.1, accordingly to previous ^1H NMR data.

Sample		C	H	N	S	DS
		[wt%]	[wt%]	[wt%]	[wt%]	
M ₇ -bHTL	Low	25.019	4.183	0.837	9.368	0.8
	Medium	20.098	3.479	0.490	12.657	1.4
	High	23.746	4.096	0.864	11.295	1.1

Table 14. Degree of sulfation per saccharidic unit of the sulfated $\text{M}_7\text{-bHTL}$ derivatives (calculated by elemental analysis).

To summarize, conditions previously developed for the synthesis of sulfated maltoheptaose derivatives were slightly modified. DMF was chosen as unique solvent for complete sulfation of products, and an acid scavenger, 2M2B, was added in order to avoid partial hydrolysis of products. These conditions

allowed to successfully prepare lightly and moderately sulfated M₇-bHTL derivatives, while the highly sulfated one could not be obtained pure and efficiently sulfated.

4.2.2.2 Synthesis of randomly sulfated M₇-rHTL

Conditions described above for the preparation of sulfated M₇-bHTL derivatives were applied for the preparation of M₇-rHTL derivatives as shown on the Scheme 54 below.



Scheme 53. Random sulfation of M₇-rHTL (**47**)

Similarly to M₇-bHTL, the obtention of lightly and moderately sulfated derivatives could be easily obtained. The preparation of highly sulfated derivative demanded more time for partially efficient sulfation: reaction time was increased from 2 hours to 2 nights, resulting in the obtention of a product who seemed more sulfated than other samples according to ¹H NMR (higher peak at 4.42 ppm and spectrum more shifted towards low field). Only the lightly sulfated derivative was purified by dialysis (the two other samples by GPC). The ¹H NMR spectra superposition of all three products is presented on the Figure 53.

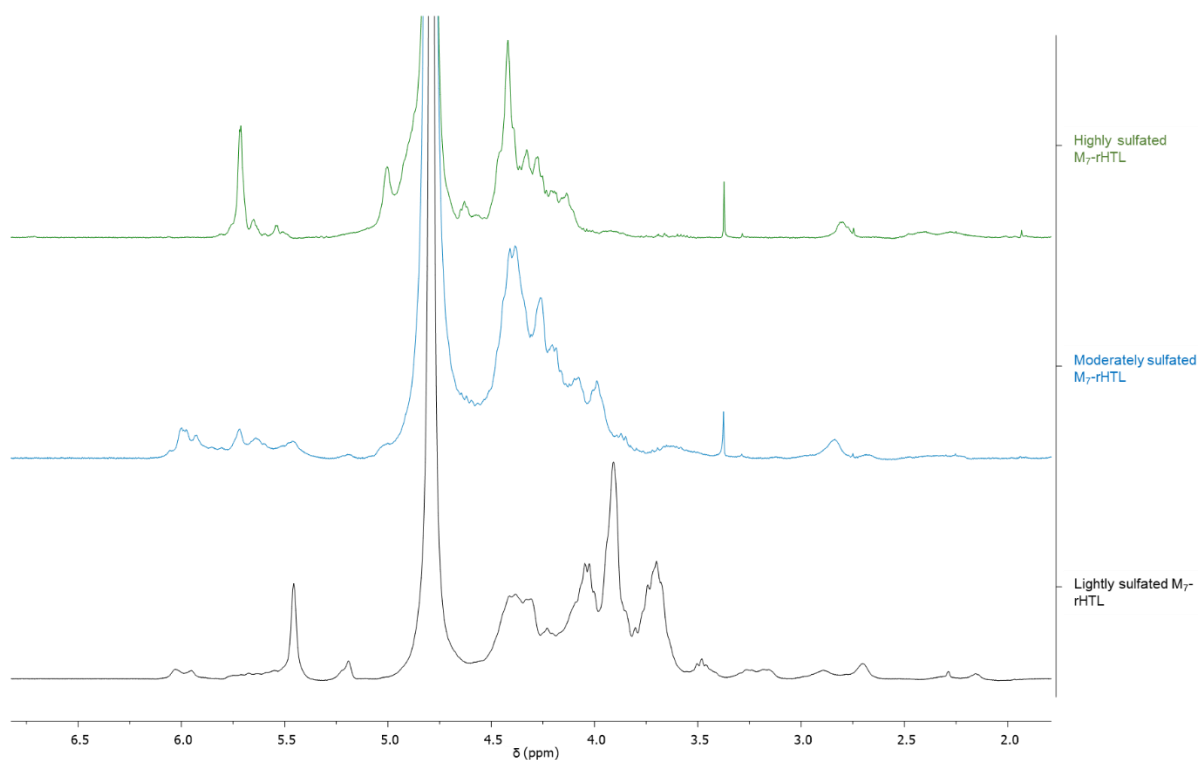


Figure 53. ¹H NMR spectra superposition of lightly (black), moderately (blue) and highly (green) sulfated M₇-rHTL in D₂O

SEC-MALS analysis of sulfated maltoheptaose indicated two populations for the lightly sulfated one with a M_w of 2822 and 3033 $\text{g}\cdot\text{mol}^{-1}$. Moderately sulfated M_7 -rHTL was characterized by two populations as well with a M_w of 2550 and 3042 $\text{g}\cdot\text{mol}^{-1}$. The population observed at 3000 $\text{g}\cdot\text{mol}^{-1}$ was present in both samples, suggesting the presence of a possible side-product in the starting material. However, the decrease of M_w between lightly sulfated sample and the moderately one was not concomitant with the data of other analysis (see ^1H NMR and elemental analysis). No conclusive data could be collected although many trials. Highly sulfated M_7 -rHTL was characterized by one unique population with a M_w of 2516 $\text{g}\cdot\text{mol}^{-1}$, which was in accordance with the ^1H NMR spectrum.

Elemental analysis of samples was conducted as previously. Data are displayed on the Table 17 below. The degree of sulfation increased from 1.1 to 2.8 sulfate moiety per unit, which was in accordance with theory.

Sample		C [wt%]	H [wt%]	N [wt%]	S [wt%]	DS
M_7 -rHTL	Low	23.048	4.127	0.483	11.597	1.1
	Medium	17.850	5.229	7.778	18.269	2.3
	High	15.563	5.035	8.351	19.641	2.8

Table 15. Degree of sulfation per saccharidic unit of the sulfated M_7 -rHTL derivatives (calculated by elemental analysis).

The preparation of sulfated M_7 -rHTL derivatives seemed to be successful although SEC-MALS analysis was not conclusive for lightly and moderately sulfated ones. M_7 -rHTL and M_7 -rHTL derivatives were not biologically assayed because the only difference with native maltooligosaccharides resided in their functionalized reducing end, which was not supposed to change the interaction (later grafted to PHOU polymer).

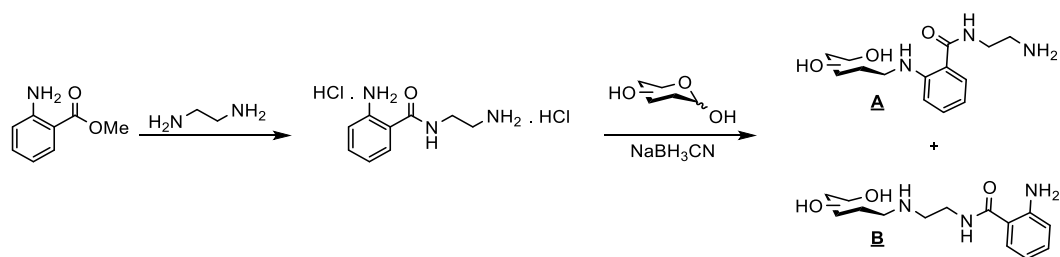
The thiol-functionalized maltoses prepared in part 4.2.1 were used to test the challenging thiol-ene coupling. Due to the difficulty to efficiently perform this photoinitiated reaction (see 5.2.1), a second more classical type of grafting was proposed to get around the thiol-ene chemistry: amidation. To do so, carbohydrates have to be amine-end-functionalized.

4.2.3 Amine end-functionalization

4.2.3.1 Introduction

Amine-end functionalization of carbohydrates was developed in the late stage of the project due to the difficulty of performing the challenging thiol-ene coupling of thiol-end functionalized maltooligosaccharides with the PHOU polymer. Therefore, only one functionalization was investigated with an anthranilic derivative bearing ethylenediamine.

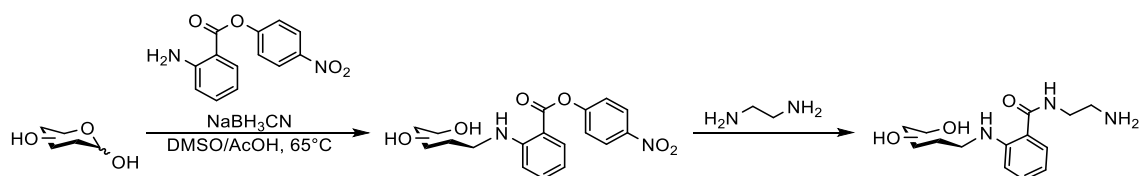
This approach was developed by Cummings and col.²³⁷ Starting from methyl anthranilate and ethylenediamine, they prepared an anthranilic derivative possessing two free amines: an aromatic one (pK_a 4-5) and an aliphatic one (pK_a 9-10). The presence of these two amines could lead to two different products after reductive amination (**A** and **B**). To achieve a chemoselective reductive amination, they converted the anthranilic derivative into its salt and an acidic medium was used to decrease the nucleophilicity of the aliphatic amine. By doing so, they dramatically dropped off the amount of product **B**, which was observed as traces. Their strategy is illustrated on the scheme 55.



Scheme 54. Preparation of amine-end functionalized carbohydrates *via* the synthesis of an anthranilamide by Cumming and col.

In the same paper, they also developed the reverse strategy. To completely avoid the formation of the compound **B**, they carried out reductive amination of their glycan with methyl anthranilate, and they then achieved the aminolysis of the anthranilic ester to afford the product **A**.

In another paper, Cummings and col.³¹⁰ described the two-step conjugation of carbohydrate reducing end to proteins with a fluorescent linker. This latter, *para*-nitrophenyl anthranilate, was chosen for its aryl amine, used for the reductive amination, and active *para*-nitrophenyl ester, that could be transformed into an amide by nucleophilic attack of protein's amino groups. Interestingly, the two opposite functional groups (amine and ester) were known to be tolerant. The aminolysis of the active ester was first tested with ethylenediamine and showed a total conversion at room temperature within thirty minutes. Applying it to protein at 37°C in a buffer showed an efficient carbohydrate-protein conjugation where the two entities were linked by a small fluorescent moiety. This approach is illustrated on the scheme 56.



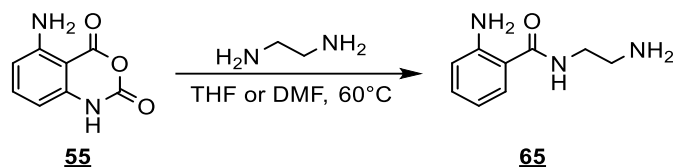
Scheme 55. Preparation of amine-end functionalized carbohydrates *via* the synthesis of a glycol-conjugate

In both papers, the use of anthranilic derivatives for biological systems was expected to be safe as anthranilic acid is the precursor of the amino acid tryptophan in the organism.

To amine-end functionalize maltoheptaose with anthranilic derivatives, both approaches were carried out.

4.2.3.2 Amine end-functionalization starting from isatoic anhydride

The first way investigated to amine-functionalize the reducing end of carbohydrates was inspired from Cummings and col.²³⁷ An ethylenediamine-bearing anthranilamide was conceived to be obtained from isatoic anhydride **55** instead of methyl anthranilate. The synthesis is shown on the scheme 57.



Scheme 56. Preparation of an ethylenediamine-bearing anthranilamide starting from isatoic anhydride

First, the reaction was performed at 60°C in tetrahydrofuran (conditions previously developed in the team, not published). To avoid the obtention of di-substituted ethylenediamine forming a symmetrical dimer, 0.5 equivalents of isatoic anhydride were added dropwise at room temperature in the reaction mixture, and then the heating proceeded. It was observed insoluble isatoic anhydride at room temperature became almost soluble at 60°C. At the end of the reaction, the ^1H NMR showed what seemed to be a mixture of product. According to mass spectrometry, the majority product was the targeted one **65**, but many side-products were also observed (Figure 54 below, **65** in blue). The same reaction was carried out with equimolar ratio of isatoic anhydride and ethylenediamine in a more diluted medium for the amine. The major product, was this time the di-substituted amine **67**, and the targeted anthranilamide **65** was present as traces. When the reaction was performed with 1.2 equivalents of amine and with a slower addition of isatoic anhydride, the same result was observed. It was hypothesized that the insolubility of isatoic anhydride in tetrahydrofuran during its addition might affect the reaction. The solvent was changed for dimethylformamide as recommended by Heindel et al.³⁰⁸ and the reaction was conducted with one, 1.2 and five equivalents of ethylenediamine. According to their mass spectrum, more side-products were observed. Higher intensities of targeted product **65** were however observed when adding great excess of ethylenediamine. The product could never be obtained pure, but many of the side-products could be identified by MS. Their structures, also described by Fadda et al.,³¹¹ are shown on the figure 54.

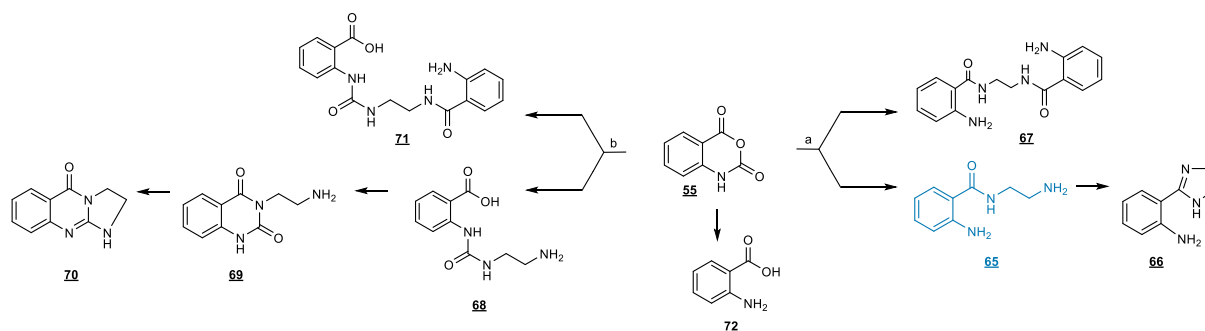


Figure 54. Products obtained from the anthranoylation of isatoic anhydride with ethylenediamine

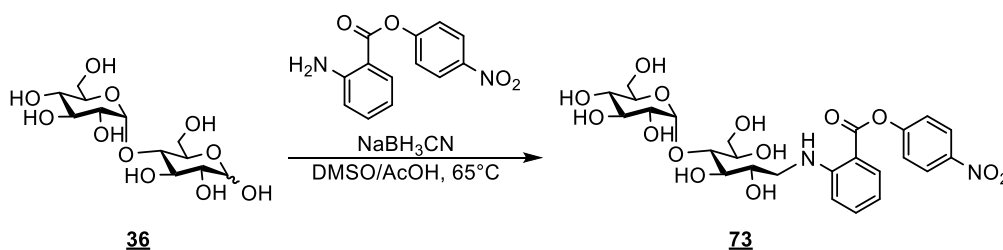
The products **65**, **66** and **67** were issued from the nucleophilic attack of ethylenediamine on the benzoyl of isatoic anhydride (pathway **a**) while compounds **68**, **69**, **70** and **71** from the attack of ethylenediamine on the carbonyl on α of the amine (pathway **b**). The targeted product **65**, could undergo a cyclization leading to the compound **66**. Issued from the pathway **b**, the side-product **68** issued could cyclize by an intramolecular attack of the secondary newly introduced amine on the carboxylic acid (**69**). Similarly to compound **65** (targeted product), this formed product could cyclize by the action of the primary amine, forming the product **70**. Compound **71**, was obtained by di-substitution of ethylenediamine by the two pathways **b** then **a** on isatoic anhydride. Di-substituted **67**, was done by the pathway **a**. No di-substituted product only from pathway **b** was observed. Finally, product **72**, was obtained by a simple hydrolysis of isatoic anhydride and forms anthranilic acid.

All these side-products, obtained from the same reaction mixture, could very hardly be separated from the targeted product by chromatography because of the structure similarities. To bypass this problem, isatoic anhydride was put aside, and the other approach developed by Cumming and col. was conceived with an anthranilic derivative possessing a leaving group stable enough to endure reductive amination.

4.2.3.3 Amine end-functionalization starting from *para*-nitrophenyl anthranilate

Instead of preparing the anthranilic derivative with ethylenediamine and then grafting it onto carbohydrates, the reverse steps were envisioned as previously described by Cummings and col.²³⁷ A reductive amination of carbohydrates with an anthranilic derivative bearing a leaving group was accomplished, although the conversion was not total (more than 80%) and later this leaving group was replaced by ethylenediamine. The anthranilic derivative chosen for this approach was *para*-nitrophenyl anthranilate (PNPA). This compound owns a nitrophenyl as leaving group, which was assumed to be stable enough to undergo reductive amination.

The introduction of PNPA onto carbohydrates was first tested on maltose. The conditions of reductive amination used were the same as previously described for homocysteine thiolactone, as shown on the scheme 58.

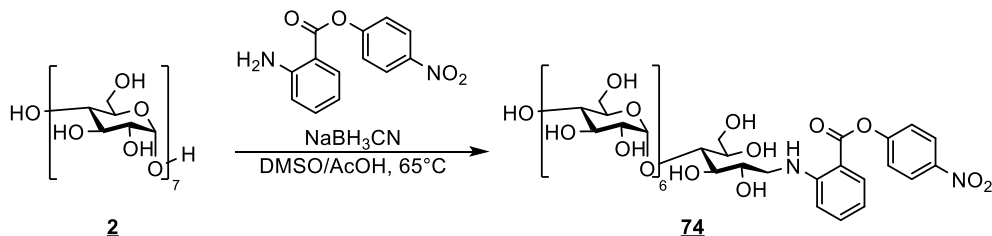


Scheme 57. Reductive amination of maltose with *para*-nitrophenyl anthranilate

Briefly, maltose **36** was either mixed with two equivalents of PNPA and eight of sodium cyanoborohydride, either ten equivalents of PNPA and thirty of reducing agent. In the first case, almost no conversion of maltose was observed according to TLC plates. And in the second case, a less polar

product was observed but also a non-UV active sugar compound more polar than maltose, which could not be isolated and identified.

Reductive amination of maltoheptaose **2** was carried out in the same conditions, as illustrated on the scheme 59.



Scheme 58. Reductive amination of maltoheptaose with *para*-nitrophenyl anthranilate

After 6h30, although maltoheptaose did not seem to be totally consumed according to the TLC plate, the reaction was treated by precipitation-centrifugation cycles. It was observed that after a while PNPA crystallizes in the supernatant providing yellow longitudinal crystals. A column was carried out in order to remove unreacted or reduced maltoheptaose. It was found that the product was very difficult to concentrate under reduced pressure because of its amphiphilic properties. These complications decreased the yield to 59%. The ¹H NMR spectrum of compound **74** is presented on the figure 55 below. Peaks attributed to maltoheptaose protons between 3.25 and 5.46 ppm and those attributed to PNPA between 6.71 and 8.41 ppm are effectively present on the spectrum of compound **74**. In addition, peak integration and the slight change of anomeric protons peak (4.70, 5.10 and 5.40 ppm) along with mass spectrum prove that reductive amination of PNPA onto maltoheptaose was successful.

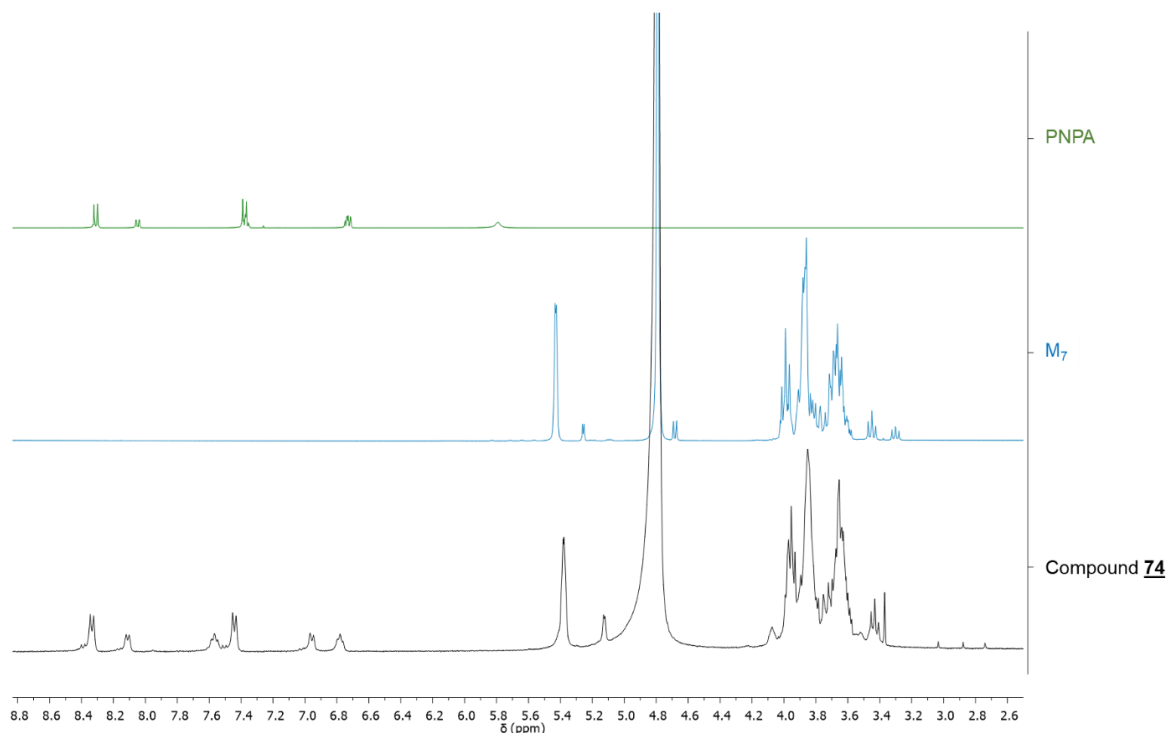
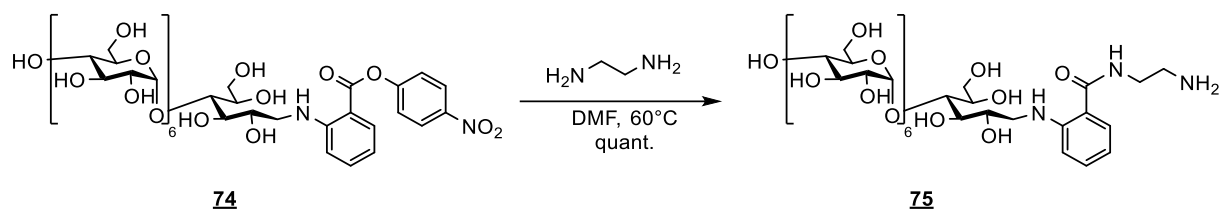


Figure 55. ¹H NMR spectra superposition of compound **74** (black, in D₂O) with native maltoheptaose (blue, in D₂O) and PNPA (green, in CDCl₃)

To replace the leaving group of the newly end-functionalized maltoheptaose **74**, a nucleophilic attack of ethylenediamine on the activated ester of **74** was achieved in dimethylformamide at 60°C, as shown on the scheme 60 below.



Scheme 59. Preparation of amine-end functionalized maltoheptaose with ethylenediamine

The reaction, after completion within 2h30, was precipitated in acetone and filtered. This simple procedure afforded a pure amine-end functionalized maltoheptaose with a quantitative yield, that was fully characterized. The ¹H NMR spectrum of compound **75** is presented on the figure 56 below. Half of PNPA signals disappeared, and two triplets corresponding to ethylenediamine methylene appeared at 3.20 and 3.45 ppm. Amine-functionalized maltoheptaose **75** was thereby successfully obtained and could be further coupled by amidation to the polymer (see 5.2.2).

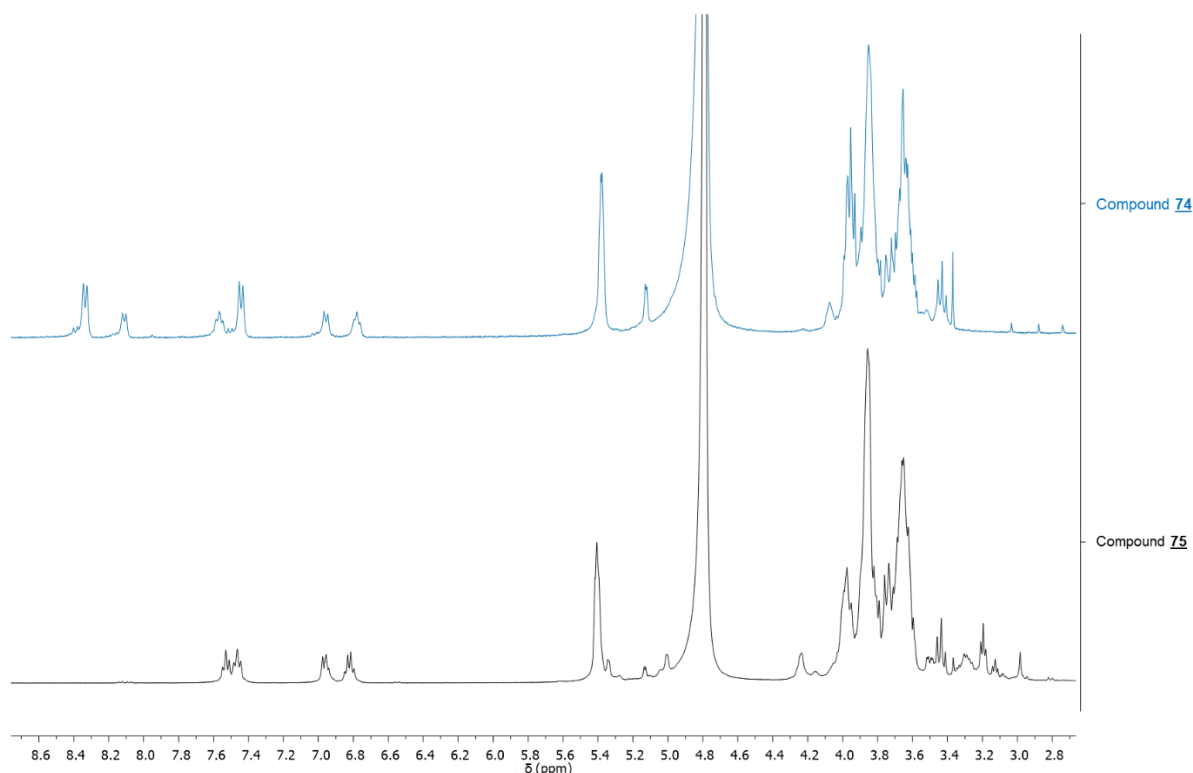


Figure 56. ¹H NMR spectra superposition of compound **75** with its precursor compound **74** (blue) in D₂O

4.3 Conclusion

Linear maltooligosaccharides were reducing end functionalized with a linker bearing a thiol or an amine moiety. For thiol-modified glycans, three strategies were investigated on maltose and maltoheptaose: cysteamine-cystamine method for which no product could be obtained, homocysteine thiolactone method for which four products could be isolated, and anthranilic derivative method for which two products were achieved. By doing so, six compounds could be synthesized whose structures are presented on the Figure 57.

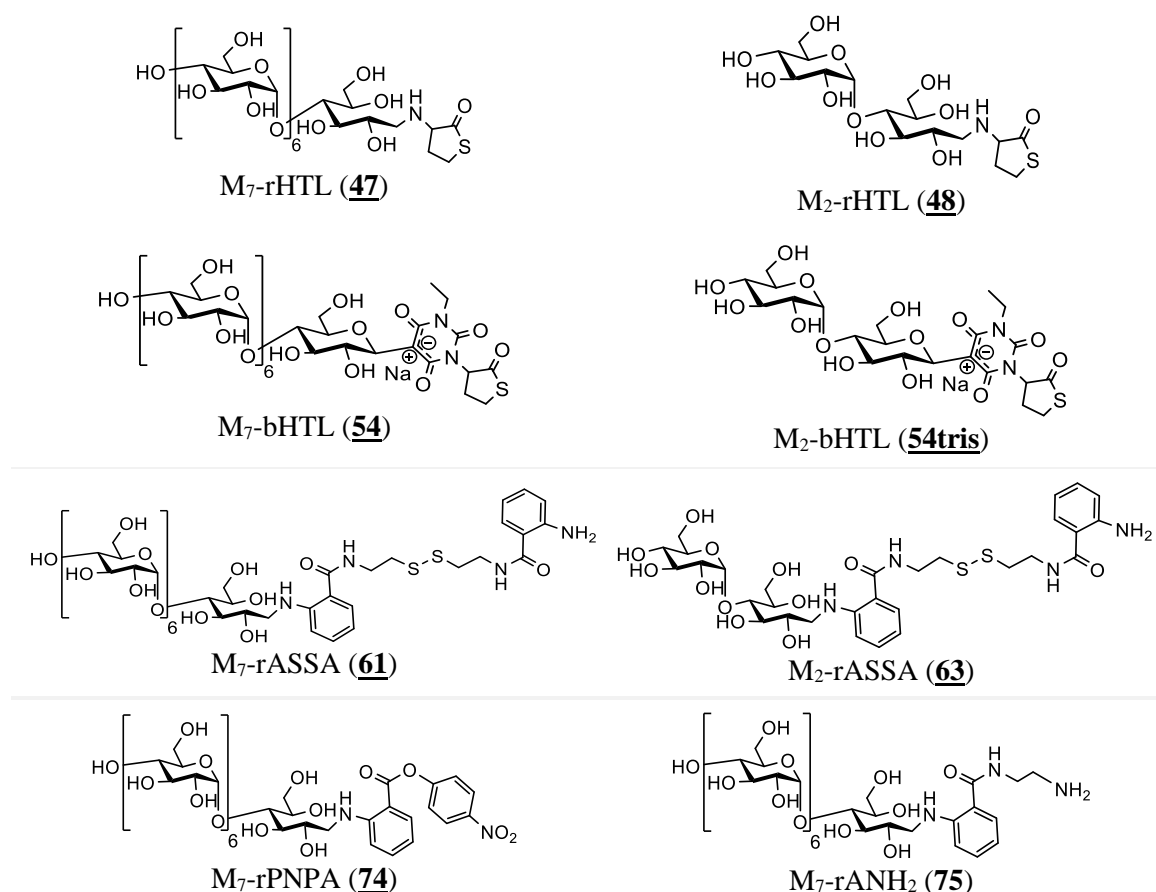


Figure 57. Scope of thiolated and aminated maltooligosaccharides that were successfully synthesized

As a final goal, several sulfated maltoheptaose (thiol- or amine-functionalized) chains were envisioned to be grafted to a polymeric skeleton (natural PHOU bearing pendant alkene functions, or PHOU-COOH bearing pendant acid carboxylic functions) in order to obtain proteoglycan mimetics.

For the next step of the project, some thiol-end-functionalized maltoheptaoses were randomly sulfated for their future coupling with PHOU, while thiol-modified maltoses were used to optimize the thiol-ene coupling.

Concerning the amine-modification that was developed in late stages of the project, only one strategy was investigated directly on maltoheptaose: the anthranilic derivative method. Two modified maltoheptaoses could be obtained including the final amine-bearing glycan **75**. Their structures are

presented on the figure 56 above. M₇-rPNPA (**74**) was submitted to random sulfation (for the future formation of PG mimetics) but PNPA was found not to be stable enough for sulfation conditions (even in the presence of acid scavenger 2M2B), and M₇-rANH₂ (**75**) to an amide coupling with biotin and a variant of PHOU bearing pendant carboxylic acids (see [5.2.2](#)).

CHAPTER 5

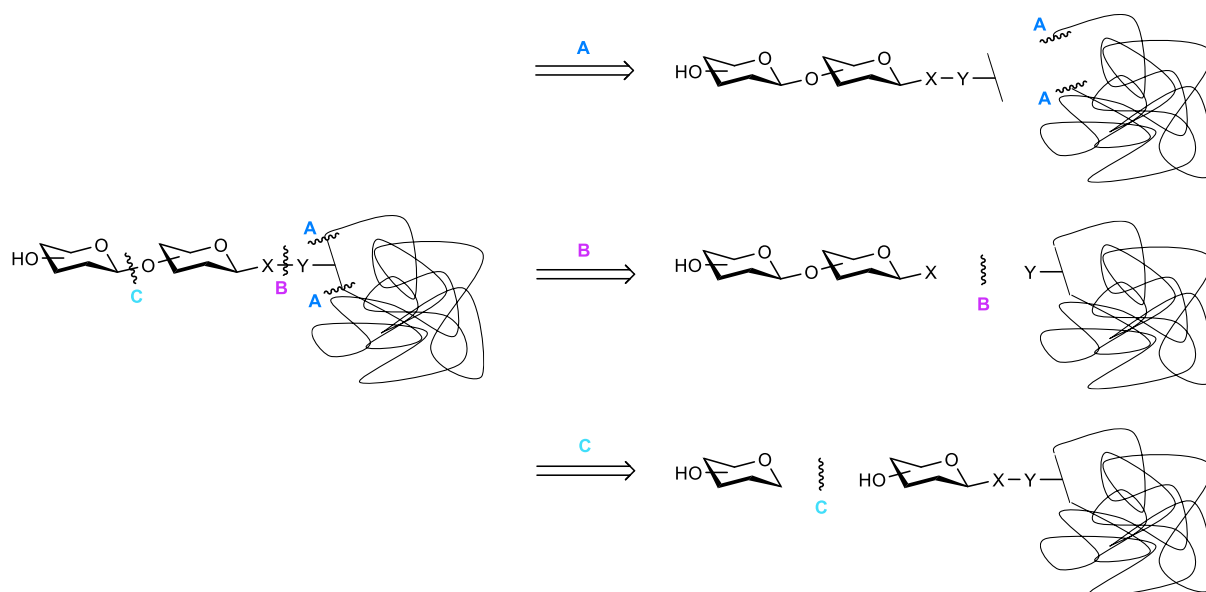
Coupling of functionalized maltooligosaccharides

5.1 Introduction

As a reminder, in Nature, many glycosaminoglycan chains can be found attached to a protein core forming a proteoglycan. This complex structure of oligosaccharides might be relevant for molecular recognition : the presence of many oligosaccharide chains that each have low affinity with carbohydrate-binding proteins or others carbohydrates might generate a “cluster” effect by increasing the local concentration³⁶ and thus the activity^{312–315} : this phenomenon is defined as multivalency. As an example, the carbohydrate-lectin interaction is characterized by a weak dissociation constant (K_d) in the order of millimolars. According to Davis group,³⁵ this weak and indiscriminating interaction is caused by the shallow, solvent-exposed binding sites of lectin, that enables few direct ligand contacts. When multiple glycan chains are well-oriented, a consequent increase of affinity and specificity are observed due to the multivalent effect.³¹⁶

The vast majority of glycans are *N*- or *O*-linked to protein amino-acids in Nature.³¹⁷ In order to produce proteoglycan mimetics, many groups have investigated the preparation of sulfated oligosaccharides chains (from mono- to poly-saccharide) grafted onto a polymer or protein core either by direct coupling either *via* a linker or spacer. Many parameters have to be taken into account for the preparation of glycoconjugates such as the terminal linkage, the density or the length of saccharide chains in the case of vaccines.³¹⁷ For example, the group of Roy reported that a spacer between oligosaccharide chains and polymer or protein might give conformational freedom and more accessibility for glycan recognition.^{312–314}

Different strategies may be employed for the construction of glycan-aglycon conjugates, herein, the aglycon being defined as a polymer or a protein. As reported by Davis³¹⁷ on the Scheme 61 below, glycans can be end-functionalized with a small portion of aglycon that would be further grafted to the rest of this aglycon (pathway **A**, one glycan per aglycon in that case) ; the strategy illustrated on the pathway **C** consists in preparing an aglycon bearing a portion of glycan that is then glycosylated to obtain longer glycan chains (long procedure) ; and the last strategy (pathway **B**) relies on the functionalization of the glycan on the one hand, and of the aglycon on the other hand with reactive groups that react together to form the final glycoconjugate. In this last strategy, the functional groups introduced are biorthogonal with the other functionalities of both aglycon and saccharides, and provide high yields of products. This methodology also provides the possibility of multivalency by attaching multiple glycan chains ; it was therefore used in our context.



Scheme 60. General strategies for preparing glycan-aglycon conjugates

A variety of coupling reactions with or without metal catalysts exist to create glycan-aglycon linkages such as amide, thioether, urea, oxime, hydrazide, alkene and so on. Among them, thiol-ene and amide coupling were chosen according to available chemical functions in PHOU polymers provided by ICMPE collaborators.

PHOU (poly(3-hydroxyoctanoate-co-3-hydroxyundecenoate) **76**) is a bacterial functionalized polymer belonging to the class of polyhydroxyalkanoates. This polyester is a statistical copolymer functionalized on its side chains by pendant pentyl and oct-1-ene chains in a 69/31 molar ratio. This alkene ratio depends on the initial bacterial feeding ratio with octanoic acid and 10-undecanoic acid.³¹⁹

PHOU is characterized by a molecular mass of 124000 g/mol (determined by SEC in THF, polystyrene equivalents). Size-defined oligomers of PHOU can be synthesized from native PHOU by methanolysis. This reaction, previously developed by ICMPE group³²⁰, enables the controlled depolymerization of PHOU as a function of reaction time without affecting the percentage of alkene functions.

These alkene functions allow post-polymerization such as transformation into epoxides³²¹, chlorine³²², bromine^{323,324}, hydroxyl³²⁵⁻³²⁷, carboxylic acid groups^{328,329} or thioether³²⁴ allowing an enhancement of water solubility and thus improving the hydrophilic character of such polymer.³³⁰ The introduced functional groups may be used for further reactions to create conjugates.³³¹

In our project, glycan-aglycon conjugates were envisioned in the goal of forming proteoglycan mimetics. As previously described, proteoglycans (PGs) are featured by a core protein where are attached multiple GAG chains. Likewise, a single PHOU chain acting like a scaffold would be attached to multiple glycan chains to create a multivalent platform capable of biological activity. PHOU oligomers (provided by ICMPE collaborators) were thereby envisioned to be coupled with end-

functionalized maltooligosaccharides previously synthesized (see [CHAPTER 4](#)) according to two strategies : thiol-ene and amide couplings that will be developed in the following chapter.

In order to limit the waste of the alkene-bearing polymer PHOU and to optimize the conditions necessary for an improved thiol-ene and amide coupling of modified maltooligosaccharides, a low molecular weight model compound was selected: D-(+)-biotin. This reagent allows for a better following of the reaction by TLC and NMR as it can be well characterized. Moreover, once attached to maltooligosaccharides, it enables to measure the glycoconjugate affinity with biomolecules *via* Surface Plasmon Resonance biological analysis (performed at IBS, Grenoble). In our case, sulfated maltooligosaccharides, acting as glycosaminoglycan mimetics, can be immobilized on the surface by forming glycan-biotin-streptavidin complexes and their interaction with analytes such as protein and growth factor can be assayed.

Initially, a thiol-ene coupling between native PHOU and maltooligosaccharides was investigated. To do so, an alkene-bearing biotin was synthesized. This latter was reacted with thiol-terminated maltose, a disaccharide model compound, in a photo-initiated thiol-ene reaction. As a result of inefficiency, an amide coupling between NHS-bearing biotin and amine-functionalized maltoheptaose was lately developed. The coupled adducts were then submitted to random sulfation. Maltoheptaose-biotin adducts were sulfated for the future SPR analysis, and maltoheptaose-PHOU adducts were sulfated in the goal of mimicking PGs.

5.2 Results and discussion

5.2.1 Thiol-ene coupling

5.2.1.1 Introduction

The addition of a thiol to a double bond is known as the thiol-ene reaction. Such fast and high yielding reaction usually requires mild conditions. However, the reactivity of thiols constitutes a limitation as these functional groups can undergo many simultaneous reactions, limiting their chemoselectivity and orthogonality to a broad range of reagents. As a consequence, thiol-ene couplings do not meet all requirements necessary for click chemistry and are therefore referred to as “thiol-inspired” reactions.³³² Their metal-free characteristic allows their extensive use for bioconjugation and biomedical applications rather than CuAAC because no toxic metal catalyst that could be detrimental for further *in vivo* and/or *in vitro* studies is employed.^{333,334}

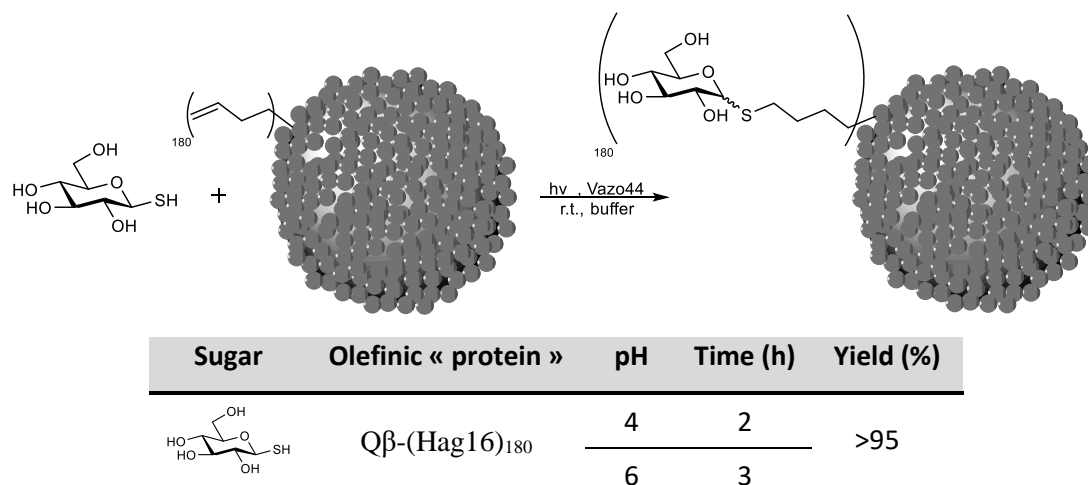
Metal-free thiol-ene couplings may be subdivided into two classes depending on the nature of unsaturated substrate. An electron-rich double bond might be thiolated by a radical mechanism while an electron deficient one by a nucleophilic mechanism, so-called thiol-Michael addition. This latter requires a strong base but can proceed at room temperature without the need of UV irradiation.³³⁵ In this chapter,

only radical thiol-ene reactions were performed and will be discussed. Such couplings, initiated thermally or photochemically, are achieved through a free-radical chain mechanism allowing the formation of robust, flexible and sterically non-demanding thioethers.³³³

On the other hand, one main disadvantage of radical thiol-ene reactions is the formation of disulfides stemming from oxidative dimerization of free thiols. Many reagents may cause this side-reaction besides atmospheric oxygen such as halogens, sulfoxides (DMSO solvent), metal ions, etc.^{336,337} In the case of photochemically induced radical thiol-ene couplings, the second case of disulfide formation is photo-oxidation (where thiols undergo a photolytic cleavage resulting in disulfide formation by radical recombination).³³² Disulfides may nevertheless be avoided by the addition of reducing agents: phosphines (tributyl-, triphenyl- and tris(2-carboxyethyl)-phosphines being the most common ones) or thiols (β -mercaptoethanol, dithiothreitol or glutathione).

Although thiol-ene reaction is an old reaction discovered in 1905 by Posner³³⁸, its application in the field of glycosciences started in the last decade with the emergence of click chemistry. From there, thiol-ene reactions allowed for the preparation of wide range of glycoconjugates such as *S*-linked oligosaccharides, calix[4]arene- or silsesquioxanes-based glycoclusters, glycodendrimers, and amino-acid-, peptide- and more interestingly protein-based glycoconjugates (for more information see^{333,339}).

As an example, Floyd et al.³⁴⁰ carried out the preparation of a *S*-linked glycoconjugate protein in aqueous and mild conditions (Scheme 62). To do so, they functionalized proteins with a non-natural amino-acid bearing an olefinic side-chain, L-homoallylglycine (L-Hag), that further reacted in a free-radical thiol-ene coupling with various 1-thioglycosyls. They further used a self-assembled multimeric virus-like particle Q β displaying 180 L-Hag moieties (Q β -(Hag16)₁₈₀) for photo-initiated glycoconjugation with β -1-thioglycosyl and obtained within 2-3 hours (depending on the pH 4 or 6) more than 95% yield of a fully glycoconjugated product on all 180 sites.



Scheme 61. Glycoconjugation of virus-like Q β -Hag16 with β -1-thioglycosyl by radical thiol-ene coupling

The radical thiol-ene coupling can also be applied to polysaccharidic structures as described by An et al.³⁴¹ They prepared thiol-incorporated cellulose nanofibers by esterification between 3,3'-dithiodipropionic acid and hydroxyl functions of glycosyl units. Next, the created disulfide bridges were cleaved releasing free thiol functions that reacted in a radical thiol-ene reaction with a complex random polymer, poly(VBC-r-VBDMH-r-AMA), bearing among others allyl groups. The coupling of both polymers was carried out using 2,2-dimethoxy-2-phenylacetophenone (DMPA) as photoinitiator in DMF under UV irradiation for three hours. The scheme of the strategy is presented on the figure 58 below.

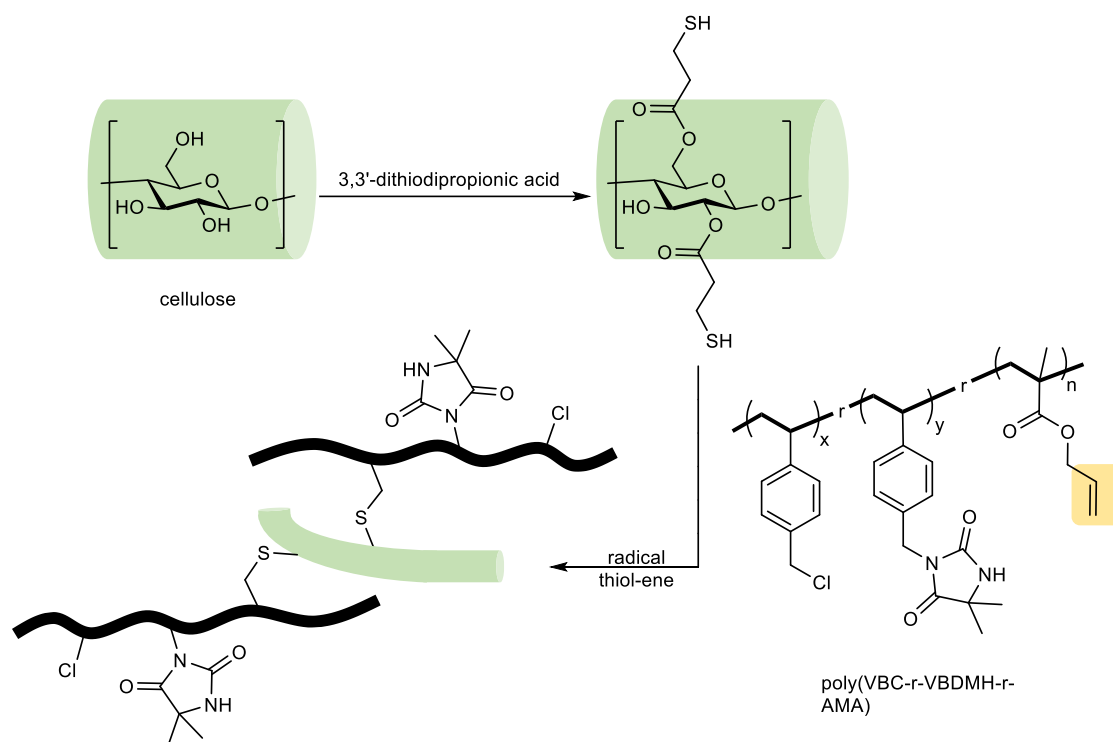


Figure 58. Thiol-ene coupling of thiol-functionalized cellulose nanofibers with the polymer poly(VBC-r-VBDMH-r-AMA)

Taking consideration of the availability of PHOU polymer bearing pendant electron-rich alkene functions and our prepared HTL-functionalized maltooligosaccharides ([CHAPTER 4](#)) for our project, an amine-thiol-ene coupling was proposed. This variant of the original radical reaction developed by du Prez and coll.³⁴²⁻³⁴⁴ with HTL-carrying polymers consists in opening the thiolactone ring of HTL by aminolysis for its further “thiol-X” chemistry in a one-pot reaction (scheme 39 illustrating the strategy in [4.2.1.2.1](#)). The amine used for the ring opening step should be saturated (no double or triple bond, no aromatic ring etc.) in view of the further radical thiol-ene coupling. The advantage of the strategy is its byproduct-free nature as no small molecules are liberated during the two steps, which facilitates purification steps.

Mainly one thiol-functionalized maltooligosaccharide was used for the amine-thiol-ene coupling, M₂-rHTL (**48**), over the two prepared that are presented on the figure 59.

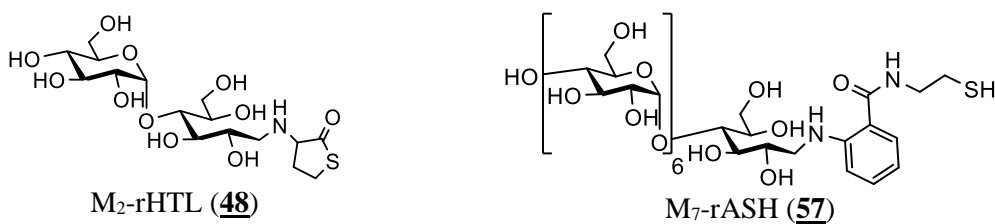
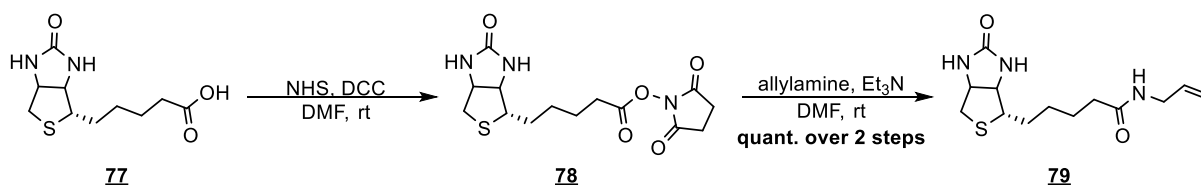


Figure 59. Structure and name of thiol-functionalized maltooligosaccharides used as model compounds for thiol-ene coupling trials

5.2.1.2 Synthesis of an alkene-bearing biotin

As previously cited, D-(+)-biotin **77** was chosen as a low molecular weight model compound to be grafted onto thiol-functionalized maltooligosaccharides for two reasons: (i) this reagent allows for a better characterization of the reaction, (ii) it enables to measure the affinity of the formed potential GAG mimetics with biomolecules such as heparin binding growth factors *via* Surface Plasmon Resonance biological analysis (performed at IBS, Grenoble). Biotin was derivatized with an alkene group for the future thiol-ene coupling.

The alkene-modified biotin (**79**) was prepared within two steps according to the procedure of Waldmann et al.³⁴⁵, as shown on the scheme 63 below. The carboxylic acid of biotin **77** was activated using *N*-hydroxysuccinimide (NHS) in the presence of dicyclohexylcarbodiimide (DCC) in DMF, forming the reactive biotin-NHS intermediate (**78**). After removal by filtration of insoluble *N,N'*-dicyclohexylurea formed during the reaction³⁴⁶, the NHS leaving group was replaced by allylamine in basic medium with triethylamine, creating biotin-allyl (**79**) with a quantitative yield over two steps.



Scheme 62. Synthesis of biotin-allyl **79** *via* biotin-NHS **78**

The final product **79**, whose ¹H NMR spectrum with peak attribution is presented on the Figure 60, did not require further purification and matches perfectly with literature data^{345,346}.

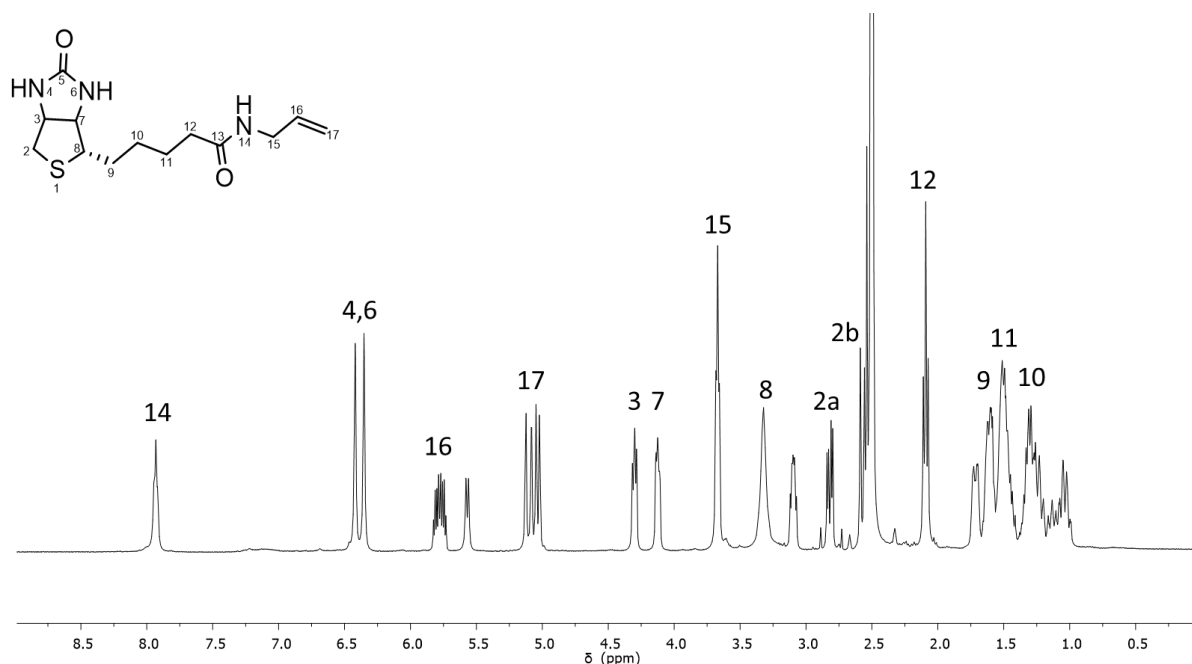
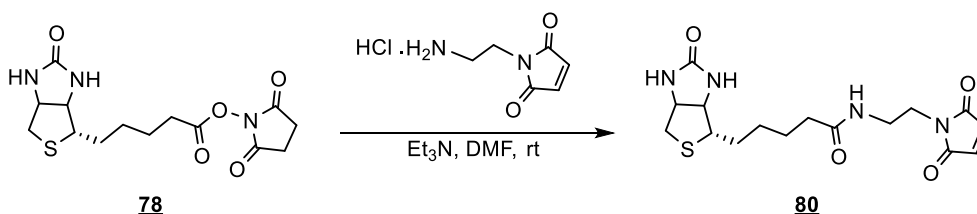


Figure 60. ^1H NMR spectrum with of compound **79** its peak attribution in DMSO-d_6

A second alkene-bearing biotin possessing an electron-deficient maleimide instead of an allyl was synthesized that could undergo a Michael-type nucleophilic thiol-ene reaction. To do so, the biotin-NHS (**78**) intermediate previously synthesized was reacted with commercially available 2-aminoethyl maleimide hydrochloride in DMF in the presence of triethylamine, as shown on the scheme 64 below³⁴⁷. Biotin-maleimide (**80**) was purified by reverse phase chromatography yielding 43% of pure product.



Scheme 63. Synthesis of biotin-maleimide **80** via biotin-NHS **78**

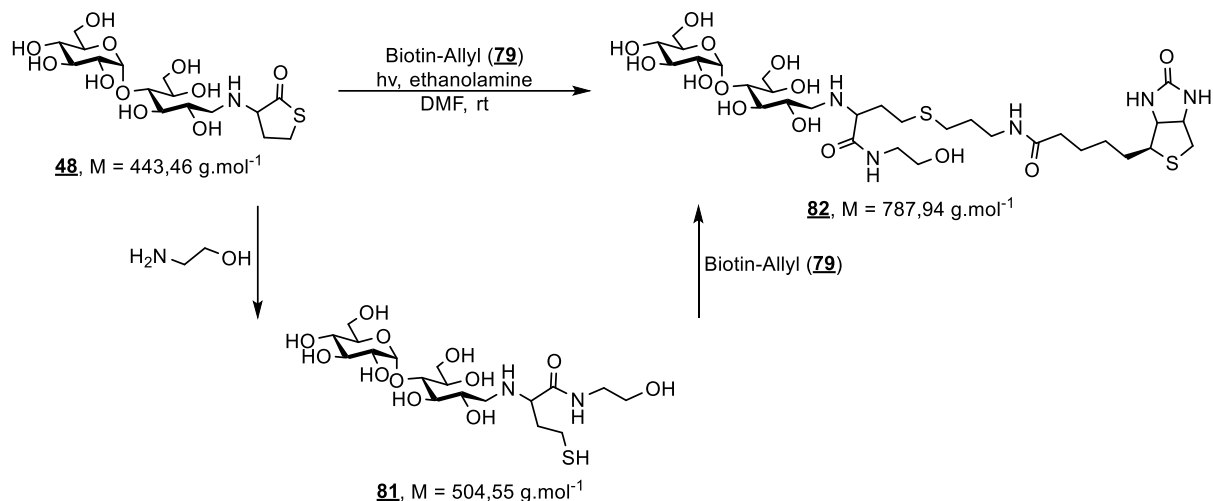
However, due to the cost of 2-aminoethyl maleimide reagent and the moderate effectiveness of the reaction, the thiol-ene coupling with this reagent was put aside to focus on biotin-allyl reaction with thiol-end functionalized maltooligosaccharides.

5.2.1.3 Preliminary tests of the thiol-ene coupling

5.2.1.3.1 Thiol-ene reaction of end-functionalized maltose with biotin-allyl

After preparation of the first thiol-end functionalized maltose **48** (see 4.2.1.2.2) and biotin-allyl (**79**, see 5.2.1.2), trials of thiol-ene coupling were started. M_2 -rHTL (**48**) and biotin-allyl (**79**) were chosen as reaction models because of their accessibility and availability. They should react together in a radical amine-thiol-ene reaction^{342,344,348} described as follows and illustrated on the scheme 65. The latent thiol

protected in the form of a thiolactone on maltose will first be released by aminolysis with ethanolamine (compound **81**). Besides its use for ring-opening, ethanolamine was chosen to bring more water-solubility to the final compound. The subsequently liberated thiol should react with the alkene moiety of modified biotin (**79**) in a radical-initiated thiol-ene reaction under UV irradiation to provide **82**.



Scheme 64. Radical amine-thiol-ene reaction of M₂-rHTL **48** and biotin-allyl **79**

Equimolar ratios of M₂-rHTL **48** and biotin-allyl **79** were reacted together with ethanolamine (two equivalents) and DMAP (nucleophilic catalyst) in DMF under UV-light (at 365 nm). No photoinitiator was used at the beginning of our tests due to possible side-reaction of the radical fragment of photoinitiator with the amine.³⁴² The reaction crude was each time analyzed by mass spectrometry to have an idea of the species present. The first trials showed a majority of aminolyzed sugar **81** and disulfide dimers. It was assessed that the aminolysis is a very quick reaction compared to the second step (photoinduced radical thiol-ene coupling). Thereby, the released thiols tended to form dimers, hampering the second step. The lengthening of reaction times (from 2 hours to 7 hours) caused the formation of more dimers, and on the contrary the portionwise addition of ethanolamine allowed for a bit less side-products. The mass spectrum displayed in figure 61 is representative of the most “efficient” trial that we obtained.

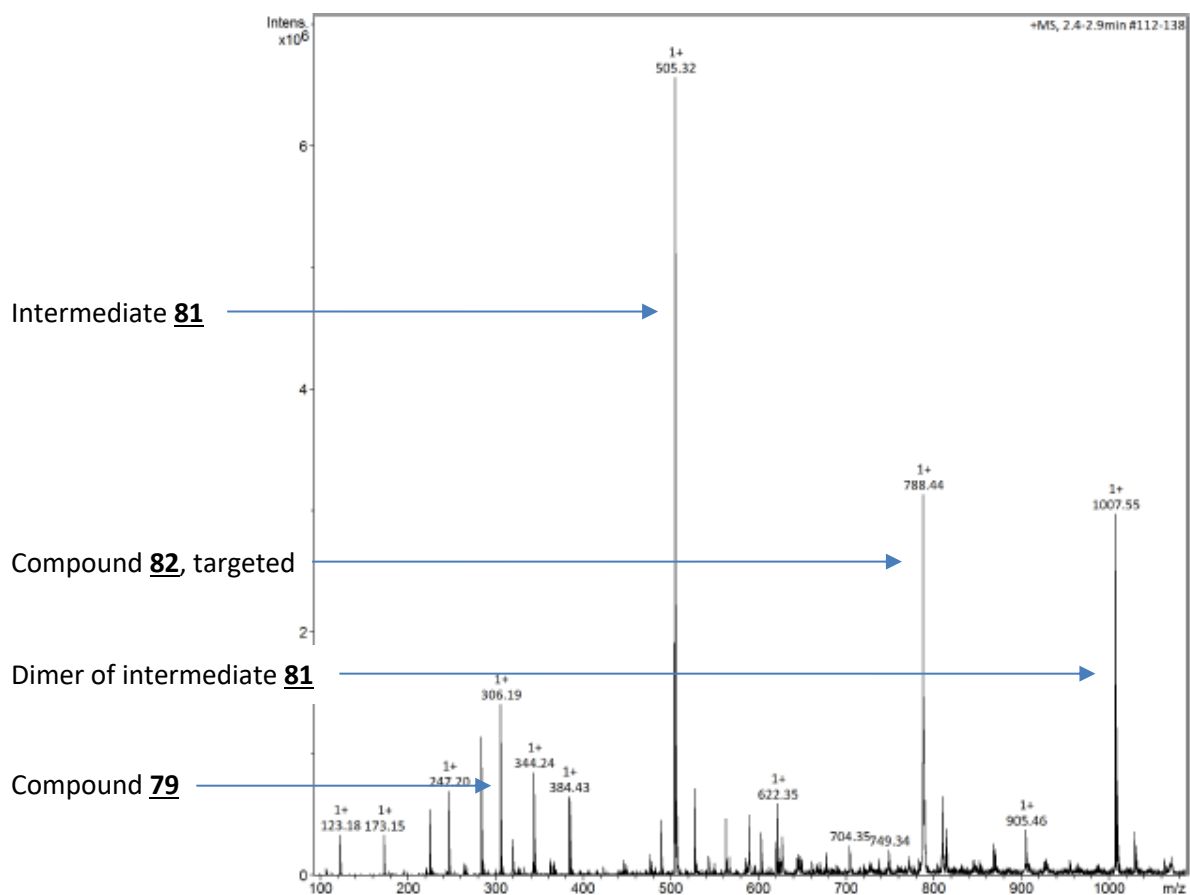


Figure 61. Mass spectrum of a thiol-ene reaction trial between M_2 -rHTL **48** and biotin-allyl **79**

A large majority of intermediate **81** at $m/z=505.32$ is present, dimers at $m/z=1007.55$ and targeted compound **82** at $m/z=788.44$ seem to be almost equally obtained, and a minority of residual biotin-allyl **79** at $m/z=306.19$ is observed. Considering the peak intensities on the mass spectrum, still a minority of targeted product was formed. Instead of the amine, the thiol-functionalized maltose was added portionwise which resulted in a large majority of side-products. It was hypothesized that the slow rate of thiol-ene step might be due to the absence of photoinitiator. So, the nucleophilic catalyst DMAP was replaced by the photoinitiator DMPA (2,2-dimethoxy-2-phenylacetophenone) in stoichiometric amount. No pic of M_2 -rHTL **48** was observed, but a new pic at $m/z=589.4$ that could not be attributed appeared. The mass spectrum is presented in the figure 62.

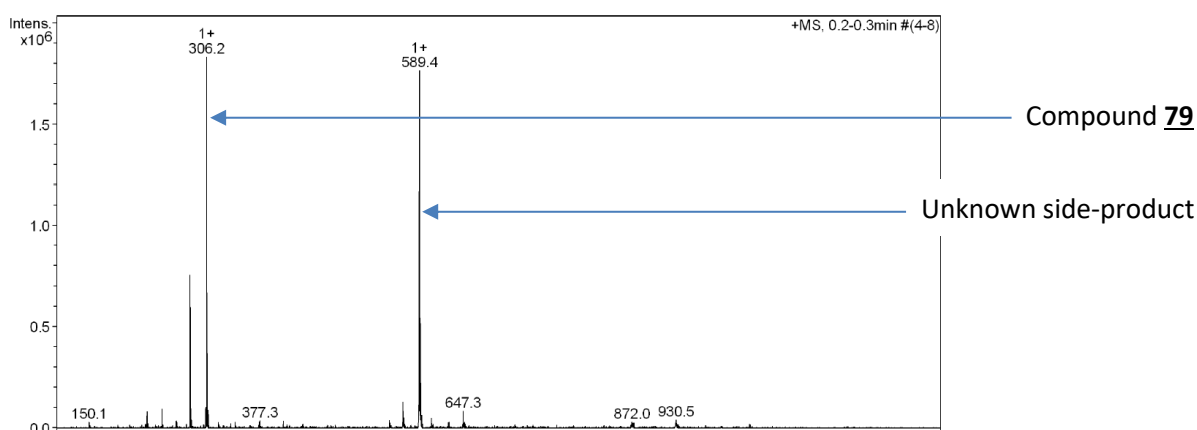
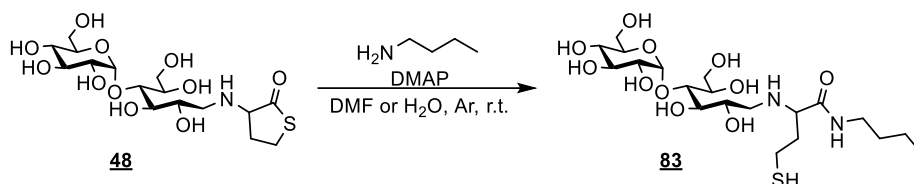


Figure 62. Mass spectrum of the thiol-ene crude after reaction between M_2 -rHTL **48** and biotin-allyl **79** in the presence of DMPA photoinitiator

When the quantities of DMPA were then drastically decreased to 6% weight, more product **82** was formed compared to dimers but the unidentifiable product was still major. Adding more quantities of functionalized maltose (2.5 equivalents) along with decreasing DMPA ratio to 3% weight did not optimize the reaction. Finally, when TCEP reducing agent was added, no dimer was formed but the targeted product **82** was present as traces as the major product was the unknown one. To resume, many parameters were modulated to avoid the disulfide as well as side-product formation such as partitioned additions of ethanolamine or of functionalized maltose, reaction times, inert conditions, photoinitiator or addition of a reducing agent. Despite all trials, the product could not be isolated with an acceptable yield. In addition, reaction times were extremely long compared to classic thiol-ene couplings (3-7 h). As a consequence, starting materials M_2 -rHTL **48** and biotin-allyl **79** were sent to our collaborators (ICMPE, Thiais), that have an expertise in radical-mediated thiol-ene chemistry on polymers.

Based on their trials with PHOU (see 5.2.1.3.2), they also observed that the aminolysis step was very quick compared to the thiol-ene step. To improve the rate of the second step, they realised the ring opening of M_2 -rHTL (**48**) prior to the thiol-ene reaction. The aminolysis (first step) was performed by mixing *n*-butylamine with M_2 -rHTL (**48**) in the presence of the base DMAP either in DMF either in water, this latter solvent being more easily removable. The reaction is illustrated on the Scheme 66 below.



Scheme 65. Aminolysis of maltose-rHTL (**48**) with *n*-butylamine

The purification step yielded about 95% of pure product **83** when the reaction was carried out in DMF and 80% in water, that was characterized by Raman spectroscopy to assess the presence of free thiols

and amide linkage (data not shown) and by ^1H NMR to observe the successful attachment of *n*-butylamine (Figure 63 below).

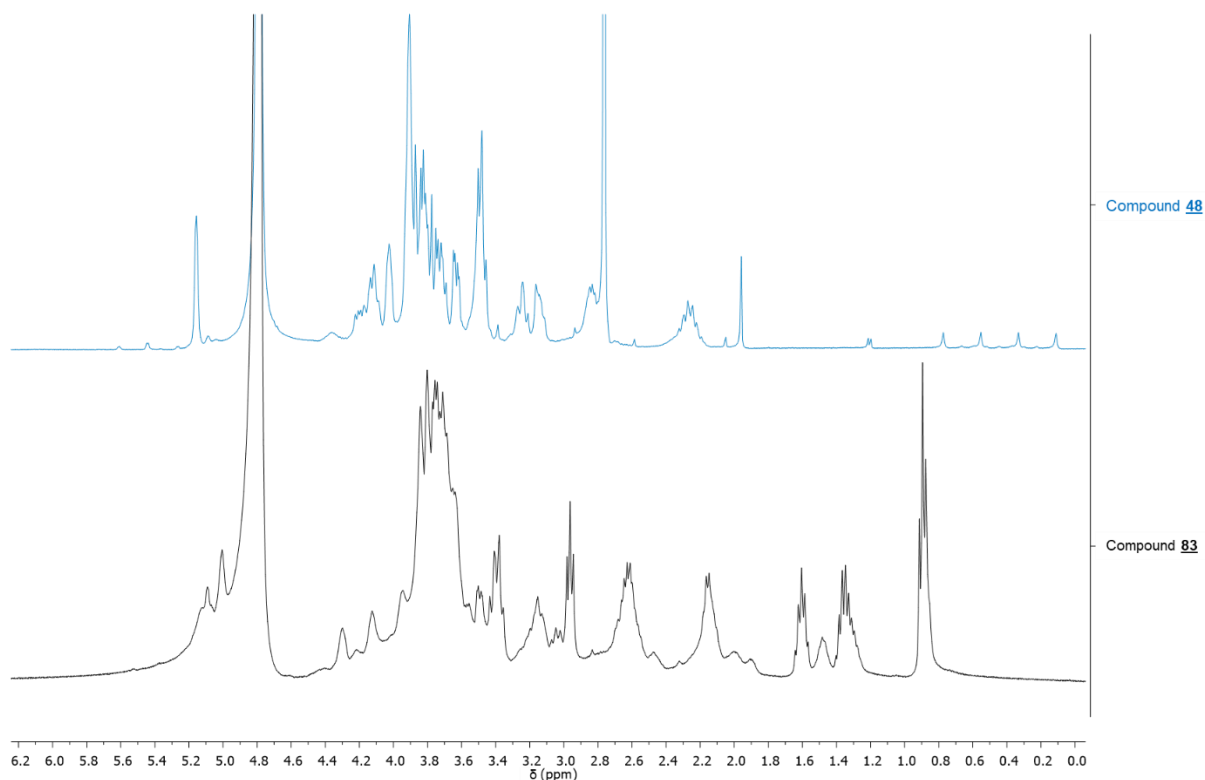
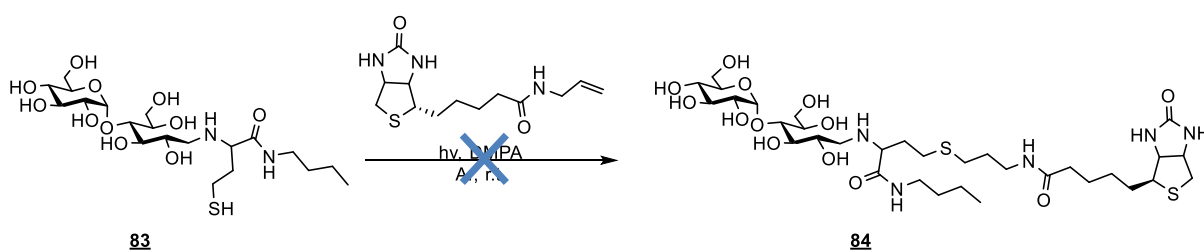


Figure 63. ^1H NMR spectra superposition of compound **83** (after aminolysis, black) and **48** (before aminolysis, blue) in D_2O

Both $\text{M}_2\text{-rHTL-SH}$ **83** and biotin-allyl **79** were dissolved in DMSO, DMPA initiator was added in methanol and the reaction mixture was irradiated during 2*5min under UV light, as illustrated on the Scheme 67.

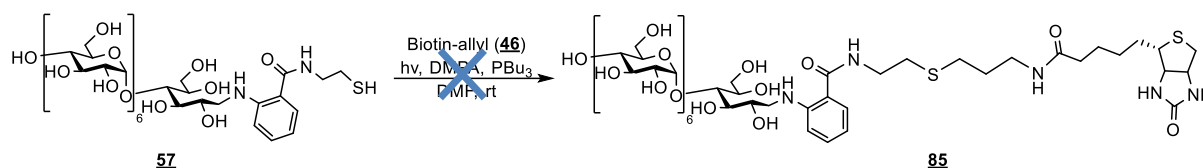


Scheme 66. Radical amine-thiol-ene reaction of $\text{M}_2\text{-rHTL-SH}$ **83** and biotin-allyl **79**

Few quantities of product were recovered after dialysis purification, but a mixture of products was supposedly formed according to the ^1H NMR spectrum. In a second trial, TCEP was dissolved with free-thiol maltose (**83**) overnight prior to the reaction in the same conditions. However, once again, no pure product could be isolated after purification according to the ^1H NMR spectrum.

The thiolactone system was hypothesized to cause problem because of the rapid ring opening step releasing the sulfhydryl moiety. To check this theory, another thiol-functionalized maltooligosaccharide was tested. The trial was directly attempted on modified maltoheptaose instead of maltose to save time.

Previously prepared and impure M₇-rASH (**57**), that was conserved under inert atmosphere in the presence of tributylphosphine, was reacted with biotin-allyl **79** and DMPA in dry DMF, as showed on the scheme 58. After one hour and by following the reaction with TLC plates, nothing occurred suggesting that the problem might come from the conditions used or the alkene system.



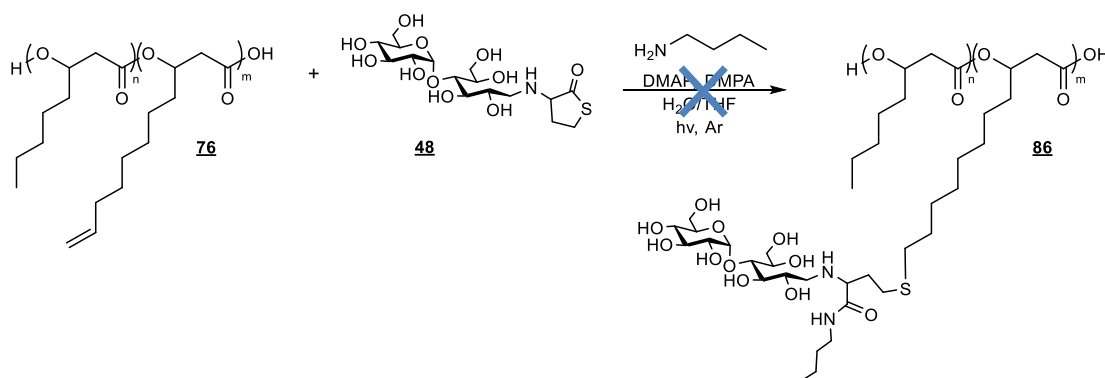
Scheme 67. Radical thiol-ene reaction of M₇-rASH **57** and biotin-allyl **79**

In parallel of these preliminary tests of amine-thiol-ene coupling on low-molecular weight compound biotin-allyl **49**, some tests were performed directly on PHOU polymer by our ICMPE collaborators.

5.2.1.3.2 Thiol-ene reaction of end-functionalized maltose with PHOU

While optimizing the thiol-ene coupling of functionalized maltose **48** with biotin-allyl **79**, the reaction was carried out with native PHOU **76**, a polyester bearing terminal alkenes whose percentage among the polymer chain varies between %_{alkene} = 31-33 % depending on the batch of PHOU. All thiol-ene trials were performed in the presence of the photoinitiator DMPA under UV irradiation (at 365 nm and 200 watts) and under argon atmosphere. When a ring opening of thiolactone was required, DMAP was used as a nucleophilic catalyst. Solvents were particularly critical for the coupling; carbohydrates being water-soluble and partially soluble in DMSO while PHOU is a very hydrophobic polymer soluble in water-miscible THF.

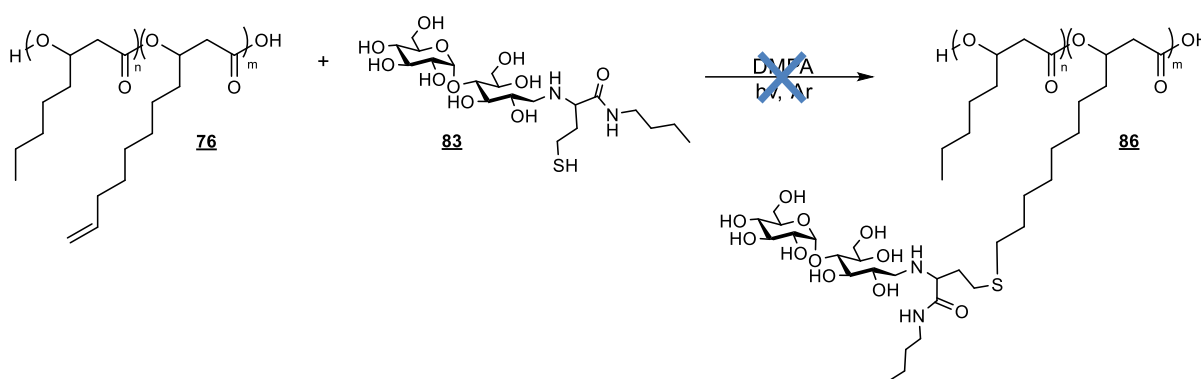
For the first trial, PHOU (**76**) and maltose-rHTL (**48**) were reacted with *n*-butylamine in a “one-pot” photo-initiated amine-thiol-ene reaction for 5 min in a mixture of THF and water (1/1 v/v), as depicted on the Scheme 69 below.



Scheme 68. “One-pot” photo-initiated thiol-ene coupling of maltose-rHTL (**48**) with PHOU (**76**)

The polymer obtained after UV irradiation precipitated due to the insolubility of PHOU in water, and the dialysis against water did not allow to recover enough product for characterization. As hypothesized previously, the first step of aminolysis was considered to be very fast compared to the thiol-ene step. The dialysis might have eliminated the aminolyzed maltose along with DMPA, DMAP and *n*-butylamine.

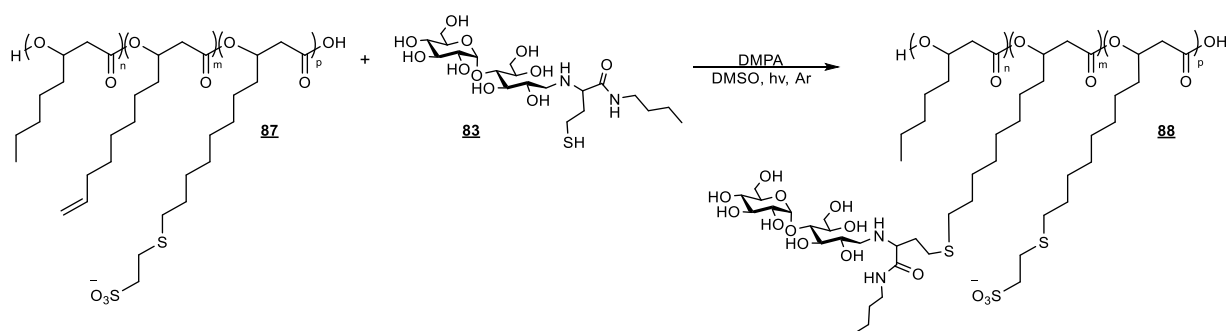
The grafting of maltose onto PHOU was then tried within two separate steps instead of a “one-pot”. The aminolysis (first step) was performed by mixing *n*-butylamine with maltose-rHTL (**48**) as previously described (see 5.2.1.3.1). Few thiol-ene couplings were then carried out by varying the solvent as shown on the Scheme 70.



Scheme 69. Photo-initiated thiol-ene coupling of maltose-rHTL-SH (**83**) with PHOU (**76**)

PHOU (**76**) was dissolved with maltose-rHTL-SH (**83**) in the presence of initiator in deuterated chloroform and DMSO for an NMR study of the reaction, showing no evolution of spectrum before and after UV irradiation. A single solvent was then used for the reaction, water, where PHOU formed a suspension. Some methanol was added with the introduction of DMPA. However, as for the very first trial, important loss of product was observed during dialysis and the product could not be characterized. Finally, a ternary mixture of solvent was assayed : THF, DMF and water (5/2/minimum v/v/v). Some TCEP was added as a reducing agent for eventual disulfide formations. The final product, purified by dialysis, could not be analyzed by NMR due to its gel consistency in deuterated chloroform and DMSO.

To increase the solubility of PHOU in DMSO, the polymer was partially grafted with sulfonate groups (anionic functions) by thiol-ene coupling: 14% of sulfonate were attached while 17% of alkene functions were left for future thiol-ene with functionalized maltose. The resulting polymer **87** and maltose-rHTL-SH (**83**) were then solubilized in DMSO and reacted together under UV irradiation for 2*5 min, as shown on the Scheme 71.



Scheme 70. Photo-initiated thiol-ene coupling of maltose-rHTL-SH (**83**) with PHOU-sulfonate (**87**)

The purified product was analyzed by ^1H NMR, showing small quantities of sugar compared to PHOU. It was assumed that a small percentage of maltose-rHTL-SH (**83**) was grafted onto the polymer.

As mentioned in the chapter 4 (4.2.1.2.2), maltose-rHTL (**48**) could not be obtained in big quantities and under pure form, ICMPE collaborators therefore carried out thiol-ene reaction tests with other maltoses differently thiol-functionalized in parallel to save product and optimize the conditions.

They assayed two aminated variants of sugar (aminated maltose and glucosamine) with *N*-acetyl HTL illustrated on the Figure 64. However, the thiol-ene reaction tests with these variants were not conclusive although many solvents were tried to solubilize both PHOU and modified carbohydrates (THF/water, THF/DMSO/water, THF/DMAc/water, DMSO/THF).

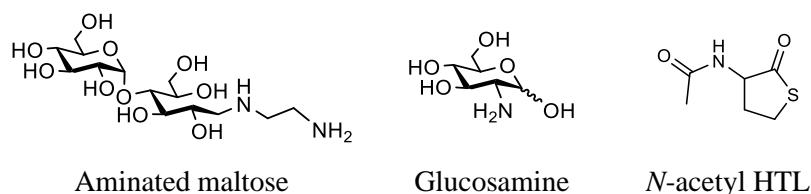


Figure 64. Structure of the variants of sugar and *N*-acetyl HTL tested for thiol-ene coupling by ICMPE collaborators

In summary, a wide panel of solvent mixtures was tried for the thiol-ene coupling, but the difference of polarity and solubility of carbohydrates and PHOU might explain the inefficiency of the reaction. As PHOU was very hard to solubilize in most of the mixtures, the cause of failure might be the inaccessibility of its alkene functions by polar thiol-bearing carbohydrates.

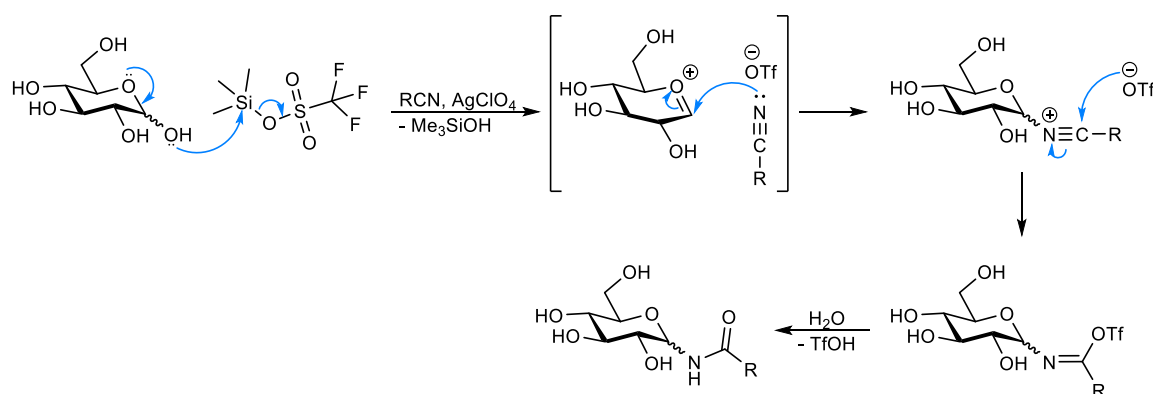
For PHOU as well as for biotin-allyl, it was presumed that the allyl group was not accessible enough for this type of reaction and that free thiols might be very reactive and unstable leading to side-products. Thus, instead of thiol-ene chemistry, a more classical amide coupling was developed, where amine-terminated maltooligosaccharides were beforehand prepared.

5.2.2 Amide coupling

5.2.2.1 Introduction

Glycosyl amide linkages are ubiquitously present in living organisms as part of glycoconjugates involving peptides or proteins. In the goal of mimicking native glyco-peptides and -protein, many methods were developed to synthesize such linkage from native or functionalized carbohydrates (for more information see ³⁷).

Ritter et al. reported the amide linkage formation from a nitrile and a carbonyl in 1948.³⁴⁹ The so-called Ritter reaction was applied to carbohydrate chemistry with little modifications and the mechanism, illustrated on the scheme 72, was elucidated by Wang group.³⁵⁰ The anomeric position of native carbohydrate was activated by a Lewis acid, providing an oxocarbenium intermediate, which was attacked by a nitrile nucleophile to form after hydration an amide linkage with β selectivity.



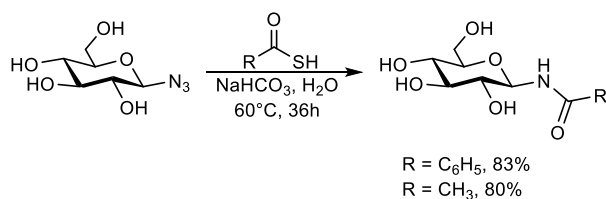
Scheme 71. Proposed mechanism for the Ritter reaction of unprotected carbohydrate with a nitrile

Another more recent method starting from native carbohydrate implies the use of a phosphine, an acid and a silylated azide. The procedure was developed by Zheng et al.³⁵¹ The scope of glycopeptides that could be prepared is presented on the Table 22.

Product	Yield (%) ^a
	76
	75
	70
	61

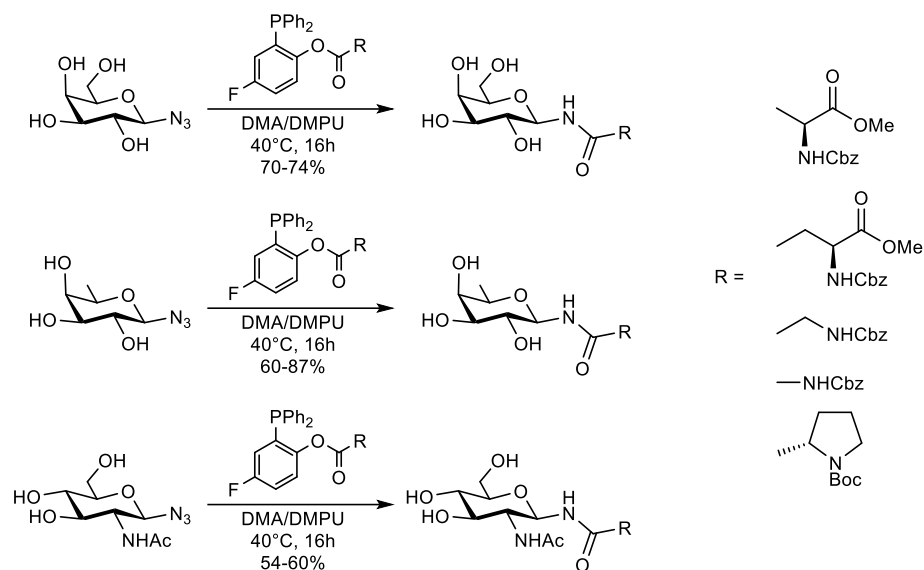
Table 16. Scope of glycopeptides prepared by Zheng et al. by reductive glycosylation of native carbohydrates with azides.^a β : α ratio >15:1

The thioacid-azide ligation results in the coupling between azides and substituted thioacids. The reaction reported by Chu and co-workers and thioacetic acid³⁵² and then exploited by Williams' group who proposed two possible mechanisms for the reaction depending on the azide type (electron-rich or -deficient)³⁵³. Unprotected azide-end-functionalized carbohydrates could be coupled to thioacetic and thiobenzoic acids in aqueous conditions with yields up to 80% as shown on the Scheme 73 below³⁵⁴. However, long reaction times were observed (also with per-protected glycosyl azides).



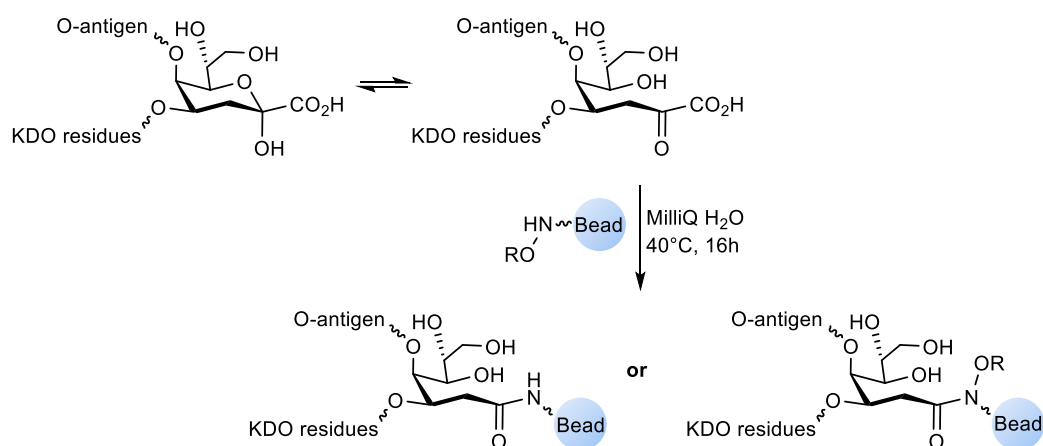
Scheme 72. Preparation of amide-linked glycoconjugate by thioacid-azide ligation

Also with the use of azide-terminated carbohydrates, traceless Staudinger ligation was developed by Raines group³⁵⁵ and Bertozzi³⁵⁶ involving phosphine functionalized ester. Nisic et al.³⁵⁷ prepared a variety of *N*-glycosyl amino acids by this method, as shown on the Scheme 74. Unprotected β -oriented glycosyl azides were converted into the corresponding amides with good yields. However, furanosyl amides and native glycans were also observed as side-products.



Scheme 73. Synthesis of *N*-glycosyl amino acids by traceless Staudinger ligation with fluorinated phosphanes

The α -ketoacid/hydroxylamine ligation was a method reported in the 00's by Bode et al.³⁵⁸. Despite the β selectivity, poor yields of glycoconjugates were obtained due to possible side-reactions of both reactants. As an example illustrated on the Scheme 75, Boas et al.³⁵⁹ performed the glycoconjugation of KDO antigen polysaccharide with oxyamine-functionalized polystyrene beads in mild conditions (40°C in water).



Scheme 74. Preparation of glycoconjugate adducts by α -ketoacid/hydroxylamine ligation with KDO antigen polysaccharide with polystyrene beads

The most widely used method for preparing amide linked glycoconjugates is the acylation of glycosylamines or amine-functionalized carbohydrates. The procedure usually requires the presence of an anhydride, acyl halide or a carboxylic acid to be activated by a coupling reagent. The disadvantage of intermediate anomerization and instability with glycosylamines may be overcome by using carbohydrates that were amine-functionalized by a spacer. As an example, Huang et al.³⁶⁰ synthesized truncated Globo H tumor antigen analogs, that were amine-end functionalized in one pot strategies.

These derivatives were then immobilized as shown on the figure 65 onto NHS-coated glass slides by formation of an amide linkage in aqueous conditions at room temperature for biological purpose ³⁶¹.

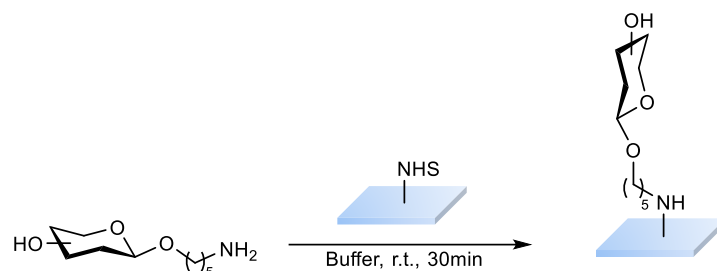


Figure 65. Immobilization of amine-terminated glycans on NHS-coated glass slides

Regarding the availability of PHOU-carboxylate **89** and amine-terminated maltooligosaccharides, an amide coupling by acylation was conceived. Due to the lack of time, the reactions were directly carried out with functionalized maltoheptaose M_7 -rANH₂ (**75**), whose structure is presented on the figure 66 below.

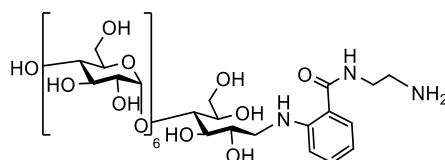
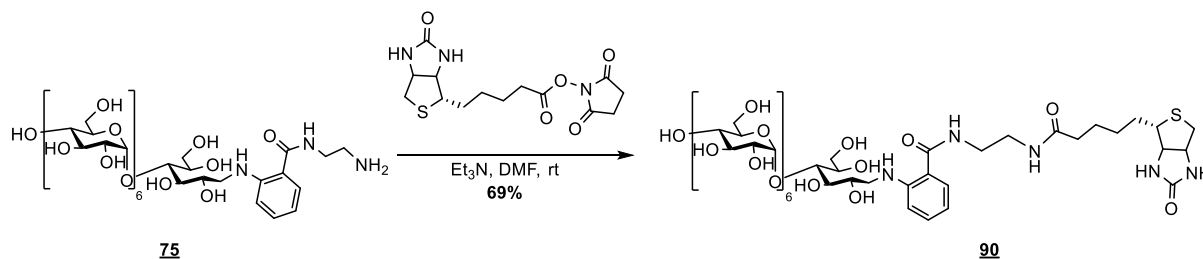


Figure 66. Structure of M_7 -rANH₂ (**75**)

5.2.2.2 Amide coupling of amine-modified maltooligosaccharides with biotin-NHS

Biotin, as a model compound and useful for strongly interacting with streptavidin, was attached to amine-terminated maltooligosaccharides by amide coupling by using the biotin-NHS intermediate (**78**) previously prepared. On the contrary to the thiol strategy, maltose was not used as a model compound due to the lack of time. The tests were directly carried out with modified maltoheptaose. M_7 -rANH₂ (**75**), in the presence of triethylamine, was reacted with biotin-NHS (**78**) in a mixture of DMF/water as illustrated on the Scheme 76 below to provide the coupled product **90** within thirty minutes with a 69% yield after purification.



Scheme 75. Amide coupling of M_7 -rANH₂ **75** with biotin-NHS **78**

The ¹H NMR spectra superposition of the product and the starting materials is presented on the Figure 67 below. On the spectrum of the product (black), the peaks attributed to sugar protons between 2.90 and 5.46 ppm seem intact as well as those attributed to the anthranilic aglycon between 6.76-7.58 ppm (blue). Peaks attributed to biotin-NHS (**78**) may have shifted due to the difference of solvent (DMSO-

d_6 for the green spectrum while D_2O for the black and blue ones) but are still present showing a successful coupling.

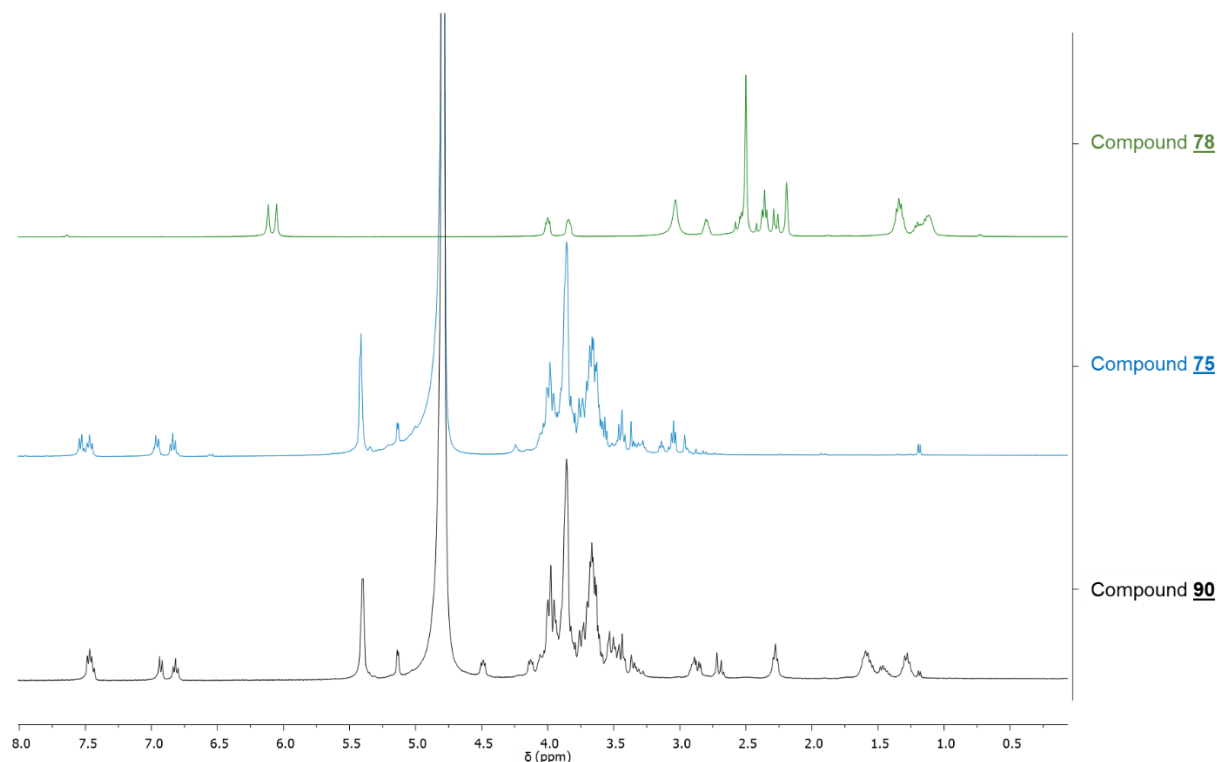
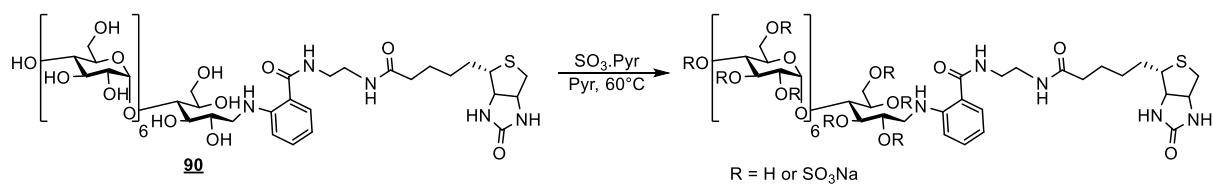


Figure 67. 1H NMR spectra superposition of compound **90** (black, in D_2O) with the starting compounds **75** (blue, in D_2O) and **78** (green, in $DMSO-d_6$)

Once the product obtained, it was randomly sulfated at different degrees to be further tested as glycosaminoglycan mimetic during SPR analysis (IBS, Grenoble).

5.2.2.3 Random sulfation of biotin-maltoheptaose conjugates

In the aim of performing surface plasmon resonance analysis (at IBS, Grenoble), compound M_7 -rANH-CO-biotin **90** was randomly sulfated at different degrees to produce biotinylated potential GAG mimetics as shown on the Scheme 77. Sulfation was carried out in the optimized conditions described for maltoheptaose derivatives (see 2.2.1). Briefly, compound **90** was dissolved in dry pyridine and reacted with different amounts of sulfur trioxide pyridine complex depending on the targeted DS. The products were then purified by GPC. By doing so, purified highly and moderately sulfated derivatives could be obtained.



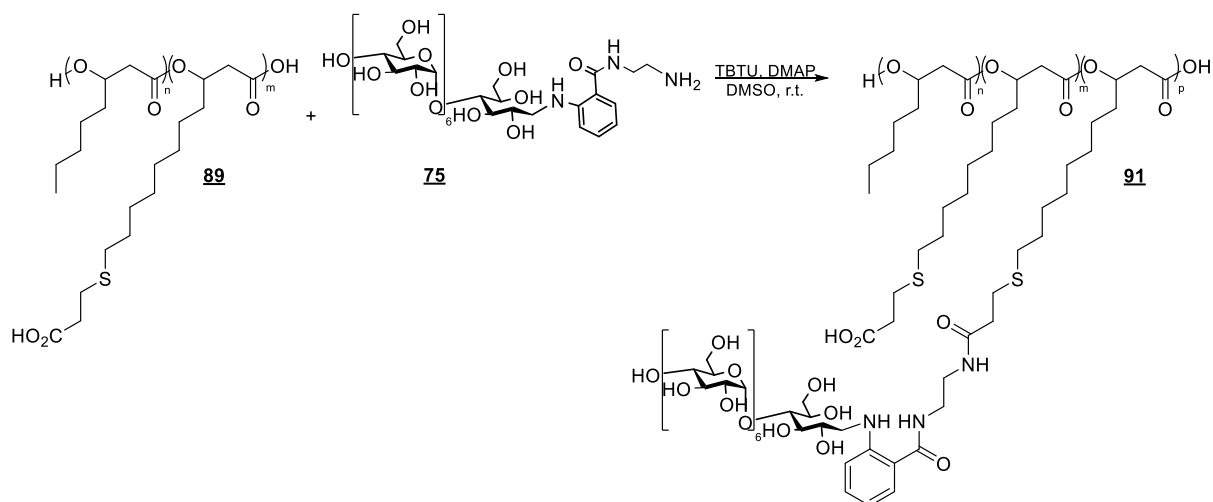
Scheme 76. Random sulfation of M_7 -rANH-CO-biotin **90**

Due to a lack of time (lockdown of COVID-19), this part could not be completed : (i) lightly sulfated derivative could not be prepared because the starting material was degraded with prolonged conversation at room temperature, (ii) the reactions did not afford enough product for complete analysis of sulfated derivatives, and they could not be relaunched, (iii) our potential GAG mimetics could not be analyzed by our collaborators at IBS (Grenoble).

The amide route being validated for amine-functionalized maltoheptaose (see 5.2.2.2), the reaction between amine-functionalized maltoheptaose **75** and PHOU-carboxylate **89** was performed by our collaborators (ICMPE, Thiais).

5.2.2.4 Amide coupling of amine-modified maltooligosaccharides with PHOU-carboxylate

ICMPE collaborators beforehand oxidized native PHOU possessing alkene functions ($\%_{\text{alkene}} = 31\%$) into carboxylates. The percentage of carboxylate functions formed was estimated to be of 31%, assessing a complete transformation of alkenes. Next, the grafting reaction between PHOU-carboxylate **89** and M₇-rANH₂ **75** was realized in DMSO in the presence of the base DMAP with the coupling reagent TBTU (*O*-(1*H*-Benzotriazol-1-yl)-*N,N,N',N'*-tetramethyluronium tetrafluoroborate), an aminium reagent known for achieving high coupling rates with few undesirable side reactions³⁶². The resulting by-products of this reagent are water-soluble, allowing an easy purification of the polymer by dialysis (mechanism of amide coupling with HBTU³⁶³). The reaction is illustrated on the Scheme 78 below.



Scheme 77. Amide coupling of M₇-rANH₂ **43** with PHOU-carboxylate **56**

The reaction was carried out for 48h, and the purified product was characterized by ¹H NMR (figure 68) showing a successful coupling of maltoheptaose on PHOU with a grafting rate of 18% (calculated by ¹H NMR), representing on average 19 monomers bearing maltoheptaose among one PHOU-carboxylate chain. Apparition of aromatic and N-H peaks between 6.42 and 8.40 ppm, along with sugar peaks from 2.90 to 5.75 ppm demonstrated the presence of maltoheptaose along with PHOU peaks in DMSO.

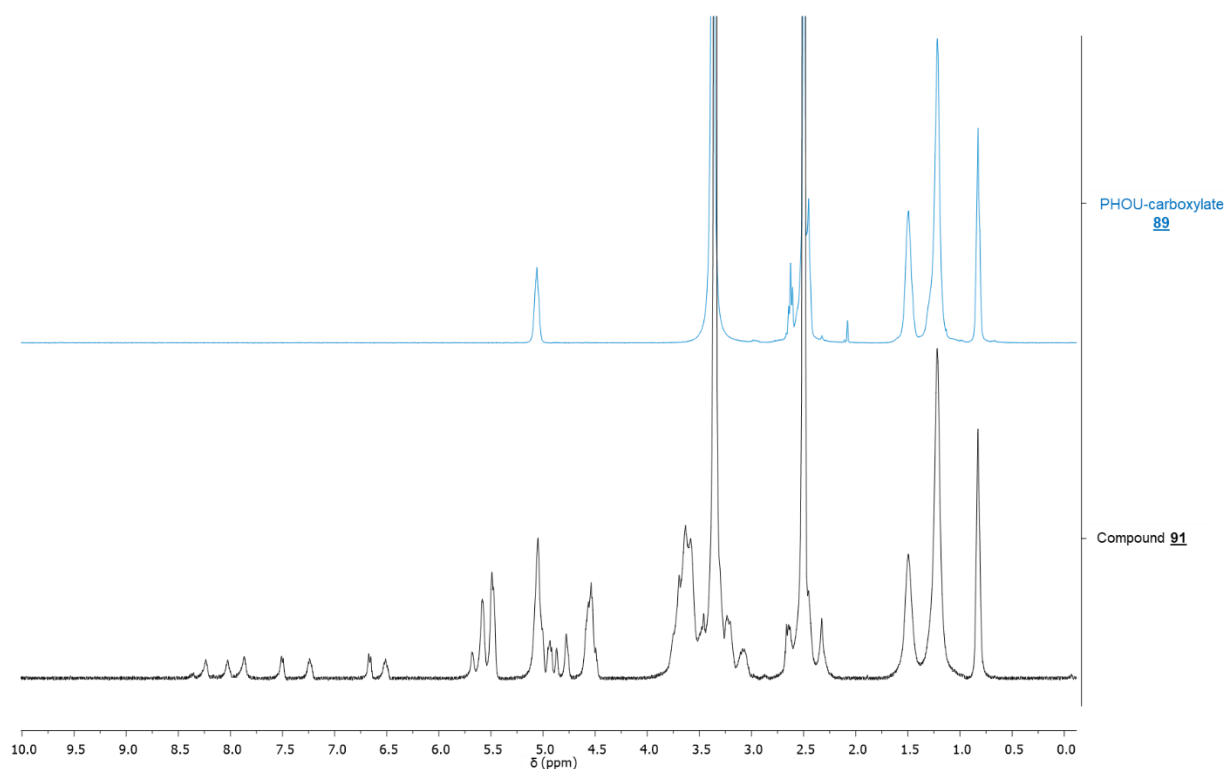


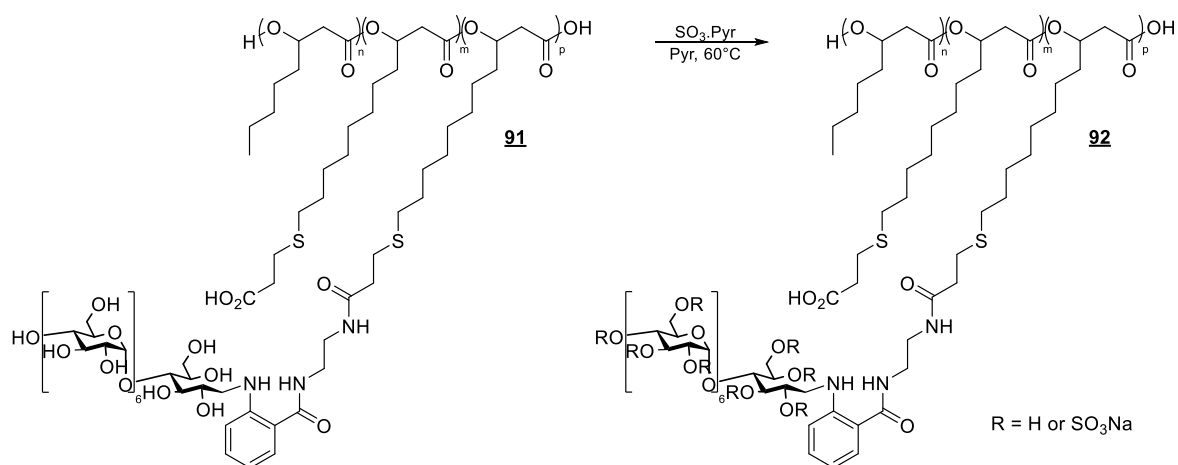
Figure 68. ^1H NMR spectra superposition of product **91** (black) and PHOU-carboxylate **89** (blue)

The coupled product was then submitted to sulfation at different degrees in order to obtain randomly sulfated glycoconjugate polymers, acting as potential proteoglycan mimetics.

5.2.2.5 Random sulfation of PHOU-maltoheptaose conjugate

To produce PG mimetics, functionalized maltoheptaose was grafted onto PHOU polymer by amide coupling. The resulting compound **91** was submitted to random sulfation. Due to the limited quantities of starting material, only one DS, the moderately one, was targeted. Prior to the reaction, solubility of compound **91** was tested in the solvents used for sulfation: the product was soluble only in DMSO and in pyridine, but not in DMF neither in water. The reaction was therefore carried out in dry pyridine as shown on the Scheme 79.

Compound **91** was solubilized for one night in dry pyridine at room temperature, leading to a clear yellowish solution. Next, the sulfating agent was introduced and the temperature was raised to 60°C for one night. The crude, not soluble in water, was neutralized with sodium bicarbonate and dialyzed against water for four nights. A brown residue was obtained after lyophilization. The ^1H NMR spectrum obtained suggested that no reaction has occurred, as the peaks were identical to those of the starting material **91**. Unfortunately, due to a lack of time, the reaction could not be relaunched.



Scheme 78. Random sulfation of M₇-rANH-CO-biotin **91**

5.3 Conclusion

In the goal of obtaining potential proteoglycan mimetics, a thiol-ene coupling of thiol-end functionalized maltooligosaccharides with the alkene-bearing PHOU polymer was envisioned. The preliminary trials were performed on the low-molecular weight model compound maltose for its accessibility and availability. Unfortunately, no product could be isolated by amine-thiol-ene reaction of maltose with biotin-allyl **79** or PHOU **76**. It was hypothesized that the alkene function of these latter was not accessible enough because of the difference of solubility of the sugar and aglycon entities.

To address this problem, a second more classic grafting was performed with amine-terminated maltoheptaose and either biotin-NHS **78** or PHOU-carboxylate **89**. The amide coupling successfully yielded the coupled products, whose structures are presented on the Figure 69 below. Compound **90** was then sulfated at two degrees (high and medium) and was aimed to be biologically evaluated as GAG mimetic by our IBS collaborators (Grenoble, work to be done). Compound **91** on the other side was aimed to be a potential PG mimetic once sulfated, however the sulfation step could not be achieved yet.

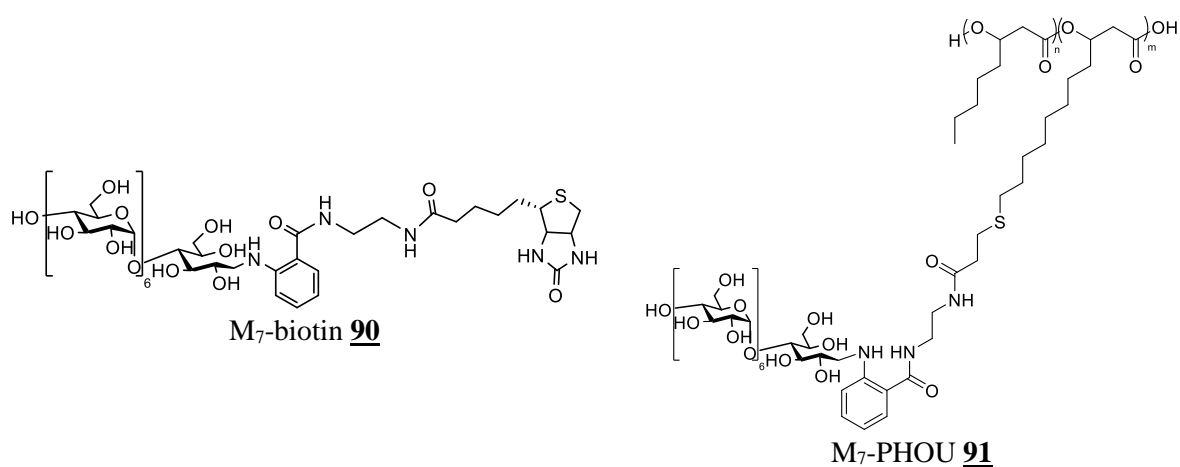


Figure 69. Scope of successfully grafted maltooligosaccharides by amide coupling

CHAPTER 6 Conclusions and perspectives

6.1 Conclusions

The project, emerged in the context of osteoarthritis, consisted in proposing a favorable environment for mesenchymal stem cells to reconstruct the articular matrix by preparing structurally simplified GAG and PG mimetics. The aim of the study was to understand the role of chain length, conformation, charge density, sulfate position and multivalency for the interaction of newly synthesized glycomimetics with proteins involved in osteoarthritis.

In practice, our multidisciplinary project was developed between four laboratories : mainly the CERMAV (Grenoble) for their expertise in glycochemistry, Gly-CRRET (Créteil) for biological assays *in vitro* and *ex vivo* skills, ICMPE (Thiais) for their knowledge in polymer chemistry, and a team at IBS (Grenoble) for their competence on GAG structure and activity elucidation.

The strategy was based on (cyclo)maltooligosaccharides of defined length, six or seven sugar units, that already proved their biological activities. The first part of the project consisted in random sulfation of potential GAG mimetics. Linear malto-hexaose & -heptaose and β -cyclodextrin (the cyclic equivalent of maltoheptaose) were randomly sulfated at different degrees (low, medium, high) and assayed to estimate the degree of sulfation and the importance of structural conformation needed to elicit biological activity as potential monovalent GAG mimetics (performed by our collaborators of Gly-CRRET, Créteil). Then, regioselective sulfation was achieved by using the chemistry of cyclomaltooligosaccharides, known for their C_n symmetry. Selectively sulfated cyclodextrins were later biologically assayed to understand the role of sulfate position on their biological activity.

Linear maltooligosaccharides were also end-functionalized for their future coupling performed by ICMPE collaborators with a biodegradable bacterial polyester polymer, PHOU (poly(3-hydroxyoctanoate-co-3-hydroxyundecenoate)), in order to get a multivalent structure able to potentially mimic PGs.

The project was structured around four main tasks, developed in the different chapters :

- 1) Random sulfation of (cyclo)maltooligosaccharides and their biological evaluation (chapter 2);
- 2) Preparation of potential cyclic GAG mimetics by regioselective sulfation and their biological evaluation (chapter 3);
- 3) Thiol- and amine-end-functionalization of potential linear GAG mimetics, and their random sulfation, for their future grafting by thiol-ene or amide coupling respectively (chapter 4);
- 4) Preparation of potential PG mimetics by grafting of potential linear GAG mimetics on a biodegradable polymer scaffold and their random sulfation (chapter 5).

We performed and optimized the protocol for randomly sulfated (cyclo)maltooligosaccharides. After being fully characterized by ^1H NMR, SEC-MALS, FT-IR and elemental analysis, the compounds were

submitted to biological assays. Two tests were carried out to evaluate their ability to mimic natural GAGs by using FGF-2 and VEGF as HPBs. The ELISA tests allowed to measure the relative affinity of sulfated (cyclo)maltooligosaccharides for growth factors, and thereby their binding abilities. The mitogenic assay on BAF32 and HUVEC cells allowed to attest their efficacy by eliciting cell growth. Globally, moderately and highly sulfated exhibited more affinity and elicited more intense responses than lightly sulfated derivatives. The minimal chain length required for biological activity was estimated at seven sugar units. Binding affinities and cell growth were different depending on the linear or cyclic conformation of oligosaccharides.

Selective chemistry on β -cyclodextrins was then used for the preparation of selectively sulfated maltooligosaccharides. Six regioselectively sulfated β -cyclodextrin derivatives were targeted in the goal of obtaining linear maltooligosaccharides with well-defined sulfation patterns. Starting from a key intermediate, heptakis-(6-*O*-*tert*-butyldimethylsilyl)- β -cyclodextrin, multiple pathways were investigated. Three cyclic derivatives were successfully obtained (6S, 2S, and 3,6S), one compound could only be partially sulfated (2,3S) and two compounds could not be prepared due to incompatible protecting groups and a lack of time (2,6S and 3S). The sulfated β -cyclodextrins were next sent to our biologist collaborators (Gly-CRRET, Créteil) for early stage assays. Unfortunately, no assumptions could be made with the preliminary results presented.

In the goal of evaluating the multivalent presentation of “GAG mimetics” on the biological activity, several sulfated maltoheptaose (thiol- or amine-functionalized) chains were envisioned to be grafted to a polymeric skeleton (natural PHOU bearing pendant alkene functions, or PHOU-COOH bearing pendant acid carboxylic functions) in order to obtain proteoglycan mimetics.

Linear maltooligosaccharides were reducing end functionalized by a thiol or amine moiety. For thiol-modified glycans, three strategies were investigated on maltose and maltoheptaose: cysteamine/cystamine method for which no product could be obtained, homocysteine thiolactone method for which four products could be isolated (two M_2 and two M_7 derivatives), and anthranilic derivative method for which two products were achieved. By doing so, six compounds could be synthesized.

For the next step of the project, some thiol-end-functionalized maltoheptaoses were randomly sulfated for their future coupling with PHOU, while thiol-modified maltoses were used to optimize the thiol-ene coupling.

Despite many tries varying the conditions, thiol-ene either on biotin or PHOU could not be achieved with acceptable yields. To overcome this problem, an amide coupling was developed in late stages of the project.

Only one strategy was investigated for the amine-modification directly on maltoheptaose: the anthranilic derivative method. Two modified maltoheptaoses could be obtained including the final amine-bearing glycan. M₇-rANH₂ was used for the amide coupling with biotin NHS-functionalized and a variant of PHOU bearing pendant carboxylic acid groups. The coupled product M₇-biotin was successfully obtained and was submitted to random sulfation at different degrees for future SPR analysis (by IBS collaborators, Grenoble). The product M₇-PHOU was also successfully obtained and remains to be sulfated prior to the evaluation of its biological properties as proteoglycan mimetic.

6.2 Perspectives

In the continuity of our work, some tasks, mainly biological assays, remain to be completed in each chapter.

More biological assays need to be performed of randomly sulfated (cyclo)maltooligosaccharides to assess the role of the DS, chain length and conformation (linear or cyclic) on the biological properties of the compounds (work in progress).

To accurately evaluate the role of sulfate group positions, two compounds remain to be prepared and once again, a majority of biological assays are missing (work in progress). Also, an interesting perspective would be to perform an acetolysis of regioselectively sulfated β -cyclodextrins. By doing so, linear maltoheptaoses with defined sulfation patterns would be obtained, and their biological properties could be compared to those of randomly sulfated maltoheptaoses.

Random sulfation of the coupled product M₇-PHOU is in progress, and once sulfated, the product will be sent to evaluate its ability to mimic PGs.

Experimental section

Materials and methods

All reagents were purchased from commercial suppliers and were used as received. *N,N'*-Dimethylformamide (DMF) and pyridine were distilled under vacuum and stored over activated molecular sieves 4Å. β -cyclodextrin was dried at 60 or 90 °C under reduced pressure in the presence of P_2O_5 and KOH until constant weight.

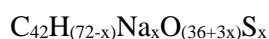
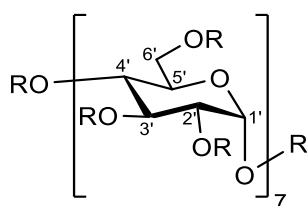
Carbohydrate modifications were followed by thin-layer chromatography on silica gel 60F254 (E. Merck) visualized by heat staining with sulfuric acid 3% solution in MeOH/H₂O (1/1 v/v). Sephadex purifications were performed with LH20 Sephadex resin using H₂O/MeOH 2/1 v/v eluent. NMR analyses were recorded at 25 °C on a Bruker Advance III DRX400 spectrometer. Chemical shifts (δ) are given in ppm. The solvent residual peaks of D₂O, DMSO-*d*₆, MeOD-*d*₄ and CDCl₃ were used as internal standards, at 4.78 ppm, 2.50 ppm, 3.31 ppm and 7.26 ppm, respectively for ¹H NMR, and at 39.52 (DMSO-*d*₆), 49.00 (MeOD-*d*₄) and 77.16 (CDCl₃) for 2D NMR. Coupling constants (J) values are given in Hertz (Hz). Signal multiplicities are described by the following abbreviations: singlet (s), broad singlet (bs), doublet (d), broad doublet (bd), doublet of doublets (dd), triplet (t) and triplet of doublets (td). 2D NMR, homonuclear correlation spectroscopy (COSY), heteronuclear single quantum coherence spectroscopy (HSQC), and heteronuclear multiple-bond correlation spectroscopy (HMBC) experiments were used for unequivocal assignment. Matrix-assisted laser desorption ionization time-of-flight (MALDI–TOF) measurements were performed on a Bruker Daltonics Autoflex Speed apparatus using 2,5-dihydroxybenzoic acid (DHB) as a matrix. High resolution mass spectrometry was carried on a Thermo Scientific LTQ Orbitrap XL (quadrupole hybrid with orthogonal acceleration time-of-flight) mass spectrometer apparatus. Sulfated oligosaccharides were purified by gel permeation chromatography (GPC) with the Superdex S30*3 system (polyacrylamide gel, Biogel P2, P4 or BIORAD) by using ammonium carbonate (0.1 M) at 1.2 mL/min flow rate. For sulfated oligosaccharides, gel permeation chromatography (SEC-MALS) measurements were performed on a Shimadzu apparatus using dextran sulfate (dn/dc=0.142) as an internal reference. The infrared measurements (FT-IR) were carried on a Perkin Elmer Spectrum Two apparatus. The elemental analysis measurements were performed on an Elementar Vario Micro Cube apparatus (Laboratoire de Mesures Physiques, Université de Montpellier, France).

Elemental analysis was performed to determine the sulfur content of each mixture of sulfated polysaccharides and to define the degree of sulfation per unit (DS) of each derivative³⁶⁴.

$$DS = \frac{\left(\frac{S\%}{\text{atomic mass of } S} \right)}{\left(\frac{C\%}{\text{atomic mass of } C \times n_C} \right) \times 7} = 2,25 \times \frac{S\%}{C\%}$$

Synthesis

Randomly sulfated maltoheptaose (Sulfated M₇)



R = H or SO₃Na

[Lightly sulfated] To a stirred solution of maltoheptaose (1 eq., 0.17 mmol, 200 mg) in anhydrous DMF (5 mL) under nitrogen atmosphere was added sulfur trioxide pyridine complex (0.5 eq./OH, 2.00 mmol, 318 mg) portionwise. The reaction mixture was heated at 80°C and was stirred for 2 hours. The reaction mixture was then cooled down to room temperature and poured in a 5% NaHCO_{3(aq)} solution (10 mL, pH 7-8). The crude was concentrated until dryness and then purified by GPC to afford, after lyophilization, a fluffy white solid (195 mg).

¹H NMR (400 MHz, D₂O, 298K) δ (ppm) : 3.17-4.58 (m, H^{2'}, ^{3'}, ^{4'}, ^{5'}, ^{6'}) ; 5.22-6.15 (m, 7H, H^{1'}).

FT-IR : ν(OH)=3282 cm⁻¹ ; ν(CH)=2913 cm⁻¹ ; ν(S=O)=1199 cm⁻¹ ; ν(C-OH ; C-O & C-C)=990 cm⁻¹ ; ν(salts)=568 cm⁻¹.

SEC-MALS: weight-average molar mass M_w of 1722 ± 53 g/mol.

[Moderately sulfated] To a stirred solution of maltoheptaose (1 eq., 0.17 mmol, 200 mg) in anhydrous DMF (5 mL) under nitrogen atmosphere was added sulfur trioxide pyridine complex (1 eq./OH, 4.00 mmol, 636 mg) portionwise. The reaction mixture was heated at 80°C and was stirred for 2 hours. The reaction mixture was then cooled down to room temperature and poured in a 5% NaHCO_{3(aq)} solution (10 mL, pH 7-8). The crude was concentrated until dryness and then purified by GPC to afford, after lyophilization, a fluffy white solid (178 mg).

¹H NMR (400 MHz, D₂O, 298K) δ (ppm) : 3.74-4.68 (m, H^{2'}, ^{3'}, ^{4'}, ^{5'}, ^{6'}) ; 5.37-6.11 (m, 7H, H^{1'}).

FT-IR : ν(OH)=3449 cm⁻¹ ; ν(CH)=2950 cm⁻¹ ; ν(S=O)=1213 cm⁻¹ ; ν(C-OH ; C-O & C-C)=990 cm⁻¹ ; ν(salts)=575 cm⁻¹.

SEC-MALS: weight-average molar mass M_w of 2415 ± 31 g/mol.

[Highly sulfated] To a stirred solution of maltoheptaose (1 eq., 86.73 μmol, 100 mg) in anhydrous DMF (4 mL) under nitrogen atmosphere was added sulfur trioxide pyridine complex (5 eq./OH, 10.01 mmol, 1.59 g) portionwise. The reaction mixture was heated at 60°C and was stirred overnight. The reaction mixture was then cooled down to room temperature and poured in H₂O (10 mL). NaHCO₃ was added until saturation (pH 9-10). The crude was concentrated until dryness and then purified by GPC to afford, after lyophilization, a fluffy white solid (212 mg).

¹H NMR (400 MHz, D₂O, 298K) δ (ppm) : 3.81-5.01 (m, H^{2'}, ^{3'}, ^{4'}, ^{5'}, ^{6'}) ; 5.53-5.74 (m, 7H, H^{1'}).

FT-IR : ν(OH)=3478 cm⁻¹ ; ν(CH)=2921 cm⁻¹ ; ν(S=O)=1218 cm⁻¹ ; ν(C-OH ; C-O & C-C)=990 cm⁻¹ ; ν(salts)=582 cm⁻¹.

SEC-MALS: weight-average molar mass M_w of 2910 ± 167 g/mol.

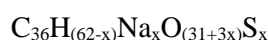
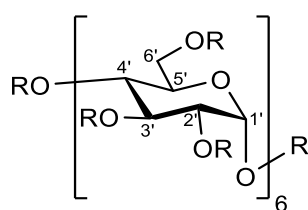
Sample	Mw		Mn		PDI (Mw/Mn)	
	Moy	±	Moy	±	Moy	±
M ₇ L	1722	53	1281	28	1.344	0.012
M ₇ M	2415	31	1320	15	1.830	0.025
M ₇ H	2910	167	1649	57	1.765	0.066

Table 17. SEC-MALS analysis of sulfated M₇

Sample	C [wt%]	H [wt%]	N [wt%]	S [wt%]	Degree of sulfation (DS)
M ₇ L	30.844	5.999	3.152	7.003	0.5
M ₇ M	20.532	5.475	5.826	14.444	1.6
M ₇ H	14.832	4.716	8.473	21.009	3.2

Table 18. Elemental analysis of sulfated M₇

Randomly sulfated maltohexaose (Sulfated M₆)



R = H or SO₃Na

[Lightly sulfated] To a stirred solution of maltohexaose (1 eq., 0.15 mmol, 150 mg) in a mixture of DMF/pyridine 2/3 v/v (5 mL) was added sulfur trioxide pyridine complex (0.5 eq./OH, 1.50 mmol, 238 mg). The reaction mixture was heated at 80°C and was stirred for 2h30. The reaction mixture was then cooled down to room temperature and poured in a 5% NaHCO_{3(aq)} solution (10 mL, pH 7-8). The crude was concentrated until dryness and then purified by dialysis against H₂O to afford, after lyophilization, a fluffy white solid (67 mg).

¹H NMR (400 MHz, D₂O, 298K) δ (ppm) : 3.23-4.72 (m, H^{2',3',4',5',6'}) ; 5.23 (d, 0.5H, H^{1'α}) ; 5.31-5.81 (m, 5.5H, H^{1'}).

FT-IR : ν(OH)=3272 cm⁻¹ ; ν(S=O)=1215 cm⁻¹ ; ν(C-OH ; C-O & C-C)=995 cm⁻¹ ; ν(salts)=576 cm⁻¹.

[Moderately sulfated] To a stirred solution of maltohexaose (1 eq., 0.15 mmol, 150 mg) in a mixture of DMF/pyridine 2/3 v/v (5 mL) was added sulfur trioxide pyridine complex (1 eq./OH, 3.00 mmol, 477 mg). The reaction mixture was heated at 80°C and was stirred for 2 hours leading to the formation of a brown residue in a colorless solvent. The hot solvent was discarded, and the residue was rinsed with MeOH (10 mL) three times. The residue was then dissolved in H₂O (7 mL) by using an ultrasound bath and concentrated until dryness. The residue was redissolved in H₂O (4 mL) and a solution of barium acetate (0.55 mM, 4 mL) was added dropwise until the pH reached a value of 6. The addition of barium acetate formed a white precipitate, that was centrifuged at 7000 g for 10 min at 4°C. The precipitate was discarded and the supernatant was concentrated. The product was then passed through an ion-exchange resin (DOWEX H⁺). The obtained product was then neutralized with ammonia 1 M (3 mL). Finally, the product was purified by dialysis against H₂O, and lyophilized to provide a white fluffy solid (288 mg).

¹H NMR (400 MHz, D₂O, 298K) δ (ppm) : 3.25-4.62 (m, H^{2',3',4',5',6'}) ; 5.20-6.08 (m, 5.5H, H^{1'}).

FT-IR : ν(OH)=3204 cm⁻¹ ; ν(S=O)=1188 cm⁻¹ ; ν(C-OH ; C-O & C-C)=993 cm⁻¹ ; ν(salts)=575 cm⁻¹.

[Highly sulfated] To a stirred solution of maltohexaose (1 eq., 0.15 mmol, 150 mg) in a mixture of DMF/pyridine 2/3 v/v (5 mL) was added sulfur trioxide pyridine complex (2 eq./OH, 6.00 mmol, 955 mg). The reaction mixture was heated at 80°C and was stirred for 2 hours leading to the formation of a brown residue in a colorless solvent. The hot solvent was discarded, and the residue was rinsed with MeOH (10 mL) in an ultrasound bath 30 min. The brown residue became a white precipitate in suspension. The crude was then filtered over a Büchner with MeOH (30 mL). The precipitate was then dissolved in H₂O (10 mL) and concentrated until dryness. Then, one more time, the product is precipitated in MeOH (10 mL) and centrifuged at 7000 g for 10 min at 4°C. The supernatant was discarded and the pellet was redissolved in H₂O (4 mL) and a solution of barium acetate (0.55 mM, 1 mL) was added dropwise until the pH reached a value of 6. The addition of barium acetate formed a white precipitate, that was centrifuged at 7000 g for 10 min at 4°C. The precipitate was discarded and the supernatant was concentrated. The product was then passed through an ion-exchange resin (DOWEX H⁺). The obtained product was then neutralized with 1 M ammonia solution (3 mL). Finally, the product was purified by dialysis against H₂O, and lyophilized to provide a white fluffy solid (99 mg).

¹H NMR (400 MHz, D₂O, 298K) δ (ppm) : 3.24-4.70 (m, H^{2',3',4',5',6'}) ; 5.23 (d, 0.5H, H^{1'a}) ; 5.34-5.68 (m, 5.5H, H^{1'}).

FT-IR : ν(OH)=3227 cm⁻¹ ; ν(S=O)=1199 cm⁻¹ ; ν(C-OH ; C-O & C-C)=996 cm⁻¹ ; ν(salts)=575 cm⁻¹.

Sample	C [wt%]	H [wt%]	N [wt%]	S [wt%]	Degree of sulfation (DS)
M ₆ L	25.451	4.496	0.016	9.259	0.8
M ₆ M	17.696	5.466	6.870	16.618	2.1
M ₆ H	28.680	5.905	3.034	7.968	0.6

Table 19. Elemental analysis of sulfated M₆

Randomly sulfated β-cyclodextrin (Sulfated ^BCD)



[Lightly sulfated] To a stirred solution of dry β-cyclodextrin (1 eq., 88.10 μmol, 100 mg) in dry DMF (4 mL) was added sulfur trioxide pyridine complex (0.5 eq./OH, 0.92 mmol, 147 mg) portionwise under nitrogen atmosphere. The reaction mixture was heated at 60°C and was stirred for 2 hours. After being cooled down to room temperature, the reaction mixture was poured in H₂O (20 mL), and NaHCO₃ was added until the pH reached a value of 9. The neutralized crude was then concentrated until dryness and purified by GPC to provide, after lyophilization, the pure product as a white solid (123 mg).

¹H NMR (400 MHz, D₂O, 298K) δ (ppm) : 3.47-4.57 (m, H^{2',3',4',5',6'}) ; 5.06-5.74 (m, H^{1'}).

SEC-MALS: weight-average molar mass Mw of 1665 ± 3 g/mol.

[Highly sulfated] To a stirred solution of dry β-cyclodextrin (1 eq., 88.10 μmol, 100 mg) in dry DMF (4 mL) was added sulfur trioxide pyridine complex (5 eq./OH, 9.24 mmol, 1.47 g) portionwise under nitrogen atmosphere. The reaction mixture was heated at 60°C and was stirred over the weekend. After being cooled down to room temperature, the reaction mixture was poured in H₂O (20 mL), and NaHCO₃

was added until the pH reached a value of 9. The neutralized crude was then concentrated until dryness and purified by GPC to provide, after lyophilization, the pure product as a white solid (91 mg).

^1H NMR (400 MHz, D_2O , 298K) δ (ppm) : 3.84-5.23 (m, $\text{H}^{2'}$, $3'$, $4'$, $5'$, $6'$) ; 5.39-5.74 (m, $\text{H}^{1'}$).

SEC-MALS: weight-average molar mass M_w of 2543 ± 39 g/mol.

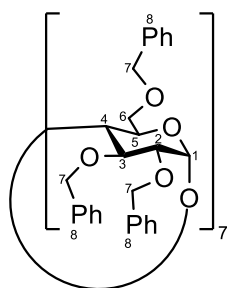
Sample	M_w		M_n		PDI (M_w/M_n)	
	Moy	\pm	Moy	\pm	Moy	\pm
$^{\text{B}}\text{CL}$	1665	3	1241	37	1.342	0.044
$^{\text{B}}\text{CM}^*$	2274	19	1477	14	1.540	0.003
$^{\text{B}}\text{CH}$	2543	39	1559	17	1.632	0.022

Table 20. SEC-MALS of sulfated $^{\text{B}}\text{CD}$. *commercially available

Sample	C [wt%]	H [wt%]	N [wt%]	S [wt%]	Degree of sulfation (DS)
$^{\text{B}}\text{CL}$	25.144	5.754	5.192	11.790	1.0
$^{\text{B}}\text{CM}^*$	17.498	3.421	0.000	14.680	1.9
$^{\text{B}}\text{CH}$	15.441	5.074	7.936	19.007	2.8

Table 21. Elemental analysis of sulfated $^{\text{B}}\text{CD}$. *commercially available

Heptakis-(2,3,6-tri-*O*-benzyl)- β -cyclodextrin **4**



$$M = 3027.61 \text{ g}\cdot\text{mol}^{-1}$$

$$\text{C}_{189}\text{H}_{196}\text{O}_{35}$$

β -Cyclodextrin was dried at 60°C *in vacuo*.

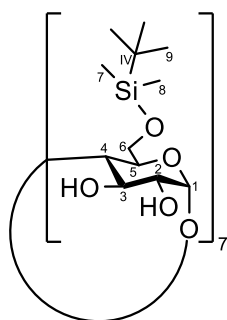
Dried β -Cyclodextrin (1 eq., 3.52 mmol, 4 g) was dissolved in dry DMSO (73 mL) under nitrogen atmosphere at room temperature. NaH (60% w/w, 2 eq./OH, 147.84 mmol, 5.92 g) was added portionwise under vigorous stirring at room temperature, forming a grey suspension. Benzyl chloride (2 eq./OH, 147.84 mmol, 17 mL) was added dropwise over an hour *via* an addition funnel under vigorous stirring. The beige suspension was stirred overnight at room temperature under nitrogen atmosphere. The reaction was followed by TLC (eluent 9/1 v/v cHexane/EtOAc). After completion, the reaction mixture was cooled down to 0°C . MeOH (100 mL) was carefully added to hydrolyze the reaction, followed by H_2O (180 mL). The crude was extracted with EtOAc three times. The combined organic layers were washed with brine, dried over Na_2SO_4 , filtered and concentrated. The product was then purified by chromatography with a gradient of 10/0 to 5/5 v/v EP/EtOAc to provide the pure product as a yellowish oil (8.89 g, 2.93 mmol, 83%).

^1H NMR (400 MHz, CDCl_3 , 298K) δ (ppm) : 3.48 (dd, 7H, 9.3/3.2 Hz, H^2) ; 3.55 (d, 7H, 10.6 Hz, H^{6a}) ; 4.01 (m, 28H, H^3 , H^4 , H^5 & H^{6b}) ; 4.35 (d, 7H, 12.1 Hz, H^{7*}) ; 4.40 (d, 7H, 12.1 Hz, H^{7*}) ; 4.46 (d, 7H, 12.8 Hz, H^{7*}) ; 4.50 (d, 7H, 12.8 Hz, H^{7*}) ; 4.77 ((d, 7H, 11.1 Hz, H^{7*}) ; 5.07 (d, 7H, 11.1 Hz, H^{7*}) ; 5.19 (d, 7H, 3.2 Hz, H^1) ; 7.19 (m, 105H, H^8).

*part of 3 AB systems

MS ESI+ : $m/z=3067.36$ [$\text{M}+\text{K}+\text{H}$] $^{2+}$; $m/z=3090.39$ [$\text{M}+\text{K}+\text{Na}+\text{H}$] $^{3+}$; $m/z=3107.32$ [$\text{M}+2\text{K}+2\text{H}$] $^{4+}$.

Heptakis-(6-*O*-*tert*-butyldimethylsilyl)- β -cyclodextrin **7**



$$M = 1934.83 \text{ g}\cdot\text{mol}^{-1}$$
$$\text{C}_{84}\text{H}_{168}\text{O}_{35}\text{Si}_7$$

Previously lyophilized β -Cyclodextrin was dried at 90°C *in vacuo* in the presence of P₂O₅ until constant weight.

β -Cyclodextrin (1 eq., 11.92 mmol, 13.53 g) was dissolved in dry pyridine (200 mL) at room temperature under nitrogen atmosphere and stirred for 1 hour. *tert*-butyldimethylsilyl chloride (8.4 eq., 100.13 mmol, 15.09 g) was added in one portion, and the resulting suspension was stirred at room temperature for 12 hours. The reaction was followed by TLC (eluent 30/5/4 v/v/v EtOAc/EtOH-96%/H₂O). To ease the chromatography purification, one portion of *tert*-butyldimethylsilyl chloride (1 eq., 11.92 mmol, 1.80 g) was added for the most polar product to be consumed. When the reaction was completed, H₂O was added to the reaction mixture (1 L) and the precipitate was filtered over a Büchner. The precipitate was washed with H₂O (200 mL), redissolved in toluene (40 mL) and concentrated under reduced pressure. The azeotropic drying with toluene was repeated three times. The crude product was then redissolved in CH₂Cl₂ (200 mL) with silica and dried to form a dry sample. The product was purified by chromatography by using 40/40/20/4 v/v/v/v CH₂Cl₂/ACN/EtOH-96%/NH_{3(aq)} to elute the side products then 40/40/20/4 v/v/v/v CH₂Cl₂/ACN/EtOH-96%/H₂O. The pure product was obtained as a white powder (19.09 g, 9.87 mmol, 83 %).

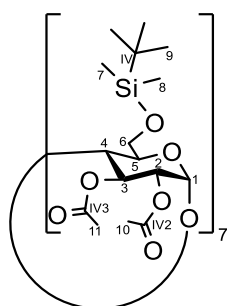
¹H NMR (400 MHz, CDCl₃, 298K) δ (ppm) : 0.03 (s, 21H, H⁷) ; 0.04 (s, 21H, H⁸) ; 0.87 (s, 63H, H⁹) ; 3.56 (t, 7H, 9.3 Hz, H⁴) ; 3.61 (bs, 7H, H⁵) ; 3.64 (dd, 7H, 9.3/3.5 Hz, H²) ; 3.71 (bd, 7H, 10.9 Hz, H^{6a}) ; 3.90 (dd, 7H, 10.9/2.8 Hz, H^{6b}) ; 4.04 (t, 7H, 9.1 Hz, H³) ; 4.89 (d, 7H, 3.5 Hz, H¹).

¹³C NMR (100MHz, CDCl₃, 298K), δ (ppm) : -5.0 (C⁷) ; -4.9 (C⁸) ; 18.4 (C^{IV}) ; 26.1 (C⁹) ; 61.8 (C⁶) ; 72.7 (C⁵) ; 73.6 (C³) ; 73.7 (C²) ; 81.9 (C⁴) ; 102.1 (C¹).

FT-IR : ν (Si-alkyl)=775 cm⁻¹ ; ν (C-H sugar + CH₂-O-Si)= 1034 cm⁻¹ ; ν (O-H)=3327 cm⁻¹

MS MALDI+ : m/z=1956.838 [M+Na]⁺

Heptakis-(6-*O*-*tert*-butyldimethylsilyl)-2,3-di-*O*-acetyl)- β -cyclodextrin **8**



$$M = 2523.35 \text{ g}\cdot\text{mol}^{-1}$$
$$\text{C}_{112}\text{H}_{196}\text{O}_{49}\text{Si}_7$$

A solution of heptakis-(6-*O*-*tert*-butyldimethylsilyl)- β -cyclodextrin **7** (1 eq., 2.58 mmol, 5 g) and acetic anhydride (excess, 26 mL) in dry pyridine (129 mL) under nitrogen atmosphere was stirred overnight at

70°C. The reaction was followed by TLC (eluent EtOAc). If the reaction was not completed, Ac₂O (5 mL) and DMAP (6 mg) were added and the reaction mixture was stirred overnight. When the reaction was finished, the reaction mixture was evaporated under reduced pressure and co-evaporated with toluene (50 mL) three times to remove pyridine. The dried residue was redissolved in EtOAc (50 mL) and washed with HCl_(aq) 1 M (50 mL) then H₂O (50 mL). The organic layer was dried over Na₂SO₄, filtered and concentrated with silica. The product was finally purified by column chromatography with a gradient of 0/10 to 10/0 v/v EtOAc/EP to obtain a colorless solid (5.36 g, 2.12 mmol, 82 %).

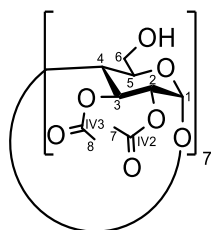
¹H NMR (400 MHz, CDCl₃, 298K) δ (ppm) : 0.03 (s, 21H, H⁷) ; 0.04 (s, 21H, H⁸) ; 0.87 (s, 63H, H⁹) ; 2.03 (s, 21H, H¹⁰) ; 2.04 (s, 21H, H¹¹) ; 3.71 (d, 7H, 11.0 Hz, H⁵) ; 3.86 (m, 14H, H⁶) ; 4.02 (d, 7H, 11.0 Hz, H⁴) ; 4.69 (dd, 7H, 3.5/10.0 Hz, H²) ; 5.14 (d, 7H, 3.5 Hz, H¹) ; 5.33 (dd, 7H, 7.9/10.0 Hz, H³).

¹³C NMR (100MHz, CDCl₃, 298K), δ(ppm) : -5.1 (C⁷) ; -4.9 (C⁸) ; 18.4 (C^{IV}) ; 20.9 (C¹⁰) ; 21.0 (C¹¹) ; 26.0 (C⁹) ; 62.0 (C⁶) ; 71.4 (C²) ; 71.7 (C³) ; 71.9 (C⁵) ; 75.4 (C⁴) ; 96.6 (C¹) ; 169.6 (C^{IV3}) ; 170.9 (C^{IV2}).

FT-IR : ν(Si-alkyl)=776 cm⁻¹ ; ν(C-H sugar and CH₂-O-Si)=1030 cm⁻¹ ; ν(C-O Ac)=1243 and 1216 cm⁻¹ ; ν(CH₃ Ac)=1370 cm⁻¹ ; ν(C=O Ac)=1749 cm⁻¹

MS MALDI+ : m/z= 2546.070 [M+Na]⁺ ; m/z=2562.067 [M+K]⁺

Heptakis-(2,3-di-*O*-acetyl)-β-cyclodextrin **9**



M = 1722.52 g.mol⁻¹
C₇₀H₉₈O₄₉

To a stirred solution of heptakis-(6-*O*-*tert*-butyldimethylsilyl)-2,3-di-*O*-acetyl)-β-cyclodextrin **8** (1 eq., 0.99 mmol, 2.5 g) in dry CH₂Cl₂ (80 mL) under nitrogen atmosphere at room temperature was added a solution of BF₃.OEt₂ (46.5% BF₃, 8 eq., 7.92 mmol, 2.42 g) in dry CH₂Cl₂ (22 mL) dropwise. The resulting mixture was stirred overnight under nitrogen atmosphere. The reaction was monitored by TLC (eluent 95/5 v/v CH₂Cl₂/MeOH). A solution of saturated NaHCO₃ (80 mL) was added and the reaction mixture was extracted. The organic phase was washed with H₂O (80 mL), dried over Na₂SO₄, filtered and concentrated with silica. The product was then purified by chromatography with a gradient of 10/0 to 8/2 v/v CH₂Cl₂/MeOH to obtain a white solid (1.38 g, 0.80 mmol, 81 %).

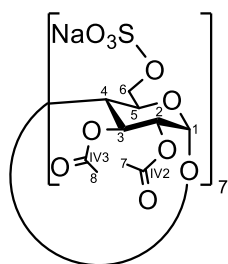
¹H NMR (400 MHz, CDCl₃, 298K) δ(ppm) : 2.00 (s, 21H, H⁷) ; 2.02 (s, 21H, H⁸) ; 3.62 (d, 7H, 11.4 Hz, H^{6a}) ; 3.78 (m, 21H, 11.4/8.2 Hz, H^{6b}, H⁵ & H⁴) ; 4.60 (dd, 7H, 3.4/10.4 Hz, H²) ; 4.77 (bs, 7H, OH⁶) ; 5.09 (d, 7H, 3.4 Hz, H¹) ; 5.25 (dd, 7H, 8.2/10.4 Hz, H³).

¹³C NMR (100MHz, CDCl₃, 298K), δ(ppm) : 20.8 (C⁷) ; 20.9 (C⁸) ; 61.1 (C⁶) ; 71.0 (C³) ; 71.1 (C²) ; 72.2 (C⁵) ; 77.3 (C⁴) ; 96.6 (C¹) ; 170.9 (C^{IV3}) ; 169.7 (C^{IV2}).

FT-IR : ν(C-H sugar)=1023 cm⁻¹ ; ν(C-O Ac)=1216 cm⁻¹ ; ν(CH₃ Ac)= 1370 cm⁻¹ ; ν((C=O Ac)=1741 cm⁻¹ ; ν(O-H)=3419 cm⁻¹

MS MALDI+ : m/z= 1745.55 [M+Na]⁺ ; m/z=881.32 [M+K]²⁺

Heptakis-(6-*O*-sulfo-2,3-di-*O*-acetyl)- β -cyclodextrin **10a**



$$M = 2437.78 \text{ g}\cdot\text{mol}^{-1}$$
$$\text{C}_{70}\text{H}_{91}\text{Na}_7\text{O}_{70}\text{S}_7$$

To a stirred solution of heptakis-(2,3-di-*O*-acetyl)- β -cyclodextrin **9** (1 eq., 0.058 mmol, 100 mg) in dry pyridine (5 mL) under nitrogen atmosphere was added sulfur trioxide pyridine complex (35 eq., 2.03 mmol, 323 mg) in one portion. The reaction mixture was stirred at 60°C overnight and was monitored by TLC (TLC eluent 8/2 v/v ACN/H₂O). When the reaction was completed, the reaction mixture was poured in H₂O (20 mL) and NaHCO₃ was added until the pH reached \approx 9. The crude was then dried with silica to form a dry sample. The product was purified by chromatography with a gradient of 10/0 to 8/2 v/v ACN/H₂O and was then lyophilized to afford a yellowish fluffy solid (118 mg, 48.40 μ mol, 84%).

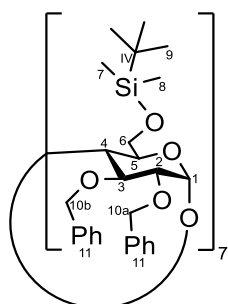
¹H NMR (400 MHz, D₂O, 298K) δ (ppm) : 2.15 (s, 21H, H⁷) ; 2.18 (s, 21H, H⁸) ; 4.14 (q, 7H, 10.3 Hz, H⁴) ; 4.24 (t, 7H, 10.3 Hz, H⁵) ; 4.39 (t, 7H, 9.9 Hz, H^{6a}) ; 4.54 (t, 7H, 9.9 Hz, H^{6b}) ; 4.95 (td, 7H, 10.3/3.5 Hz, H²) ; 5.33 (dd, 7H, 11.5/3.5 Hz, H¹) ; 5.42 (q, 7H, 10.3 Hz, H³).

¹³C NMR (100MHz, D₂O, 298K), δ (ppm) : 20.4 (C⁷) ; 20.5 (C⁸) ; 66.5 (C⁶) ; 70.0 (C⁵) ; 70.8 (C²) ; 71.3 (C³) ; 74.7 (C⁴) ; 96.4 (C¹) ; 172.9 (C^{IV3}) ; 173.0 (C^{IV2}).

FT-IR : ν (C-O aliphatic)=1133 cm⁻¹ ; ν (sulfate)=1210 cm⁻¹ ; ν (C=O ester)=1735 cm⁻¹ ; ν (C-H aliphatic)=2958 cm⁻¹

MS ESI- : m/z =325.02 [M-7Na]⁻ ; m/z =283.03 [M-6Na]⁻ ; m/z =464.23 [M-5Na]⁻ ; m/z =586.03 [M-4Na]⁻ ; m/z =789.04 [M-3Na]⁻

Heptakis-(6-*O*-*tert*-butyldimethylsilyl)-2,3-di-*O*-benzyl)- β -cyclodextrin **11**



$$M = 3196.58 \text{ g}\cdot\text{mol}^{-1}$$
$$\text{C}_{182}\text{H}_{252}\text{O}_{35}\text{Si}_7$$

heptakis-(6-*O*-*tert*-butyldimethylsilyl)- β -cyclodextrin **7** (1 eq., 1.03 mmol, 2 g) was dissolved in dry THF (20 mL) in a round-bottom flask under inert atmosphere. The vigorously stirred solution was cooled down to a temperature between 0-10°C. Crushed KOH (92 eq., 94.76 mmol, 5.32g) was added portionwise. After that, Methyltriphenylphosphonium bromide (0.5 eq., 0.52 mmol, 186 mg) was added in one portion. The initially colorless solution became a white gel, and was vigorously stirred for 2 hours at 0-10°C under inert atmosphere. Then, benzyl bromide (15.5 eq., 15.97 mmol, 1.90 mL) was added dropwise at 5-10°C. The reaction mixture was warmed up to room temperature and left overnight. The reaction was monitored by TLC (eluent 9/1.5/1.2 v/v/v EtOAc/EtOH/H₂O and 9/1 v/v Hexane/EtOAc). KOH (49 eq., 50.46 mmol, 2.83 g, crushed) and BnBr (8 eq., 8.41 mmol, 1 mL) were added at 10°C until the reaction was completed. The reaction mixture was filtered through a Büchner

and the white solid was washed with THF (100 mL). The filtrate was concentrated until about 10 mL were left and poured in MeOH (120 mL) vigorously stirred. A yellowish solid precipitated. The solid was decanted and the operation was repeated three times. The precipitate was then filtered through a Büchner with H₂O (50 mL) five times and H₂O/MeOH 9/1 v/v (50 mL) once, leading to a very hydrophobic white solid. The product was finally isolated by chromatography with a gradient of 10/0 to 5/5 v/v EP/CH₂Cl₂ in the form of a white powder (2.44 g, 0.76 mmol, 74%).

¹H NMR (400 MHz, CDCl₃, 298K) δ (ppm) : 0.00 (s, 21H, H⁷); 0.01 (s, 21H, H⁸); 0.84 (s, 63H, H⁹) ; 3.36 (dd, 7H, 9.2/3.0 Hz, H²); 3.70 (m, 14H, H⁵ & H^{6a}); 4.01 (td, 14H, 21.6/9.2 Hz, H³ & H⁴); 4.24 (d, 7H, 10.8 Hz, H^{6b}); 4.46 (d*, 7H, 12.3 Hz, H^{10a}); 4.51 (d*, 7H, 12.3 Hz, H^{10a}); 4.68 (d*, 7H, 10.8 Hz, H^{10b}) ; 5.05 (d*, 7H, 10.8 Hz, H^{10b}); 5.29 (d, 7H, 3.0 Hz, H¹); 7.11 (m, 70H, H¹¹).

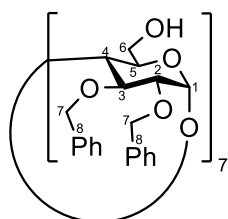
*part of 2 AB systems

¹³C NMR (100MHz, CDCl₃, 298K), δ(ppm) : -4.9 (C⁷) ; -4.6 (C⁸) ; 18.5 (C^{IV}) ; 26.1 (C⁹) ; 62.5 (C⁶) ; 72.6 (C⁵) ; 72.7 (C^{10a}) ; 75.6 (C^{10b}) ; 77.8 (C⁴) ; 79.4 (C²) ; 81.0 (C³) ; 98.1 (C¹) ; 126.9, 127.4, 127.7, 127.8, 128.0, 128.2, 138.5, 139.5 (C¹¹).

FT-IR : ν(Si-alkyl)=776 cm⁻¹ ; ν(benzyl)=831-694 cm⁻¹ ; ν(C-H sugar and CH²-O-Si)=1028 cm⁻¹ ; ν(benzyl)=1454 cm⁻¹

MS MALDI+ : m/z= 3218.301 [M=Na]⁺ ; m/z= 3234.276 [M+K]⁺

Heptakis-(2,3-di-*O*-benzyl)-β-cyclodextrin 12



M = 2396.74 g.mol⁻¹
C₁₄₀H₁₅₄O₃₅

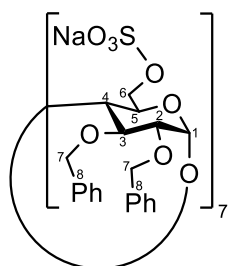
To a stirred solution of heptakis-(6-*O*-tert-butyldimethylsilyl)-2,3-di-*O*-benzyl)-β-cyclodextrin 11 (1 eq., 0.16 mmol, 500 mg) in THF (20 mL) was added tetrabutylammonium fluoride trihydrate (16 eq., 2.56 mmol, 808 mg) portionwise at room temperature. The colorless solution became yellow during the addition, and was stirred at room temperature overnight. The reaction was monitored by TLC (eluent 9/1 v/v CH₂Cl₂/MeOH). When the reaction was completed, the reaction mixture was concentrated. MeOH (10 mL) was added and the mixture was concentrated three times until dryness. The product was suspended in H₂O (50 mL), and filtered over a Büchner with H₂O (10 mL) six times, then with H₂O/MeOH 9/1 v/v (10 mL) four times until obtention of an odorless white solid. The precipitate was redissolved in EtOAc (30 mL) and collected by filtration through a Büchner. The dried product was obtained as a white solid (231 mg, quantitative yield).

¹H NMR (400 MHz, DMSO-d₆, 298K) δ (ppm) : 3.41 (dd, 7H, 9.1/2.7 Hz, H²) ; 3.66 (dd, 7H, 11.1/3.6 Hz, H^{6a}) ; 3.86 (m, 28H, H⁵, H⁴, H^{6b}, H³) ; 4.51 (d, 7H, 13.2 Hz, H^{7*}) ; 4.54 (d, 7H, 13.2 Hz, H^{7*}) ; 4.60 (t, 7H, 5.8 Hz, H⁶) ; 4.63 (d, 7H, 11.5 Hz, H⁷) ; 4.93 (d, 7H, 11.5 Hz, H⁷) ; 5.27 (d, 7H, 2.7 Hz, H¹) ; 7.14 (m, 70H, H⁸).

*part of an AB system

MS MALDI+ : m/z=2419.025 [M+Na]⁺ ; m/z=2435.017 [M+K]⁺

Heptakis-(6-*O*-sulfo-2,3-di-*O*-benzyl)- β -cyclodextrin **10b**



$$M = 3108.60 \text{ g}\cdot\text{mol}^{-1}$$
$$C_{147}H_{147}Na_7O_{56}S_7$$

To a stirred solution of heptakis-(2,3-di-*O*-benzyl)- β -cyclodextrin **12** (1 eq., 32.13 μmol , 77 mg) in dry pyridine (4 mL) was added sulfur trioxide pyridine complex (35 eq., 1.12 mmol, 169 mg) in one portion. The reaction was heated at 60°C and left stirring under nitrogen atmosphere over the weekend. When the reaction was completed (TLC eluent 85/15 v/v ACN/H₂O), the reaction mixture was poured in H₂O (20 mL) and treated with NaHCO₃ to reach a pH around 9 (to replace the pyridinium salts on sulfate moieties by sodium salts). The crude was then dried with silica to be later purified by chromatography with a gradient of 10/0 to 8/2 v/v ACN/H₂O to provide the pure product in the form of a white solid (319 mg, quantitative yield).

¹H NMR (400 MHz, DMSO-d₆, 298K) δ (ppm) : 3.34 (d, 7H, 2.3 Hz, H²) ; 3.86 (t, 7H, 8.9 Hz, H⁴) ; 3.97 (t, 7H, 8.9 Hz, H³) ; 4.01 (d, 7H, 10.0/1.8 Hz, H⁵) ; 4.12 (d, 7H, 10.8 Hz, H⁷ or H⁶) ; 4.36 (d, 7H, 10.8 Hz, H⁷ or H⁶) ; 4.44* (d, 7H, 12.3 Hz, H⁷ or H⁶) ; 4.49* (d, 7H, 12.3 Hz, H⁷ or H⁶) ; 4.62 (d, 7H, 11.0 Hz, H⁷ or H⁶) ; 4.91 (d, 7H, 11.0 Hz, H⁷ or H⁶) ; 5.53 (d, 7H, 2.3 Hz, H¹) ; 7.06 (m, 70H, H⁸).

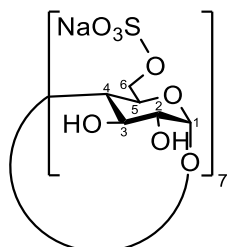
¹³C NMR (100MHz, DMSO-d₆, 298K), δ (ppm) : 65.5 (C⁶ or C⁷) ; 70.4 (C⁵) ; 71.2 (C⁶ or C⁷) ; 74.4 (C⁶ or C⁷) ; 77.2 (C⁴) ; 78.7 (C²) ; 80.0 (C³) ; 96.4 (C¹) ; 126.7, 127.0, 127.1, 127.3, 127.7, 127.9, 138.3, 139.2 (C⁸).

*part of an AB system

FT-IR : ν (C-H aromatic)=695 + 730 cm⁻¹ ; ν (C-O aliphatic)=990 cm⁻¹ ; ν (C-O ether aliphatic)=1053 cm⁻¹ ; ν (sulfate)=1210 cm⁻¹ ; ν (C-H aliphatic)=2895 cm⁻¹

HRMS-ESI-: calculated for [M+4H-7Na]³⁻ m/z=983.90098, found 983.89633 (one pic for each loss of Na)

Heptakis-(6-*O*-sulfo)- β -cyclodextrin **13**



$$M = 1849.26 \text{ g}\cdot\text{mol}^{-1}$$
$$C_{42}H_{63}Na_7O_{56}S_7$$

To a stirred solution of heptakis-(6-*O*-sulfo-2,3-di-*O*-acetyl)- β -cyclodextrin **10a** (1 eq., 0.12 mmol, 292 mg) in absolute methanol (6 mL) under nitrogen atmosphere was added a solution of freshly prepared sodium methoxide (1 M in MeOH, 0.08 eq., 0.01 mmol, 10 μL) dropwise at room temperature. The reaction mixture became trouble during the addition. The reaction mixture was stirred overnight and was monitored by TLC (8/2 v/v ACN/H₂O). When the reaction was completed, water (2 mL) was added to quench sodium methoxide, and then NaHCO₃ was added until pH 9-10. The crude was then concentrated and purified by GPC to afford, after lyophilization, a white solid (176 mg, 79%).

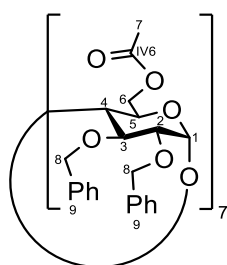
^1H NMR (400 MHz, D_2O , 298K) δ (ppm) : 3.56 (dd, 7H, 9.8/3.1 Hz, H^2) ; 3.67 (t, 7H, 9.8 Hz, H^4) ; 3.96 (t, 7H, 9.8 Hz, H^3) ; 4.09 (d, 7H, 9.8 Hz, H^5) ; 4.24 (d, 7H, 10.8 Hz, H^{6a}) ; 4.32 (d, 7H, 10.8 Hz, H^{6b}) ; 5.15 (d, 7H, 3.1 Hz, H^1).

^{13}C NMR (100 MHz, D_2O , 298K), δ (ppm) : 66.6 (C^6) ; 69.4 (C^5) ; 71.9 (C^2) ; 72.8 (C^3) ; 78.6 (C^4) ; 100.4 (C^1).

FT-IR : $\nu(\text{C-O aliphatic})=1055 \text{ cm}^{-1}$; $\nu(\text{S=O sulfate})=1206 \text{ cm}^{-1}$; $\nu(\text{O-H})=3220 \text{ cm}^{-1}$

HRMS-ESI- : calculated for $[\text{M}+2\text{H}-7\text{Na}]^{5-}$ $m/z=337.80622$, found 337.80580

Heptakis-(6-*O*-acetyl-2,3-di-*O*-benzyl)- β -cyclodextrin **5**



$M = 2691.00 \text{ g}\cdot\text{mol}^{-1}$

$\text{C}_{154}\text{H}_{168}\text{O}_{42}$

To a stirred solution of heptakis-(2,3-di-*O*-benzyl)- β -cyclodextrin **12** (1 eq., 93.88 μmol , 225 mg) in dry pyridine (4 mL) was added anhydride acetic (excess, 9.96 mmol, 942 μL) and DMAP (cat., 3 mg) at room temperature. The reaction mixture was heated and stirred at 70°C overnight. The reaction mixture was followed by TLC (2/8 v/v EP/EtOAc). When the reaction was completed, the reaction mixture was dried, and pyridine was co-evaporated with toluene (10 mL) three times. The brown residue was redissolved in EtOAc (10 mL) and washed with $\text{HCl}_{(\text{aq})}$ 1M (10 mL) and H_2O (10 mL). The organic layer was dried over Na_2SO_4 , filtered and dried providing a brown solid (260 mg, quantitative yield).

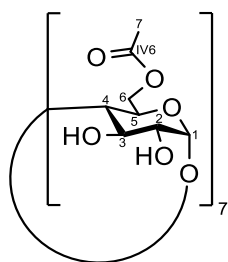
^1H NMR (400 MHz, CDCl_3 , 298K) δ (ppm) : 2.03 (s, 21H, H^7) ; 3.46 (dd, 7H, 3.3/8.8 Hz, H^2) ; 3.67 (t, 7H, 8.8 Hz, H^4) ; 3.99 (t, 7H, 8.8 Hz, H^3) ; 4.05 (dd, 7H, 3.7/8.8 Hz, H^5) ; 4.36 (dd, 7H, 3.7/12.3 Hz, H^{6a}) ; 4.40 (d, 7H, 12.7 Hz, H^8 of $\text{C}^2\text{-Bn}$) ; 4.44 (dd, 7H, 3.7/12.3 Hz, H^{6b}) ; 4.55 (d, 7H, 12.7 Hz, H^8 of $\text{C}^2\text{-Bn}$) ; 4.73 (d, 7H, 11.0 Hz, H^8 of $\text{C}^3\text{-Bn}$) ; 4.93 (d, 7H, 3.3 Hz, H^1) ; 5.00 (d, 7H, 11.0 Hz, H^8 of $\text{C}^3\text{-Bn}$) ; 7.10-7.25 (m, 70H, H^9).

^{13}C NMR (100MHz, CDCl_3 , 298K), δ (ppm) : 21.5 (C^7) ; 64.2 (C^6) ; 70.6 (C^5) ; 73.8 (C^8 of $\text{C}^2\text{-Bn}$) ; 76.0 (C^8 of $\text{C}^3\text{-Bn}$) ; 79.3 (C^2) ; 80.4 (C^4) ; 81.1 (C^3) ; 99.7 (C^1) ; 127.8, 127.9, 128.4, 128.6, 128.8, 128.9, 139.0 & 140.0 (C^9) ; 171.2 ($\text{C}^{\text{IV}6}$).

FT-IR : $\nu(\text{C-H aromatic})=695 + 732 \text{ cm}^{-1}$; $\nu(\text{C-O aliphatic})=1023 \text{ cm}^{-1}$; $\nu(\text{C-O ether aliphatic})=1092 \text{ cm}^{-1}$; $\nu(\text{C=O ester})=1737 \text{ cm}^{-1}$; $\nu(\text{C-H aliphatic})=2908 \text{ cm}^{-1}$

MALDI+ : $m/z=2623.400$ $[\text{M}'+\text{Na}]^+$ corresponding to the product with one loss of Bn ; $m/z=2713.469$ $[\text{M}+\text{Na}]^+$.

Heptakis-(6-*O*-acetyl)- β -cyclodextrin 6



$$M = 1429.25 \text{ g}\cdot\text{mol}^{-1}$$
$$\text{C}_{56}\text{H}_{84}\text{O}_{42}$$

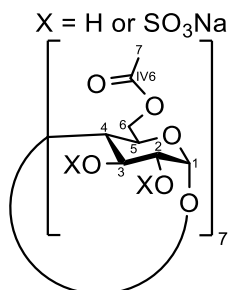
To a stirred solution of heptakis-(6-*O*-acetyl-2,3-di-*O*-benzyl)- β -cyclodextrin 5 (1 eq., 0.037 mmol, 100 mg) in MeOH/DCM (5.2/0.2 v/v) was carefully added palladium on carbon (10% weight, 1.8 eq., 0.067 mmol, 71 mg). After three purging cycles, the flask was stirred under 5 atmospheres of H₂ overnight. The crude was then filtered on celite over a Büchner with MeOH (5 x 10 mL) and EtOH (2 x 10 mL), and the filtrate was dried providing a white solid (53 mg, 100%).

¹H NMR (400 MHz, DMSO-d₆, 298K) δ (ppm) : 1.99 (s, 21H, H⁷) ; 3.44 (m, 14H, H² & H⁴) ; 3.63 (t, 7H, 9.3 Hz, H³) ; 3.85 (m, 7H, H⁵) ; 4.13 (dd, 7H, 11.4/6.2 Hz, H^{6a}) ; 4.35 (d, 7H, 11.4 Hz, H^{6b}) ; 4.89 (d, 7H, 3.6 Hz, H¹) ; 5.89 (sl, 14H, OH).

¹³C NMR (100MHz, DMSO-d₆, 298K), δ (ppm) : 20.3 (C⁷) ; 63.1 (C⁶) ; 69.1 (C⁵) ; 72.0 (C²) ; 72.8 (C³) ; 82.1 (C⁴) ; 102.0 (C¹) ; 170.1 (C^{IV6}).

FT-IR : ν (C-O aliphatic)=1029 cm⁻¹ ; ν (C=O ester)=1742 cm⁻¹ ; ν (C-H aliphatic)=2933 cm⁻¹ ; ν (O-H)=3323 cm⁻¹.

Partially 2,3-*O*-sulfated heptakis-(6-*O*-acetyl)- β -cyclodextrin 16'

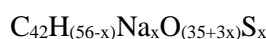
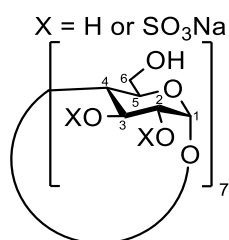


$$\text{C}_{56}\text{H}_{(84-x)}\text{Na}_x\text{O}_{(42+3x)}\text{S}_x$$

To a stirred solution of heptakis-(6-*O*-acetyl)- β -cyclodextrin 6 (1 eq., 0.077 mg, 111 mg) in dry pyridine (5 mL) was added sulfur trioxide pyridine complex (70 eq., 5.39 mmol, 858 mg) at room temperature. The reaction mixture was heated at 60°C for four days. When the reaction was not evolving anymore (TLC eluent 8/2 v/v ACN/H₂O or 10/2 v/v EtOH/H₂O), the crude was purified by size exclusion chromatography on Sephadex column then ionic exchange resin Dowex Na⁺ form (eluent 2/1 v/v H₂O/MeOH). The lyophilized mixture of products was afforded as a white solid (135 mg).

¹H NMR (400 MHz, D₂O, 298K) δ (ppm) : 3.36 (s, 21H, H⁷) ; 3.47-5.60 (m, H¹, H², H³, H⁴, H⁵ & H⁶).

Partially 2,3-*O*-sulfated β -cyclodextrin **17'**



To a stirred solution of partially 2,3-*O*-sulfated heptakis-(6-*O*-acetyl)- β -cyclodextrin **16'** (1 eq., 135 mg) in absolute MeOH (5 mL) was added sodium methoxide (1M in MeOH, 200 μ L) under nitrogen atmosphere. The reaction mixture was stirred at room temperature under nitrogen atmosphere, and was monitored by TLC (eluent 7/3 v/v ACN/H₂O). Extra portions of sodium methoxide could be eventually added. After 4 days, IR120 H⁺ form was added in the reaction mixture until the pH reached 7. The crude was then filtered over Büchner with MeOH and purified by GPC, affording a white cottonous solid after lyophilization (67 mg).

¹H NMR (400 MHz, D₂O, 298K) δ (ppm) : 3.41-5.69 (m, H¹, H², H³, H⁴, H⁵ & H⁶).

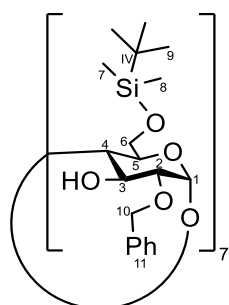
Sample	C [wt%]	H [wt%]	N [wt%]	S [wt%]	Degree of sulfation (DS)
<i>Per</i> -2,3S- β -cyclodextrin	23.975	5.460	5.637	12.912	1.2

Table 22. Elemental analysis of *per*-2,3S- β -cyclodextrin **17'**

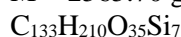
Sample	Mw		Mn		PDI (Mw/Mn)	
	Moy	\pm	Moy	\pm	Moy	\pm
<i>Per</i> -2,3S- β -cyclodextrin	2103	81	1492	4	1.409	0.055

Table 23. SEC-MALS of *per*-2,3S- β -cyclodextrin **17'**

Heptakis-(6-*O*-*tert*-butyldimethylsilyl-2-*O*-benzyl)- β -cyclodextrin **19**



$$M = 2565.70 \text{ g}\cdot\text{mol}^{-1}$$



In a round-bottom flask was dissolved heptakis-(6-*O*-*tert*-butyldimethylsilyl)- β -cyclodextrin **7** (1 eq., 0.52 mmol, 1g) in dry THF (10 mL) at rt under nitrogen atmosphere. NaH (10 eq., 5.17 mmol, 207 mg) was added portionwise and the reaction mixture was stirred for 45 minutes at room temperature. Benzyl bromide (10 eq., 5.17 mmol, 615 μ L) was added dropwise and the mixture was stirred at room temperature over the weekend. The reaction was followed by TLC (eluent 8/2 v/v Hex/EtOAc). When the reaction was completed, NaH was neutralized by the addition of EtOAc (100 mL). H₂O (100 mL) was also added, and the product was extracted from the aqueous phase with EtOAc two times. The organic layer was dried over Na₂SO₄, filtered and concentrated with silica. The product was purified by chromatography with a slow gradient of 10/0 to 8/2 v/v Hex/EtOAc. The pure product was obtained in the form of a white solid (698 mg, 0.27 mmol, 52%).

¹H NMR (400 MHz, CDCl₃, 298K) δ (ppm) : -0.05 (s, 21H, H⁷) ; -0.04 (s, 21H, H⁸) ; 0.82 (s, 63H, H⁹) ; 3.31 (dd, 7H, 9.3/3.0 Hz, H²) ; 3.42 (dd, 7H, 9.3/9.1 Hz, H⁴) ; 3.53 (dd, 7H, 9.1/1.4 Hz, H⁵) ; 3.59 (dd,

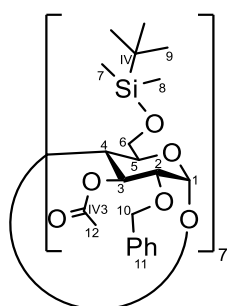
7H, 10.8/1.4 Hz, H^{6a}); 3.84 (dd, 7H, 10.8/1.4 Hz, H^{6b}); 3.99 (t, 7H, 9.3 Hz, H³); 4.70 (d, 7H, 11.6 Hz, H^{10a}); 4.75 (d, 7H, 3.0 Hz, H¹); 4.90 (bs, 7H, OH); 4.95 (d, 7H, 11.6 Hz, H^{10b}); 7.34 (m, 35H, H¹¹).

¹³C NMR (100MHz, CDCl₃, 298K), δ(ppm) : -5.1 (C⁷); -4.9 (C⁸); 18.4 (C^{IV}); 26.1 (C⁹); 61.9 (C⁶); 71.8 (C⁵); 73.7 (C³); 74.1 (C¹⁰); 79.2 (C²); 82.2 (C⁴); 101.4 (C¹); 128.0, 128.5, 128.9, 137.9 (C¹¹).

FT-IR : ν(CH₂)=746 cm⁻¹; ν(Si-alkyl)=777 cm⁻¹; ν(C-H aromatic)=696 + 2931 cm⁻¹; ν(Si-O-C)=829 + 1079 cm⁻¹; ν(C-O aliphatic)=1042 cm⁻¹; ν(Si-CH₃)=1248 cm⁻¹; ν(C-H sp³)=2879 cm⁻¹; ν(O-H)=3419 cm⁻¹

MS MALDI+: m/z= 2588.138 [M+Na]⁺; m/z=2604.107 [M+K]⁺ (and then one pic for each loss of TBDMS, Δ=91).

Heptakis-(6-*O*-*tert*-butyldimethylsilyl-2-*O*-benzyl-3-*O*-acetyl)-β-cyclodextrin **20**



M = 2859.96 g.mol⁻¹
C₁₄₇H₂₂₄O₄₂Si₇

To a stirred solution of heptakis-(6-*O*-*tert*-butyldimethylsilyl-2-*O*-benzyl)-β-cyclodextrin **19** (1eq., 77.95 μmol, 200 mg) in dry pyridine (5 mL) was added acetic anhydride (excess, 868 μL) at room temperature. The reaction mixture was then heated at 70°C and stirred over the weekend. The reaction was monitored by TLC (eluent 7/3 v/v Hex/EtOAc). If needed, DMAP (cat., 5 mg) and Ac₂O (500 μL) were added. When the reaction was completed, the reaction mixture was dried, and co-evaporated with toluene (10 mL) three times to remove traces of pyridine. The obtained almost-red solid was redissolved in EtOAc (20 mL) and washed with HCl_(aq) 1M (20 mL) and then H₂O (20 mL). The organic layer was dried over Na₂SO₄, filtered, and dried to afford a yellow solid (248 mg, quantitative yield).

¹H NMR (400 MHz, CDCl₃, 298K) δ (ppm) : -0.01 (s, 21H, H⁷); 0.00 (s, 21H, H⁸); 0.86 (s, 63H, H⁹); 1.77 (s, 21H, H¹²); 3.31 (dd, 7H, 9.6/3.0 Hz, H²); 3.65* (d, 7H, 11.7 Hz, H^{6a}); 3.79 (m, 14H, H⁵ & H⁴); 4.11* (d, 7H, 11.7 Hz, H^{6b}); 4.46 (d, 7H, 12.3 Hz, H^{10a}); 4.58 (d, 7H, 12.3 Hz, H^{10b}); 5.00 (d, 7H, 3.0 Hz, H¹); 5.25 (t, 7H, 9.6 Hz, H³); 7.26 (m, 35H, H¹¹).

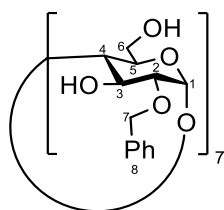
*part of an AB system

¹³C NMR (100MHz, CDCl₃, 298K), δ(ppm) : -5.0 (C⁷); -4.7 (C⁸); 21.0 (C¹²); 26.1 (C⁹); 62.3 (C⁶); 72.4 (C⁵); 72.6 (C¹⁰); 73.2 (C³); 77.1 (C⁴); 77.9 (C²); 98.7 (C¹); 127.8, 128.1 & 128.5 (C¹¹); 138.4 (C^{IV} C¹¹).

FT-IR : ν(C-H aromatic)=699 + 748 cm⁻¹; ν(Si-alkyl)=778 cm⁻¹; ν(Si-O-C)=832 cm⁻¹; ν(C-O aliphatic)=1032 cm⁻¹; ν(Si-CH₃)=1233 cm⁻¹; ν(C-H aliphatic)=2935 cm⁻¹; ν(O-H)=3419 cm⁻¹.

MS MALDI+: m/z=2880.489 [M+Na]⁺

Heptakis-(2-*O*-benzyl)- β -cyclodextrin 25



$$M = 1765.84 \text{ g}\cdot\text{mol}^{-1}$$
$$\text{C}_{91}\text{H}_{112}\text{O}_{35}$$

To a stirred solution of heptakis-(6-*O*-*tert*-butyldimethylsilyl-2-*O*-benzyl)- β -cyclodextrin 19 (1 eq., 58.46 μmol , 150 mg) in THF (4 mL) was added tetrabutylammonium fluoride trihydrate (16 eq., 0.93 mmol, 295 mg) portionwise. The yellowish reaction was stirred at room temperature overnight, and the reaction was monitored by TLC (95/5 v/v $\text{CH}_2\text{Cl}_2/\text{MeOH}$). When the reaction was completed, the reaction mixture was dried and redissolved in the minimum of MeOH. The product was precipitated in H_2O (60 mL) and filtered over a Büchner with H_2O (5 x 20 mL) and with $\text{H}_2\text{O}/\text{MeOH}$ 9/1 v/v (3 x 20 mL). The odorless precipitate was dried at 60°C *under vacuo* to provide the pure product as a white solid (70 mg, 0.04 mmol, 69%).

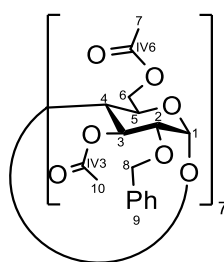
^1H NMR (400 MHz, DMSO-d_6 , 298K) δ (ppm) : 3.33 (m, 7H, 3.0 Hz, H^2) ; 3.38 (t, 7H, 9.0 Hz, H^4) ; 3.58 (m, 21H, H^5 & H^6) ; 3.85 (t, 7H, 9.0 Hz, H^3) ; 4.73 (dd, 7H, 11.9/2.5 Hz, H^{7a}) ; 4.83 (dd, 7H, 11.9/2.6 Hz, H^{7b}) ; 4.90 (d, 7H, 3.0 Hz, H^1) ; 7.38 (m, 35H, H^9).

^{13}C NMR (100 MHz, DMSO-d_6 , 298K), δ (ppm) : 59.7 (C^6) ; 71.5 (C^5) ; 72.9 (C^3) ; 73.0 (C^7) ; 79.0 (C^2) ; 82.0 (C^4) ; 100.1 (C^1) ; 127.7, 128.2 (C^8) ; 137.7 (C^{IV} C^8).

FT-IR : $\nu(\text{C-H aromatic})=697 + 749 \text{ cm}^{-1}$; $\nu(\text{C-O aliphatic})=1035 \text{ cm}^{-1}$; $\nu(\text{C-H aliphatic})=2922 \text{ cm}^{-1}$; $\nu(\text{O-H})=3390 \text{ cm}^{-1}$.

MS MALDI+ : $m/z=1787.676 [\text{M}+\text{Na}]^+$; $1804.677 [\text{M}+\text{K}]^+$

Heptakis-(3,6-di-*O*-acetyl-2-*O*-benzyl)- β -cyclodextrin 26



$$M = 2352.85 \text{ g}\cdot\text{mol}^{-1}$$
$$\text{C}_{119}\text{H}_{140}\text{O}_{49}$$

To a stirred solution of heptakis-(2-*O*-benzyl)- β -cyclodextrin 25 (1 eq., 0.17 mmol, 300 mg) in dry pyridine (7 mL) was added acetic anhydride (excess, 18.01 mmol, 1.7 mL) at room temperature under nitrogen atmosphere. The brown solution was heated and stirred at 70°C overnight and the reaction was monitored by TLC (eluent 85/15 v/v $\text{CH}_2\text{Cl}_2/\text{MeOH}$ and 2/8 v/v EP/EtOAc). If needed, DMAP (cat. 3 mg) was added. When the reaction was finished, the reaction mixture was dried and traces of pyridine were co-evaporated with toluene (20 mL) three times. The brown residue was redissolved in EtOAc (10 mL) and washed with $\text{HCl}_{(\text{aq})}$ 1 M (10 mL) and H_2O (10 mL). The organic layer was then dried over Na_2SO_4 , filtered and evaporated until dryness providing a brown residue (445 mg, quantitative yield).

^1H NMR (400 MHz, CDCl_3 , 298K) δ (ppm) : 3.40 (dd, 7H, 9.7/3.0 Hz, H^2) ; 3.52 (t, 7H, 9.1 Hz, H^4) ; 4.03 (dd, 7H, 9.9/3.6 Hz, H^5) ; 4.23* (dd, 7H, 12.3/4.7 Hz, H^{6a}) ; 4.41* (d, 7H, 12.1 Hz, H^{6b}) ; 4.56 (s, 14H, H^8) ; 4.72 (d, 7H, 2.8 Hz, H^1) ; 5.28 (t, 7H, 9.1 Hz, H^3) ; 7.22-7.34 (m, 35H, H^9).

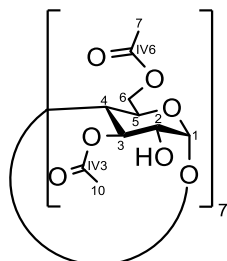
*part of an AB system

^{13}C NMR (100 MHz, CDCl_3 , 298K), δ (ppm) : 63.2 (C^6) ; 69.9 (C^5) ; 72.5 (C^3) ; 73.2 (C^8) ; 77.4 (C^2) ; 78.7 (C^4) ; 99.4 (C^1) ; 128.1, 128.3, 128.6, 138.1 (C^9).

FT-IR : $\nu(\text{C-H aromatic})=699 + 743 \text{ cm}^{-1}$; $\nu(\text{C-O aliphatic})=1024 \text{ cm}^{-1}$; $\nu(\text{C=O ester})=1740 \text{ cm}^{-1}$; $\nu(\text{C-H aliphatic})=2917 \text{ cm}^{-1}$

HRMS-ESI+ : calculated for $[\text{M}+\text{Na}]^+$ $m/z=2375.83554$, found 2375.83435

Heptakis-(3,6-di-*O*-acetyl)- β -cyclodextrin **27**



$M = 1723.51 \text{ g}\cdot\text{mol}^{-1}$

$\text{C}_{70}\text{H}_{98}\text{O}_{49}$

To a stirred solution of heptakis-(3,6-di-*O*-acetyl-2-*O*-benzyl)- β -cyclodextrin **26** (1 eq., 0.042 mmol, 100 mg) in MeOH/EtOAc (3/min. v/v) was carefully added palladium on carbon (10% weight, 1eq., 0.042 mmol, 45 mg). The reaction mixture under 5 atmospheres of H_2 at room temperature overnight. When the reaction was finished (TLC eluent 9/1 v/v ACN/ H_2O), the reaction mixture was filtered on celite over a Büchner with EtOH (3 x 10 mL) and MeOH (5 x 10 mL), and the filtrate was concentrated until dryness affording a white solid (116 mg, quantitative yield).

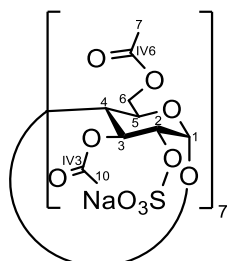
^1H NMR (400 MHz, MeOD- d_4 , 298K) δ (ppm) : 2.06 (s, 21H, H^{10}) ; 2.09 (s, 21H, H^7) ; 3.54 (dd, 7H, 9.7/3.2 Hz, H^2) ; 3.69 (t, 7H, 9.7 Hz, H^4) ; 4.06 (dd, 7H, 9.7/4.5 Hz, H^5) ; 4.30 (dd, 7H, 11.9/4.5 Hz, H^{6a}) ; 4.56 (d, 7H, 11.9 Hz, H^{6b}) ; 4.89 (d, 7H, 3.2 Hz, H^1) ; 5.23 (t, 7H, 9.7 Hz, H^3).

^{13}C NMR (100 MHz, MeOD- d_4 , 298K), δ (ppm) : 21.0 (C^7) ; 21.7 (C^{10}) ; 64.8 (C^6) ; 71.2 (C^5) ; 71.8 (C^2) ; 74.9 (C^3) ; 80.5 (C^4) ; 102.9 (C^1) ; 172.7 ($\text{C}^{\text{IV}3}$ & $\text{C}^{\text{IV}6}$).

FT-IR : $\nu(\text{C-O aliphatic})=1016 \text{ cm}^{-1}$; $\nu(\text{C=O ester})=1743 \text{ cm}^{-1}$; $\nu(\text{C-H aliphatic})=2925 \text{ cm}^{-1}$; $\nu(\text{O-H})=3274 \text{ cm}^{-1}$

MS MALDI+ : $m/z= 1704.476 [\text{M}-1\text{Ac}+\text{Na}]^+$ (minor) ; $1746.495 [\text{M}+\text{Na}]^+$ (major)

Heptakis-(3,6-di-*O*-acetyl-2-*O*-sulfo)- β -cyclodextrin **28**



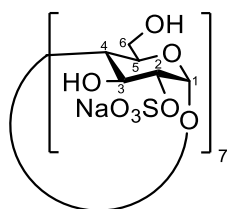
$M = 2437.78 \text{ g}\cdot\text{mol}^{-1}$

$\text{C}_{70}\text{H}_{91}\text{Na}_7\text{O}_{70}\text{S}_7$

To a stirred solution of heptakis-(3,6-di-*O*-acetyl)- β -cyclodextrin **27** (1 eq., 0.041 mmol, 71 mg) in dry pyridine (5 mL) was added sulfur trioxide pyridine complex (35 eq., 1.442 mmol, 229 mg) under nitrogen atmosphere. The reaction mixture was heated at 60°C and the reaction was followed by TLC (eluent 8/2 v/v ACN/ H_2O). After 6h30, the reaction mixture was poured in H_2O (15 mL) and NaHCO_3

was added portionwise until the pH was up to 8. The crude was then concentrated until dryness and used without further purification for the next step.

Heptakis-(2-*O*-sulfo)- β -cyclodextrin 29



$$M = 1847.94 \text{ g.mol}^{-1}$$

$$C_{42}H_{63}Na_7O_{56}S_7$$

To a stirred solution of heptakis-(3,6-di-*O*-acetyl-2-*O*-sulfo)- β -cyclodextrin 28 (1 eq., 0.041 mmol, crude) in absolute MeOH (5 mL) was added sodium methoxide (1M in MeOH, 0.08 eq., 3 μ L) under nitrogen atmosphere at room temperature. The reaction was monitored by TLC (eluent 7/3 v/v ACN/H₂O) and extra portions of sodium methoxide were added until the reaction was finished. Water (10 mL) was added and IR120 H⁺ form was introduced portionwise until the pH reached 7. The crude was then filtered over a Büchner with H₂O (5 x 10 mL), and the filtrate was concentrated until dryness. The pure product was then afforded after GPC purification and lyophilization in the form of a beige cottonous solid (44mg, 58%).

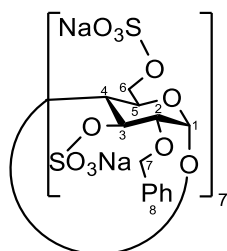
¹H NMR (400 MHz, D₂O, 298K) δ (ppm) : 3.80 (t, 7H, 8.8 Hz, H⁴) ; 3.92 (m, 21H, H⁵ & H⁶) ; 4.13 (dd, 7H, 10.1/8.8 Hz, H³) ; 4.23 (dd, 7H, 10.1/3.6 Hz, H²) ; 5.53 (d, 7H, 3.6 Hz, H¹).

¹³C NMR (100 MHz, D₂O, 298K), δ (ppm) : 60.3 (C⁶) ; 70.1 (C³) ; 71.0 (C⁵) ; 77.4 (C²) ; 78.3 (C⁴) ; 97.6 (C¹).

FT-IR : ν (C-O aliphatic)=987 cm⁻¹ ; ν (S=O)=1213 cm⁻¹ ; ν (O-H)=3237 cm⁻¹

HRMS (ESI-) : calculated for [M+3H-7Na]⁴⁺ m/z=422.50959, found 422.50959

Heptakis-(3,6-di-*O*-sulfo-2-*O*-benzyl)- β -cyclodextrin 30



$$M = 3194.47 \text{ g.mol}^{-1}$$

$$C_{91}H_{98}Na_{14}O_{77}S_{14}$$

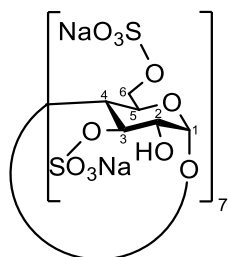
To a stirred solution of heptakis-(2-*O*-benzyl)- β -cyclodextrin 25 (1 eq., 36.81 μ mol, 65 mg) in dry pyridine (3 mL) was added sulfur trioxide pyridine complex (70 eq., 2.58 mmol, 410 mg) portionwise. The reaction mixture was heated at 60°C over the weekend, and the reaction was followed by TLC (eluent 8/2 v/v ACN/H₂O). When the reaction was completed, the reaction mixture was poured in H₂O (10 mL) and NaHCO₃ was added until the pH reached a value of 9. The neutralized solution was concentrated until dryness and purified by GPC to provide, after lyophilization, the pure product as a white solid (58 mg, 18.16 μ mol, 49%).

¹H NMR (400 MHz, D₂O, 298K) δ (ppm) : 3.91 (dl, 7H, 8.4 Hz, H⁵) ; 4.00 (sl, 7H, H²) ; 4.19 (dd, 7H, 8.6/3.8 Hz, H⁴) ; 4.26 (sl, 14H, H⁶) ; 4.55 (sl, 14H, H⁷) ; 4.78 (sl, H³) ; 5.23 (d, 7H, 3.8 Hz, H¹) ; 7.22 (t, 7H, 7.1 Hz,) ; 7.27-7.38 (m, 35H, H⁸).

^{13}C NMR (100 MHz, D_2O , 298K), δ (ppm) : 67.1 (C^6) ; 70.0 (C^5) ; 73.0 (C^7) ; 74.6 (C^2) ; 75.7 (C^4) ; 97.4 (C^1) ; 127.8 (C^8) ; 128.3 (C^8) ; 138.4 ($\text{C}^{\text{IV}} \text{C}^8$).

HRMS-ESI- : calculated for $[\text{M}+9\text{H}-14\text{Na}]^{5-}$ $m/z=575.81149$, found 575.81105

Heptakis-(3,6-di-*O*-sulfo)- β -cyclodextrin **31**



$M = 2563.53 \text{ g}\cdot\text{mol}^{-1}$
 $\text{C}_{42}\text{H}_{56}\text{Na}_{14}\text{O}_{77}\text{S}_{14}$

To a stirred solution of heptakis-(3,6-di-*O*-sulfo-2-*O*-benzyl)- β -cyclodextrin **30** (1 eq., 0.031 mmol, 100 mg) in MeOH (3 mL) was carefully added palladium on carbon (10% weight, 0.9 eq., 0.028 mmol, 30 mg). The reaction mixture was stirred under 5 atmospheres of H_2 at room temperature overnight. The reaction was monitored by TLC (eluent 8/2 v/v ACN/ H_2O), and relaunched if not finished. When the reaction was finished, the reaction mixture was filtered on celite over a Büchner with H_2O (6 x 10 mL) and MeOH (3 x 10 mL), and the filtrate was concentrated until dryness affording a white solid (44 mg, 56%).

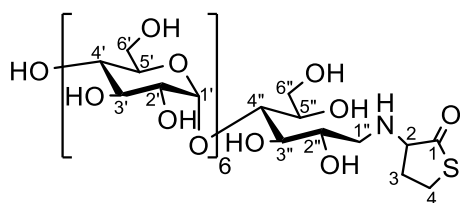
^1H NMR (400 MHz, D_2O , 298K) δ (ppm) : 3.71 (dd, 7H, 8.9/3.5 Hz, H^2) ; 3.93 (t, 7H, 8.9 Hz, H^4) ; 4.15 (d, 7H, 8.9 Hz, H^5) ; 4.29 (d, 7H, 11.5 Hz, H^{6a}) ; 4.54 (d, 7H, 11.5 Hz, H^{6b}) ; 4.64 (t, 7H, 8.9 Hz, H^3) ; 5.20 (d, 7H, 3.58 Hz, H^1).

^{13}C NMR (100 MHz, D_2O , 298K), δ (ppm) : 66.9 (C^6) ; 69.2 (C^5) ; 70.1 (C^2) ; 76.6 (C^4) ; 80.0 (C^3) ; 99.5 (C^1).

FT-IR : $\nu(\text{C}-\text{O} \text{ aliphatic})=1000 \text{ cm}^{-1}$; $\nu(\text{S}=\text{O})=1205 \text{ cm}^{-1}$; $\nu(\text{O}-\text{H})=3213 \text{ cm}^{-1}$.

MS ESI- : $m/z=764.90$ $[\text{M}+9\text{H}-12\text{Na}]^{3-}$; $m/z=772.23$ $[\text{M}+8\text{H}-11\text{Na}]^{3-}$; $m/z=779.56$ $[\text{M}+7\text{H}-10\text{Na}]^{3-}$; $m/z=786.88$ $[\text{M}+6\text{H}-9\text{Na}]^{3-}$.

M₇-rHTL **47**



$M = 1254,17 \text{ g}\cdot\text{mol}^{-1}$
 $\text{C}_{46}\text{H}_{79}\text{NO}_{36}\text{S}$

To a stirred solution of maltoheptaose (1 eq., 0.17 mmol, 200 mg) and homocysteine thiolactone hydrochloride (10 eq., 1.70 mmol, 261 mg) in a mixture of DMSO/AcOH 7/3 v/v (5.2 mL) was added sodium cyanoborohydride (30 eq., 5.10 mmol, 320 mg) portionwise at room temperature. The reaction mixture was heated and stirred at 65°C and was monitored by TLC (5/3/2 v/v/v EtOH/*n*-BuOH/ H_2O). After 5 hours, the reaction mixture was cooled down to room temperature and precipitated in an excess of ACN. The white suspension was centrifuged at 9000 g for 10 min at 4°C . The supernatant was discarded, and the pellet was triturated in ACN (50 mL), and centrifuged in the same conditions. This operation was repeated four times. The residue was redissolved in the minimum of H_2O (5 mL), precipitated once again in acetonitrile, and centrifuged in the same conditions as above. After

concentration and lyophilization of the residue, the pure product was obtained in the form of a white fluffy solid (212 mg, 0.17 mmol, 99%).

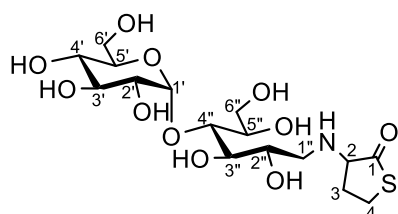
$^1\text{H NMR}$ (400 MHz, D_2O , 298K) δ (ppm) : 2.32 (m, 1H, H3a) ; 2.89 (m, 1H, H3b) ; 3.17-4.37 (m, 60H, H4, H $^{1''}$, 3 $''$, 4 $''$, 5 $''$, 6 $''$, 2 $''$, 3 $''$, 4 $''$, 5 $''$, 6 $''$, OH 2 , OH 3 , OH 4 , OH 5 & OH 6) 5.16 (bs, 1H, H $^{2''}$) ; 5.40 (bs, 6H, H $^{1'}$).

HRMS-ESI+ : calculated for $[\text{M}+\text{H}]^+$ $m/z=1254.41752$, found 1254.41834

FT-IR : $\nu(\text{OH})=3297\text{ cm}^{-1}$; $\nu(\text{C-H})=2926\text{ cm}^{-1}$; $\nu(\text{C=O})=1691\text{ cm}^{-1}$; $\nu(\text{C-N})=1148\text{ cm}^{-1}$; $\nu(\text{C-O, C-C \& C-OH})=1015\text{ cm}^{-1}$.

SEC-MALS: weight-average molar mass M_w of $1240 \pm 65\text{ g/mol}$.

M₂-rHTL 48



$M = 443.47\text{ g}\cdot\text{mol}^{-1}$
 $\text{C}_{16}\text{H}_{29}\text{NO}_{11}\text{S}$

Three methods possible for the synthesis of **48**, method A & B were used for small quantities, and method C for the scale-up :

[Method A] To a stirred solution of D-maltose (1 eq., 0.28 mmol, 100 mg) and homocysteine thiolactone hydrochloride (1 eq., 0.28 mmol, 43 mg) in DMSO/AcOH 7/3 v/v (2.7 mL) was added sodium cyanoborohydrate (8 eq., 2.24 mmol, 141 mg) in one portion at room temperature. The reaction mixture was heated and stirred at 65°C and the reaction was followed by TLC (eluent 7/3 v/v ACN/ H_2O). After 2h30, the reaction mixture was cooled down to room temperature and precipitated in ACN (100 mL). The white suspension was then centrifuged at 7000 g for 10 min. The supernatant was discarded and the pellet was triturated in ACN (50 mL) and centrifuged four times in the same conditions. The white precipitate was redissolved in H_2O (5 mL), concentrated and lyophilized to provide the pure product as a white fluffy solid (99 mg, 0.22 mmol, 80%).

[Method B] To a stirred solution of D-maltose (1 eq., 0.28 mmol, 100 mg) in a mixture of $\text{H}_2\text{O}/\text{MeOH}$ 1/1 v/v (1 mL) was added AcOH until the pH reached a value of 4-5. Homocysteine thiolactone hydrochloride (2 eq., 0.56 mmol, 86 mg) then sodium cyanoborohydrate (2 eq., 0.56 mmol, 35 mg) were added in one portion at room temperature. The colorless solution was heated at 80°C and the reaction was followed by TLC (7/3 v/v ACN/ H_2O). After 5 hours, the reaction mixture was cooled down to room temperature and precipitated in acetone (100 mL). The white suspension was centrifuged at 9000 g for 10 min at 4°C . The colorless supernatant was discarded and the pellet was redispersed in acetone (50 mL) to be centrifuged four times in the same conditions as above. The precipitate was redissolved in H_2O (5 mL), concentrated and lyophilized to provide the product as a white fluffy solid (122 mg, 0,27 mmol, 98%).

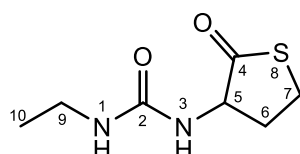
[Method C] To a stirred solution of D-maltose (1 eq., 11.1 mmol, 4 g) and homocysteine thiolactone hydrochloride (2 eq., 22.20 mmol, 3,41 g) in DMSO/AcOH 7/3 v/v (121 mL) was added sodium cyanoborohydrate (8 eq., 88.80 mmol, 5.580 g) in one portion at room temperature. The reaction mixture was heated at 65°C and the reaction was followed by TLC (eluent 7/3 v/v ACN/ H_2O). After 2h30, the reaction mixture was cooled down to room temperature and precipitated in an excess of ACN. The white suspension was then centrifuged at 9000 g for 10 min. The supernatant was discarded and the pellet was

trituated in ACN (250 mL) and centrifuged six times in the same conditions. The white precipitate was redissolved in H₂O (30 mL), concentrated and lyophilized to provide the pure product as a white fluffy solid (3.32 g, 7.50 mmol, 68%). According to SM ESI+, 7% of di-HTL side product **48a** present in this sample.

¹H NMR (400 MHz, D₂O, 298K) δ (ppm) : 2.16 (m, 1H, H^{3a}) ; 2.75 (m, 1H, H^{3b}) ; 3.05 (m, 2H, H⁴) ; 3.37-4.36 (m, 21H, H², H^{3''}, ^{4''}, ^{5''}, ^{6''}, ^{2'}, ^{3'}, ^{4'}, ^{5'}, ^{6'}, OH², OH³, OH⁴, OH⁵ & OH⁶) ; 4.78 (bs, 1H, H^{2''}) ; 5.14 (bs, 1H, H^{1'}).

HRMS-ESI+ : calculated for [M+H]⁺ m/z=444.15341 ; found 444.15332

1-ethyl-3-(2-oxotetrahydrothiophen-3-yl)urea (urea-HTL) **52**



M = 188.25 g.mol⁻¹
C₇H₁₂N₂O₂S

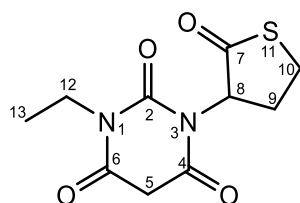
To a stirred solution of homocysteine thiolactone hydrochloride (1 eq., 3.25 mmol, 500 mg) in dry CH₂Cl₂ (0.1 M, 32 mL) at room temperature under nitrogen atmosphere was added ethyl isocyanate (1.1 eq., 3.58 mmol, 283 μL) dropwise and triethylamine (1.5 eq., 4.88 mmol, 678 μL). The reaction mixture was stirred overnight under nitrogen atmosphere at room temperature and was followed by TLC plates (eluent 95/5 v/v DCM/MeOH). When the reaction was finished, the mixture was washed with brine (30 mL). And the aqueous layer was extracted three times with CH₂Cl₂ (30 mL). The organic layers were assembled, dried with Na₂SO₄, filtered and concentrated under reduced pressure to give the urea intermediate, which was used without further purification.

¹H NMR (400MHz, CDCl₃, 298K), δ(ppm) : 1.12 (t, 3H, 7.2 Hz, H¹⁰) ; 1.92 (qd, 1H, 12.4/6.7 Hz, H^{6b}) ; 2.88 (td x2, 1H, 1.1/12.4 Hz, H^{6a}) ; 3.20 (q, 2H, 7.2 Hz, H⁹) ; 3.20 (m, 1H, H^{7b}) ; 3.32 (td, 1H, 11.7/5.3 Hz, H^{7a}) ; 4.42 (td x2, 1H, 12.4/1.1 Hz, H⁵) ; 4.68 (bs, 1H, NH¹) ; 4.98 (d, 1H, 1 Hz, NH³).

¹³C NMR (100MHz, CDCl₃, 298K), δ(ppm) : 15.5 (C¹⁰) ; 27.7 (C⁷) ; 33.1 (C⁶) ; 35.6 (C⁹) ; 60.7 (C⁵) ; 157.9 (C²) ; 207.6 (C⁴).

FT-IR : ν(C-S) = 1305 ou 1383 cm⁻¹ ; ν(C=O) = 1692 cm⁻¹ (thin pic) ; ν(CO-NH) = 2959 + 1560 cm⁻¹ ; ν(N-H) = 3302 + 1560 cm⁻¹.

1-ethyl-3-(2-oxotetrahydrothiophen-3-yl)pyrimidine-2-4-6-(1H,3H,5H)-trione (barbiturate-HTL) **53**



M = 256.28 g.mol⁻¹
C₁₀H₁₂N₂O₄S

To a stirred solution of urea-HTL **52** (1eq., 0.73 mmol, 138 mg) in dry CH₂Cl₂ (40 mL) at room temperature under nitrogen atmosphere was added malonyl chloride (1.1 eq., 0.80 mmol, 78 μL). The reaction mixture was stirred overnight and followed by TLC plates (eluent 7/3 v/v EtOAc/EtOH). When

the reaction was completed, the reaction mixture was concentrated and the product was purified by chromatography with a gradient from 10/0 to 7/3 v/v EtOAc/EtOH to give the final product (90%).

[Sequential One-Pot Reaction] To a stirred solution of homocysteine thiolactone hydrochloride (1 eq., 6.51 mmol, 1 g) in dry CH₂Cl₂ (65 mL) at room temperature under nitrogen atmosphere was added ethyl isocyanate (1.1 eq, 7.16 mmol, 567 μL) dropwise and triethylamine (1.5 eq., 9.76 mmol, 1.36 mL). The reaction mixture was stirred for 2 hours at room temperature under nitrogen atmosphere and was followed by TLC (eluent 95/5 v/v CH₂Cl₂/MeOH). If needed, ethyl isocyanate was added to complete the first step of the reaction. Then, malonyl chloride (1.1 eq., 7.16 mmol, 696 μL) and dry CH₂Cl₂ (290 mL) were added to the flask. The reaction mixture was stirred for 2 more hours and followed by TLC (eluent 7/3 v/v EtOAc/EtOH). When the reaction was completed, the reaction mixture was concentrated and the product was purified by chromatography with an isocratic elution of CH₂Cl₂ with 0.2% of AcOH to provide the final product as a yellowish solid (1.61 g, 6.28 mmol, 96%).

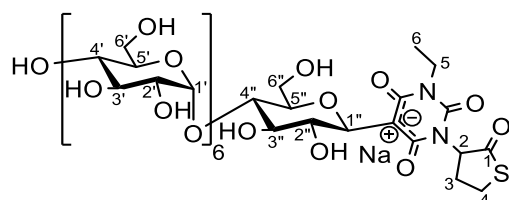
¹H NMR (400MHz, CDCl₃, 298K), δ(ppm) : 1.71 (t, 3H, 7.1 Hz, H¹³) ; 2.49 (tdd, 1H, 2.4/12.1 Hz, H^{10b}) ; 2.74 (ddd, 1H, 1/8.4/11.4/12.0 Hz, H^{10a}) ; 3.36 (m, 2H, 7.6/12.1 Hz, H⁹) ; 3.67 (s, 2H, H⁵) ; 3.89 (q, 2H, 7.1Hz, H¹²) ; 5.38 (dd, 1H, 7.6/12.1 Hz, H⁸).

¹³C NMR (100MHz, CDCl₃, 298K), δ(ppm) : 13.1 (C¹³) ; 26.8 (C¹⁰) ; 27.1 (C⁹) ; 37.5 (C¹²) ; 39.7 (C⁵) ; 60.3 (C⁸) ; 164.2 (C²) ; 202.7 (C⁷).

FT-IR : ν(C-S) = 1305 ou 1383 cm⁻¹ ; ν(C=O) = 1692 cm⁻¹ ; ν(CO-NH) = 2959 + 1560 cm⁻¹ ; ν(N-H) = 3302 + 1560 cm⁻¹.

HRMS - : calculated for [M-H]⁻ m/z=255.04340, found 255.04387.

M₇-bHTL **54**



M = 1413.24 g.mol⁻¹
C₅₂H₈₁N₂NaO₃₉S

To a stirred solution of maltoheptaose (1 eq., 2.70 mmol, 3.11 g) in a phosphate buffer (40 mL, pH 7.2, 0.1 M) was added barbiturate-HTL **53** (1 eq., 2.70 mmol, 693 mg). The reaction mixture was heated and stirred at 60°C to allow the barbiturate derivative to solubilize. The reaction was monitored by TLC (eluent 7/3 v/v ACN/H₂O). When the reaction was completed (after three days), the reaction mixture was concentrated with silica. The product was purified by chromatography with a gradient of 10/0 to 7/3 v/v ACN/H₂O, and was obtained, after lyophilization, in the form of a white solid (3.15 g, 2.23 mmol, 83%).

¹H NMR (400 MHz, D₂O, 298K) δ (ppm) : 1.13 (m, 3H, H⁶) ; 2.54 (m, 1H, H^{3a}) ; 2.69 (m, 1H, H^{3b}) ; 3.37-4.06 (m, 64H, H^{4,5}, H^{2',3',4',5',6',3'',4'',5'',6''}, OH², OH³, OH⁶, OH⁴) ; 4.36 (t, 1H, 8.9 Hz, H^{2''}) ; 4.53 (dd, 1H, 9.6/2.7 Hz, H^{1''}) ; 5.40 (d, 5H, 3.6 Hz, H^{1'}) ; 5.44 (d, 1H, 3.6 Hz, H^{1'?}) ; 5.53 (m, 0.5H, H²) ; 5.74 (m, 0.5H, H²).

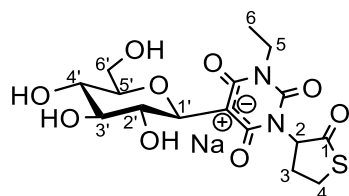
¹³C NMR (100 MHz, D₂O, 298K), δ(ppm) : 12.8 (C⁶) ; 27.6 (C³ & C⁴) ; 60.7 (C²) ; 60.4, 60.5, 69.3, 71.1, 71.2, 71.5, 71.6, 71.7, 72.7, 72.9, 73.3, 73.4, 76.7, 76.9, 77.1, 78.2, 78.6 (C^{2',3',4',5',6',2'',3'',4'',5'',6''}) ; 99.6 (C¹).

MS MALDI⁺ : m/z=1413.387 [M+H]⁺

FT-IR : $\nu(\text{OH})=3298 \text{ cm}^{-1}$; $\nu(\text{C-H})=2912 \text{ cm}^{-1}$; $\nu(\text{C=O HTL})= 1663 \text{ cm}^{-1}$; $\nu(\text{C=O barbiturate})= 1575 \text{ cm}^{-1}$; $\nu(\text{C-C, C-O, C-OH})=1021 \text{ cm}^{-1}$.

SEC-MALS: weight-average molar mass M_w of $1552 \pm 61 \text{ g/mol}$.

Glu-bHTL 54bis



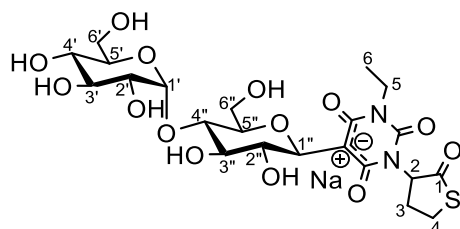
$M = 440.40 \text{ g.mol}^{-1}$
 $\text{C}_{16}\text{H}_{21}\text{N}_2\text{NaO}_9\text{S}$

To a stirred solution of D-glucose (1 eq., 0.96 mmol, 173 mg) in a phosphate buffer (14 mL, pH 7.2, 0.1 M) was added barbiturate-HTL 53 (1.1 eq., 1.06 mmol, 272 mg). The reaction mixture was heated and stirred at 80°C to allow the barbiturate derivative to solubilize. The reaction was monitored by TLC (eluent 8/2 v/v ACN/H₂O). When the reaction was completed (5 hours), the reaction mixture was concentrated with silica. The product was purified by chromatography with a gradient of 10/0 to 7/3 v/v ACN/H₂O and then by reverse chromatography with a gradient of 10/0 to 0/10 H₂O/MeOH, and was obtained, after lyophilization, in the form of a white fluffy solid (268 mg, 0.61 mmol, 63%).

$^1\text{H NMR}$ (400 MHz, D₂O, 298K) δ (ppm) : 1.12 (m, 3H, H⁶) ; 2.53 (bs, 1H, H^{3a}) ; 2.68 (m, 1H, H^{3b}) ; 3.37-3.60 (m, 5H, H⁴, H^{3'}, 4', 6') ; 3.72-3.93 (m, 4H, H⁵, H^{5'}, 6') ; 4.32 (t, 1H, 9.5 Hz, H^{2'}) ; 4.51 (dd, 1H, 9.5/2.6 Hz, H^{1'}) ; 5.53 (m, 0.5H, H²) ; 5.74 (m, 0.5H, H²).

SM ESI- : $m/z=417.0$ [M-Na]⁻

M₂-bHTL 54tris



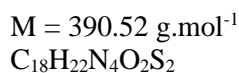
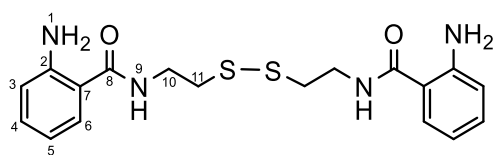
$M = 602.54 \text{ g.mol}^{-1}$
 $\text{C}_{22}\text{H}_{31}\text{N}_2\text{NaO}_{14}\text{S}$

To a stirred solution of D-maltose (1 eq., 0.55 mmol, 200 mg) in a phosphate buffer (8 mL, pH 7.2, 0.1 M) was added barbiturate-HTL 53 (1.1 eq., 0.61 mmol, 156 mg). The reaction mixture was heated and stirred at 80°C to allow the barbiturate derivative to solubilize. The reaction was monitored by TLC (eluent 7/3 v/v ACN/H₂O). When the reaction was completed (overnight), the reaction mixture was concentrated with silica. The product was purified by chromatography with a gradient of 10/0 to 7/3 v/v ACN/H₂O, and was obtained, after lyophilization, in the form of a yellowish fluffy solid (224 mg, 0.37 mmol, 68%).

$^1\text{H NMR}$ (400 MHz, D₂O, 298K) δ (ppm) : 1.10 (m, 3H, H⁶) ; 2.51 (bs, 1H, H^{3a}) ; 2.66 (m, 1H, H^{3b}) ; 3.34-3.92 (m, 14H, H^{4,5,2',3',4',5',6',3'',4'',5'',6''}) ; 4.33 (t, 1H, 9.5 Hz, H^{2''}) ; 4.50 (dd, 1H, 9.5/2.0 Hz, H^{1''}) ; 5.41 (d, 1H, 3.8 Hz, H^{1'}) ; 5.50 (m, 0.5H, H²) ; 5.71 (m, 0.5H, H²).

SM ESI- : $m/z=579.23$ [M-Na]⁻

N,N'-(disulfaneylbis(ethane-2,1-diyl))bis(2-aminobenzamide) (ASSA) **58**



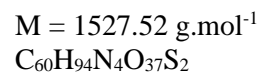
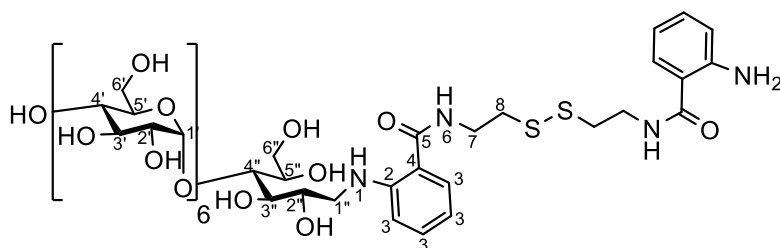
Cystamine dihydrochloride (1 eq., 8.87 mmol, 2 g) was dissolved in H₂O (240 mL) and a solution of NaOH (2 eq., 17.74 mmol, 709 mg, 0.15 M) in H₂O was added. The mixture was stirred for 1 hour and was then dried. The crude was dissolved in CH₂Cl₂ (30 mL) and was filtered through a Büchner with CH₂Cl₂ (100 mL) to remove the insoluble salts. The filtrate was dried to afford a yellowish liquid, cystamine free base, used without further purification. Cystamine free base was dissolved in THF (50 mL), and isatoic anhydride (2 eq., 17.74 mmol, 2.89 g) was added in one portion to the solution at room temperature. The formed brown suspension was heated at 60°C, allowing isatoic anhydride to solubilize, and was stirred overnight. The reaction was monitored by TLC (eluent 6/4 v/v EP/EtOAc). When the reaction was completed, the reaction mixture was dried to provide a sticky brown solid (3.52 g, quantitative yield), that was used without further purification.

¹H NMR (400 MHz, DMSO-d₆, 298K) δ (ppm) : 2.91 (t, 4H, 7.0 Hz, H¹¹) ; 3.51 (q, 4H, 6.4 Hz, H¹⁰) ; 6.39 (bs, 4H, NH¹) ; 6.50 (td, 2H, 7.5/1.2 Hz, H⁵) ; 6.68 (dd, 2H, 8.2/1.2 Hz, H³) ; 7.13 (td, 2H, 7.7/1.2 Hz, H⁴) ; 7.47 (dd, 2H, 7.8/1.2 Hz, H⁶) ; 8.36 (t, 2H, 5.5 Hz, NH⁶).

HRMS-ESI+: calculated for [M+H]⁺ m/z=391.12569, found 391.12575

FT-IR : ν(C-H aromatic) = 659 + 745 + 3051 cm⁻¹ ; ν(C-S) = 670 cm⁻¹ ; ν(C-N) = 1150 cm⁻¹ ; ν(N-H) = 1536 cm⁻¹ ; ν(primary amine) = 1539 + 3476 + 3360 cm⁻¹ ; ν(C=O amide) = 1624 cm⁻¹ ; ν(C-H aliphatic) = 2904 cm⁻¹ ; ν(substituted amide) = 3275 cm⁻¹.

M₇-rASSA **61**

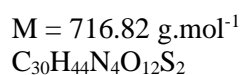
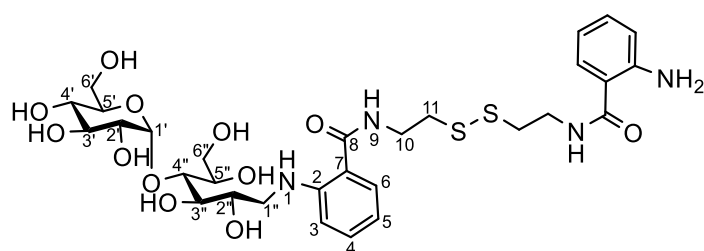


To a stirred solution of maltoheptaose (1 eq., 86.73 μmol, 100 mg) and ASSA **58** (10 eq., 0.87 mmol, 338 mg) in DMSO/AcOH 7/3 v/v (5 mL) was added sodium cyanoborohydrate (30 eq., 2.60 mmol, 163 mg) in one portion at room temperature. The brown suspension was heated to allow the anthranilic derivative to solubilize and the formed solution was stirred at 65°C. The reaction was followed by TLC (eluent 7/3 v/v ACN/H₂O). After 4 hours, the reaction mixture was cooled down to room temperature and precipitated in ACN (100 mL). The brown suspension was then centrifuged at 9000 g for 5 min. The supernatant was discarded and the pellet was triturated in ACN (40 mL) and centrifuged three times in the same conditions. The almost-white precipitate was redissolved in H₂O (10 mL), concentrated and lyophilized to provide the pure product as a grey fluffy solid (168 mg, 0.11 mmol, quantitative yield).

¹H NMR (400 MHz, D₂O, 298K) δ (ppm) : 3.02 (m, 6H, H⁷ & H⁸?) ; 3.37-4.25 (m, H², 3', 4', 5', 6', 2'', 3'', 4'', 5'', 6'') ; 5.03 (m, 1H, H¹'?) ; 5.37 (bs, 7H, H¹' & H¹'') ? ; 6.85 (m, 4H, H³) ; 7.40 (m, 4H, H³).

HRMS-ESI+: calculated for [M+Na]⁺ m/z=1549.49305, found 1549.49441

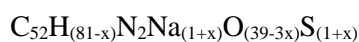
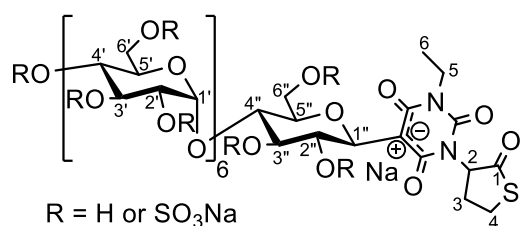
M₂-rASSA **63**



To a stirred solution of D-maltose (1 eq., 0.80 mmol, 288 mg) and ASSA **58** (10 eq., 8.05 mmol, 3.14 g) in DMSO/AcOH 7/3 v/v (10 mL) was added sodium cyanoborohydrate (30 eq., 24.15 mmol, 1.52 g) in one portion at room temperature. The brown suspension was heated and stirred at 65°C and the reaction was followed by TLC (eluent 8/2 v/v ACN/H₂O). After 2 hours, the reaction mixture was cooled down to room temperature and precipitated in ACN (150 mL). The suspension was then centrifuged at 9000 g for 5 min. The supernatant was discarded and the pellet was triturated in ACN (60 mL) and centrifuged three times in the same conditions. The almost-white precipitate was redissolved in H₂O (10 mL), concentrated and lyophilized to provide the pure product as a grey fluffy solid (435 mg, 0.61 mmol, 76%).

SM ESI⁺ : m/z=359.15 [M+2H]²⁺ ; m/z=541.17 [M'+K]²⁺ (symmetrical dimer, 15%) ; m/z=598.21 [maltose+K]⁺ (starting material, 11%) ; m/z=717.23 [M+H]⁺ (very major pic) ; m/z=1043.31 [M'+H]⁺ (symmetrical dimer).

Sulfated M₇-bHTL



R = H or SO₃Na

[Lightly sulfated] To a stirred solution of M₇-bHTL **54** (1 eq., 0.14 mmol, 200 mg) in DMF (3 mL) was added 2-methyl-2-butene (88 eq., 12.32 mmol, 1.3 mL) and sulfur trioxide pyridine complex (0.5 eq./OH, 1.54 mmol, 245 mg) at room temperature. The reaction mixture was heated at 30°C and stirred for 2 hours. After being cooled down, the reaction mixture was poured in a 5% solution of NaHCO_{3(aq)} (4 mL) and concentrated until dryness. The product was then purified by dialysis against H₂O and lyophilized to afford a white fluffy solid (193 mg).

¹H NMR (400 MHz, D₂O, 298K) δ (ppm) : 1.15 (m, 3H, H⁶) ; 2.56 (m, 1H, H^{3a}) ; 2.71 (m, 1H, H^{3b}) ; 3.37-4.70 (m, H^{4,5}, H^{2',3',4',5',6',2'',3'',4'',5'',6''}) ; 5.33-6.04 (m, 8H, 3.6 Hz, H^{1'} & H²).

FT-IR : ν(OH)=3408 cm⁻¹ ; ν(C=O HTL)= 1674 cm⁻¹ ; ν(C=O barbiturate)= 1583 cm⁻¹ ; ν(S=O)= 1216 cm⁻¹ ; ν(C-C, C-O, C-OH)=996 cm⁻¹.

SEC-MALS: weight-average molar mass M_w of 2233 ± 12 g/mol.

[Moderately sulfated] To a stirred solution of M₇-bHTL **54** (1 eq., 0.07 mmol, 100 mg) in DMF (2 mL) was added 2-methyl-2-butene (176 eq., 12.32 mmol, 1.3 mL) and sulfur trioxide pyridine complex (1 eq./OH, 1.54 mmol, 245 mg) at room temperature. The reaction mixture was heated at 30°C and stirred for 2 hours. After being cooled down, the reaction mixture was poured in a 5% solution of NaHCO_{3(aq)}

(4 mL) and concentrated until dryness. The product was then purified by dialysis against H₂O and lyophilized to afford a fluffy white solid (160 mg).

¹H NMR (400 MHz, D₂O, 298K) δ (ppm) : 1.15 (m, 3H, H⁶) ; 2.56 (m, 1H, H^{3a}) ; 2.71 (m, 1H, H^{3b}) ; 3.37-4.66 (m, H^{4,5}, H^{2',3',4',5',6',2'',3'',4'',5'',6''}) ; 5.33-6.04 (m, 8H, 3.6 Hz, H^{1'} & H²).

FT-IR : ν(OH)=3426 cm⁻¹ ; ν(C=O HTL)= 1677 cm⁻¹ ; ν(C=O barbiturate)= 1586 cm⁻¹ ; ν(S=O)= 1229 cm⁻¹ ; ν(C-C, C-O, C-OH)=998 cm⁻¹.

SEC-MALS: weight-average molar mass Mw of 2560 ± 110 g/mol.

[Highly sulfated] To a stirred solution of M₇-bHTL **54** (1 eq., 0.14 mmol, 200 mg) in DMF (6 mL) was added 2-methyl-2-butene (352 eq., 49.28 mmol, 5.2 mL) and sulfur trioxide pyridine complex (2 eq./OH, 6.16 mmol, 980 mg) at room temperature. The reaction mixture was heated at 30°C and stirred for 2h15. After being cooled down, the reaction mixture was poured in a 5% solution of NaHCO_{3(aq)} (16 mL) and concentrated until dryness. The product was then purified by dialysis against H₂O and lyophilized to afford a brown solid (117 mg).

¹H NMR (400 MHz, D₂O, 298K) δ (ppm) : 1.20 (bs, 3H, H⁶) ; 2.69 (m, 2H, H³) ; 3.40-4.72 (m, H^{4,5}, H^{2',3',4',5',6',2'',3'',4'',5'',6''}) ; 5.36-6.09 (m, 8H, 3.6 Hz, H^{1'} & H²).

FT-IR : ν(OH)=3426 cm⁻¹ ; ν(C=O HTL)= 1681 cm⁻¹ ; ν(C=O barbiturate)= 1591 cm⁻¹ ; ν(S=O)= 1223 cm⁻¹ ; ν(C-C, C-O, C-OH)=996 cm⁻¹.

SEC-MALS: weight-average molar mass Mw of 2839 ± 17 g/mol.

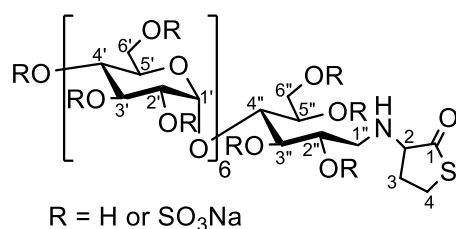
Sample M ₇ -bHTL	Mw		Mn		PDI (Mw/Mn)	
	Moy	±	Moy	±	Moy	±
Low	2233	12	1693	19	1.319	0.012
Medium	2560	110	1722	58	1.486	0.017
High	2839	17	2014	17	1.410	0.007

Table 24. SEC-MALS of sulfated M₇-bHTL. (Mw, Mn and Ip measured on triplicates, here the mean value Moy is given. Standard deviation “±” calculated with the triplicate measured values)

Sample M ₇ -bHTL	C [wt%]	H [wt%]	N [wt%]	S [wt%]	Degree of sulfation (DS)
Low	25.019	4.183	0.837	9.368	0.8
Medium	20.098	3.479	0.490	12.657	1.4
High	23.746	4.096	0.864	11.295	1.1

Table 25. Elemental analysis of sulfated M₇-bHTL

Sulfated M₇-rHTL



[RUR124 – Low DS] To a stirred solution of M₇-rHTL **47** (1 eq., 0.16 mmol, 200 mg) in DMF (2 mL) was added 2-methyl-2-butene (88 eq., 14.08 mmol, 1.5 mL) and sulfur trioxide pyridine complex (0.5 eq./OH, 1.76 mmol, 280 mg) at room temperature. The reaction mixture was heated at 30°C and stirred for 2 hours. After being cooled down, the reaction mixture was poured in a 5% solution of NaHCO_{3(aq)}

(5 mL) and concentrated until dryness. The product was then purified by dialysis against H₂O and lyophilized to afford a white fluffy solid (207 mg).

¹H NMR (400 MHz, D₂O, 298K) δ (ppm) : 2.24 (m, 1H, H^{3a}) ; 2.78 (m, 1H, H^{3b}) ; 3.10-4.57 (m, H⁴, H^{1''}, 3'', 4'', 5'', 6'', 2', 3', 4', 5', 6')

SEC-MALS: weight-average molar mass Mw of 2822 ± 11 g/mol.

[RUR292 – Medium DS] To a stirred solution of M₇-rHTL **47** (1 eq., 0.08 mmol, 100 mg) in dry DMF (5 mL) was added 2-methyl-2-butene (46 eq., 3.68 mmol, 390 μL) and sulfur trioxide pyridine complex (1 eq./OH, 1.84 mmol, 293 mg) at room temperature under nitrogen atmosphere. The reaction mixture was heated at 30°C and stirred overnight. After being cooled down, the reaction mixture was poured in H₂O (10 mL) and neutralized with NaHCO₃ until the pH reached a value of 9. The crude was then concentrated until dryness and purified by GPC to provide, after lyophilization, the pure product as a white fluffy solid (96 mg).

¹H NMR (400 MHz, D₂O, 298K) δ (ppm) : 2.34 (m, 1H, H^{3a}) ; 2.82 (m, 1H, H^{3b}) ; 3.45-5.10 (m, H⁴, H^{1''}, 3'', 4'', 5'', 6'', 2', 3', 4', 5', 6')

SEC-MALS: weight-average molar mass Mw of 3123 ± 147 g/mol.

[RUR291 – High DS] To a stirred solution of M₇-rHTL **47** (1 eq., 0.08 mmol, 100 mg) in dry DMF (5 mL) was added 2-methyl-2-butene (167 eq., 13.40 mmol, 1.95 mL) and sulfur trioxide pyridine complex (5 eq./OH, 9.20 mmol, 1.46 g) at room temperature under nitrogen atmosphere. The reaction mixture was heated at 30°C and stirred over the weekend. After being cooled down, the reaction mixture was poured in H₂O (10 mL) and neutralized with NaHCO₃ until the pH reached a value of 9. The crude was then concentrated until dryness and purified by GPC to provide, after lyophilization, the pure product as a white fluffy solid (77 mg).

¹H NMR (400 MHz, D₂O, 298K) δ (ppm) : 2.34 (m, 1H, H^{3a}) ; 2.80 (m, 1H, H^{3b}) ; 3.50-5.10 (m, H⁴, H^{1''}, 3'', 4'', 5'', 6'', 2', 3', 4', 5', 6')

SEC-MALS: weight-average molar mass Mw of 2516 ± 64 g/mol.

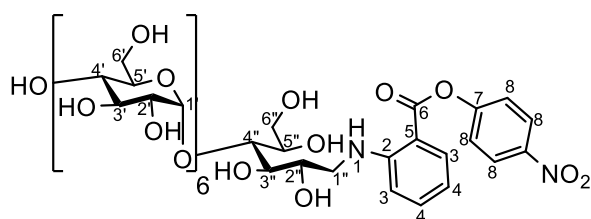
Sample M ₇ -rHTL	Mw		Mn		PDI (Mw/Mn)	
	Moy	±	Moy	±	Moy	±
Low	2822	11	2188	4.9	1.290	0.007
Medium	3123	147	2471	68	1.264	0.025
High	2516	64	1937	52	1.299	0.008

Table 26. SEC-MALS of sulfated M₇-rHTL. (Mw, Mn and Ip measured on triplicates, here the mean value Moy is given. Standard deviation “±” calculated with the triplicate measured values)

Sample M ₇ -rHTL	C [wt%]	H [wt%]	N [wt%]	S [wt%]	Degree of sulfation (DS)
Low	23.048	4.127	0.483	11.597	1.1
Medium	17.850	5.229	7.778	18.269	1.9
High	15.563	5.035	8.351	19.641	2.8

Table 27. Elemental analysis of sulfated M₇-rHTL

M₇-rAPNP 74



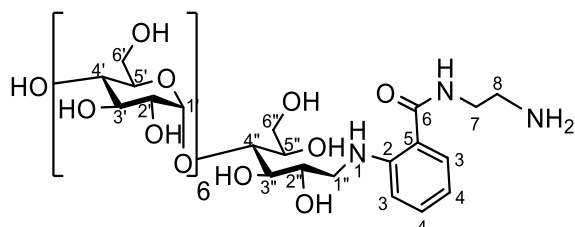
M = 1395.23 g.mol⁻¹
C₅₅H₈₂N₂O₃₉

To a stirred solution of maltoheptaose (1 eq., 0.87 mmol, 1 g) and 4-nitrophenyl anthranilate (10 eq., 8.67 mmol, 2.24 g) in DMSO/AcOH 7/3 v/v (26 mL) was added sodium cyanoborohydrate (30 eq., 26.01 mmol, 1.63 g) in one portion at room temperature. The fluorescent yellow solution was heated and stirred at 65°C. The reaction was followed by TLC (eluent 7/3 v/v ACN/H₂O). After 6 hours, the reaction mixture was cooled down to room temperature and precipitated in ACN (250 mL). The yellow suspension was then centrifuged at 9000 g for 5 min at 4°C. The supernatant was discarded and the pellet was triturated in ACN (100 mL) and centrifuged two times in the same conditions. The fluorescent yellow precipitate was redissolved in H₂O (10 mL), concentrated and purified by chromatography with a gradient of 10/0 to 7/3 v/v ACN/H₂O to remove the residual maltoheptaose. The pure product was obtained, after lyophilized, as a yellow solid (884 mg, 0.63 mmol, 84% based on conversion rate (58% if the reaction was finished, and conversion rate 69%).

¹H NMR (400 MHz, D₂O, 298K) δ (ppm) : 3.33-4.12 (m, H^{2'}, 3', 4', 5', 6', 2'', 3'', 4'', 5'', 6''); 5.12 (d, 2H, 3.8 Hz, H^{1''}); 5.37 (d, 6H, 3.8 Hz, H^{1'}); 6.77 (t, 1H, 7.6 Hz, H⁴); 6.95 (d, 1H, 8.7 Hz, H⁴); 7.43 (d, 2H, 8.7 Hz, H⁸); 7.56 (t, 1H, 7.6 Hz, H⁴); 8.10 (d, 1H, 7.6 Hz, H³); 8.32 (d, 2H, 8.7 Hz, H⁸).

SM ESI⁺ : m/z=717.19 [M+K]⁺ ; m/z=956.24 [2M+2K]³⁺ ; m/z=1066.27 [3M+2H+2K]⁴⁺ ; m/z=1414.84 [2M+K]²⁺.

M₇-rANH₂ 75



M = 1316.22 g.mol⁻¹
C₅₁H₈₅N₃O₃₆

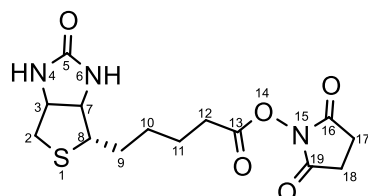
To a stirred solution of M₇-rAPNP (1 eq., 71.67 μmol, 100 mg) in dry DMF (1 mL) was added ethylenediamine (2 eq., 0.14 mmol, 10 μL) at room temperature. The reaction mixture was heated at 60°C and the reaction was followed by TLC (eluent 7/3 v/v ACN/H₂O). After 2 hours, the reaction was dried to obtain a fluorescent yellow residue. The residue was redissolved in H₂O, and precipitated in acetone (100 mL). The yellow suspension was filtered over a Büchner with acetone. The precipitate was recovered with H₂O, and the product was obtained, after lyophilization, as a yellow solid (98 mg, 71.67 μmol, quantitative yield).

¹H NMR (400 MHz, D₂O, 298K) δ (ppm) : 2.91-4.28 (m, H⁷, H⁸, H^{2'}, 3', 4', 5', 6', 2'', 3'', 4'', 5'', 6''); 5.13 (d, 2H, 3.9 Hz, H^{1''}); 5.41 (d, 6H, 3.9 Hz, H^{1'}); 6.83 (t, 1H, 7.6 Hz, H⁴); 6.95 (d, 1H, 8.4 Hz, H³); 7.46 (t, 1H, 7.6 Hz, H⁴); 7.53 (d, 1H, 7.6 Hz, H³).

¹³C NMR (100 MHz, D₂O, 298K), δ(ppm) : 37.3 (C⁷) ; 37.4 (C⁸) ; 58.1, 58.2, 59.9, 66.9, 67.1, 68.7, 69.0, 69.2, 69.3, 69.5, 70.2, 70.5, 70.7, 71.1, 74.6 (C^{2'}, 3', 4', 5', 6', 2'', 3'', 4'', 5'', 6''); 97.4 (C^{1'}) ; 98.0 (C^{1''}) ; 110.8 (C⁴) ; 114.8 (C³) ; 126.4 (C⁴) ; 131.0 (C³) ; 170.0 (C⁶).

SM MALDI+ : $m/z=1338.514 [M+Na]^+$

***N*-allyl-5-(2-oxohexahydro-1*H*-thieno[3,4-*d*]imidazole-4-yl)pentanamide (biotin-NHS) 78**



$M = 341.38 \text{ g.mol}^{-1}$
 $C_{14}H_{19}N_3O_5S$

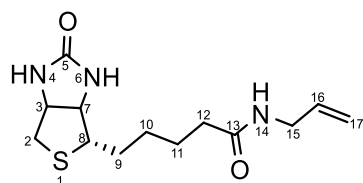
D(+)-biotin (1 eq., 16.37 mmol, 4 g) was dissolved in DMF (64 mL) by heating the flask at 80°C and was then cooled down to room temperature. *N*-hydroxysuccinimide (1.3 eq., 21.28 mmol, 2.44 g) and *N,N'*-dicyclohexylcarbodiimide (1.1 eq., 18.00 mmol, 3.71 g) were added, and the reaction solution was stirred at room temperature overnight. The reaction was monitored by TLC (eluent 75/25 v/v $CH_2Cl_2/MeOH$). When the reaction was completed, the mixture was filtered through celite with DMF (100 mL), and the filtrate was concentrated. The product was precipitated with the addition of Et_2O , and filtered over a Büchner with Et_2O extensively. The white precipitate was then washed with H_2O (2 x 20 mL), MeOH (2 x 20 mL) and cold *i*-PrOH (20 mL). The product was finally dried to provide a white solid (3.96 g, 11.62 mmol, 71%).

1H NMR (400 MHz, $DMSO-d_6$, 298K) δ (ppm) : 1.53 (m, 2H, H^9 , H^{10} & H^{11}) ; 2.58 (d, 1H, 12.3 Hz, H^{2a}) ; 2.67 (t, 2H, 7.4 Hz, H^{12}) ; 2.81 (t, 4H, 31.9 Hz, H^{17} & H^{18}) ; 2.83 (dd, 1H, 12.3/4.8 Hz, H^{2b}) ; 3.10 (m, 1H, H^8) ; 4.14 (m, 1H, H^7) ; 4.31 (m, 1H, H^3) ; 6.36 (bs, 1H, NH^4) ; 6.42 (bs, 1H, NH^6).

MS ESI+ : $m/z=342.15 [M+H]^+$; $m/z=380.12 [M+K]^+$; $m/z=683.37 [2M+H]^+$

FT-IR : $\nu(C=O) = 654 \text{ cm}^{-1}$; $\nu(C-N) = 1071 \text{ cm}^{-1}$; $\nu(C-O \text{ ester}) = 1211 \text{ cm}^{-1}$; $\nu(C=O) = 1696 \text{ cm}^{-1}$; $\nu(C-H) = 2938 \text{ cm}^{-1}$; $\nu(N-H \text{ amide}) = 3224 \text{ cm}^{-1}$.

***N*-allyl-5-(2-oxohexahydro-1*H*-thieno[3,4-*d*]imidazole-4-yl)pentanamide (biotin-allyl) 79**



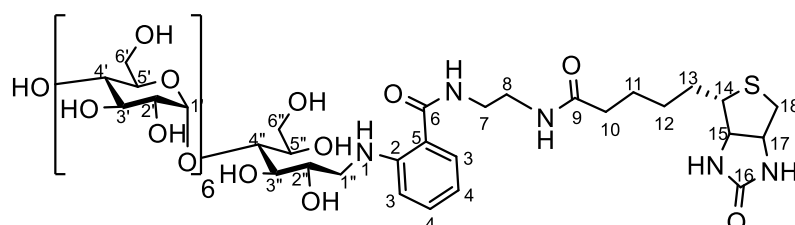
$M = 283.39 \text{ g.mol}^{-1}$
 $C_{13}H_{21}N_3O_2S$

D(+)-biotin (1 eq., 4.09 mmol, 1 g) was dissolved in DMF (16 mL) by heating the flask at 80°C and was then cooled down to room temperature. *N*-hydroxysuccinimide (1.3 eq., 5.32 mmol, 612 mg) and *N,N'*-dicyclohexylcarbodiimide (1.1 eq., 4.50 mmol, 928 mg) were added, and the reaction solution was stirred at room temperature overnight. The reaction was monitored by TLC (eluent 75/25 v/v $CH_2Cl_2/MeOH$). When the reaction was completed, the mixture was filtered through celite with DMF (80 mL), and the filtrate was concentrated until ≈ 20 mL were left. Then, allylamine (2 eq., 8.18 mmol, 614 μ L) and triethylamine (3 eq., 12.27 mmol, 1.71 mL) were added to the flask forming a milky solution, and the reaction mixture was stirred overnight. The reaction was followed by TLC (eluent 9/1 v/v ACN/ H_2O). When the reaction was finished, the reaction mixture was dried, redissolved in the minimum of MeOH, precipitated in Et_2O and filtered through a Büchner with Et_2O (100 mL). The precipitate, once dried, afforded a greyish solid (1.25 g, quantitative yield), that was used without further purification.

^1H NMR (400 MHz, DMSO- d_6 , 298K) δ (ppm) : 1.30 (m, 2H, H^{10}) ; 1.51 (m, 2H, H^{11}) ; 1.60 (m, 2H, H^9) ; 2.09 (t, 2H, 7.0 Hz, H^{12}) ; 2.57 (d, 1H, 12.3 Hz, H^{2a}) ; 2.82 (dd, 1H, 12.3/4.8 Hz, H^{2b}) ; 3.10 (td, 1H, 7.1/3.4 Hz, H^8) ; 3.67 (t, 2H, 5.4 Hz, H^{15}) ; 4.13 (m, 1H, H^7) ; 4.30 (t, 1H, 4.8 Hz, H^3) ; 5.08 (m, 2H, H^{17}) ; 5.78 (tdd, 1H, 10.9/5.4/1.1 Hz, H^{16}) ; 6.36 (bs, 1H, NH^4) ; 6.43 (bs, 1H, NH^6) ; 7.94 (bs, 1H, NH^{14}).

MS ESI+: $m/z=306.11$ [$\text{M}+\text{Na}$] $^+$; $m/z=589.21$ [$2\text{M}+\text{Na}$] $^+$

M₇-rANH-CO-biotin **90**



$M = 1542.51 \text{ g}\cdot\text{mol}^{-1}$
 $\text{C}_{61}\text{H}_{99}\text{N}_5\text{O}_{38}\text{S}$

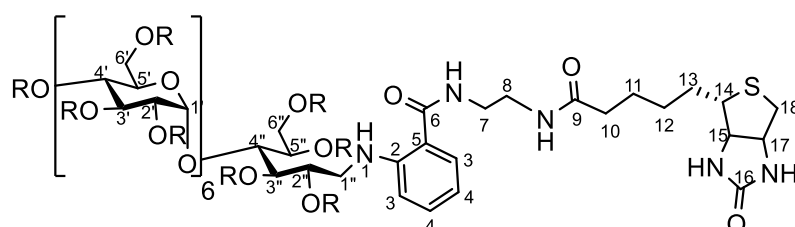
To a stirred solution of M₇-rANH₂ **75** (1 eq., 0.18 mmol, 236 mg) in a mixture of DMF/H₂O 1/1 v/v (6 mL) was added triethylamine (1 eq., 0.18 mmol, 25 μL) and biotin-NHS (2 eq., 0.36 mmol, 122 mg). The reaction mixture was stirred at room temperature for 30 min, and was monitored by TLC (eluent 7/3 v/v ACN/H₂O). Then, the reaction mixture was mixed with silica and concentrated until dryness. The crude was purified by chromatography with a gradient of 10/0 to 7/3 v/v ACN/H₂O to afford, after lyophilization, the pure product as a white solid (193 mg, 0.13 mmol, 69%).

^1H NMR (400 MHz, D₂O, 298K) δ (ppm) : 1.23-1.67 (m, 6H, H^{11} , H^{12} & H^{13}) ; 2.27 (t, 2H, 6.9 Hz, H^{10}) ; 2.70 (d, 1H, 12.8 Hz, H^{18a}) ; 2.86 (dd, 1H, 13.3/5.0 Hz, H^{18b}) ; 2.90 (m, 1H, H^{14}) ; 3.26-4.07 (m, $\text{H}^{2'}$, $3'$, $4'$, $5'$, $6'$, $2''$, $3''$, $4''$, $5''$, $6''$) ; 4.12 (m, 1H, H^{15}) ; 4.48 (m, 1H, H^{17}) ; 5.13 (d, 2H, 3.7 Hz, $\text{H}^{1''}$) ; 5.39 (d, 6H, 3.5 Hz, $\text{H}^{1'}$) ; 6.81 (t, 1H, 7.3 Hz, H^4) ; 6.92 (d, 1H, 8.3 Hz, H^3) ; 7.43 (d, 1H, 7.6 Hz, H^4) ; 7.47 (d, 1H, 7.6 Hz, H^3).

^{13}C NMR (100 MHz, D₂O, 298K), δ (ppm) : 25.2 (C^{11}) ; 27.7 (C^{12} & C^{13}) ; 35.6 (C^{10}) ; 38.6 (C^7) ; 38.8 (C^8) ; 39.7 (C^{18}) ; 55.0 (C^{14}) ; 60.2 (C^{17}) ; 61.8 (C^{15}) ; 45.7, 60.3, 60.4, 62.2, 69.1, 69.3, 71.0, 71.2, 71.4, 71.6, 71.7, 72.4, 72.7, 72.9, 73.3, 76.8, 77.1, 77.2, 77.3, 82.2 ($\text{C}^{2'}$, $3'$, $4'$, $5'$, $6'$, $2''$, $3''$, $4''$, $5''$, $6''$) ; 99.7 ($\text{C}^{1'}$) ; 100.4 ($\text{C}^{1''}$) ; 112.7 (C^3) ; 116.7 (C^4) ; 117.4 (C^5) ; 128.7 (C^4) ; 133.2 (C^3) ; 147.9 (C^2) ; 165.2 (C^{16}) ; 171.7 (C^6) ; 177.1 (C^9).

HRMS-ESI+ : calculated for [$\text{M}+\text{H}$] $^+$ $m/z=1542.57615$, found 1542.57801

Sulfated M₇-rANH-CO-biotin



$\text{C}_{61}\text{H}_{(99-x)}\text{N}_5\text{Na}_x\text{O}_{(38+3x)}\text{S}_{(1+x)}$

R = H or SO_3Na

[Moderately sulfated] To a stirred solution of M₇-rANH-CO-biotin **90** (1 eq., 0.032 mmol, 50 mg) in dry pyridine (2 mL) was added sulfur trioxide pyridine complex (1 eq./OH, 0.746 mmol, 119 mg) in one portion under nitrogen atmosphere. The reaction mixture was stirred at 60°C for 24h. The crude was poured in water and neutralized with the portionwise addition of NaHCO_3 until the pH reached 9. The crude was then dried and purified by GPC to afford, after lyophilization, a beige solid (35 mg).

^1H NMR (400 MHz, D_2O , 298K) δ (ppm) : 1.12-1.79 (m, 6H, H^{11} , H^{12} & H^{13}) ; 2.28 (sl, 2H, H^{10}) ; 2.66-3.00 (m, 2H, H^{18}) ; 3.32-4.80 ($\text{H}^{2',3',4',5',6',1'',2'',3'',4'',5'',6''}$, H^{15} , H^{17}) ; 5.41-6.07 (m, 6H, $\text{H}^{1'}$) ; 6.79 (m, 1H, H^4) ; 7.04 (m, 1H, H^3) ; 7.44 (m, 2H, H^3 & H^4).

[Highly sulfated] To a stirred solution of $\text{M}_7\text{-rANH-CO-biotin}$ **90** (1 eq., 0.032 mmol, 50 mg) in dry pyridine (2 mL) was added sulfur trioxide pyridine complex (5 eq./OH, 3.728 mmol, 593 mg) in one portion under nitrogen atmosphere. The reaction mixture was stirred at 60°C for 20h. The crude was poured in water and neutralized with the portionwise addition of NaHCO_3 until the pH reached 9. The crude was then dried and purified by GPC to afford, after lyophilization, a beige solid (70 mg).

^1H NMR (400 MHz, D_2O , 298K) δ (ppm) : 1.09-1.98 (m, 6H, H^{11} , H^{12} & H^{13}) ; 2.30 (sl, 2H, H^{10}) ; 2.98-3.30 (m, 2H, H^{18}) ; 3.32-4.80 ($\text{H}^{2',3',4',5',6',1'',2'',3'',4'',5'',6''}$, H^{15} , H^{17}) ; 5.41-6.07 (m, 6H, $\text{H}^{1'}$) ; 6.79 (m, 1H, H^4) ; 7.06 (m, 1H, H^3) ; 7.46 (m, 2H, H^3 & H^4).

References

1. Merceron C, Portron S, Vignes-Colombeix C, et al. Pharmacological Modulation of Human Mesenchymal Stem Cell Chondrogenesis by a Chemically Oversulfated Polysaccharide of Marine Origin: Potential Application to Cartilage Regenerative Medicine. *STEM CELLS*. 2012;30(3):471-480. doi:10.1002/stem.1686
2. Alexander PG, Gottardi R, Lin H, Lozito TP, Tuan RS. Three-dimensional osteogenic and chondrogenic systems to model osteochondral physiology and degenerative joint diseases. *Exp Biol Med Maywood NJ*. 2014;239(9):1080-1095. doi:10.1177/1535370214539232
3. Chen FH, Rousche KT, Tuan RS. Technology Insight: adult stem cells in cartilage regeneration and tissue engineering. *Nat Clin Pract Rheumatol*. 2006;2(7):373-382. doi:10.1038/ncprheum0216
4. Zamli Z, Sharif M. Chondrocyte apoptosis: a cause or consequence of osteoarthritis? *Int J Rheum Dis*. 2011;14(2):159-166. doi:10.1111/j.1756-185X.2011.01618.x
5. Musumeci G, Aiello FC, Szychlinska MA, Di Rosa M, Castrogiovanni P, Mobasher A. Osteoarthritis in the XXIst Century: Risk Factors and Behaviours that Influence Disease Onset and Progression. *Int J Mol Sci*. 2015;16(3):6093-6112. doi:10.3390/ijms16036093
6. Sandell LJ, Aigner T. Articular cartilage and changes in Arthritis: Cell biology of osteoarthritis. *Arthritis Res Ther*. 2001;3(2):107. doi:10.1186/ar148
7. Rizkalla G, Reiner A, Bogoch E, Poole AR. Studies of the articular cartilage proteoglycan aggrecan in health and osteoarthritis. Evidence for molecular heterogeneity and extensive molecular changes in disease. *J Clin Invest*. 1992;90(6):2268-2277. doi:10.1172/JCI116113
8. Joint Replacements & Osteoarthritis - Max Superspecialty Ortho Clinic. Accessed October 17, 2020. <http://www.orthohyd.com/hip-knee-replacements-1>
9. Reynard LN, Loughlin J. Genetics and epigenetics of osteoarthritis. *Maturitas*. 2012;71(3):200-204. doi:10.1016/j.maturitas.2011.12.001
10. Ramos YFM, Hollander W den, Bovée JVMG, et al. Genes Involved in the Osteoarthritis Process Identified through Genome Wide Expression Analysis in Articular Cartilage; the RAAK Study. *PLOS ONE*. 2014;9(7):e103056. doi:10.1371/journal.pone.0103056
11. Veronese N, Stubbs B, Solmi M, et al. Association between lower limb osteoarthritis and incidence of depressive symptoms: data from the osteoarthritis initiative. *Age Ageing*. 2017;46(3):470-476. doi:10.1093/ageing/afw216
12. Vina ER, Kwok CK. Epidemiology of osteoarthritis: literature update. *Curr Opin Rheumatol*. 2018;30(2):160–167. doi:10.1097/BOR.0000000000000479
13. Murray CJL, Lopez AD, Organization WH, Bank W, Health HS of P. *The Global Burden of Disease : A Comprehensive Assessment of Mortality and Disability from Diseases, Injuries, and*

- Risk Factors in 1990 and Projected to 2020 : Summary.* World Health Organization; 1996. Accessed October 17, 2020. <https://apps.who.int/iris/handle/10665/41864>
14. WHO Scientific Group on the Burden of Musculoskeletal Conditions at the Start of the New Millennium. (2003 : Geneva S. *The Burden of Musculoskeletal Conditions at the Start of the New Millennium : Report of a WHO Scientific Group.* Geneve : World Health Organization; 2003. Accessed October 6, 2020. <https://apps.who.int/iris/handle/10665/42721>
 15. Felson DT, Zhang Y. An update on the epidemiology of knee and hip osteoarthritis with a view to prevention. *Arthritis Rheum.* 1998;41(8):1343-1355. doi:10.1002/1529-0131(199808)41:8<1343::AID-ART3>3.0.CO;2-9
 16. Allman-Farinelli MA, Aitken RJ, King LA, Bauman AE. Osteoarthritis — the forgotten obesity-related epidemic with worse to come. *Med J Aust.* 2008;188(5):317. doi:10.5694/j.1326-5377.2008.tb01634.x
 17. Valdes AM, Stocks J. Osteoarthritis and Ageing. *European Medical Journal.* Published March 1, 2018. Accessed October 17, 2020. <https://www.emjreviews.com/rheumatology/article/osteoarthritis-and-ageing/>
 18. Quintana R, Silvestre AMR, Goñi M, et al. Prevalence of musculoskeletal disorders and rheumatic diseases in the indigenous Qom population of Rosario, Argentina. *Clin Rheumatol.* 2016;35(1):5-14. doi:10.1007/s10067-016-3192-2
 19. Del Río Nájera D, Santana N, Peláez-Ballestas I, González-Chávez SA, Quiñonez-Flores CM, Pacheco-Tena C. Prevalence of rheumatic diseases in Raramuri people in Chihuahua, Mexico: a community-based study. *Clin Rheumatol.* 2016;35(1):43-52. doi:10.1007/s10067-016-3225-x
 20. Lee S, Kim S-J. Prevalence of knee osteoarthritis, risk factors, and quality of life: The Fifth Korean National Health And Nutrition Examination Survey. *Int J Rheum Dis.* 2017;20(7):809-817. doi:10.1111/1756-185X.12795
 21. Pal CP, Singh P, Chaturvedi S, Pruthi KK, Vij A. Epidemiology of knee osteoarthritis in India and related factors. *Indian J Orthop.* 2016;50(5):518-522. doi:10.4103/0019-5413.189608
 22. Kodama R, Muraki S, Oka H, et al. Prevalence of hand osteoarthritis and its relationship to hand pain and grip strength in Japan: The third survey of the ROAD study. *Mod Rheumatol.* 2016;26(5):767-773. doi:10.3109/14397595.2015.1130673
 23. Davatchi F, Sandoughi M, Moghimi N, et al. Epidemiology of rheumatic diseases in Iran from analysis of four COPCORD studies. *Int J Rheum Dis.* 2016;19(11):1056-1062. doi:10.1111/1756-185X.12809
 24. Le Pen C, Reygrobelle C, Gérentes I. Financial cost of osteoarthritis in France: The “COART” Study. *Joint Bone Spine.* 2005;72(6):567-570. doi:10.1016/j.jbspin.2005.01.011
 25. Stitik TP, Altschuler E, Foye PM. Pharmacotherapy of Osteoarthritis. *Am J Phys Med Rehabil.* 2006;85(11):S15. doi:10.1097/01.phm.0000245512.85085.a0
 26. Mobasheri A, Kalamegam G, Musumeci G, Batt ME. Chondrocyte and mesenchymal stem cell-based therapies for cartilage repair in osteoarthritis and related orthopaedic conditions. *Maturitas.* 2014;78(3):188-198. doi:10.1016/j.maturitas.2014.04.017

27. Pomin VH, Mulloy B. Glycosaminoglycans and Proteoglycans. *Pharmaceuticals*. 2018;11(1):27. doi:10.3390/ph11010027
28. Chevalier F. Les glycosaminoglycane : implication dans la régénération tissulaire après ischémie et utilisation de mimétiques comme agents potentialisateurs des progéniteurs endothéliaux humains pour la régénération vasculaire. Published online September 30, 2013. Accessed October 17, 2020. <http://www.theses.fr/2013PEST0104>
29. Weyers A, Linhardt RJ. Neoproteoglycans in tissue engineering. *FEBS J*. 2013;280(10):2511-2522. doi:10.1111/febs.12187
30. Whitelock JM, Melrose J, Iozzo RV. Diverse Cell Signaling Events Modulated by Perlecan. *Biochemistry*. 2008;47(43):11174-11183. doi:10.1021/bi8013938
31. Kjellén L, Lindahl U. Proteoglycans: Structures and Interactions. *Annu Rev Biochem*. 1991;60(1):443-475. doi:10.1146/annurev.bi.60.070191.002303
32. Lindahl U, Couchman J, Kimata K, Esko JD. Proteoglycans and Sulfated Glycosaminoglycans. In: Varki A, Cummings RD, Esko JD, et al., eds. *Essentials of Glycobiology*. 3rd ed. Cold Spring Harbor Laboratory Press; 2015. Accessed October 8, 2020. <http://www.ncbi.nlm.nih.gov/books/NBK453033/>
33. Mihov D, Spiess M. Glycosaminoglycans: Sorting determinants in intracellular protein traffic. *Int J Biochem Cell Biol*. 2015;68:87-91. doi:10.1016/j.biocel.2015.08.019
34. Varki A, Cummings R, Esko J, Freeze H, Hart G, Marth J. Proteoglycans and Glycosaminoglycans. In: *Essentials of Glycobiology*. Cold Spring Harbor Laboratory Press; 1999:229–248. Accessed October 5, 2020. <https://www.ncbi.nlm.nih.gov/books/NBK20693/>
35. Davis BG. Recent developments in glycoconjugates. *J Chem Soc Perkin 1*. 1999;(22):3215-3237. doi:10.1039/A809773I
36. Varki A. Biological roles of oligosaccharides: all of the theories are correct. *Glycobiology*. 1993;3(2):97-130. doi:10.1093/glycob/3.2.97
37. Villadsen K, Martos-Maldonado MC, Jensen KJ, Thygesen MB. Chemoselective Reactions for the Synthesis of Glycoconjugates from Unprotected Carbohydrates. *ChemBioChem*. 2017;18(7):574-612. doi:10.1002/cbic.201600582
38. Almond A, Sheehan JK. Glycosaminoglycan conformation: do aqueous molecular dynamics simulations agree with x-ray fiber diffraction? *Glycobiology*. 2000;10(3):329-338. doi:10.1093/glycob/10.3.329
39. Rodríguez-Carvajal MA, Imberty A, Pérez S. Conformational behavior of chondroitin and chondroitin sulfate in relation to their physical properties as inferred by molecular modeling. *Biopolymers*. 2003;69(1):15-28. doi:10.1002/bip.10304
40. Li J-P, Kusche-Gullberg M. Chapter Six - Heparan Sulfate: Biosynthesis, Structure, and Function. In: Jeon KW, ed. *International Review of Cell and Molecular Biology*. Vol 325. International Review of Cell and Molecular Biology. Academic Press; 2016:215-273. doi:10.1016/bs.ircmb.2016.02.009

41. Habuchi H, Habuchi O, Kimata K. Sulfation pattern in glycosaminoglycan: Does it have a code? *Glycoconj J*. 2004;21(1):47-52. doi:10.1023/B:GLYC.0000043747.87325.5e
42. Martinez P, Denys A, Delos M, et al. Macrophage polarization alters the expression and sulfation pattern of glycosaminoglycans. *Glycobiology*. 2015;25(5):502-513. doi:10.1093/glycob/cwu137
43. Zong C, Venot A, Li X, et al. Heparan Sulfate Microarray Reveals That Heparan Sulfate–Protein Binding Exhibits Different Ligand Requirements. *J Am Chem Soc*. 2017;139(28):9534-9543. doi:10.1021/jacs.7b01399
44. Gama CI, Tully SE, Sotogaku N, et al. Sulfation patterns of glycosaminoglycans encode molecular recognition and activity. *Nat Chem Biol*. 2006;2(9):467-473. doi:10.1038/nchembio810
45. Imberty A, Lortat-Jacob H, Pérez S. Structural view of glycosaminoglycan–protein interactions. *Carbohydr Res*. 2007;342(3):430-439. doi:10.1016/j.carres.2006.12.019
46. Paluck SJ, Nguyen TH, Maynard HD. Heparin-Mimicking Polymers: Synthesis and Biological Applications. *Biomacromolecules*. 2016;17(11):3417-3440. doi:10.1021/acs.biomac.6b01147
47. Mehta AY, Cummings RD. GlycoGlyph: a glycan visualizing, drawing and naming application. *Bioinformatics*. 2020;36(11):3613-3614. doi:10.1093/bioinformatics/btaa190
48. Smith RAA, Meade K, Pickford CE, Holley RJ, Merry CLR. Glycosaminoglycans as regulators of stem cell differentiation. *Biochem Soc Trans*. 2011;39(1):383-387. doi:10.1042/BST0390383
49. Huynh MB, Villares J, Sepúlveda Díaz JE, et al. Glycosaminoglycans from aged human hippocampus have altered capacities to regulate trophic factors activities but not A β 42 peptide toxicity. *Neurobiol Aging*. 2012;33(5):1005.e11-1005.e22. doi:10.1016/j.neurobiolaging.2011.09.030
50. Salbach J, Rachner TD, Rauner M, et al. Regenerative potential of glycosaminoglycans for skin and bone. *J Mol Med*. 2012;90(6):625-635. doi:10.1007/s00109-011-0843-2
51. Ishihara M, Tyrrell DJ, Stauber GB, Brown S, Cousens LS, Stack RJ. Preparation of affinity-fractionated, heparin-derived oligosaccharides and their effects on selected biological activities mediated by basic fibroblast growth factor. *J Biol Chem*. 1993;268(7):4675-4683.
52. Urban JPG, Hall AC, Gehl KA. Regulation of matrix synthesis rates by the ionic and osmotic environment of articular chondrocytes. *J Cell Physiol*. 1993;154(2):262-270. doi:10.1002/jcp.1041540208
53. Linhardt RJ, Toida T. Role of Glycosaminoglycans in Cellular Communication. *Acc Chem Res*. 2004;37(7):431-438. doi:10.1021/ar030138x
54. Iozzo RV, Karamanos N. Proteoglycans in health and disease: emerging concepts and future directions. *FEBS J*. 2010;277(19):3863-3863. doi:10.1111/j.1742-4658.2010.07796.x
55. Theocharis AD, Skandalis SS, Tzanakakis GN, Karamanos NK. Proteoglycans in health and disease: novel roles for proteoglycans in malignancy and their pharmacological targeting. *FEBS J*. 2010;277(19):3904-3923. doi:10.1111/j.1742-4658.2010.07800.x

56. Ruoslahti E, Yamaguchi Y. Proteoglycans as modulators of growth factor activities. *Cell*. 1991;64(5):867-869. doi:10.1016/0092-8674(91)90308-L
57. Kato S, Ishii T, Hara H, Sugiura N, Kimata K, Akamatsu N. Hepatocyte Growth Factor Immobilized onto Culture Substrates through Heparin and Matrigel Enhances DNA Synthesis in Primary Rat Hepatocytes. *Exp Cell Res*. 1994;211(1):53-58. doi:10.1006/excr.1994.1058
58. Madihally SV, Flake AW, Matthew HWT. Maintenance of CD34 Expression During Proliferation of CD34+ Cord Blood Cells on Glycosaminoglycan Surfaces. *STEM CELLS*. 1999;17(5):295-305. doi:10.1002/stem.170295
59. Aviezer D, Levy E, Safran M, et al. Differential structural requirements of heparin and heparan sulfate proteoglycans that promote binding of basic fibroblast growth factor to its receptor. *J Biol Chem*. 1994;269(1):114-121.
60. Yayon A, Klagsbrun M, Esko JD, Leder P, Ornitz DM. Cell surface, heparin-like molecules are required for binding of basic fibroblast growth factor to its high affinity receptor. *Cell*. 1991;64(4):841-848. doi:10.1016/0092-8674(91)90512-W
61. Barbucci R, Magnani A, Rappuoli R, Lamponi S, Consumi M. Immobilisation of sulphated hyaluronan for improved biocompatibility. *J Inorg Biochem*. 2000;79(1):119-125. doi:10.1016/S0162-0134(00)00007-6
62. van der Smissen A, Hintze V, Scharnweber D, et al. Growth promoting substrates for human dermal fibroblasts provided by artificial extracellular matrices composed of collagen I and sulfated glycosaminoglycans. *Biomaterials*. 2011;32(34):8938-8946. doi:10.1016/j.biomaterials.2011.08.025
63. Köhling S, Blaszkiewicz J, Ruiz-Gómez G, et al. Syntheses of defined sulfated oligohyaluronans reveal structural effects, diversity and thermodynamics of GAG–protein binding. *Chem Sci*. 2019;10(3):866-878. doi:10.1039/C8SC03649G
64. Gandhi NS, Mancera RL. The Structure of Glycosaminoglycans and their Interactions with Proteins. *Chem Biol Drug Des*. 2008;72(6):455-482. doi:10.1111/j.1747-0285.2008.00741.x
65. Lindahl U, Bäckström G, Thunberg L, Leder IG. Evidence for a 3-O-sulfated D-glucosamine residue in the antithrombin-binding sequence of heparin. *Proc Natl Acad Sci*. 1980;77(11):6551-6555. doi:10.1073/pnas.77.11.6551
66. Atha DH, Lormeau JC, Petitou M, Rosenberg RD, Choay J. Contribution of monosaccharide residues in heparin binding to antithrombin III. *Biochemistry*. 1985;24(23):6723-6729. doi:10.1021/bi00344a063
67. Capila I, Linhardt RJ. Heparin–Protein Interactions. *Angew Chem Int Ed*. 2002;41(3):390-412. doi:10.1002/1521-3773(20020201)41:3<390::AID-ANIE390>3.0.CO;2-B
68. Rapraeger AC, Krufka A, Olwin BB. Requirement of heparan sulfate for bFGF-mediated fibroblast growth and myoblast differentiation. *Science*. 1991;252(5013):1705-1708. doi:10.1126/science.1646484
69. Guimond S, Maccarana M, Olwin BB, Lindahl U, Rapraeger AC. Activating and inhibitory heparin sequences for FGF-2 (basic FGF). Distinct requirements for FGF-1, FGF-2, and FGF-4. *J Biol Chem*. 1993;268(32):23906-23914.

70. Ishihara M, Takano R, Kanda T, et al. Importance of 6-O-Sulfate Groups of Glucosamine Residues in Heparin for Activation of FGF-1 and FGF-2. *J Biochem (Tokyo)*. 1995;118(6):1255-1260. doi:10.1093/oxfordjournals.jbchem.a125015
71. Seffouh A, Milz F, Przybylski C, et al. HSulf sulfatases catalyze processive and oriented 6-O-desulfation of heparan sulfate that differentially regulates fibroblast growth factor activity. *FASEB J*. 2013;27(6):2431-2439. doi:10.1096/fj.12-226373
72. Frescaline G, Boudierlique T, Huynh MB, Papy-Garcia D, Courty J, Albanese P. Glycosaminoglycans mimetics potentiate the clonogenicity, proliferation, migration and differentiation properties of rat mesenchymal stem cells. *Stem Cell Res*. 2012;8(2):180-192. doi:10.1016/j.scr.2011.09.005
73. Ferdous Z, Grande-Allen KJ. Utility and Control of Proteoglycans in Tissue Engineering. *Tissue Eng*. 2007;13(8):1893-1904. doi:10.1089/ten.2006.0056
74. Geutjes PJ, Daamen WF, Buma P, Feitz WF, Faraj KA, van Kuppevelt TH. From Molecules to Matrix: Construction and Evaluation of Molecularly Defined Bioscaffolds. In: Fisher JP, ed. *Tissue Engineering*. Advances in Experimental Medicine and Biology. Springer US; 2007:279-295.
75. Mucci A, Schenetti L, Volpi N. ¹H and ¹³C nuclear magnetic resonance identification and characterization of components of chondroitin sulfates of various origin. *Carbohydr Polym*. 2000;41(1):37-45. doi:10.1016/S0144-8617(99)00075-2
76. Pummill PE, Brown SH. Recombinant Production of Hyaluronic Acid. *Curr Pharm Biotechnol*. 2008;9(4):239-241.
77. Casper CL, Yang W, Farach-Carson MC, Rabolt JF. Coating Electrospun Collagen and Gelatin Fibers with Perlecan Domain I for Increased Growth Factor Binding. *Biomacromolecules*. 2007;8(4):1116-1123. doi:10.1021/bm061003s
78. Yang W d., Gomes R r., Alicknavitch M, Farach-Carson M c., Carson D d. Perlecan Domain I Promotes Fibroblast Growth Factor 2 Delivery in Collagen I Fibril Scaffolds. *Tissue Eng*. 2005;11(1-2):76-89. doi:10.1089/ten.2005.11.76
79. Yang W, Gomes RR, Brown AJ, et al. Chondrogenic Differentiation on Perlecan Domain I, Collagen II, and Bone Morphogenetic Protein-2–Based Matrices. *Tissue Eng*. 2006;12(7):2009-2024. doi:10.1089/ten.2006.12.2009
80. Mende M, Bednarek C, Wawryszyn M, et al. Chemical Synthesis of Glycosaminoglycans. *Chem Rev*. 2016;116(14):8193-8255. doi:10.1021/acs.chemrev.6b00010
81. Tabata Y. Biomaterial technology for tissue engineering applications. *J R Soc Interface*. 2009;6(Suppl 3):S311-S324. doi:10.1098/rsif.2008.0448.focus
82. Mauzac M, Jozefonvicz J. Anticoagulant activity of dextran derivatives. Part I: Synthesis and characterization. *Biomaterials*. 1984;5(5):301-304. doi:10.1016/0142-9612(84)90078-4
83. Powell AK, Ahmed YA, Yates EA, Turnbull JE. Generating heparan sulfate saccharide libraries for glycomics applications. *Nat Protoc*. 2010;5(5):821-833. doi:10.1038/nprot.2010.17

84. Wang M, Liu X, Lyu Z, Gu H, Li D, Chen H. Glycosaminoglycans (GAGs) and GAG mimetics regulate the behavior of stem cell differentiation. *Colloids Surf B Biointerfaces*. 2017;150:175-182. doi:10.1016/j.colsurfb.2016.11.022
85. Zubkova OV, Ahmed YA, Guimond SE, et al. Dendrimer Heparan Sulfate Glycomimetics: Potent Heparanase Inhibitors for Anticancer Therapy. *ACS Chem Biol*. 2018;13(12):3236-3242. doi:10.1021/acscchembio.8b00909
86. Meddahi A, Brée F, Papy-Garcia D, Gautron J, Barritault D, Caruelle J-P. Pharmacological studies of RGTA11, a heparan sulfate mimetic polymer, efficient on muscle regeneration. *J Biomed Mater Res*. 2002;62(4):525-531. doi:10.1002/jbm.10283
87. Arlov Ø, Achmann FL, Sundan A, Espevik T, Skjåk-Bræk G. Heparin-Like Properties of Sulfated Alginates with Defined Sequences and Sulfation Degrees. *Biomacromolecules*. 2014;15(7):2744-2750. doi:10.1021/bm500602w
88. Ruvinov E, Freeman I, Fredo R, Cohen S. Spontaneous Coassembly of Biologically Active Nanoparticles via Affinity Binding of Heparin-Binding Proteins to Alginate-Sulfate. *Nano Lett*. 2016;16(2):883-888. doi:10.1021/acs.nanolett.5b03598
89. Ronghua H, Yumin D, Jianhong Y. Preparation and in vitro anticoagulant activities of alginate sulfate and its quaterized derivatives. *Carbohydr Polym*. 2003;52(1):19-24. doi:10.1016/S0144-8617(02)00258-8
90. Wang Z-M, Xiao K-J, Li L, Wu J-Y. Molecular weight-dependent anticoagulation activity of sulfated cellulose derivatives. *Cellulose*. 2010;17(5):953-961. doi:10.1007/s10570-010-9441-7
91. Groth T, Wagenknecht W. Anticoagulant potential of regioselective derivatized cellulose. *Biomaterials*. 2001;22(20):2719-2729. doi:10.1016/S0142-9612(01)00013-8
92. Yang J, Cai J, Wu K, et al. Preparation, characterization and anticoagulant activity in vitro of heparin-like 6-carboxylchitin derivative. *Int J Biol Macromol*. 2012;50(4):1158-1164. doi:10.1016/j.ijbiomac.2012.01.007
93. Suwan J, Zhang Z, Li B, et al. Sulfonation of papain-treated chitosan and its mechanism for anticoagulant activity. *Carbohydr Res*. 2009;344(10):1190-1196. doi:10.1016/j.carres.2009.04.016
94. Ding K, Wang Y, Wang H, et al. 6-O-Sulfated Chitosan Promoting the Neural Differentiation of Mouse Embryonic Stem Cells. *ACS Appl Mater Interfaces*. 2014;6(22):20043-20050. doi:10.1021/am505628g
95. Zou Y, Khor E. Preparation of sulfated-chitins under homogeneous conditions. *Carbohydr Polym*. 2009;77(3):516-525. doi:10.1016/j.carbpol.2009.01.031
96. Hirano S, Tanaka Y, Hasegawa M, Tobetto K, Nishioka A. Effect of sulfated derivatives of chitosan on some blood coagulant factors. *Carbohydr Res*. 1985;137:205-215. doi:10.1016/0008-6215(85)85161-2
97. Vongchan P, Sajomsang W, Subyen D, Kongtawelert P. Anticoagulant activity of a sulfated chitosan. *Carbohydr Res*. 2002;337(13):1239-1242. doi:10.1016/S0008-6215(02)00098-8

98. Liu Q, Chen G, Chen H. Chemical synthesis of glycosaminoglycan-mimetic polymers. *Polym Chem.* 2018;10(2):164-171. doi:10.1039/C8PY01338A
99. Zhou H, Qian J, Wang J, et al. Enhanced bioactivity of bone morphogenetic protein-2 with low dose of 2-N, 6-O-sulfated chitosan in vitro and in vivo. *Biomaterials.* 2009;30(9):1715-1724. doi:10.1016/j.biomaterials.2008.12.016
100. Cao L, Wang J, Hou J, Xing W, Liu C. Vascularization and bone regeneration in a critical sized defect using 2-N,6-O-sulfated chitosan nanoparticles incorporating BMP-2. *Biomaterials.* 2014;35(2):684-698. doi:10.1016/j.biomaterials.2013.10.005
101. Yu Y, Chen J, Chen R, et al. Enhancement of VEGF-Mediated Angiogenesis by 2-N,6-O-Sulfated Chitosan-Coated Hierarchical PLGA Scaffolds. *ACS Appl Mater Interfaces.* 2015;7(18):9982-9990. doi:10.1021/acsami.5b02324
102. Peng X, Yu Y, Wang Z, Zhang X, Wang J, Liu C. Potentiation effect of HB-EGF on facilitating wound healing via 2-N,6-O-sulfated chitosan nanoparticles modified PLGA scaffold. *RSC Adv.* 2017;7(68):43161-43171. doi:10.1039/C7RA07719J
103. Yu Y, Chen R, Sun Y, et al. Manipulation of VEGF-induced angiogenesis by 2-N, 6-O-sulfated chitosan. *Acta Biomater.* 2018;71:510-521. doi:10.1016/j.actbio.2018.02.031
104. Changotade SIT, Korb G, Bassil J, et al. Potential effects of a low-molecular-weight fucoidan extracted from brown algae on bone biomaterial osteoconductive properties. *J Biomed Mater Res A.* 2008;87A(3):666-675. doi:10.1002/jbm.a.31819
105. Deux J-F, Meddahi-Pellé A, Bree F, Bataille I, Michel J-B, Letourneur D. Comparative Studies on the Mechanisms of Action of Four Polysaccharides on Arterial Restenosis. *J Biomater Sci Polym Ed.* 2009;20(5-6):689-702. doi:10.1163/156856209X426493
106. Tillman J, Ullm A, Madihally SV. Three-dimensional cell colonization in a sulfate rich environment. *Biomaterials.* 2006;27(32):5618-5626. doi:10.1016/j.biomaterials.2006.07.006
107. Mauzac M, Aubert N, Jozefonvicz J. Antithrombic activity of some polysaccharide resins. *Biomaterials.* 1982;3(4):221-224. doi:10.1016/0142-9612(82)90023-0
108. Baldwin AD, Kiick KL. Polysaccharide-Modified Synthetic Polymeric Biomaterials. *Biopolymers.* 2010;94(1):128-140. doi:10.1002/bip.21334
109. Ikeda Y, Charef S, Ouidja M-O, et al. Synthesis and biological activities of a library of glycosaminoglycans mimetic oligosaccharides. *Biomaterials.* 2011;32(3):769-776. doi:10.1016/j.biomaterials.2010.09.043
110. Albanese P, Caruelle D, Frescaline G, et al. Glycosaminoglycan mimetics–induced mobilization of hematopoietic progenitors and stem cells into mouse peripheral blood: Structure/function insights*. *Exp Hematol.* 2009;37(9):1072-1083. doi:10.1016/j.exphem.2009.06.005
111. Papy-Garcia D, Barbier-Chassefière V, Rouet V, et al. Nondegradative Sulfation of Polysaccharides. Synthesis and Structure Characterization of Biologically Active Heparan Sulfate Mimetics. *Macromolecules.* 2005;38(11):4647-4654. doi:10.1021/ma048485p

112. Rouet V, Meddahi-Pellé A, Miao H-Q, Vlodavsky I, Caruelle J-P, Barritault D. Heparin-like synthetic polymers, named RGTAs, mimic biological effects of heparin in vitro. *J Biomed Mater Res A*. 2006;78A(4):792-797. doi:10.1002/jbm.a.30723
113. D B, Jp C. [Regenerating agents (RGTAs): a new therapeutic approach]. *Ann Pharm Fr*. 2006;64(2):135-144. doi:10.1016/s0003-4509(06)75306-8
114. Charef S, Petit E, Barritault D, Courty J, Caruelle J-P. Effects on coagulation of a synthetic heparan mimetic given intraperitoneally or orally. *J Biomed Mater Res A*. 2007;83A(4):1024-1031. doi:10.1002/jbm.a.31385
115. Sutton A, Friand V, Papy-Garcia D, et al. Glycosaminoglycans and their synthetic mimetics inhibit RANTES-induced migration and invasion of human hepatoma cells. *Mol Cancer Ther*. 2007;6(11):2948-2958. doi:10.1158/1535-7163.MCT-07-0114
116. Friand V, Haddad O, Papy-Garcia D, et al. Glycosaminoglycan mimetics inhibit SDF-1/CXCL12-mediated migration and invasion of human hepatoma cells. *Glycobiology*. 2009;19(12):1511-1524. doi:10.1093/glycob/cwp130
117. Khammari Chebbi C, Kichenin K, Amar N, et al. Étude pilote d'un nouvel agent de thérapie matricielle (RGTA OTR4120®) dans les ulcères de cornée et les dystrophies cornéennes rebelles. *J Fr Ophtalmol*. 2008;31(5):465-471. doi:10.1016/S0181-5512(08)72462-8
118. Sweeney EA, Lortat-Jacob H, Priestley GV, Nakamoto B, Papayannopoulou T. Sulfated polysaccharides increase plasma levels of SDF-1 in monkeys and mice: involvement in mobilization of stem/progenitor cells. *Blood*. 2002;99(1):44-51. doi:10.1182/blood.V99.1.44
119. Frenette PS, Weiss L. Sulfated glycans induce rapid hematopoietic progenitor cell mobilization: evidence for selectin-dependent and independent mechanisms. *Blood*. 2000;96(7):2460-2468. doi:10.1182/blood.V96.7.2460
120. Colliec Jouault S, Chevolut L, Helley D, et al. Characterization, chemical modifications and in vitro anticoagulant properties of an exopolysaccharide produced by *Alteromonas infernus*. *Biochim Biophys Acta BBA - Gen Subj*. 2001;1528(2):141-151. doi:10.1016/S0304-4165(01)00185-4
121. Matou S, Colliec-Jouault S, Galy-Fauroux I, et al. Effect of an oversulfated exopolysaccharide on angiogenesis induced by fibroblast growth factor-2 or vascular endothelial growth factor in vitro. *Biochem Pharmacol*. 2005;69(5):751-759. doi:10.1016/j.bcp.2004.11.021
122. Cheng JWM. Fondaparinux: A new antithrombotic agent. *Clin Ther*. 2002;24(11):1757-1769. doi:10.1016/S0149-2918(02)80077-7
123. Wall D, Douglas S, Ferro V, Cowden W, Parish C. Characterisation of the Anticoagulant Properties of a Range of Structurally Diverse Sulfated Oligosaccharides. *Thromb Res*. 2001;103(4):325-335. doi:10.1016/S0049-3848(01)00314-0
124. Tully SE, Mabon R, Gama CI, Tsai SM, Liu X, Hsieh-Wilson LC. A Chondroitin Sulfate Small Molecule that Stimulates Neuronal Growth. *J Am Chem Soc*. 2004;126(25):7736-7737. doi:10.1021/ja0484045
125. Foxall C, Wei Z, Schaefer ME, et al. Sulfated malto-oligosaccharides bind to basic FGF, inhibit endothelial cell proliferation, and disrupt endothelial cell tube formation. *J Cell Physiol*.

- 1996;168(3):657-667. doi:10.1002/(SICI)1097-4652(199609)168:3<657::AID-JCP18>3.0.CO;2-W
126. Parish CR, Freeman C, Brown KJ, Francis DJ, Cowden WB. Identification of Sulfated Oligosaccharide-based Inhibitors of Tumor Growth and Metastasis Using Novel in Vitro Assays for Angiogenesis and Heparanase Activity. *Cancer Res.* 1999;59(14):3433-3441.
 127. Miura Y, Fukuda T, Seto H, Hoshino Y. Development of glycosaminoglycan mimetics using glycopolymers. *Polym J.* 2016;48(3):229-237. doi:10.1038/pj.2015.110
 128. Miura Y, Yasuda K, Yamamoto K, Koike M, Nishida Y, Kobayashi K. Inhibition of Alzheimer Amyloid Aggregation with Sulfated Glycopolymers. *Biomacromolecules.* 2007;8(7):2129-2134. doi:10.1021/bm0701402
 129. Miura Y, Mizuno H. Interaction Analyses of Amyloid β Peptide (1–40) with Glycosaminoglycan Model Polymers. *Bull Chem Soc Jpn.* 2010;83(9):1004-1009. doi:10.1246/bcsj.20100094
 130. Lee S-G, Brown JM, Rogers CJ, et al. End-functionalized glycopolymers as mimetics of chondroitin sulfate proteoglycans. *Chem Sci.* 2010;1(3):322-325. doi:10.1039/C0SC00271B
 131. Rawat M, Gama CI, Matson JB, Hsieh-Wilson LC. Neuroactive Chondroitin Sulfate Glycomimetics. *J Am Chem Soc.* 2008;130(10):2959-2961. doi:10.1021/ja709993p
 132. Oh YI, Sheng GJ, Chang S-K, Hsieh-Wilson LC. Tailored Glycopolymers as Anticoagulant Heparin Mimetics. *Angew Chem.* 2013;125(45):12012-12015. doi:10.1002/ange.201306968
 133. Sheng GJ, Oh YI, Chang S-K, Hsieh-Wilson LC. Tunable Heparan Sulfate Mimetics for Modulating Chemokine Activity. *J Am Chem Soc.* 2013;135(30):10898-10901. doi:10.1021/ja4027727
 134. Grande D, Baskaran S, Chaikof EL. Glycosaminoglycan Mimetic Biomaterials. 2. Alkene- and Acrylate-Derivatized Glycopolymers via Cyanoxyl-Mediated Free-Radical Polymerization. *Macromolecules.* 2001;34(6):1640-1646. doi:10.1021/ma001680t
 135. Grande D, Baskaran S, Baskaran C, Gnanou Y, Chaikof EL. Glycosaminoglycan-Mimetic Biomaterials. 1. Nonsulfated and Sulfated Glycopolymers by Cyanoxyl-Mediated Free-Radical Polymerization. *Macromolecules.* 2000;33(4):1123-1125. doi:10.1021/ma991579s
 136. Baskaran S, Grande D, Sun X-L, Yayon A, Chaikof EL. Glycosaminoglycan-Mimetic Biomaterials. 3. Glycopolymers Prepared from Alkene-Derivatized Mono- and Disaccharide-Based Glycomonomers. *Bioconjug Chem.* 2002;13(6):1309-1313. doi:10.1021/bc0255485
 137. Sun X-L, Grande D, Baskaran S, Hanson SR, Chaikof EL. Glycosaminoglycan Mimetic Biomaterials. 4. Synthesis of Sulfated Lactose-Based Glycopolymers That Exhibit Anticoagulant Activity. *Biomacromolecules.* 2002;3(5):1065-1070. doi:10.1021/bm025561s
 138. Guan R, Sun X-L, Hou S, Wu P, Chaikof EL. A Glycopolymer Chaperone for Fibroblast Growth Factor-2. *Bioconjug Chem.* 2004;15(1):145-151. doi:10.1021/bc034138t
 139. Christman KL, Vázquez-Dorbatt V, Schopf E, et al. Nanoscale Growth Factor Patterns by Immobilization on a Heparin-Mimicking Polymer. *J Am Chem Soc.* 2008;130(49):16585-16591. doi:10.1021/ja803676r

140. Nguyen TH, Kim S-H, Decker CG, Wong DY, Loo JA, Maynard HD. A heparin-mimicking polymer conjugate stabilizes basic fibroblast growth factor. *Nat Chem*. 2013;5(3):221-227. doi:10.1038/nchem.1573
141. Ma L, Qin H, Cheng C, et al. Mussel-inspired self-coating at macro-interface with improved biocompatibility and bioactivity via dopamine grafted heparin-like polymers and heparin. *J Mater Chem B*. 2014;2(4):363-375. doi:10.1039/C3TB21388A
142. Arslan E, Guler MO, Tekinay AB. Glycosaminoglycan-Mimetic Signals Direct the Osteo/Chondrogenic Differentiation of Mesenchymal Stem Cells in a Three-Dimensional Peptide Nanofiber Extracellular Matrix Mimetic Environment. *Biomacromolecules*. 2016;17(4):1280-1291. doi:10.1021/acs.biomac.5b01637
143. Lee EC, Davis-Poynter N, Nguyen CTH, et al. GAG mimetic functionalised solid and mesoporous silica nanoparticles as viral entry inhibitors of herpes simplex type 1 and type 2 viruses. *Nanoscale*. 2016;8(36):16192-16196. doi:10.1039/C6NR03878F
144. Place LW, Sekyi M, Kipper MJ. Aggrecan-Mimetic, Glycosaminoglycan-Containing Nanoparticles for Growth Factor Stabilization and Delivery. *Biomacromolecules*. 2014;15(2):680-689. doi:10.1021/bm401736c
145. Werz DB, Ranzinger R, Herget S, Adibekian A, von der Lieth C-W, Seeberger PH. Exploring the Structural Diversity of Mammalian Carbohydrates ("Glycospace") by Statistical Databank Analysis. *ACS Chem Biol*. 2007;2(10):685-691. doi:10.1021/cb700178s
146. Pashkuleva I, Reis RL. Sugars: burden or biomaterials of the future? *J Mater Chem*. 2010;20(40):8803-8818. doi:10.1039/C0JM01605E
147. Kuriki T, Imanaka T. The concept of the α -amylase family: Structural similarity and common catalytic mechanism. *J Biosci Bioeng*. 1999;87(5):557-565. doi:10.1016/S1389-1723(99)80114-5
148. Ornitz DM, Itoh N. Fibroblast growth factors. *Genome Biol*. 2001;2(3):reviews3005.1. doi:10.1186/gb-2001-2-3-reviews3005
149. Holmes K, Roberts OL, Thomas AM, Cross MJ. Vascular endothelial growth factor receptor-2: Structure, function, intracellular signalling and therapeutic inhibition. *Cell Signal*. 2007;19(10):2003-2012. doi:10.1016/j.cellsig.2007.05.013
150. Ornitz DM. FGFs, heparan sulfate and FGFRs: complex interactions essential for development. *BioEssays*. 2000;22(2):108-112. doi:10.1002/(SICI)1521-1878(200002)22:2<108::AID-BIES2>3.0.CO;2-M
151. Ashikari-Hada S, Habuchi H, Kariya Y, Kimata K. Heparin Regulates Vascular Endothelial Growth Factor165-dependent Mitogenic Activity, Tube Formation, and Its Receptor Phosphorylation of Human Endothelial Cells COMPARISON OF THE EFFECTS OF HEPARIN AND MODIFIED HEPARINS. *J Biol Chem*. 2005;280(36):31508-31515. doi:10.1074/jbc.M414581200
152. Gitay-Goren H, Soker S, Vlodavsky I, Neufeld G. The binding of vascular endothelial growth factor to its receptors is dependent on cell surface-associated heparin-like molecules. *J Biol Chem*. 1992;267(9):6093-6098.

153. Gospodarowicz D, Cheng J. Heparin protects basic and acidic FGF from inactivation. *J Cell Physiol.* 1986;128(3):475-484. doi:10.1002/jcp.1041280317
154. Park M, Lee S-T. The Fourth Immunoglobulin-like Loop in the Extracellular Domain of FLT-1, a VEGF Receptor, Includes a Major Heparin-Binding Site. *Biochem Biophys Res Commun.* 1999;264(3):730-734. doi:10.1006/bbrc.1999.1580
155. Dougher AM, Wasserstrom H, Torley L, et al. Identification of a Heparin Binding Peptide on the Extracellular Domain of the KDR VEGF Receptor. *Growth Factors.* 1997;14(4):257-268. doi:10.3109/08977199709021524
156. Ornitz DM, Yayon A, Flanagan JG, Svahn CM, Levi E, Leder P. Heparin is required for cell-free binding of basic fibroblast growth factor to a soluble receptor and for mitogenesis in whole cells. *Mol Cell Biol.* 1992;12(1):240-247.
157. Njau F, Shushakova N, Schenk H, et al. Calcium dobesilate reduces VEGF signaling by interfering with heparan sulfate binding site and protects from vascular complications in diabetic mice. *bioRxiv.* Published online June 5, 2019:661793. doi:10.1101/661793
158. Ellman MB, Yan D, Ahmadiania K, Chen D, An HS, Im HJ. Fibroblast growth factor control of cartilage homeostasis. *J Cell Biochem.* 2013;114(4):735-742. doi:10.1002/jcb.24418
159. Pufe T, Petersen W, Tillmann B, Mentlein R. The splice variants VEGF121 and VEGF189 of the angiogenic peptide vascular endothelial growth factor are expressed in osteoarthritic cartilage. *Arthritis Rheum.* 2001;44(5):1082-1088. doi:10.1002/1529-0131(200105)44:5<1082::AID-ANR188>3.0.CO;2-X
160. Pufe T, Lemke A, Kurz B, et al. Mechanical Overload Induces VEGF in Cartilage Discs via Hypoxia-Inducible Factor. *Am J Pathol.* 2004;164(1):185-192.
161. Yeh C-J, Ku C-C, Lin W-C, et al. Single-Step Per-O-Sulfonation of Sugar Oligomers with Concomitant 1,6-Anhydro Bridge Formation for Binding Fibroblast Growth Factors. *ChemBioChem.* 2019;20(2):237-240. doi:10.1002/cbic.201800464
162. Li L-Y, Seddon AP. Fluorospectrometric Analysis of Heparin Interaction with Fibroblast Growth Factors. *Growth Factors.* 1994;11(1):1-7. doi:10.3109/08977199409015046
163. Shing Y, Folkman J, Weisz PB, Joullie MM, Ewing WR. Affinity of fibroblast growth factors for β -cyclodextrin tetradecasulfate. *Anal Biochem.* 1990;185(1):108-111. doi:10.1016/0003-2697(90)90263-9
164. Bachinsky WB, Barnathan ES, Liu H, et al. Sustained inhibition of intimal thickening. In vitro and in vivo effects of polymeric beta-cyclodextrin sulfate. *J Clin Invest.* 1995;96(6):2583-2592. doi:10.1172/JCI118322
165. Usov AI. NMR Spectroscopy of Red Seaweed Polysaccharides: Agars, Carrageenans, and Xylans. *Bot Mar.* 1984;27(5):189-202. doi:10.1515/botm.1984.27.5.189
166. Chuang CY, Lord MS, Melrose J, et al. Heparan Sulfate-Dependent Signaling of Fibroblast Growth Factor 18 by Chondrocyte-Derived Perlecan. *Biochemistry.* 2010;49(26):5524-5532. doi:10.1021/bi1005199

167. Quarto N, Amalric F. Heparan sulfate proteoglycans as transducers of FGF-2 signalling. *J Cell Sci.* 1994;107(11):3201-3212.
168. Xu M, McCanna DJ, Sivak JG. Use of the viability reagent PrestoBlue in comparison with alamarBlue and MTT to assess the viability of human corneal epithelial cells. *J Pharmacol Toxicol Methods.* 2015;71:1-7. doi:10.1016/j.vascn.2014.11.003
169. Qi Q, Zimmermann W. Cyclodextrin glucanotransferase: from gene to applications. *Appl Microbiol Biotechnol.* 2005;66(5):475-485. doi:10.1007/s00253-004-1781-5
170. Freudenberg KD, Cramer FD, Plieninger HD. A process for the preparation of inclusion compounds of physiologically active organic compounds. 1953;(DE895769C). Accessed October 6, 2020. <https://patents.google.com/patent/DE895769C/en>
171. Szejtli J. Introduction and General Overview of Cyclodextrin Chemistry. *Chem Rev.* 1998;98(5):1743-1754. doi:10.1021/cr970022c
172. Gelb RI, Schwartz LM, Bradshaw JJ, Laufer DA. Acid dissociation of cyclohexaamylose and cycloheptaamylose. *Bioorganic Chem.* 1980;9(3):299-304. doi:10.1016/0045-2068(80)90039-5
173. Khan AR, Forgo P, Stine KJ, D'Souza VT. Methods for Selective Modifications of Cyclodextrins. *Chem Rev.* 1998;98(5):1977-1996. doi:10.1021/cr970012b
174. Řezanka M. Synthesis of substituted cyclodextrins. *Environ Chem Lett.* Published online July 18, 2018. doi:10.1007/s10311-018-0779-7
175. Hayashida K, Higashi T, Kono D, Motoyama K, Wada K, Arima H. Preparation and evaluation of cyclodextrin polypseudorotaxane with PEGylated liposome as a sustained release drug carrier. *Beilstein J Org Chem.* 2014;10(1):2756-2764. doi:10.3762/bjoc.10.292
176. Hu Q-D, Tang G-P, Chu PK. Cyclodextrin-Based Host–Guest Supramolecular Nanoparticles for Delivery: From Design to Applications. *Acc Chem Res.* 2014;47(7):2017-2025. doi:10.1021/ar500055s
177. Rajewski RA, Stella VJ. Pharmaceutical applications of cyclodextrins. 2. in vivo drug delivery. *J Pharm Sci.* 1996;85(11):1142-1169. doi:10.1021/js960075u
178. Wang L, Li L, Fan Y, Wang H. Host–Guest Supramolecular Nanosystems for Cancer Diagnostics and Therapeutics. *Adv Mater.* 2013;25(28):3888-3898. doi:10.1002/adma.201301202
179. Zhao Y, Sakai F, Su L, et al. Progressive Macromolecular Self-Assembly: From Biomimetic Chemistry to Bio-Inspired Materials. *Adv Mater.* 2013;25(37):5215-5256. doi:10.1002/adma.201302215
180. Umezawa S, Tatsuta K. Studies of Aminosugars. XVIII. Syntheses of Amino Derivatives of Schardinger α -Dextrin and Raffinose. *Bull Chem Soc Jpn.* 1968;41(2):464-468. doi:10.1246/bcsj.41.464
181. Gadelle A, Defaye J. Selective Halogenation at Primary Positions of Cyclomaltooligosaccharides and a Synthesis of Per-3,6-anhydro Cyclomaltooligosaccharides. *Angew Chem Int Ed Engl.* 1991;30(1):78-80. doi:10.1002/anie.199100781

182. Takeo K, Ueraura K, Mitoh H. Derivatives Of α -Cyclodextrin and the Synthesis of 6-O- α -D-Glucopyranosyl- α -Cyclodextrin. *J Carbohydr Chem*. 1988;7(2):293-308. doi:10.1080/07328308808058926
183. Takeo K, Mitoh H, Uemura K. Selective chemical modification of cyclomalto-oligosaccharides via tert-butyldimethylsilylation. *Carbohydr Res*. 1989;187(2):203-221. doi:10.1016/0008-6215(89)80004-7
184. Zhang P, Wang A, Cui L, Ling C-C. First Per-6-O-tritylation of Cyclodextrins. *Org Lett*. 2012;14(6):1612-1615. doi:10.1021/ol300358u
185. Boger J, Corcoran RJ, Lehn J-M. Selective modification of all primary hydroxyl groups of α - and β -cyclodextrins. *Helv Chim Acta*. 1978;61(6):2190-2218. doi:10.1002/hlca.19780610622
186. Rong D, D'Souza VT. A convenient method for functionalization of the 2-position of cyclodextrins. *Tetrahedron Lett*. 1990;31(30):4275-4278. doi:10.1016/S0040-4039(00)97599-3
187. Ward S, Calderon O, Zhang P, et al. Investigation into the role of the hydrogen bonding network in cyclodextrin-based self-assembling mesophases. *J Mater Chem C*. 2014;2(25):4928-4936. doi:10.1039/C4TC00448E
188. Vincent JB, Kirby DM, Nguyen TV, Vigh G. A Family of Single-Isomer Chiral Resolving Agents for Capillary Electrophoresis. 2. Hepta-6-sulfato- β -cyclodextrin. *Anal Chem*. 1997;69(21):4419-4428. doi:10.1021/ac970418o
189. Chen F-TA, Shen G, Evangelista RA. Characterization of highly sulfated cyclodextrins. *J Chromatogr A*. 2001;924(1):523-532. doi:10.1016/S0021-9673(01)00757-9
190. Cai H, Nguyen TV, Vigh G. A Family of Single-Isomer Chiral Resolving Agents for Capillary Electrophoresis. 3. Heptakis(2,3-dimethyl-6-sulfato)- β -cyclodextrin. *Anal Chem*. 1998;70(3):580-589. doi:10.1021/ac970822n
191. Rousseau C, Ortega-Caballero F, Nordstrøm LU, Christensen B, Petersen TE, Bols M. Artificial Glycosyl Phosphorylases. *Chem – Eur J*. 2005;11(17):5094-5101. doi:10.1002/chem.200500364
192. Dubes A, Bouchu D, Lamartine R, Parrot-Lopez H. An efficient regio-specific synthetic route to multiply substituted acyl-sulphated β -cyclodextrins. *Tetrahedron Lett*. 2001;42(52):9147-9151. doi:10.1016/S0040-4039(01)01992-X
193. Tutu E, Vigh G. Synthesis, analytical characterization and initial capillary electrophoretic use in an acidic background electrolyte of a new, single-isomer chiral resolving agent: Heptakis(2-O-sulfo-3-O-methyl-6-O-acetyl)- β -cyclodextrin. *Electrophoresis*. 2011;32(19):2655-2662. doi:10.1002/elps.201100104
194. Maynard DK, Vigh G. Synthesis and analytical characterization of the sodium salt of heptakis(2-O-methyl-3,6-di-O-sulfo)cyclomaltoheptaose, a chiral resolving agent candidate for capillary electrophoresis. *Carbohydr Res*. 2000;328(3):277-285. doi:10.1016/S0008-6215(00)00114-2
195. Takeo K, Mitoh H, Uemura K. Selective chemical modification of cyclomalto-oligosaccharides via tert-butyldimethylsilylation. *Carbohydr Res*. 1989;187(2):203-221. doi:10.1016/0008-6215(89)80004-7

196. Fügedi P. Synthesis of heptakis(6-O-tert-butyldimethylsilyl)cyclomaltoheptaose and octakis(6-O-tert-butyldimethylsilyl)cyclomalto-octaose. *Carbohydr Res.* 1989;192:366-369. doi:10.1016/0008-6215(89)85197-3
197. Baumann R, Rys P. Metachromatic activity of beta-cyclodextrin sulfates as heparin mimics. *Int J Biol Macromol.* 1999;24(1):15-18.
198. Lecourt T, Herault A, Pearce AJ, Sollogoub M, Sinaÿ P. Triisobutylaluminium and Diisobutylaluminium Hydride as Molecular Scalpels: The Regioselective Stripping of Perbenzylated Sugars and Cyclodextrins. *Chem - Eur J.* 2004;10(12):2960-2971. doi:10.1002/chem.200305683
199. Angibeaud P, Utille JP. Cyclodextrin chemistry. Part I : application of a regioselective acetolysis method for benzyl ethers. *SYNTHESIS.* 1991;9:737-738.
200. Sutyagin AA, Glazyrin AE, Kurochkina GI, Grachev MK, Nifant'ev EE. Regioselective Acetylation of β -Cyclodextrin. *Russ J Gen Chem.* 2002;72(1):147-150. doi:10.1023/A:1015378203469
201. Ashton PR, Königer R, Stoddart JF, Alker D, Harding VD. Amino Acid Derivatives of β -Cyclodextrin. *J Org Chem.* 1996;61(3):903-908. doi:10.1021/jo951396d
202. Vogel C, Murphy P. *Carbohydrate Chemistry: Proven Synthetic Methods, Volume 4.* Vol 4. CRC Press; 2018. Accessed January 8, 2019. <https://www.crcpress.com/Carbohydrate-Chemistry-Proven-Synthetic-Methods-Volume-4/Vogel-Murphy/p/book/9781498726917>
203. Gou P-F, Zhu W-P, Xu N, Shen Z-Q. Synthesis and characterization of well-defined cyclodextrin-centered seven-arm star poly(ϵ -caprolactone)s and amphiphilic star poly(ϵ -caprolactone-b-ethylene glycol)s. *J Polym Sci Part Polym Chem.* 2008;46(19):6455-6465. doi:10.1002/pola.22955
204. Dolgopyatova NV, Novikov VYu, Konovalova IN, Putintsev NM. Mechanism of acid hydrolysis of N-acetyl-D-glucosamine. *Russ J Appl Chem.* 2013;86(7):986-991. doi:10.1134/S1070427213070070
205. McKee JA, Green TK. Synthesis of 2,3-O-dibenzyl-6-O-sulfobutyl- α and β cyclodextrins: new chiral surfactants for capillary electrophoresis. *Tetrahedron Lett.* 2015;56(30):4451-4454. doi:10.1016/j.tetlet.2015.05.057
206. Czernecki S, Georgoulis C, Provelenghiou C. Nouvelle methode de benzylation d'hydroxyles glucidiques encombrés. *Tetrahedron Lett.* 1976;17(39):3535-3536. doi:10.1016/S0040-4039(00)71351-7
207. Assam Evoung JN. Utilisation et Modification de la β -cyclodextrine et de système mono-oxidique en angiogenèse. Published online December 21, 2012. Accessed October 18, 2020. <http://www.theses.fr/2012ENCM0027>
208. Bálint M, Darcsi A, Benkovics G, Varga E, Malanga M, Béni S. Synthesis of the chiral selector heptakis(6-O-methyl)- β -cyclodextrin by phase-transfer catalysis and hydrazine-mediated transfer-hydrogenation. *ELECTROPHORESIS.* 2019;40(15):1941-1950. doi:10.1002/elps.201900065

209. Starks CM, Liotta CL, Halpern ME. Basic Concepts in Phase-Transfer Catalysis. In: Starks CM, Liotta CL, Halpern ME, eds. *Phase-Transfer Catalysis: Fundamentals, Applications, and Industrial Perspectives*. Springer Netherlands; 1994:1-22. doi:10.1007/978-94-011-0687-0_1
210. Uccello-Barretta G, Sicoli G, Balzano F, Salvadori P. NMR spectroscopy: a powerful tool for detecting the conformational features of symmetrical persubstituted mixed cyclomaltoheptaoses (β -cyclodextrins). *Carbohydr Res*. 2005;340(2):278-281. doi:10.1016/j.carres.2004.11.022
211. Fatema MK, Nonami H, Ducatti DRB, et al. Matrix-assisted laser desorption/ionization time-of-flight (MALDI-TOF) mass spectrometry analysis of oligosaccharides and oligosaccharide alditols obtained by hydrolysis of agaroses and carrageenans, two important types of red seaweed polysaccharides. *Carbohydr Res*. 2010;345(2):275-283. doi:10.1016/j.carres.2009.10.009
212. Meppen M, Wang Y, Cheon H-S, Kishi Y. Synthetic 6-O-Methylglucose-Containing Polysaccharides (sMGPs): Design and Synthesis. *J Org Chem*. 2007;72(6):1941-1950. doi:10.1021/jo061990v
213. Oike H, Yoshioka Y, Kobayashi S, Nakashima M, Tezuka Y, Goethals EJ. Benzylic triflates prepared in-situ: novel initiators for mono-, bi- and trifunctional living poly(THF)s. *Macromol Rapid Commun*. 2000;21(17):1185-1190. doi:10.1002/1521-3927(20001101)21:17<1185::AID-MARC1185>3.0.CO;2-N
214. Ashton PR, Boyd SE, Gattuso G, et al. A Novel Approach to the Synthesis of Some Chemically-Modified Cyclodextrins. *J Org Chem*. 1995;60(12):3898-3903. doi:10.1021/jo00117a049
215. Hamelin B, Jullien L, Laschewsky A, Penhoat CH du. Self-assembly of Janus Cyclodextrins at the Air-Water Interface and in Organic Solvents. *Chem – Eur J*. 1999;5(2):546-556. doi:10.1002/(SICI)1521-3765(19990201)5:2<546::AID-CHEM546>3.0.CO;2-I
216. Gingras M, Chabre YM, Roy M, Roy R. How do multivalent glycodendrimers benefit from sulfur chemistry? *Chem Soc Rev*. 2013;42(11):4823-4841. doi:10.1039/C3CS60090D
217. Bernardes GJL, Gamblin DP, Davis BG. The Direct Formation of Glycosyl Thiols from Reducing Sugars Allows One-Pot Protein Glycoconjugation. *Angew Chem Int Ed*. 2006;45(24):4007-4011. doi:10.1002/anie.200600685
218. Park SS, Hsieh H-W, Gervay-Hague J. Anomeric O-Functionalization of Carbohydrates for Chemical Conjugation to Vaccine Constructs. *Mol J Synth Chem Nat Prod Chem*. 2018;23(7). doi:10.3390/molecules23071742
219. G.M. Wuts P. *Greene's Protective Groups in Organic Synthesis, 5th Edition* | Wiley. Vol 5th edition. John Wiley&Sons.; 2014. Accessed February 26, 2020. <https://www.wiley.com/en-fr/Greene%27s+Protective+Groups+in+Organic+Synthesis%2C+5th+Edition-p-9781118057483>
220. Roth PJ, Boyer C, Lowe AB, Davis TP. RAFT Polymerization and Thiol Chemistry: A Complementary Pairing for Implementing Modern Macromolecular Design. *Macromol Rapid Commun*. 2011;32(15):1123-1143. doi:10.1002/marc.201100127
221. Carbohydrate Chemistry: Proven Synthetic Methods, Volume 4. CRC Press. Accessed January 8, 2019. <https://www.crcpress.com/Carbohydrate-Chemistry-Proven-Synthetic-Methods-Volume-4/Vogel-Murphy/p/book/9781498726917>

222. G.M. Wuts P. Protection for the Thiol Group. In: *Greene's Protective Groups in Organic Synthesis.* ; 2014:837-894. doi:10.1002/9781118905074.ch06
223. Falconer RA. The S-xanthenyl group: potential for application in the synthesis of thioglycosides. *Tetrahedron Lett.* 2002;43(47):8503-8505. doi:10.1016/S0040-4039(02)02070-1
224. Yanase M, Funabashi M. Stereoselective 1,2-CIS-1-Thioglycosidation of Aldohexoses with Tert-Butyl Mercaptan in 90% Trifluoroacetic Acid. *J Carbohydr Chem.* 2000;19(1):53-66. doi:10.1080/07328300008544064
225. Funabashi M, Arai S, Shinohara M. Novel Syntheses of Diphenyl and/or Trimethylene Dithioacetals of Mono- and Oligosaccharides in 90% Trifluoroacetic Acid. *J Carbohydr Chem.* 1999;18(3):333-341. doi:10.1080/07328309908543999
226. Tanaka T, Matsumoto T, Noguchi M, Kobayashi A, Shoda S. Direct Transformation of Unprotected Sugars to Aryl 1-Thio- β -glycosides in Aqueous Media Using 2-Chloro-1,3-dimethylimidazolium Chloride. *Chem Lett.* 2009;38(5):458-459. doi:10.1246/cl.2009.458
227. Stick RV, Stubbs KA. From glycoside hydrolases to thioglycoligases: the synthesis of thioglycosides. *Tetrahedron Asymmetry.* 2005;16(2):321-335. doi:10.1016/j.tetasy.2004.12.004
228. Lian G, Zhang X, Yu B. Thioglycosides in Carbohydrate Research. *Carbohydr Res.* 2015;403:13-22. doi:10.1016/j.carres.2014.06.009
229. Kahne D, Walker S, Cheng Y, Van Engen D. Glycosylation of unreactive substrates. *J Am Chem Soc.* 1989;111(17):6881-6882. doi:10.1021/ja00199a081
230. Nicolaou KC, Dolle RE, Papahatjis DP. Practical synthesis of oligosaccharides. Partial synthesis of avermectin B1a. *J Am Chem Soc.* 1984;106(15):4189-4192. doi:10.1021/ja00327a021
231. Christensen MK, Meldal M, Bock K. Synthesis of mannose 6-phosphate-containing disaccharide threonine building blocks and their use in solid-phase glycopeptide synthesis. *J Chem Soc Perkin 1.* 1993;(13):1453-1460. doi:10.1039/P19930001453
232. Yoshida N, Fujieda T, Kobayashi A, Ishihara M, Noguchi M, Shoda S. Direct Introduction of Detachable Fluorescent Tag into Oligosaccharides. *Chem Lett.* 2013;42(9):1038-1039. doi:10.1246/cl.130379
233. Goethals F, Frank D, Du Prez F. Protected thiol strategies in macromolecular design. *Prog Polym Sci.* 2017;64:76-113. doi:10.1016/j.progpolymsci.2016.09.003
234. Prasanphanich NS, Song X, Heimbürg-Molinari J, et al. Intact Reducing Glycan Promotes the Specific Immune Response to Lacto-N-neotetraose-BSA Neoglycoconjugates. *Bioconjug Chem.* 2015;26(3):559-571. doi:10.1021/acs.bioconjchem.5b00036
235. Ruhaak LR, Zauner G, Huhn C, Bruggink C, Deelder AM, Wuhrer M. Glycan labeling strategies and their use in identification and quantification. *Anal Bioanal Chem.* 2010;397(8):3457-3481. doi:10.1007/s00216-010-3532-z

236. Villadsen K, Martos-Maldonado MC, Jensen KJ, Thygesen MB. Chemoselective Reactions for the Synthesis of Glycoconjugates from Unprotected Carbohydrates. *ChemBioChem*. 2017;18(7):574-612. doi:10.1002/cbic.201600582
237. Song X, Xia B, Stowell SR, Lasanajak Y, Smith DF, Cummings RD. Novel Fluorescent Glycan Microarray Strategy Reveals Ligands for Galectins. *Chem Biol*. 2009;16(1):36-47. doi:10.1016/j.chembiol.2008.11.004
238. Tomiya N, Kurono M, Ishihara H, et al. Structural analysis of N-linked oligosaccharides by a combination of glycopeptidase, exoglycosidases, and high-performance liquid chromatography. *Anal Biochem*. 1987;163(2):489-499. doi:10.1016/0003-2697(87)90253-3
239. Bigge JC, Patel TP, Bruce JA, Goulding PN, Charles SM, Parekh RB. Nonselective and Efficient Fluorescent Labeling of Glycans Using 2-Amino Benzamide and Anthranilic Acid. *Anal Biochem*. 1995;230(2):229-238. doi:10.1006/abio.1995.1468
240. Xia B, Kawar ZS, Ju T, Alvarez RA, Sachdev GP, Cummings RD. Versatile fluorescent derivatization of glycans for glycomic analysis. *Nat Methods*. 2005;2(11):845-850. doi:10.1038/nmeth808
241. Breitenbach BB, Steiert E, Konhäuser M, et al. Double stimuli-responsive polysaccharide block copolymers as green macrosurfactants for near-infrared photodynamic therapy. *Soft Matter*. 2019;15(6):1423-1434. doi:10.1039/C8SM02204F
242. Guerry A, Bernard J, Samain E, Fleury E, Cottaz S, Halila S. Aniline-Catalyzed Reductive Amination as a Powerful Method for the Preparation of Reducing End-“Clickable” Chitooligosaccharides. *Bioconjug Chem*. 2013;24(4):544-549. doi:10.1021/bc3003716
243. Likhoshesterov LM, Novikova OS, Derevitskaja VA, Kochetkov NK. A new simple synthesis of amino sugar β -d-glycosylamines. *Carbohydr Res*. 1986;146(1):C1-C5. doi:10.1016/0008-6215(86)85037-6
244. Petrelli A, Borsali R, Fort S, Halila S. Oligosaccharide-based block copolymers: Metal-free thiol-maleimide click conjugation and self-assembly into nanoparticles. *Carbohydr Polym*. 2015;124:109-116. doi:10.1016/j.carbpol.2015.01.079
245. Kwase YA, Cochran M, Nitz M. Protecting-Group-Free Glycoconjugate Synthesis: Hydrazide and Oxyamine Derivatives in N-Glycoside Formation. In: *Modern Synthetic Methods in Carbohydrate Chemistry*. John Wiley & Sons, Ltd; 2013:67-96. doi:10.1002/9783527658947.ch3
246. Zhi Z, Powell AK, Turnbull JE. Fabrication of Carbohydrate Microarrays on Gold Surfaces: Direct Attachment of Nonderivatized Oligosaccharides to Hydrazide-Modified Self-Assembled Monolayers. *Anal Chem*. 2006;78(14):4786-4793. doi:10.1021/ac060084f
247. Flinn NS, Quibell M, Monk TP, Ramjee MK, Urch CJ. A Single-Step Method for the Production of Sugar Hydrazides: Intermediates for the Chemoselective Preparation of Glycoconjugates. *Bioconjug Chem*. 2005;16(3):722-728. doi:10.1021/bc050041q
248. Munneke S, Prevost JRC, Painter GF, Stocker BL, Timmer MSM. The Rapid and Facile Synthesis of Oxyamine Linkers for the Preparation of Hydrolytically Stable Glycoconjugates. *Org Lett*. 2015;17(3):624-627. doi:10.1021/ol503634j

249. Lee M, Shin I. Facile Preparation of Carbohydrate Microarrays by Site-Specific, Covalent Immobilization of Unmodified Carbohydrates on Hydrazide-Coated Glass Slides. *Org Lett.* 2005;7(19):4269-4272. doi:10.1021/ol051753z
250. Park S, Lee M-R, Shin I. Construction of Carbohydrate Microarrays by Using One-Step, Direct Immobilizations of Diverse Unmodified Glycans on Solid Surfaces. *Bioconjug Chem.* 2009;20(1):155-162. doi:10.1021/bc800442z
251. Carrasco MR, Nguyen MJ, Burnell DR, MacLaren MD, Hengel SM. Synthesis of neoglycopeptides by chemoselective reaction of carbohydrates with peptides containing a novel N'-methyl-aminooxy amino acid. *Tetrahedron Lett.* 2002;43(33):5727-5729. doi:10.1016/S0040-4039(02)01212-1
252. Carrasco MR, Brown RT, Serafimova IM, Silva O. Synthesis of N-Fmoc-O- (N'-Boc-N'-methyl)-aminohomoserine, an Amino Acid for the Facile Preparation of Neoglycopeptides. *J Org Chem.* 2003;68(1):195-197. doi:10.1021/jo026641p
253. Peri F, Dumy P, Mutter M. Chemo- and stereoselective glycosylation of hydroxylamino derivatives: A versatile approach to glycoconjugates. *Tetrahedron.* 1998;54(40):12269-12278. doi:10.1016/S0040-4020(98)00763-7
254. Leung C, Chibba A, Gómez-Biagi RF, Nitz M. Efficient synthesis and protein conjugation of β -(1 \rightarrow 6)-d-N-acetylglucosamine oligosaccharides from the polysaccharide intercellular adhesin. *Carbohydr Res.* 2009;344(5):570-575. doi:10.1016/j.carres.2008.12.021
255. Likhoshesterov LM, Novikova OS, Shibaev VN. New Efficient Synthesis of β -Glucosylamines of Mono- and Disaccharides with the Use of Ammonium Carbamate. *Dokl Chem.* 2002;383(4):89-92. doi:10.1023/A:1015428720733
256. Lubineau A, Augé J, Drouillat B. Improved synthesis of glycosylamines and a straightforward preparation of N-acylglycosylamines as carbohydrate-based detergents. *Carbohydr Res.* 1995;266(2):211-219. doi:10.1016/0008-6215(94)00275-K
257. Monsigny M, Quétard C, Bourgerie S, et al. Glycotargeting: The preparation of glyco-amino acids and derivatives from unprotected reducing sugars. *Biochimie.* 1998;80(2):99-108. doi:10.1016/S0300-9084(98)80016-3
258. Kallin E, Lönn H, Norberg T, Elofsson M. Derivatization Procedures for Reducing Oligosaccharides, Part 3: Preparation of Oligosaccharide Glycosylamines, and Their Conversion Into Glycosaccharide - Acrylamide Copolymers. *J Carbohydr Chem.* 1989;8(4):597-611. doi:10.1080/07328308908048020
259. ISBELL HS, FRUSH HL. Mutarotation, Hydrolysis, and Rearrangement Reactions of Glycosylamines1. *J Org Chem.* 1958;23(9):1309-1319. doi:10.1021/jo011103a019
260. Vetter D, Gallop MA. Strategies for the Synthesis and Screening of Glycoconjugates. 1. A Library of Glycosylamines. *Bioconjug Chem.* 1995;6(3):316-318. doi:10.1021/bc00033a013
261. Bruyn CAL de, Franchimont APN. Dérivés ammoniacaux cristallisés d'hydrates de carbone: (Communication provisoire). *Recl Trav Chim Pays-Bas.* 1893;12(11):286-289. doi:10.1002/recl.18930121103

262. Bruyn CAL de, Leent FH van. Dérivés ammoniacaux de la mannose, de la sorbose et de la galactose. *Recl Trav Chim Pays-Bas*. 1896;15(3):81-83. doi:10.1002/recl.18960150303
263. Isbell HS, Frush HL. Mechanisms for the mutarotation and hydrolysis of the glycosylamines and the mutarotation of the sugars. In: ; 1951. doi:10.6028/jres.046.020
264. Mitts E, Hixon RM. The Reaction of Glucose with Some Amines. *J Am Chem Soc*. 1944;66(3):483-486. doi:10.1021/ja01231a055
265. Danishefsky SJ, Hu S, Cirillo PF, Eckhardt M, Seeberger PH. A Highly Convergent Total Synthetic Route to Glycopeptides Carrying a High-Mannose Core Pentasaccharide Domain N-linked to a Natural Peptide Motif. *Chem – Eur J*. 1997;3(10):1617-1628. doi:10.1002/chem.19970031011
266. Liu X, Zhang G, Chan K, Li J. Microwave-assisted Kochetkov amination followed by permanent charge derivatization: a facile strategy for glycomics. *Chem Commun*. 2010;46(39):7424-7426. doi:10.1039/C0CC01732A
267. Huang Z-H, Shen T, Wu J, Gage DA, Watson JT. Protein Sequencing by Matrix-Assisted Laser Desorption Ionization–Postsource Decay–Mass Spectrometry Analysis of the N-Tris(2,4,6-trimethoxyphenyl)phosphine-Acetylated Tryptic Digests. *Anal Biochem*. 1999;268(2):305-317. doi:10.1006/abio.1998.3085
268. Kuyama H, Sonomura K, Shima K, Nishimura O, Tsunasawa S. An improved method for de novo sequencing of arginine-containing, N α -tris(2,4,6-trimethoxyphenyl)phosphonium-acetylated peptides. *Rapid Commun Mass Spectrom*. 2008;22(13):2063-2072. doi:10.1002/rcm.3587
269. Chen W, Lee PJ, Shion H, Ellor N, Gebler JC. Improving de Novo Sequencing of Peptides Using a Charged Tag and C-Terminal Digestion. *Anal Chem*. 2007;79(4):1583-1590. doi:10.1021/ac061670b
270. Lingome CE, Pourceau G, Gobert-Deveaux V, Wadouachi A. Efficient synthesis of glycosylamines in solventless conditions promoted by mechanical milling. *RSC Adv*. 2014;4(68):36350-36356. doi:10.1039/C4RA04321A
271. Beckmann HSG, Wittmann V. Azides in Carbohydrate Chemistry. In: *Organic Azides*. John Wiley & Sons, Ltd; 2010:469-490. doi:10.1002/9780470682517.ch16
272. de Barros ALB, Cardoso VN, Mota L das G, Leite EA, Oliveira MC de, Alves RJ. Synthesis and biological evaluation of technetium-labeled d-glucose-MAG3 derivative as agent for tumor diagnosis. *Bioorg Med Chem Lett*. 2009;19(9):2497-2499. doi:10.1016/j.bmcl.2009.03.059
273. Ding Y, Swayze EE, Hofstadler SA, Griffey RH. Efficient synthesis of neomycin B related aminoglycosides. *Tetrahedron Lett*. 2000;41(21):4049-4052. doi:10.1016/S0040-4039(00)00586-4
274. Vlist J van der, Faber M, Loen L, Dijkman TJ, Asri LATW, Loos K. Synthesis of Hyperbranched Glycoconjugates by the Combined Action of Potato Phosphorylase and Glycogen Branching Enzyme from *Deinococcus geothermalis*. *Polymers*. 2012;4(1):674-690. doi:10.3390/polym4010674

275. Gauche C, Soldi V, Fort S, Borsali R, Halila S. Xyloglucan-based diblock co-oligomer: Synthesis, self-assembly and steric stabilization of proteins. *Carbohydr Polym.* 2013;98(2):1272-1280. doi:10.1016/j.carbpol.2013.07.064
276. Shi L, Wang F, Zhu W, et al. Self-Healing Silk Fibroin-Based Hydrogel for Bone Regeneration: Dynamic Metal-Ligand Self-Assembly Approach. *Adv Funct Mater.* 2017;27(37):1700591. doi:10.1002/adfm.201700591
277. Battistella C, Klok H-A. Reversion of P-gp-Mediated Drug Resistance in Ovarian Carcinoma Cells with PHPMA-Zosuquidar Conjugates. *Biomacromolecules.* 2017;18(6):1855-1865. doi:10.1021/acs.biomac.7b00291
278. Zhang M, Liu J, Kuang Y, et al. "Stealthy" chitosan/mesoporous silica nanoparticle based complex system for tumor-triggered intracellular drug release. *J Mater Chem B.* 2016;4(19):3387-3397. doi:10.1039/C5TB02548F
279. Zugates GT, Anderson DG, Little SR, Lawhorn IEB, Langer R. Synthesis of Poly(β -amino ester)s with Thiol-Reactive Side Chains for DNA Delivery. *J Am Chem Soc.* 2006;128(39):12726-12734. doi:10.1021/ja061570n
280. Espeel P, Du Prez FE. One-pot multi-step reactions based on thiolactone chemistry: A powerful synthetic tool in polymer science. *Eur Polym J.* 2015;62:247-272. doi:10.1016/j.eurpolymj.2014.07.008
281. Kraatz U, Wamhoff H, Korte F. Heterocyclen aus Lactonen, Lactamen und Thiollactonen, XII Synthese von α -Isocyanato- γ -thiolbutyrolacton und funktionellen Derivaten sowie deren Umlagerung in Hydantoine und 1.2.4-Triazine. *Justus Liebigs Ann Chem.* 1972;758(1):177-184. doi:10.1002/jlac.19727580119
282. Stamenović MM, Espeel P, Baba E, Yamamoto T, Tezuka Y, Prez FED. Straightforward synthesis of functionalized cyclic polymers in high yield via RAFT and thiolactone–disulfide chemistry. *Polym Chem.* 2012;4(1):184-193. doi:10.1039/C2PY20751F
283. Reinicke S, Espeel P, Stamenović MM, Du Prez FE. One-Pot Double Modification of p(NIPAAm): A Tool for Designing Tailor-Made Multiresponsive Polymers. *ACS Macro Lett.* 2013;2(6):539-543. doi:10.1021/mz4002222
284. Martens S, Van den Begin J, Madder A, Du Prez FE, Espeel P. Automated Synthesis of Monodisperse Oligomers, Featuring Sequence Control and Tailored Functionalization. *J Am Chem Soc.* 2016;138(43):14182-14185. doi:10.1021/jacs.6b07120
285. Kaya NU, Prez FED, Badi N. Multifunctional Dendrimer Formation Using Thiolactone Chemistry. *Macromol Chem Phys.* 2017;218(18):1600575. doi:10.1002/macp.201600575
286. Espeel P, Goethals F, Du Prez FE. One-Pot Multistep Reactions Based on Thiolactones: Extending the Realm of Thiol–Ene Chemistry in Polymer Synthesis. *J Am Chem Soc.* 2011;133(6):1678-1681. doi:10.1021/ja1098098
287. Okumura K, Oda T, Kondo K, et al. Vitamin B6 derivatives. 13. Synthesis of tetrahydrothiazine derivatives of vitamin B6 and their biological properties. *J Med Chem.* 1971;14(3):226-229. doi:10.1021/jm00285a012

288. Goethals F, Martens S, Espeel P, van den Berg O, Du Prez FE. Diversely Substituted Polyamide Structures through Thiol–Ene Polymerization of Renewable Thiolactone Building Blocks. *Macromolecules*. 2014;47(1):61-69. doi:10.1021/ma4022423
289. Biltz H, Wittke H. Über alkylierte und acylierte Barbitursäuren. *Berichte Dtsch Chem Ges B Ser*. 1921;54(5):1035-1058. doi:10.1002/cber.19210540519
290. Xia G, Benmohamed R, Kim J, et al. Pyrimidine-2,4,6-trione Derivatives and Their Inhibition of Mutant SOD1-Dependent Protein Aggregation. Toward a Treatment for Amyotrophic Lateral Sclerosis. *J Med Chem*. 2011;54(7):2409-2421. doi:10.1021/jm101549k
291. Kang S, Cooper G, Dunne SF, et al. CaV1.3-selective L-type calcium channel antagonists as potential new therapeutics for Parkinson's disease. *Nat Commun*. 2012;3(1):1-7. doi:10.1038/ncomms2149
292. Kang S, Cooper G, Dunne SF, Luan C-H, Surmeier DJ, Silverman RB. Structure–Activity Relationship of N,N'-Disubstituted Pyrimidinetriones as CaV1.3 Calcium Channel-Selective Antagonists for Parkinson's Disease. *J Med Chem*. 2013;56(11):4786-4797. doi:10.1021/jm4005048
293. Gonzalez MA, Jimenez Requejo JL, Palacios Albarran JC, Gabis Perez JA. Facile preparation of C-glycosylbarbiturates and C-glycosylbarbituric acids. *Carbohydr Res*. 1986;158:53-66. doi:10.1016/0008-6215(86)84005-8
294. Bueno Martinez M, Zamora Mata F, Muñoz Ruiz A, Galbis Perez JA, Jaime Cardiel C. Synthesis and conformational analysis of C-glycosylbarbiturates. *Carbohydr Res*. 1990;199(2):235-238. doi:10.1016/0008-6215(90)84265-V
295. Critchley P, Clarkson GJ. Carbohydrate–protein interactions at interfaces: comparison of the binding of Ricinus communis lectin to two series of synthetic glycolipids using surface plasmon resonance studies. *Org Biomol Chem*. 2003;1(23):4148-4159. doi:10.1039/B306784J
296. Portier F, Solier J, Halila S. N,N'-Disubstituted Barbituric Acid: A Versatile and Modular Multifunctional Platform for Obtaining β -C-Glycoconjugates from Unprotected Carbohydrates in Water. *Eur J Org Chem*. 2019;2019(36):6158-6162. doi:10.1002/ejoc.201901251
297. Sureshbabu VV, Basavaprabhu null. N,N'-Carbonyldiimidazole-Mediated DBU-Catalyzed One-Pot Synthesis of Urea-Tethered Glycosyl Amino Acids and Glycoconjugates. *Synlett*. 2011;2011(08):1160-1164. doi:10.1055/s-0030-1259958
298. Knölker H-J, Braxmeier T, Schlechtingen G. A Novel Method for the Synthesis of Isocyanates Under Mild Conditions. *Angew Chem Int Ed Engl*. 1995;34(22):2497-2500. doi:10.1002/anie.199524971
299. Bergman PW and J. The Chemistry of Anthranilic Acid. *Curr Org Synth*. 2006;3(3):379-402. doi:10.2174/157017906777934926
300. Coppola GM. The Chemistry of Isatoic Anhydride. *Synthesis*. 1980;1980(7):505-536. doi:10.1055/s-1980-29110
301. Shvekhgeimer M-GA. Synthesis of Heterocyclic Compounds Based on Isatoic Anhydrides (2H-3,1-Benzoxazine-2,4-diones). (Review). *Chem Heterocycl Compd*. 2001;37(4):385-443. doi:10.1023/A:1017631318971

302. Kolbe H. Beiträge zur Ermittlung der chemischen Constitution des Isatins. *J Für Prakt Chem.* 1884;30(1):467-483. doi:10.1002/prac.18850300144
303. Sheibley FE. 6,8-DICHLOROBENZOYLENE UREA, AND THE INTERACTION OF 5,7-DIHALOGEN ISATOIC ANHYDRIDES WITH AMMONIA.—A NEW REAGENT FOR SODIUM. *J Org Chem.* 1938;03(5):414-423. doi:10.1021/jo01222a004
304. Sheibley FE. 6,8-DIODOBENZOYLENEUREA, AND THE INTERACTION OF 5,7-DIHALOGENOISATOIC ANHYDRIDES WITH AMMONIA AND WITH ETHYLAMINE. 3-ETHYL-6,8-DIHALOGENOBENZOYLENEUREAS. *J Org Chem.* 1947;12(6):743-751. doi:10.1021/jo01170a001
305. Staiger RP, Wagner EC. Isatoic anhydride. II. Reactions of isatoic anhydride with ammonia. *J Org Chem.* 1948;13(3):347-352. doi:10.1021/jo01161a004
306. Jacobs RL. The synthesis of o-Amino-N-substituted benzamides and 3-substituted 2,4 (1H,3H)-quinazolinediones from isatoic anhydride. *J Heterocycl Chem.* 1970;7(6):1337-1345. doi:10.1002/jhet.5570070617
307. Staiger RP, Wagner EC. Isatoic Anhydride. III. Reactions with Primary and Secondary Amines. *J Org Chem.* 1953;18(10):1427-1439. doi:10.1021/jo50016a024
308. Heindel ND, Fives WP, Lemke TF, Carrano RA. Synthesis and selected pharmacology of anthranilamides. *J Pharm Sci.* 1971;60(5):703-707. doi:10.1002/jps.2600600509
309. Ayers JT, Anderson SR. A Preparative Scale Reduction of Alkyl Disulfides with Tributyl Phosphine and Water. *Synth Commun.* 1999;29(3):351-358. doi:10.1080/00397919908085777
310. Luyai A, Lasanajak Y, Smith DF, Cummings RD, Song X. Facile Preparation of Fluorescent Neoglycoproteins Using p-Nitrophenyl Anthranilate as a Heterobifunctional Linker. *Bioconjug Chem.* 2009;20(8):1618-1624. doi:10.1021/bc900189h
311. Fadda AA, Refat HM, Zaki MEA, Monir E. Reaction of Isatoic Anhydride with Bifunctional Reagents: Synthesis of Some New Quinazolone Fused Heterocycles, 2-Substituted Anilinoheterocyclic Derivatives and Other Related Compounds. *Synth Commun.* 2001;31(22):3537-3545. doi:10.1081/SCC-100106216
312. Gamian A, Chomik M, Laferrière CA, Roy R. Inhibition of influenza A virus hemagglutinin and induction of interferon by synthetic sialylated glycoconjugates. *Can J Microbiol.* 1991;37(3):233-237. doi:10.1139/m91-035
313. Roy R, Laferrière CA. Synthesis of antigenic copolymers of N-acetylneuraminic acid binding to wheat germ agglutinin and antibodies. *Carbohydr Res.* 1988;177:c1-c4. doi:10.1016/0008-6215(88)85068-7
314. Roy R, Andersson FO, Harms G, Kelm S, Schauer R. Synthesis of Esterase-resistant 9-O-Acetylated Polysialoside as Inhibitor of Influenza C Virus Hemagglutinin. *Angew Chem Int Ed Engl.* 1992;31(11):1478-1481. doi:10.1002/anie.199214781
315. Spaltenstein A, Whitesides GM. Polyacrylamides bearing pendant .alpha.-sialoside groups strongly inhibit agglutination of erythrocytes by influenza virus. *J Am Chem Soc.* 1991;113(2):686-687. doi:10.1021/ja00002a053

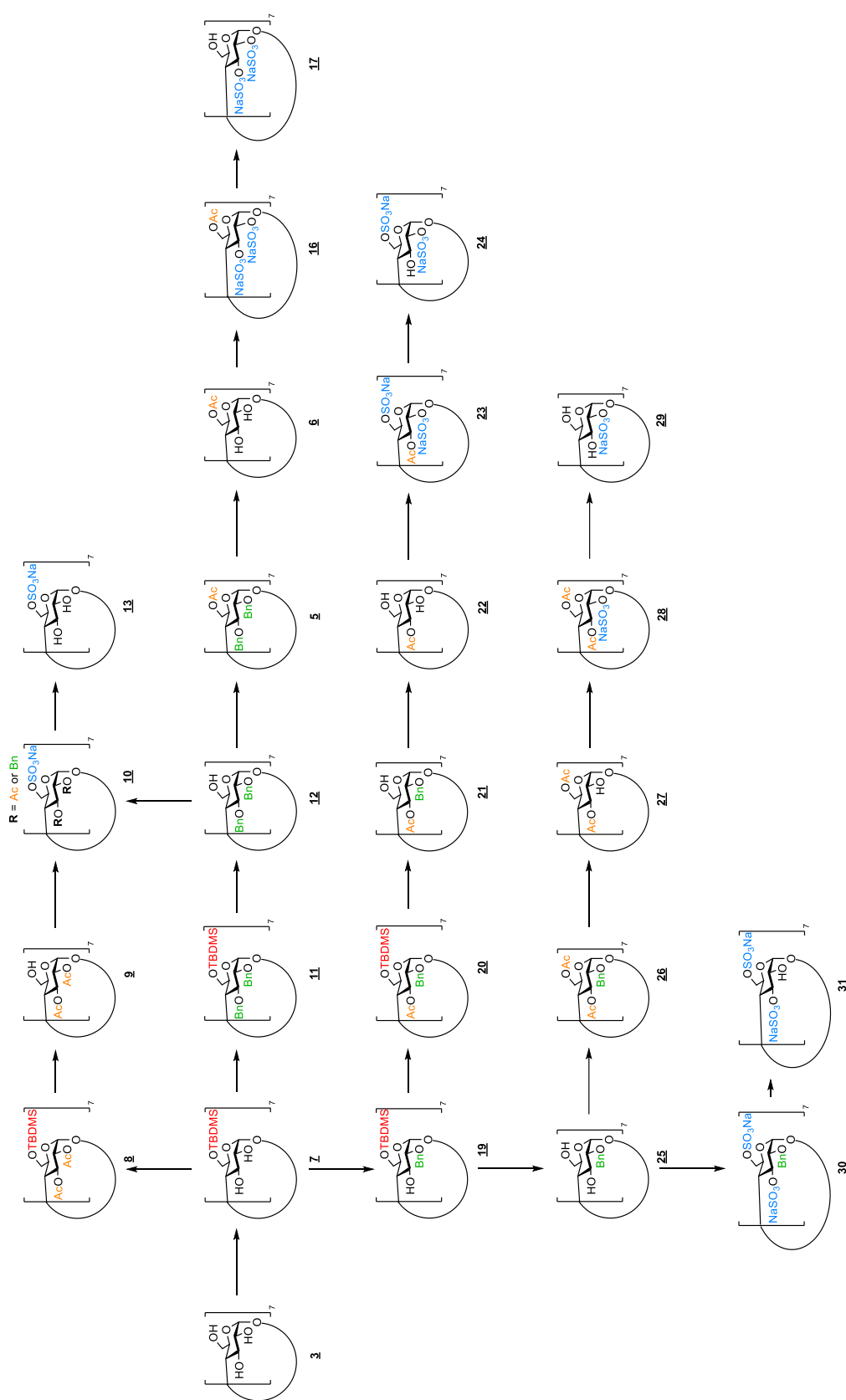
316. Kiessling LL, Pohl NL. Strength in numbers: non-natural polyvalent carbohydrate derivatives. *Chem Biol.* 1996;3(2):71-77. doi:10.1016/S1074-5521(96)90280-X
317. Davis BG. Synthesis of Glycoproteins. *Chem Rev.* 2002;102(2):579-602. doi:10.1021/cr0004310
318. Pozsgay V, Kubler-Kielb J. Conjugation Methods toward Synthetic Vaccines. In: *Carbohydrate-Based Vaccines*. Vol 989. ACS Symposium Series. American Chemical Society; 2008:36-70. doi:10.1021/bk-2008-0989.ch003
319. Babinot J, Guigner J-M, Renard E, Langlois V. Poly(3-hydroxyalkanoate)-derived amphiphilic graft copolymers for the design of polymersomes. *Chem Commun.* 2012;48(43):5364-5366. doi:10.1039/C2CC30482A
320. Timbart L, Renard E, Tessier M, Langlois V. Monohydroxylated Poly(3-hydroxyoctanoate) Oligomers and Its Functionalized Derivatives Used as Macroinitiators in the Synthesis of Degradable Diblock Copolyesters. *Biomacromolecules.* 2007;8(4):1255-1265. doi:10.1021/bm060981t
321. Bear M-M, Leboucher-Durand M-A, Langlois V, Lenz RW, Goodwin S, Guérin P. Bacterial poly-3-hydroxyalkanoates with epoxy groups in the side chains. *React Funct Polym.* 1997;34(1):65-77. doi:10.1016/S1381-5148(97)00024-2
322. Arkin AH, Hazer B, Borcakli M. Chlorination of Poly(3-hydroxy alkanoates) Containing Unsaturated Side Chains. *Macromolecules.* 2000;33(9):3219-3223. doi:10.1021/ma991535j
323. Kılıçay E, Hazer B, Çoban B, Scholz C. Synthesis and Characterization of the Poly(ethylene glycol) Grafted Unsaturated Microbial Polyesters. *Hacet J Biol Chem.* 2010;38(1):9-17.
324. Constantin M, Simionescu CI, Carpov A, Samain E, Driguez H. Chemical modification of poly(hydroxyalkanoates). Copolymers bearing pendant sugars. *Macromol Rapid Commun.* 1999;20(2):91-94. doi:10.1002/(SICI)1521-3927(19990201)20:2<91::AID-MARC91>3.0.CO;2-E
325. Eroğlu MS, Hazer B, Ozturk T, Caykara T. Hydroxylation of pendant vinyl groups of poly(3-hydroxy undec-10-enoate) in high yield. *J Appl Polym Sci.* 2005;97(5):2132-2139. doi:10.1002/app.21943
326. Lee MY, Park WH, Lenz RW. Hydrophilic bacterial polyesters modified with pendant hydroxyl groups. *Polymer.* 2000;41(5):1703-1709. doi:10.1016/S0032-3861(99)00347-X
327. Renard E, Poux A, Timbart L, Langlois V, Guérin P. Preparation of a Novel Artificial Bacterial Polyester Modified with Pendant Hydroxyl Groups. *Biomacromolecules.* 2005;6(2):891-896. doi:10.1021/bm049337+
328. Kurth N, Renard E, Brachet F, Robic D, Guerin P, Bourbouze R. Poly(3-hydroxyoctanoate) containing pendant carboxylic groups for the preparation of nanoparticles aimed at drug transport and release. *Polymer.* 2002;43(4):1095-1101. doi:10.1016/S0032-3861(01)00692-9
329. Stigers DJ, Tew GN. Poly(3-hydroxyalkanoate)s Functionalized with Carboxylic Acid Groups in the Side Chain. *Biomacromolecules.* 2003;4(2):193-195. doi:10.1021/bm025728h
330. Hazer DB, Kılıçay E, Hazer B. Poly(3-hydroxyalkanoate)s: Diversification and biomedical applications: A state of the art review. *Mater Sci Eng C.* 2012;32(4):637-647. doi:10.1016/j.msec.2012.01.021

331. Babinot J, Renard E, Langlois V. Preparation of Clickable Poly(3-hydroxyalkanoate) (PHA): Application to Poly(ethylene glycol) (PEG) Graft Copolymers Synthesis. *Macromol Rapid Commun.* 2010;31(7):619-624. doi:10.1002/marc.200900803
332. Goethals F, Frank D, Du Prez F. Protected thiol strategies in macromolecular design. *Prog Polym Sci.* 2017;64:76-113. doi:10.1016/j.progpolymsci.2016.09.003
333. Dondoni A, Marra A. Free-Radical Thiol-Ene and Thiol-Yne Couplings as Click Processes for Glycoconjugation. In: *Click Chemistry in Glycoscience*. John Wiley & Sons, Ltd; 2013:45-75. doi:10.1002/9781118526996.ch3
334. Babinot J, Renard E, Droumaguet BL, et al. Facile Synthesis of Multicompartment Micelles Based on Biocompatible Poly(3-hydroxyalkanoate). *Macromol Rapid Commun.* 2013;34(4):362-368. doi:10.1002/marc.201200692
335. Nair DP, Podgórski M, Chatani S, et al. The Thiol-Michael Addition Click Reaction: A Powerful and Widely Used Tool in Materials Chemistry. *Chem Mater.* 2014;26(1):724-744. doi:10.1021/cm402180t
336. Capozzi G, Modena G. Oxidation of thiols. In: *The Thiol Group (1974)*. John Wiley & Sons, Ltd; 2010:785-839. doi:10.1002/9780470771327.ch7
337. Witt D. Recent Developments in Disulfide Bond Formation. *Synthesis.* 2008;2008(16):2491-2509. doi:10.1055/s-2008-1067188
338. Posner T. Beiträge zur Kenntniss der ungesättigten Verbindungen. II. Ueber die Addition von Mercaptanen an ungesättigte Kohlenwasserstoffe. *Berichte Dtsch Chem Ges.* 1905;38(1):646-657. doi:10.1002/cber.190503801106
339. Dondoni A, Marra A. Recent applications of thiol-ene coupling as a click process for glycoconjugation. *Chem Soc Rev.* 2012;41(2):573-586. doi:10.1039/C1CS15157F
340. Floyd N, Vijayakrishnan B, Koeppe JR, Davis BG. Thiol Glycosylation of Olefinic Proteins: S-Linked Glycoconjugate Synthesis. *Angew Chem Int Ed.* 2009;48(42):7798-7802. doi:10.1002/anie.200903135
341. An S, Jeon B, Bae JH, et al. Thiol-based chemistry as versatile routes for the effective functionalization of cellulose nanofibers. *Carbohydr Polym.* 2019;226:115259. doi:10.1016/j.carbpol.2019.115259
342. Espeel P, Goethals F, Du Prez FE. One-Pot Multistep Reactions Based on Thiolactones: Extending the Realm of Thiol-Ene Chemistry in Polymer Synthesis. *J Am Chem Soc.* 2011;133(6):1678-1681. doi:10.1021/ja1098098
343. Espeel P, Goethals F, Driessen F, Nguyen L-TT, Prez FED. One-pot, additive-free preparation of functionalized polyurethanes via amine-thiol-ene conjugation. *Polym Chem.* 2013;4(8):2449-2456. doi:10.1039/C3PY00004D
344. Uygun M, Tasdelen MA, Yagci Y. Influence of Type of Initiation on Thiol-Ene "Click" Chemistry - Uygun - 2010 - Macromolecular Chemistry and Physics - Wiley Online Library. *Macromol Chem Phys.* 2010;211:103-110.

345. Weinrich D, Köhn M, Jonkheijm P, et al. Preparation of Biomolecule Microstructures and Microarrays by Thiol–ene Photoimmobilization. *ChemBioChem*. 2010;11(2):235-247. doi:10.1002/cbic.200900559
346. Alcock LJ, Farrell KD, Akol MT, et al. Norbornene probes for the study of cysteine oxidation. *Tetrahedron*. 2018;74(12):1220-1228. doi:10.1016/j.tet.2017.11.011
347. Munneke S, Dangerfield EM, Stocker BL, Timmer MSM. The versatility of N-alkyl-methoxyamine bi-functional linkers for the preparation of glycoconjugates. *Glycoconj J*. 2017;34(5):633-642. doi:10.1007/s10719-017-9785-4
348. Mangeon C, Modjinou T, Rios de Anda A, Thevenieau F, Renard E, Langlois V. Renewable Semi-Interpenetrating Polymer Networks Based on Vegetable Oils Used as Plasticized Systems of Poly(3-hydroxyalkanoate)s. *ACS Sustain Chem Eng*. 2018;6(4):5034-5042. doi:10.1021/acssuschemeng.7b04692
349. Ritter JJ, Minieri PP. A New Reaction of Nitriles. I. Amides from Alkenes and Mononitriles. *J Am Chem Soc*. 1948;70(12):4045-4048. doi:10.1021/ja01192a022
350. Wang ZD, Sheikh SO, Cox S, Zhang Y, Massey K. Direct Preparation of N-Glycosidic Bond-Linked Nonionic Carbohydrate-Based Surfactant (NICBS) via Ritter Reaction. *Eur J Org Chem*. 2007;2007(14):2243-2247. doi:10.1002/ejoc.200700079
351. Zheng J, Urkalan KB, Herzon SB. Direct Synthesis of β -N-Glycosides by the Reductive Glycosylation of Azides with Protected and Native Carbohydrate Donors. *Angew Chem Int Ed*. 2013;52(23):6068-6071. doi:10.1002/anie.201301264
352. Rosen T, Lico IM, Chu DTW. A convenient and highly chemoselective method for the reductive acetylation of azides. *J Org Chem*. 1988;53(7):1580-1582. doi:10.1021/jo00242a051
353. Kolakowski RV, Shangguan N, Sauers RR, Williams LJ. Mechanism of Thio Acid/Azide Amidation. *J Am Chem Soc*. 2006;128(17):5695-5702. doi:10.1021/ja057533y
354. Shangguan N, Katukojvala S, Greenberg R, Williams LJ. The Reaction of Thio Acids with Azides: A New Mechanism and New Synthetic Applications. *J Am Chem Soc*. 2003;125(26):7754-7755. doi:10.1021/ja0294919
355. Nilsson BL, Kiessling LL, Raines RT. Staudinger Ligation: A Peptide from a Thioester and Azide. *Org Lett*. 2000;2(13):1939-1941. doi:10.1021/ol0060174
356. Saxon E, Armstrong JI, Bertozzi CR. A "Traceless" Staudinger Ligation for the Chemoselective Synthesis of Amide Bonds. *Org Lett*. 2000;2(14):2141-2143. doi:10.1021/ol006054v
357. Nisic F, Andreini M, Bernardi A. Stereoselective Synthesis of N-Glycosyl Amino Acids by Traceless Staudinger Ligation of Unprotected Glycosyl Azides. *Eur J Org Chem*. 2009;2009(33):5744-5751. doi:10.1002/ejoc.200900692
358. Bode JW, Fox RM, Baucom KD. Chemoselective Amide Ligations by Decarboxylative Condensations of N-Alkylhydroxylamines and α -Ketoacids. *Angew Chem Int Ed*. 2006;45(8):1248-1252. doi:10.1002/anie.200503991
359. Boas U, Lind P, Riber U. Method to conjugate polysaccharide antigens to surfaces for the detection of antibodies. *Anal Biochem*. 2014;465:73-80. doi:10.1016/j.ab.2014.07.005

360. Huang C-Y, Thayer DA, Chang AY, et al. Carbohydrate microarray for profiling the antibodies interacting with Globo H tumor antigen. *Proc Natl Acad Sci*. 2006;103(1):15-20. doi:10.1073/pnas.0509693102
361. Blixt O, Head S, Mondala T, et al. Printed covalent glycan array for ligand profiling of diverse glycan binding proteins. *Proc Natl Acad Sci*. 2004;101(49):17033-17038. doi:10.1073/pnas.0407902101
362. Balalaie S, Mahdidoust M, Eshaghi-Najafabadi R. 2-(1H-Benzotriazole-1-yl)-1,1,3,3-Tetramethyluronium Tetrafluoro Borate (TBTU) as an Efficient Coupling Reagent for the Esterification of Carboxylic acids with Alcohols and Phenols at Room Temperature. *Chin J Chem*. 2008;26(6):1141-1144. doi:10.1002/cjoc.200890204
363. Vrettos EI, Sayyad N, Mavrogiannaki EM, et al. Unveiling and tackling guanidinium peptide coupling reagent side reactions towards the development of peptide-drug conjugates. *RSC Adv*. 2017;7(80):50519-50526. doi:10.1039/C7RA06655D
364. Moura Neto É de, Maciel J da S, Cunha PLR, dePaula RCM, Feitosa JPA. Preparation and characterization of a chemically sulfated cashew gum polysaccharide. *J Braz Chem Soc*. 2011;22(10):1953-1960. doi:10.1590/S0103-50532011001000017

Appendix



Appendix 1. General strategy employed for the synthesis of regioselectively sulfated β -cyclodextrins